The Use of Immediate-Early Gene Expression to Map Relationships Between Limbic Structures Supporting Memory

Mathieu M. Albasser

School of Psychology

CARDIFF UNIVERSITY
PRIFYSGOL CAERDYDD

Ph.D 2009

ProQuest LLC
789 East Eisenhower Parkway
P.O. Box 1346
Ann Arbor, MI 48106-1346

CARDIFF UNIVERSITY
PRIFYSGOL CAERDYDD

DECLARATION

This work has not previously been accepted in substance for any degree and is not concurrently submitted in candidature for any degree.

Signed ..... (candidate) Date ....30/10/09.....

STATEMENT 1

This thesis is being submitted in partial fulfillment of the requirements for the degree of .....(insert MCh, MD, MPhil, PhD etc, as appropriate)

Signed ..... (candidate) Date ....30/10/09.....

STATEMENT 2

This thesis is the result of my own independent work/investigation, except where otherwise stated. Other sources are acknowledged by explicit references.

Signed ..... (candidate) Date ....30/10/09.....

STATEMENT 3

I hereby give consent for my thesis, if accepted, to be available for photocopying and for inter-library loan, and for the title and summary to be made available to outside organisations.

Signed ..... (candidate) Date ....30/10/09.....

STATEMENT 4: PREVIOUSLY APPROVED BAR ON ACCESS

I hereby give consent for my thesis, if accepted, to be available for photocopying and for inter-library loans **after expiry of a bar on access previously approved by the Graduate Development Committee.**

Signed ..... (candidate) Date ....30/10/09.....

The Use of Immediate-Early Gene Expression to Map Relationships Between Limbic Structures Supporting Memory

Mathieu M. Albasser (BSc, MSc)

School of Psychology

CARDIFF UNIVERSITY
PRIFYSGOL CAERDYDD

Thesis submitted to Cardiff University

For the Degree of Doctor of Philosophy

November 2009

Table of Contents

Acknowledgments

I would like to thank my supervisor John Aggleton for all his support and guidance over the three and a half years. It was, and still is, a pleasure to be part of his team. For me, John is more than my supervisor, thank you for taking a chance on me.

Very special thanks go to my love Carine, without whom I probably would not have made it. I am grateful for her constant support and understanding, even during the hard time of my PhD.

I would also like to thank Seralynne for having always been present, and for being a great friend. A special thanks to Guillaume Poirier, Eman Amin and Rachel Kyd for their help in teaching me many of the techniques that were used in this thesis. Thank you to all my colleagues and everybody in the labs, in particular Jeff, Moira, Either.

In addition to this amazing work environment, I would like to thank all the fantastic people I met during my PhD: Dean (the best office mate ever!), Adam, Jemma, James, Helen, Mariah, Mikael, Fred, Chris. Un grand merci to the French team that was always there to help me not to forget my French: Elsa, Anais, Caroline.

My PhD was surrounded by music, and my band "Draw me Stories" helped me to go through and is a great part of my life, so a special thanks to Carl and Sam, DMS forever!

Finally, I wish to thank my mum, my dad, Tim, Marc and the rest of my family, who have always believed in me.

Summary

This thesis explores the influence of brain regions within the "extended hippocampal memory system" on the activity of the retrosplenial cortex in the rat. One of the first goals was to use lesion studies to improve the understanding of the vulnerability of the retrosplenial cortex, especially in the context of diencephalic and temporal lobe amnesia. The second was to assess what are the brain areas within the temporal lobe involved in object recognition and how they interact.

These two objectives were made possible by visualising immediate-early gene expression. By combining this technique with lesions, distal effects of different lesions (hippocampus, mammillothalamic tract and fornix) on the activity of the retrosplenial cortex were measured. For object recognition, the immediate-early gene imaging enabled the assessment of normal brain activity in rats associated with behavioural discrimination of novelty.

The lesion studies provide information about the specific and common vulnerability of the retrosplenial cortex, as all three distal lesions resulted in a decrease of immediate-early gene activity in the retrosplenial cortex. In addition, these findings unify diencephalic amnesia with temporal amnesia, and emphasize the need to study networks or systems instead of individual structure. The immediate-early gene/object recognition experiment implicated the caudal part of the perirhinal cortex (and Te2) and of the hippocampus in object recognition, and highlighted the importance of mapping brain region relationships within a connected system.

Taken together, these experiments provide clear support for the concept of an extended hippocampal memory system, but also show how this system may interact with other structures involved in different forms of memory. The findings underlie the potential afforded by use of immediate-early gene expression techniques in animal studies.

Publications

"Hippocampal lesions halve immediate-early gene protein counts in retrosplenial cortex: distal dysfunctions in a spatial memory system" Albasser MM, Poirier GL, Warburton EC, Aggleton JP (2007) Eur J Neurosci 26:1254-1266.

"Magnitude of the object recognition deficit associated with perirhinal cortex damage in rats: Effects of varying the lesion extent and the duration of the sample period" Albasser MM, Davies M, Futter JE, Aggleton JP (2009) Behav Neurosci 123:115-124.

"Hippocampal, retrosplenial, and prefrontal hypoactivity in a model of diencephalic amnesia: Evidence towards an interdependent subcortical-cortical memory network" Vann SD & Albasser MM (2009) Hippocampus 19(11):1090-1102.

"Granular and dysgranular retrosplenial cortices provide qualitatively different contributions to spatial working memory: evidence from immediate-early gene imaging in rats" Pothuizen HJ, Davies M, Albasser MM, Aggleton JP, Vann SD (2009) European Journal of Neuroscience, 30(5):877-88

"Qualitatively different modes of perirhinal - hippocampal engagement when rats explore novel versus familiar objects as revealed by c-Fos imaging" Albasser MM, Poirier GL, Aggleton JP (2009) European Journal of Neuroscience, *in press.*

Chapter 1

General Introduction

Immediate-early genes

What is an IEG

The term immediate-early gene (IEG) was originally used exclusively for viral genes. These genes are the first to be activated following virus integration into the infected cell and are responsible for transcriptional reprogramming of the host to promote virus replication. Eukaryotic homologues of retroviral proto-oncogenes have been discovered and referred to as cellular IEGs, such as c-*fos*, *zif*268, and c-*jun*. The nomenclature originates in virology in which viral genes are defined as "early" or "late" depending on whether their expression occurs before or after replication of the viral genome. Moreover, a set of viral genes are expressed rapidly or "immediately "after infection of the cell. Thus, the term "viral immediate-early gene" (e.g. v-*fos*) was adopted and modified to "cellular immediate-early gene" (e.g. c-*fos*). Like their viral relatives, cellular IEGs show rapid and transient expression in the absence of *de novo* protein synthesis.

Stimulation of neurons can activate two different mechanisms by which they process and transmit information: electrophysiological activity, and the longer-acting second messenger signal cascades that evoke production of transcription factor proteins that then initiate transcription or repression of other genes. Immediate-early genes are those genes that are first expressed following cell stimulation, their induction requiring no prior protein synthesis

(Tischmeyer and Grimm, 1999). There are two classes of IEGs: inducible and constitutive. Inducible IEGs exhibit low baselines, and their rapid expression is controlled by pre-existing constitutive IEGs present in quiescent or unstimulated cells (Herdegen and Leah, 1998). In addition, IEGs can be divided into transcription factors (e.g. c-*fos*, c-*jun*, *zif*268, *krox* 20) and effector proteins (*arc*, *homer* 1*a*). Transcription factors modulate the transcription of other genes, whereas effector proteins produce direct changes in the cell. Using subtractive hybridization techniques, Lanahan and Worley (1998) estimate that 30 to 40 genes constitute the total neuronal IEG response, of which 10 to 15 genes encode the transcription factors and the rest encode effector proteins.

Why these IEGs

One of the first and most widely studied IEG is c-*fos,* an activity-dependent inducible transcription factor (Herrera and Robertson, 1996). c-*fos* and its protein product c-Fos are used as markers for identifying activated cells in the central nervous system (Morgan and Curran, 1991; Kovacs, 2008). More importantly, c-Fos is a neural marker associated with neuronal plasticity and learning (Nikolaev et al., 1991; Herdegen and Leah, 1998; Tischmeyer and Grimm, 1999; Kasahara et al., 2001; Fleischmann et al., 2003). Even though these IEGs have been used widely, there remain some limitations and pitfalls (see the section "potential problems related to IEG); thus, the process of IEG visualisation has to be employed with great care (Fritschy, 2008; Kovacs, 2008).

Mechanism of c-fos and zif268 induction

The first studies suggesting that IEG expression could have a role in neuronal functioning were conducted *in vitro* on P12 cell cultures (Morgan and Curran, 1986). It has since been found that (1) neuronal depolarisation, (2) influx of calcium, (3) neurotrophic factors, and (4) neurotransmitters, all result in expression of c-*fos* (Milbrandt, 1986; Morgan and Curran, 1986; Sheng and

Greenberg, 1990; Ghosh et al., 1994; Hughes and Dragunow, 1995; Gaiddon et al., 1996). c-*fos* and zif268 are induced by multiple intracellular second messengers acting through distinct upstream regulatory elements.

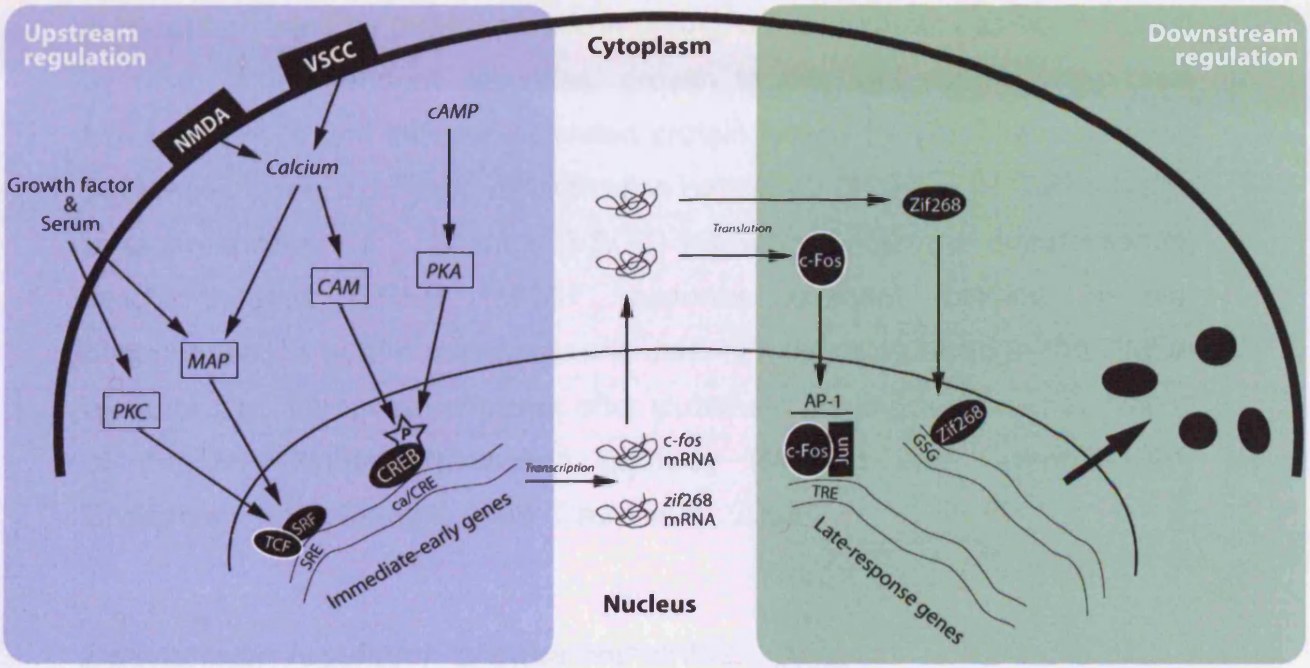

Figure 1. Schematic representation of the upstream (blue) and downstream (green) molecular pathways involved in induction of two IEGs, c-*fos* and *zif268*, in neurons (based on Chaudhuri, 1997; Kovacs, 1998). Abbreviations: AP-1, activator-protein-1; CAM, calmodulin kinase; cAMP, cyclic adenosine monophospate; CRE, cAMP response element; CREB, cAMP response element binding; GSG, promoter sequence; MAP, mitogen-activated protein kinase; NMDA, N-methyl-D-aspartic acid; PKA, protein kinase A; PKC, protein kinase C; SRE, specific sequence; SRF, transcription factor; TCF, transcription factor; TRE, promoter sequence; VSCC, voltage sensitive Ca^{2+} channels

Upstream regulation of c-fos and zif268

Increases of cyclic adenosine monophosphate (cAMP) levels in neurons result in c-*fos* and *zif*268 activation via CRE (cAMP response element) which is phosphorylated by protein kinase A (PKA). c-*fos* products can be mediated by other interdependent cascades, growth factors and serum, via protein kinase C (PKC) and mitogen-activated protein kinase (MAP). The c-*fos* gene possesses two distinct calcium activation pathways: (1) influx of Ca^{2+} through voltage sensitive Ca^{2+} channels (VSCC) following membrane depolarisation, which induces CREB (cAMP response element binding protein) phosphorylation by the calmoduline kinase, (2) signalling through the NMDA receptor Ca^{2+} ionophore complex after glutamate binding results in activation of the MAP-kinase transaction pathway (Morgan and Curran, 1991; Chaudhuri, 1997; Kovacs, 1998; Davis et al., 2003).

Downstream regulation of c-fos and zif268

The c-Fos protein is able to form heterodimeric transcription complexes with members of the Jun family, which can bind to activator-protein-1 (AP-1, Morgan and Curran, 1991). AP-1 and IEG may either stimulate or repress the candidate gene after binding to a specific promoter sequence (respectively TRE/c-Fos and GSG/Zif268, see Figure 1). The convergence of signals upon its promoter region in combination with their ability to regulate other late-response genes means that both of these IEGs are able to have a commanding influence on extra and intracellular signals in short- and long-term responses (Morgan and Curran, 1991; Chaudhuri, 1997; Davis et al., 2003).

Discrepancies between c-fos and zif268

Even though both c-*fos* and *zif*268 are induced by the same cascades, their basal expression levels are different. c-Fos has a low basal expression level,

which is due to two reasons: (1) c-*fos* mRNA is relatively unstable; (2) c-Fos protein down regulates its own transcription. Thus, c-Fos is potentially more informative when the animal has been exposed to a novel stimulus. Since Zif268 does not have the auto regulation of c-Fos, its basal expression level remains higher in many neuronal structures. This leads to the notion that *zif*268 expression is linked to ongoing synaptic activity whereas c-*fos* expression is reliant upon activity being triggered after a period of neural quiescence or after exposure to a novel stimulus (Chaudhuri, 1997). Often, studies have shown that both c-Fos and Zif268 have the same pattern of activation in same brain regions (Jenkins et al., 2004a; Albasser et al., 2007). However, previous studies have shown, for example, that certain auditory areas related to the birdsong system express Zif268, but not c-Fos (Kimpo and Doupe, 1997). Another difference is that only *zif*268 has been correlated to long term potentiation (Abraham et al., 1991, 1993).

Why use IEGs for functional mapping

To understand which brain regions are involved in different cognitive processes, such as memory formation, it is important to find the right tools. The first genes that undergo regulation of expression following cellular stimulation are the IEGs. Their induction does not require prior protein synthesis, and occurs rapidly and transiently during acquisition and early phases of consolidation of a memory trace (Tischmeyer and Grimm, 1999). An example is the use of c-Fos staining as an indicator of neuronal activity (Hunt et al., 1987; Morgan et al., 1987; Sagar et al., 1988).

c-Fos immunostaining may provide a method to map the pattern of postsynaptic stimulation within the intact nervous system with single-cell resolution. There are several advantages of using the detection of c-Fos expression. In the majority of cell types, the basal level of c-*fos* mRNA and protein expression are relatively low (Morgan and Curran, 1991; Hughes et al., 1992), although there are some cells that maintain relatively high levels of expression (Herdegen et al., 1995; Herdegen and Leah, 1998). IEGs are

widespread throughout the brain (Dragunow et al., 1987). The inducible expression of mRNA and protein products can be used as a marker of neural activity for mapping areas of the nervous system. The rapid accumulation of IEG products in activated neurons, combined with histological methods that offer detection at a cellular level, has led to their increasing use in visualising activated regions in non-human brains. IEGs have also been studied in human brain tissues in patients who were operated on for treatment of intractable seizures (Dragunow et al., 1990) and in post mortem patients after Alzheimer's disease (MacGibbon et al., 1997).

Indeed, IEG localisation can give a very high spatial resolution which makes it possible to study small brain regions (e.g. anterior thalamic nuclei), subfields of a specific region (dentate gyrus and CA fields of the hippocampus), as well as different cellular layers of the cortex (e.g. superficial and deep layers of the retrosplenial cortex). Even though new non-invasive techniques are developing, such as high field magnetic resonance imaging, their spatial resolution is not as powerful compared to IEG visualisation techniques. Thus mapping IEG expression becomes a valuable tool to understand neuroplasticity, memory formation and behaviour.

Potential problems related to IEG expression mapping

Immediate-early genes have been widely used as a neuronal marker of activity. However, this technique has some limitations, and a number of potential problems have been highlighted during the last two decades. Hughes and Dragunow (1995) showed that Fos-like immunoreactivity can be found after mechanical injury in non-nerve cells in white matter tracts (corpus callosum, fimbria-fornix), and in grey matter (the hippocampus, cortex, thalamus, striatum). It was also found that different types of neurons produce different levels of c-Fos protein following peripheral stimulation (Bullitt, 1990). Moreover, unstimulated neurons can show Fos-like immunoreactivity, indicating that this class of gene is expressed under resting physiological conditions and, therefore, cannot always be associated with learning and

memory (Morgan and Curran, 1991) – assuming that the latter requires changes in neuronal activity. The converse situation can also occur i.e. neuronal activity but no c-Fos upregulation. Consistent with the findings of Hunt et al. (1987), Bullitt (1990) found no IEG immunolabelling in either motor neurons or in the dorsal column nuclei following peripheral stimulation. These results indicate that although the presence of neuronal labelling may be interpreted as indicative of neuronal activation, the absence of such labelling cannot be used to exclude the possibility of neuronal excitation (Kovacs, 2008).

Another problem concerns the design of the IEG experiment. First, it is known that IEGs can be induced by a wide range of factors such as stress (Hughes and Dragunow, 1995; Herrera and Robertson, 1996; Tischmeyer and Grimm, 1999). Even different types of handling (rough vs. gentle) associated with saline injections can give opposite effects on basal Fos levels (Asanuma and Ogawa, 1994). Therefore, stress before sacrifice should be avoided, as basal levels of brain activity may be influenced by the past history, from 1 to 12 h prior to the experiment (Dragunow and Faull, 1989). A further issue noted by Chaudhuri (1997) is that neurons stained for an IEG product cannot be distinguished under conditions where multiple stimuli are applied. For example, if auditory and visual stimuli are used simultaneously, no conclusion can be made whether the IEG changes are induced by auditory or visual stimuli. Another shortcoming is that in certain regions such as the mammillary bodies or substantia nigra (personal findings, Dragunow and Faull, 1989) neurons cannot safely be visualised by Fos imaging as the count levels are typically so low i.e. there are problems with floor effects. Finally, drugs, such as ketamine can interfere with Fos induction (Dragunow and Faull, 1989).

IEG protein imaging versus RNA imaging (in situ hybridisation)

IEGs have been used to indicate specific cellular activation including the identification of neurons activated by various internal and external stimuli. IEG' products can be detected using two techniques. The IEG mRNA,

localised in the cytoplasm, can be revealed by *in situ* hybridisation whereas the protein, localised in the nucleus, can be visualised using immunohistochemical techniques. mRNA expression of c-*fos* reaches peak levels 30 minutes after the stimuli, whereas protein expression lags behind. By 90 minutes after the onset of the stimulation, the situation is reversed with now a peak of protein expression whereas mRNA expression is back to baseline (Bisler et al., 2002; Zangenehpour and Chaudhuri, 2002). Due to its short half-life, mRNA yields a high signal-to-noise ratio (Guzowski, 2002). One shortcoming of mRNA and protein visualisation is, therefore, that they have a poor temporal resolution. As mentioned before, the kinetics of the c-Fos (or the mRNA) response to acute stimuli is transient, with a specific peak-time point occurring 90 minutes (or 30 minutes for the mRNA) after the event. Therefore, any behavioural procedure used to stimulate c-Fos must be really precise to ensure that the measure of c-*fos* activity can realistically be related to the studied event. For example, the task used must be sensitive enough to activate c-*fos* expression (can increase number of stimuli, or length of the task). Since it is know that IEGs can be activated by numerous conditions (e.g. light), it is important to limit activation (background noise) that is not part of the target task itself (e.g. transport of the animals to the test room). That is why placing the animals in a quiet, dark, environment 30 minutes before and 90 minutes after stimulation should attenuate background noise (Dragunow and Faull, 1989). Because it is known that a new environment (Vann et al., 2000c) is enough to stimulate IEGs, the animals have to be habituated, for several days, to the dark, quiet room used before the experiment.

One shortcoming of *in situ* hybridisation, because it reveals the mRNA, not the protein, is that it gives a more indirect measure of activity following the stimuli; the immunohistochemistry technique localises the actual protein in activated neurons. Moreover, it is the protein, not the mRNA, which regulates the late-response genes (Chaudhuri, 1997).

IEG imaging versus 2-deoxyglucose

Autoradiography of 2-deoxyglucose levels provides a measure of glucose utilisation throughout the cell that can be used for mapping of local functional activity in the central nervous system (Sokoloff et al., 1977; Sokoloff, 1981). This technique seems to be more sensitive to alterations in functional activity in the neuropil compared to the nucleus (Schwartz et al., 1979). Both 2-deoxyglucose and IEG immunohistochemistry methods have been used to measure regional metabolic activity and map functional activity. However, discrepancies have been found between the two approaches. For example, *fos* induction can occur even when deoxyglucose uptake is unchanged or reduced (Sagar et al., 1988).

The 2-deoxyglucose approach cannot distinguish between altered glucose metabolism of neurons intrinsic to a brain region from that of terminals of afferent fibres (Sagar et al., 1988). Moreover, it is still unclear whether it occurs in neurons and/or glial cells and whether it occurs at the presynaptic or postsynaptic level (Sharp et al., 1993). With the 2-deoxyglucose technique, it is also difficult to identify the source of the increased glucose metabolism. Since immunohistochemistry stains activated cells, it allows the identification of specific neurons by adding specific morphological feature analyses (e.g. size of cells).

Application of IEGs to research

The interest in IEGs as a functional tool keeps growing. There are 17827 citations listed in PubMed with the search term "c-*fos*". IEGs have been widely used as a reliable marker for identifying activated cells and nervous central system circuits. It has been found that IEGs can respond to various stimuli (Morgan and Curran, 1991), such as physiological (sleep/wake cycle, Novak et al., 2000), environmental (light, noise, Campeau and Watson, 1997), pharmacological (Curran et al., 1996), and many stress challenges (Kovacs, 2008). More importantly, IEGs have been associated with learning and

memory (Nikolaev et al., 1991; Herdegen and Leah, 1998; Tischmeyer and Grimm, 1999; Kasahara et al., 2001; Fleischmann et al., 2003). Application of IEGs to research is very varied, but the next part will just focus on the relevance of c-*fos* expression in neuroplasticity, memory, behaviour and lesion studies.

Neuroplasticity and c-fos

Neuroplasticity refers to the changes that occur in the organisation of the brain as a result of experience. Neuroplasticity and memory consolidation are thought to rely on long-lasting, activity dependent modifications of synaptic strength and remodelling of neural network connectivity. That is why artificially induced long-term plasticity can be used as a model to study activity-dependent plasticity that may underlie learning and memory. Long-term potentiation (LTP) refers to an increased efficacy of synaptic transmission evoked by high frequency electrical stimulation of afferents of the hippocampus, whereas long-term depression (LTD) results are a persistent weak synaptic stimulation. The term long-term comes from the fact that this increase (potentiation) or decrease (depression) in synaptic strength lasts a very long time compared to other processes that affect synaptic strength. LTP or LTD occurs depending on the timing and frequency of the input. One of the first such studies showed that brief episodes of tetanic activation of the perforant path input to the dentate gyrus result in a persistent increase (LTP), in the synaptic efficacy of this monosynaptic excitatory pathway (Bliss and Lomo, 1973). Since then, both LTP and LTD have been widely used to model long-term plasticity (Cotman et al., 1988; Collingridge et al., 1991; Dudek and Bear, 1992; Malenka and Bear, 2004).

It has been established that there is at least an early and late phase of LTP, which rely on different cellular and molecular mechanisms. The early phase is under the control of second messengers and kinases (Bliss and Collingridge, 1993), whereas the mechanisms underlying the late phase of long-term plasticity are believed to rely on *de novo* protein synthesis, but not on mRNA

synthesis (Otani et al., 1989; Manahan-Vaughan et al., 2000). Indeed, blocking the translation but not the transcription prevents LTD (that persisted for more than 8h). Furthermore, the protein synthesis concerned appears to be performed using existing mRNA (Manahan-Vaughan et al., 2000). Therefore, it is likely that LTP and LTD are associated with IEG activity. Although it has been shown that stimuli that trigger LTP will also induce c-*fos* expression, they are not strongly correlated, as LTP can occur without the induction of IEGs. Indeed, high frequency stimulation of granule cells in the dentate gyrus induces c-*fos* expression, but at lower stimulation levels, that still evoke LTP, no induction of c-*fos* expression was found in anaesthetised animals (Douglas et al., 1988). However, in unanaesthetised rats, high-frequency stimulation of the perforant path was sufficient to produce LTP and to induce c-*fos* expression. But again the degree of LTP induction did not correlate with the degree of c-*fos* induction (Dragunow et al., 1989). Agents that interfered with the production of LTP (e.g. NMDA antagonists) also prevented c-fos induction (Dragunow et al., 1989). Similarly, sodium pentobarbital, which blocks the induction of Fos expression, also blocked a long-duration form of LTP (Jeffery et al., 1990). Finally, high frequency stimulation leading to the establishment of LTP provokes elevated expression of c-*fos* (Nikolaev et al., 1991). Thus, while there is often an association between c-*fos* and LTP, this relationship is unlikely to be directly causal.

Interestingly, for *zif*268, a clearer correlation is found between its upregulation and the persistence of LTP, but not the magnitude of induction (Abraham et al., 1993). Given that c-*fos* shows no or unreliable upregulation with tetanising stimuli to induce LTP, it is suggested that *zif*268 may play a critical role in the stabilisation of the later phases of the maintenance of LTP (Abraham et al., 1991; Abraham et al., 1993; Davis et al., 2003).

An intriguing hypothesis for the role of IEGs in memory consolidation (a protein-synthesis-dependent process of memory stabilisation) has been proposed by Clayton (2000). She described the activation of IEGs to function in a similar way as a physiological action potential, and referred to it as the "genomic action potential". Its functions would be to integrate the effects of

multiple stimuli on individual neurons within a circuit. Clayton (2000) suggested that rather than the IEGs playing a role in a linear sequence of events leading to the consolidation or long-term storage of memories, they act as a "memory rheostat" preparing the cell to consolidate incoming information within their defined temporal windows of activation. A recent review of Abraham (2008) highlights the importance of protein synthesis in metaplasticity. He points out an additional role of protein synthesis (different to memory consolidation), where protein synthesis can also raise the threshold for reversing plasticity as a metaplasticity mechanism. Metaplasticity refers to the plasticity of the synaptic plasticity where synapse's previous history of activity can determine its current plasticity.

Memory, behaviour and c-fos

In normal animals

As discussed before, memory can be studied at the synaptic level by examining neuroplasticity. Nevertheless, in order to understand what causes these changes, it becomes essential to find a way to assess memory at a system level. Brain imaging can help to get a better understanding of the role of different brain regions in a specific type of memory. In humans, behavioural experiments are now often combined with imaging techniques, such as functional magnetic resonance imaging (fMRI) to map brain activity. Similar techniques can be also used in animals. However, even though advances in imagery are growing constantly, fMRI resolution remains relatively low to map brain activity in small animals such as rodents. In addition, although one main advantage of the fMRI is that it is non-invasive, this technique becomes problematic for studying freely moving rats. That is why the use of cellular imaging, such as IEG imaging as a marker of neural activity, remains a highly informative approach and a better tool to map brain activity in rodents. Normal animals can be studied; they can move freely while they are performing the behavioural task. This technique is not invasive during the behavioural test and, therefore, has no impact on the behaviour proper. Indeed, the

immunohistochemistry procedure often starts 90 minutes after the animal has performed the task. Finally, the spatial resolution is much higher with immunohistochemistry compared to fMRI, though the temporal resolution is poor.

IEGs have been widely used to uncover the selective role of brain regions in different behavioural tasks. These tasks include a large range of memory functions (Tischmeyer and Grimm, 1999), such as odour or auditory discriminations (Hess et al., 1995a; Zuschratter et al., 1995), and active avoidance brightness discriminations (Tischmeyer et al., 1990; Nikolaev et al., 1992). However, a problem is raised with the latter task, as it incorporates an aversive stimulus component. Indeed stress brought about as a result of aversive stimuli has been shown to be sufficient to induce IEG expression (Kovacs, 1998). This highlights the fact that IEG studies associated with behaviour must be carefully designed with appropriate control conditions.

Two different basic approaches have been used to study IEGs: (1) parametric progression that is correlated with degree of activity, and (2) subtraction of active versus control conditions. The first approach is used to compare activity of brain regions in groups that differ in the level of training. Guzowski and colleagues (2006) compared *arc* mRNA after a single novel exposure, daily sessions (repeated over 9 days) or repeated exposure within a day. It was found that *arc* activity dramatically decreased in the CA1 field of the hippocampus after short but repeated exposures within a day compared to novel or spaced exposure, despite a stable electrophysiological activity during all sessions. These results suggest that *arc* transcription is not just linked to habituation and novelty. This state dependence of neuronal transcriptional coupling provides a mechanism of metaplasticity and may regulate the capacity for synaptic modification in neural networks (Guzowski et al., 2006). Porte and colleagues (2008) also looked at the effect of extended levels of training (from one to nine days) in a spatial reference memory task. They found that hippocampal activity increased with extended training. In a recent study, animals were trained in a radial-arm maze task. Two different groups were trained with "early" (two sessions) or "late" (five sessions) learning

(Poirier et al., 2008). Even though no overall differences in the number of Zif268-positive cells were found between the groups, a correlation was found between the performance and the *zif*268 activity of the dentate gyrus in the "early" training but not in the "late" one. In contrast, correlations between the performance and the CA fields were found in the "late" group but not in the "early" group.

The second approach (subtraction) compares the difference in IEG levels between an experimental group and a control group. For this approach, it is extremely important to match as well as possible the behaviour of the different groups used in the experiment. Quite often the major difficulty of the experiment remains in finding the right control for the appropriate experiment (Shires and Aggleton, 2008). That is why the matching between experimental and control groups becomes crucial in order to fully understand the role of IEGs in the task proper. Several examples of the subtracted approach in different behavioural tasks will be presented in the next paragraphs, which highlight the importance of having a well-matched control group.

A good example was the studies designed by Vann and colleagues (Vann et al., 2000a; Vann et al., 2000c), in which they examined c-Fos levels in the brains of rats following a spatial working memory task in a radial arm maze. The experimental group was trained on a series of radial maze trials within a single session, whereas the control group was "yoked". They received the same amount of rewards and visited the same number of arms as the experimental group. The difference was that the control group could only run up and down one arm, so there were no specific memory requirements. This same spatial task has been shown to be highly sensitive to damage in the hippocampal system (Olton et al., 1979). Consistent with these lesion findings, the IEG study showed that the radial-arm maze spatial working memory task involved activation of the hippocampus, as well as the subiculum and entorhinal cortex (Vann et al., 2000c). Different aspects of spatial memory combined to IEG imaging were also investigated to understand the role of the temporal lobe in the Morris water task (Jenkins et al., 2003), and in a variant of the radial arm maze task (Poirier et al., 2008).

Another study that used the Morris water maze helped to reveal the critical importance of control conditions (Shires and Aggleton, 2008). This study compared an experimental group trained on a spatial working memory task with several control groups: home cage control, swimming-free and a new control group (procedural task), which made it possible for the first time to match swim time, swim distance and escape learning with the experimental group (working memory). Comparison of the experimental group with the home cage and free-swimming controls revealed an overall increase of brain region activity in the working memory group. However, comparison between the experimental group and the procedural control only revealed a regional-specific increase of IEGs in the prefrontal cortex of the working memory group (i.e. no difference in sites such as the hippocampus).

As shown previously, IEG imaging reveals brain areas that are activated by specific mnemonic functions. This mapping provides counts of IEG-positive cells activated in different regions. It is known that brain regions are not just working as single elements. Therefore, getting more information about relationships between those structures becomes essential. Structural equation modelling (SEM) makes it possible to determine inter-relationships between the different regions. SEM is a statistical technique for testing and estimating causal relationships using a combination of statistical data (raw counts) and qualitative causal assumptions, which in this case are based on neuroanatomy. For example, different patterns across the parahippocampal regions and the hippocampus were found in two water maze tasks. In the allocentric place task, an association between activity in the entorhinal cortices and the hippocampus was found, whereas in the non-allocentric landmark task this relationship was replaced by an association from the entorhinal cortices to the subiculum (Jenkins et al., 2003). SEM technique will be used in Chapter 5, in a study assessing brain region activity involved in a new object recognition paradigm.

Recognition memory is another form of memory that has been much studied with IEG. First, it has been shown that exposure to a novel environment was

enough to activate c-Fos immunoreactivity in certain brain regions. Placing an animal once in a new room (Vann et al., 2000c) or in a new apparatus (Hess et al., 1995b), or repeatedly in an open field, each in a novel environment (Wirtshafter, 2005), all resulted in an increase of c-Fos expression levels in the hippocampus. Second, c-Fos expression has been studied after exposure of novel individual visual stimuli. Animals were exposed to novel or familiar objects briefly displayed behind a mirror system. Presentation of novel objects increased c-Fos counts in perirhinal cortex and area Te2 in the group seeing only novel objects compared to the group seeing just familiar objects (Zhu et al., 1996; Wan et al., 1999).

A methodology specifically designed to examine recognition memory is the "paired-viewing task" (Figure 2, Zhu et al., 1996). In this task, single different stimuli (novel or familiar pictures, figure 3A) are shown to the left and right visual field but are being initially processed in the opposite hemisphere of the rat brain. In the optic chiasm, the nerves connected to the right eye that attend to the right temporal visual field cross to the left hemisphere of the brain, while the nerves from the left eye that attend to the left temporal visual field cross to the right half of the brain. By simultaneously presenting novel pictures to one eye and familiar pictures to the other one, it is feasible to compare brain region activity within an animal, by comparing c-Fos levels between its two hemispheres. Increase of activity in the perirhinal cortex and area Te2, but not in the hippocampus was induced in the hemisphere opposite to where the novel visual stimuli were presented (Zhu et al., 1996; Wan et al., 1999).

Using the same procedure, Wan et al. (1999) looked as well at c-*fos* activation following exposure to familiar stimuli set in a novel arrangement. They found that the regions of the rat brain associated with presenting novel or familiar individual items differed from those responding to a spatial array of items (figure 3B). Indeed, with spatial rearrangements of familiar visual stimuli c-*fos* activity was induced in the hippocampus, but not in the perirhinal cortex (Wan et al., 1999; Aggleton and Brown, 2005). Moreover, the same pattern of activation (activity changes in the hippocampus, but not in the perirhinal

cortex) was found in another study looking at rearrangements of visual stimuli around a radial-arm maze (Jenkins et al., 2004b).

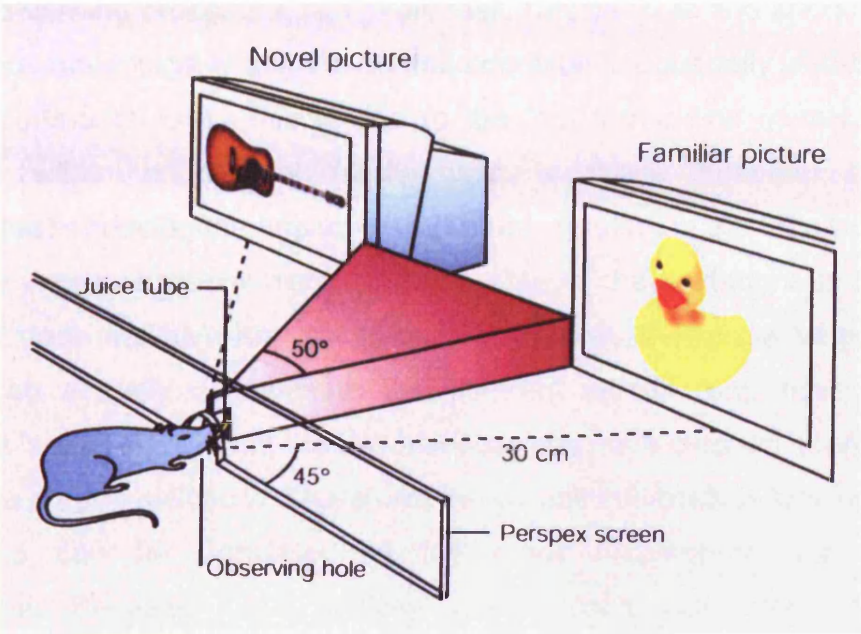

Figure 2. The paired-viewing procedure for simultaneously presenting novel and familiar stimuli. A rat views two pictures simultaneously, one novel and the other seen many times previously, while its head is in a hole in a Perspex screen. A central partition ensures that each picture is seen by only one eye and is initially processed by the opposite cerebral hemisphere. In this way, novel and familiar stimuli can be shown under the same conditions of alertness and motivation, and with similar eye movements (Zhu et al., 1996).

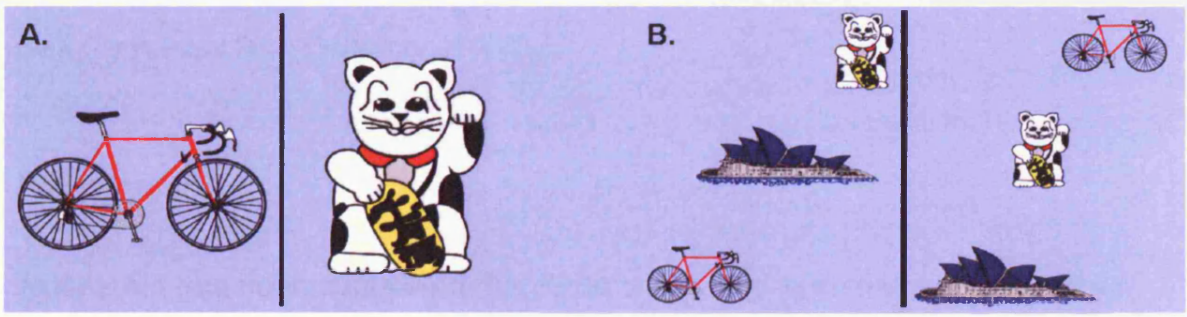

Figure 3. A. Different stimuli used for the paired-viewing procedure. For the single stimuli, one familiar (left) and one novel (right) image were presented. **B.** Example of stimuli used in spatial configuration task. Rats are repeatedly exposed to specific stimuli in fixed spatial arrangements (left), but on the test

day one eye is presented with novel spatial arrangements of the same individual stimuli (right).

The paired-viewing procedure, like every task, has benefits and shortcomings. One obvious advantage is that the control condition is unusually well-matched to the experimental one. This is due to the fact that c-Fos counts can be compared within an animal (comparison is made between the two hemispheres), reducing the impact of individual variation in the rat's behaviour and in the immunohistochemistry process. One of the limitations is that this procedure does not give any behavioural measures that show whether the animals can actually discriminate the different stimuli (e.g. novel versus familiar). It is also known that the two hemispheres have crossed connections, e.g. via the corpus callosum. Therefore, the stimuli information arriving in one hemisphere can be translated to the other hemisphere via crossed connections. Because brain activity comparisons are made between hemispheres, any null results become difficult to interpret. Indeed, these null results could be due to the fact that the region of interest is not involved in the mnemonic demands of the experiment or that there is a transfer of information from one hemisphere to the other. For this reason, as presented in Chapter 5 of this thesis, I designed a new procedure where active behavioural discrimination of the rats can be measured and where c-Fos mapping can be evaluated in an object recognition task. This new bow-tie maze combines features of the delayed nonmatching-to-sample task (Mishkin and Delacour, 1975; Aggleton, 1985; Mumby et al., 1990) with the spontaneous exploration task (Ennaceur and Delacour, 1988).

Knockout mice

Although it has been suggested that IEGs play a role in memory, it is not clear whether IEGs are necessary for memory formation. To address this question, one approach is to knockout a specific gene and to assess its effect on the animal's performance on a specific memory test. A study using *zif*268 mutant mice (Jones et al., 2001) revealed that the transgenic animals have no deficit in spatial working memory (spontaneous alternation in a T-maze), whereas

their longer term memory was impaired (social transmission of food, object recognition, and spatial memory in the Morris water maze). This temporal discrepancy between shorter (e.g. typical working memory task) and longer term memory is relevant as in many working memory tasks the retention interval being tested is much less than 90 min expression time – the time when protein production is at its peak. This temporal mismatch may explain why the knockout mice were not impaired in the shorter working memory task. Another study using mice lacking c-*fos* in the central system nervous system, demonstrated that the transgenic mice showed normal general motor behaviour e.g. locomotor activity and rotarod task, as well as affective behaviours e.g. anxiety in the light/dark box. However, these same animals were specifically impaired in spatial (the Morris water maze) and associative (contextual conditioning) hippocampal-dependent tasks (Fleischmann et al., 2003). A general caveat with this gene manipulation approach is that the results of knocking out a gene can be difficult to interpret because of molecular compensation and developmental defects (unless it is possible to use a site-specific mutant under a controlled 'on' and 'off' signal).

Using antisense

Another approach to understanding the role of IEGs in memory formation is to determine whether blocking IEG protein production can have an impact on the behavioural performance of the animal. Antisense oligonucleotides are a complementary sequence to a specific mRNA. By its binding, normal mRNA expression is inhibited, and thus induces a blockade of the protein synthesis. The translation stage is blocked and the transfer of genetic information from DNA to protein is prevented (Dias and Stein, 2002). The antisense oligonucleotides can be injected into a specific region of the rat brain where its effect is local and temporary. Many studies have investigated the consequences of different antisenses and showed with this approach the importance of IEG for memory. Animals receiving a c-Fos antisense injection in the CA1 region of the dorsal hippocampus were impaired in retention but not acquisition of a shock-motivated brightness discrimination task (Grimm et

al., 1997). Microinjections of c-Fos antisense in the CA3 region of the hippocampus impaired spatial memory in rats (reference and working memory) in the radial-arm maze (He et al., 2002). Similar experiments using *arc* or *zif*268 have confirmed the importance of the role of IEGs in memory consolidation (for review see Guzowski, 2002). In object recognition, antisense infusion blocking c-Fos expression in the perirhinal cortex showed that animals were not able to discriminate novelty from familiarity with intervals of 3h and 24h and found deficits at 3h and 24h when infusions were made 1h before the sample phase (Seoane and Brown, 2007). In conclusion, c-*fos* activity is a critical element of effective, stable memory in rats.

Lesion studies and c-fos

A recent further application of IEGs to research is to combine IEG imaging with lesion studies. The traditional lesion method has been extensively utilized and has proved to be very productive for understanding the roles of many brain structures. However, there exist some inherent limitations of this approach. The principle is to lesion a target area and to assess its effect on the animal's behaviour. Then if a deficit is found, it is concluded that this deficit is mainly due to the missing region. Nevertheless, one dilemma is that the behaviour reflects how the rest of the intact brain functions, and hence, does not reflect directly what the lesioned region does. Consequently, mapping IEGs in this way can help to inform the repercussions of the lesion on other distal regions (see covert pathology). Examples will be given later in the introduction because chapters 2-4 focus on IEG mapping following lesions (hippocampus, mammillothalamic tract and fornix), with a particular interest in retrosplenial cortex activity. Therefore, an introduction to the brain regions that are involved in memory and especially the retrosplenial cortex (its neuroanatomy and function) will be presented in the next sections.

The role of the retrosplenial cortex in memory

One of the main goals in neuroscience is to understand the mechanisms necessary for learning and memory. Great progress has been made to characterise the role of specific brain regions in memory functions. Over fifty years ago, a patient study revealed the importance of the medial temporal lobe (Scoville and Milner, 1957). The patient, H.M., was suffering from epilepsy. His seizures were uncontrollable even by maximum medication doses. For medical reasons, it was decided to remove parts of his temporal lobe as a treatment. This bilateral medial temporal lobe (MTL) resection was followed by a striking and unpredicted loss of recent memory. In this same study, eight other cases suffering from schizophrenia, who had also failed to respond to other forms of treatment, underwent the same procedure. Persistent memory impairments were found when the bilateral medial temporal lobe removal damaged appreciable portions of the hippocampus (Scoville and Milner, 1957). Since then, myriad studies have helped to confirm that damage to the MTL can cause permanent memory deficits.

The structures defined as being part of the MTL comprise the hippocampal formation, the entorhinal cortex, the perirhinal cortex and the parahippocampal cortex. Studies of amnesia in humans and animals have confirmed the important role of MTL structures for memory. More specifically these MTL structures have been defined as being critical for declarative (explicit) memory (Squire and Zola-Morgan, 1991). Anterograde amnesia is a loss of memory for what happened after the event that caused the amnesia. Symptoms of anterograde amnesia highlight specific memory dysfunctions, characterised by severe and permanent deficits in the recollection of recent events, as well as poorer recognition memory. In contrast, short term memory, IQ, semantic memory, skill learning, priming, perceptual learning, and simple classical conditioning are often spared (Parkin, 1997). Although temporal lobe amnesia has been widely investigated, with critical attention given to the role of the hippocampus, clinical descriptions of amnesia also relate to the effects of pathology centred in the medial diencephalon. Sergeievich Korsakoff first

described the confusion and amnesia (both retrograde and anterograde) that are associated with nutritional (thiamine) deficiency (Korsakoff, 1887). One diencephalic region that has often been implicated in this syndrome is the mammillary bodies (Victor et al., 1971; Vann and Aggleton, 2004b), but other diencephalic structures have often been implicated in anterograde amnesia. These structures include the anterior thalamic nuclei and the medial dorsal thalamic nucleus (Victor, 1987; Harding et al., 2000).

These two forms of amnesia (temporal lobe and diencephalic) share many similarities. Indeed, Delay and Brion (1969) proposed the existence of a network in which the hippocampus, the fornix, the mammillary bodies and the anterior thalamic nuclei formed part of a relay system whereby information from the parahippocampal cortex/temporal lobe reaches the cingulate cortex. Since then, numerous neuropsychological and neuroanatomical findings support the evidence of a specific role of some form of "extended hippocampal memory system" (Aggleton and Saunders, 1997; Gaffan and Hornak, 1997; Aggleton and Brown, 1999; Aggleton, 2008), which links the medial temporal and medial diencephalic structures.

A review by Aggleton and Brown (2006) presented a summary of the main connections (see Figure 4) between the structures (diencephalon and MTL) of this system involved in memory (and amnesia). In this schema, the fornix largely carries information from the hippocampus to the mammillary bodies, the anterior thalamic nuclei, and the medial prefrontal cortex. Patient (Gaffan and Gaffan, 1991; Aggleton et al., 2000; Tsivilis et al., 2008; Vann et al., 2008) and animal (Olton et al., 1978; Cassel et al., 1998) studies have found that bilateral fornix damage is sufficient to induce anterograde amnesia or memory impairments. Next the mammillothalamic tract sends information from the mammillary bodies to the anterior thalamic nuclei (Vann et al., 2007). A unique patient B.J. developed marked memory impairments following an accident with a snooker cue that bilaterally damaged his mammillary bodies (Dusoir et al., 1990). Animal studies have helped to confirm the importance for memory of the mammillary bodies (Vann and Aggleton, 2003) and the anterior thalamic nuclei (Aggleton et al., 1996; Byatt and Dalrymple-Alford, 1996).

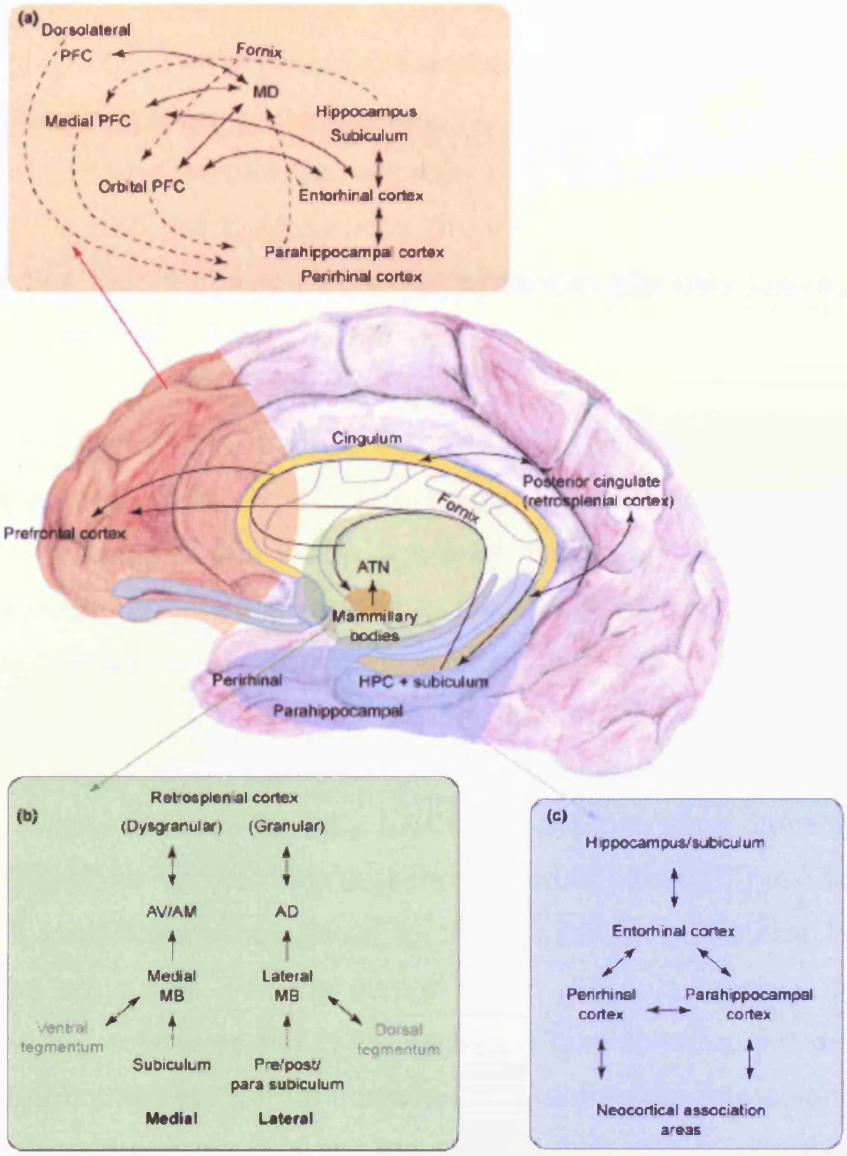

Figure 4. Schematic drawing of some of the main connections between the brain regions that underlie episodic memory. (a) The principal connections between the prefrontal cortex and the medial temporal lobe are shown in more detail. (b) The parallel components of the extended hippocampal system, which anatomically form medial and lateral subsystems. (c) The main links between the parahippocampal region and the hippocampus. Abbreviations: AD, anterior dorsal thalamic nucleus; AM, anterior medial thalamic nucleus; ATN, anterior thalamic nuclei; AV, anterior ventral thalamic nucleus; cingulum, cingulum bundle; HPC, hippocampus; MB, mammillary bodies; MD, medial dorsal thalamic nucleus; PFC, prefrontal cortex (taken from Aggleton and Brown, 2006)

Finally the anterior thalamic nuclei project back to the hippocampus, directly via the cingulum bundle (Mufson and Pandya, 1984), or indirectly through the retrosplenial cortex (part of the posterior cingulate cortex in humans). The retrosplenial cortex shares dense reciprocal connections with both the anterior thalamic nuclei and the hippocampus (from CA1 and from the subiculum). Human studies reveal that retrosplenial cortex damage may cause amnesia (Valenstein et al., 1987; Maguire, 2001a).

Lesion studies have often been used in animals to understand the role of specific structures. In such studies, damage to a single target region is assessed. A variant of this lesion approach has been used to understand specific connections between regions in the extended hippocampal memory system. The concept of a disconnection study is to test whether two regions work together. Cross-disconnection studies involve unilateral lesions in two brain structures, but in opposite hemispheres. So if the two regions are part of the same serial network with only few crossed projections, then lesions in these two regions in contralateral hemispheres should provide similar behavioural impairments compared to those seen with bilateral lesions of either of the structures. For the control group, animals received the same lesion of the two structures but in the ipsilateral hemispheres. Sutherland and Hoesing (1993) showed that the connections between the retrosplenial cortex and the hippocampus, as well as the retrosplenial cortex with the anterior thalamic nuclei, are important for spatial memory. Thus, animals with contralateral lesions were more impaired in acquisition of a water maze task compared to animals with both lesions in the same hemisphere. Another study showed that disconnection of the anterior thalamic nuclei from their hippocampal inputs (contralateral lesions of the anterior thalamic nuclei and the fornix) produced impairments in memory tasks, such as T-maze alternation and object-in-place learning (Warburton et al., 2000). One more example of a disconnection study tested whether the anterior thalamic nuclei and the hippocampus form components of the same network. Animals with lesions made in contralateral hemispheres were significantly more impaired than animals with ipsilateral lesions when tested on T-maze alternation, radial-arm maze and Morris water maze (Warburton et al., 2001).

In the next sections, the retrosplenial cortex will be described in more detail because one of my main focuses in my thesis is the role of the retrosplenial cortex in this extended hippocampal memory system.

The neuroanatomy of the retrosplenial cortex

Subdivisions within the retrosplenial cortex

In primates, the retrosplenial cortex comprises area 29 and 30. These areas with the addition of area 23 and 31 form the posterior cingulate region. In rats, there are no areas 23, 30 and 31. Thus in rodents, but not in primates, the terms retrosplenial cortex and posterior cingulate cortex refer to the same region (Vogt, 1993). The retrosplenial cortex (area 29) in the rat occupies an extensive portion of cortex posterior to the anterior cingulate. The retrosplenial cortex is situated in the medial surface of the hemispheres and extends rostrocaudally from the fornix to almost the caudal limit of the cerebral cortex. The retrosplenial cortex is located both physically and connectionally between the hippocampal formation and the neocortex. The retrosplenial cortex is divided into two main parts (Figure 5): granular and dysgranular (Rdg). The retrosplenial granular cortex is further subdivided into granular b (Rgb) and granular a (Rga) sub-regions. The terms granular and dysgranular refers respectively to the presence or the absence of distinct granular layer.

Lateral to Rdg, the retrosplenial cortex is bordered rostrally next to the motor cortex, caudally next to the visual cortex (area 18b). Ventral to Rga, is located the postsubiculum. The border between Rdg and Rgb is characterised by; (1) wider layers II-III compared to Rgb, accompanied by a reduction in cell packing density, and (2) a wider layer IV and larger cell bodies of the neurons in layer V of Rdg (see Figure 5). The separation of Rgb and Rga can be delimited by; (1) a wider layer II and the presence of smaller cells in Rgb, and (2) a thinner layer III and the presence of pyramid body cells that are more randomly spaced in Rga (Vogt and Peters, 1981).

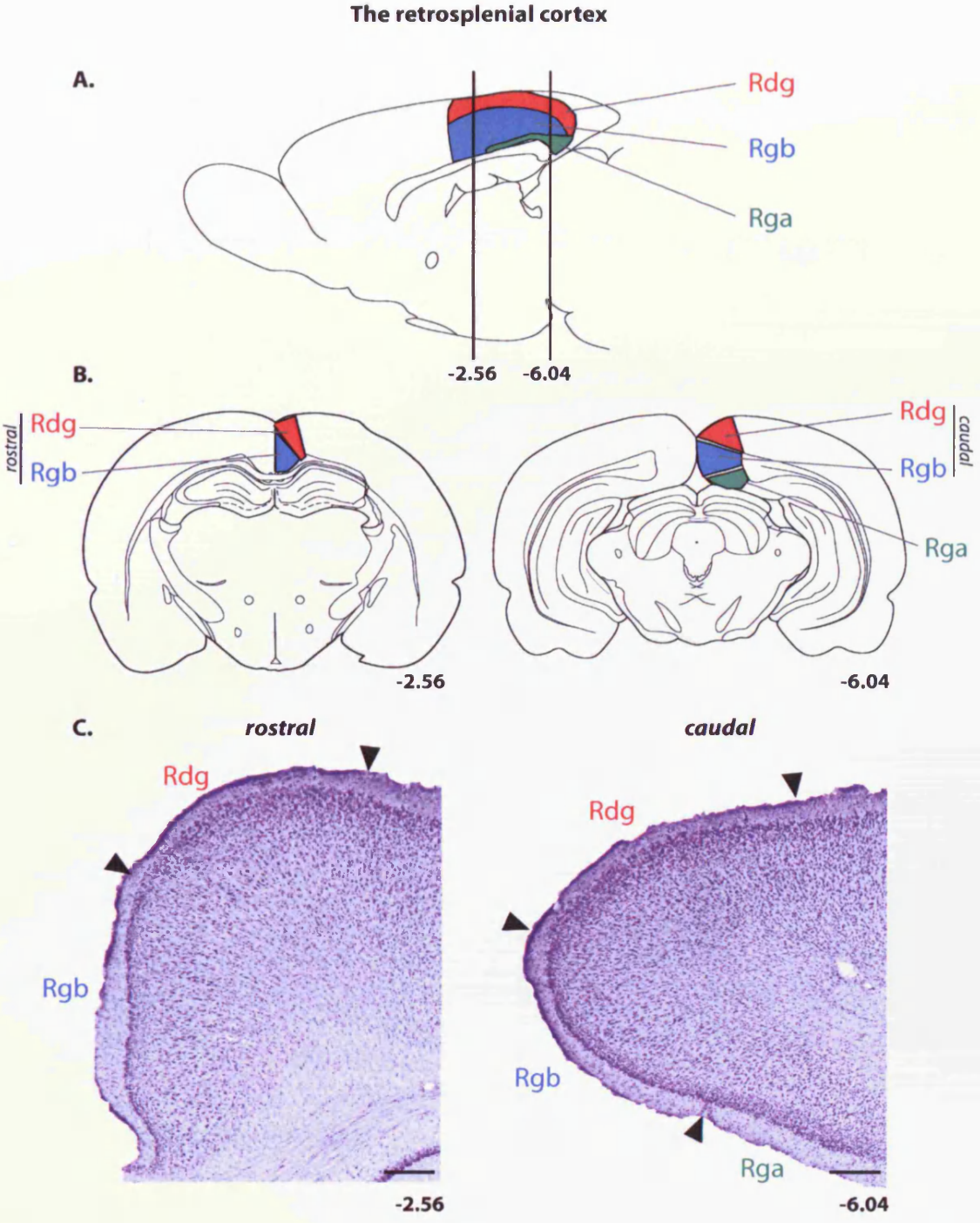

Figure 5. A. The inset depicts a sagital section of the rat brain illustrating the retrosplenial cortex at two rostral-caudal levels. **B.** The coronal sections show the location of the retrosplenial cortex sub-regions. **C.** Coronal sections showing the borders of the retrosplenial cortex sub-regions. The numbers refer to the distance (mm) from Bregma according to the atlas of Paxinos & Watson (1997). Abbreviations: Rdg, retrosplenial dysgranular cortex; Rgb, retrosplenial granular b cortex; Rga, retrosplenial granular a cortex.

The combinations of anterograde and retrograde tracing techniques facilitate precise characterisations of the origin and termination of projections. The next paragraphs will present the main cortical and subcortical connections of the retrosplenial cortex.

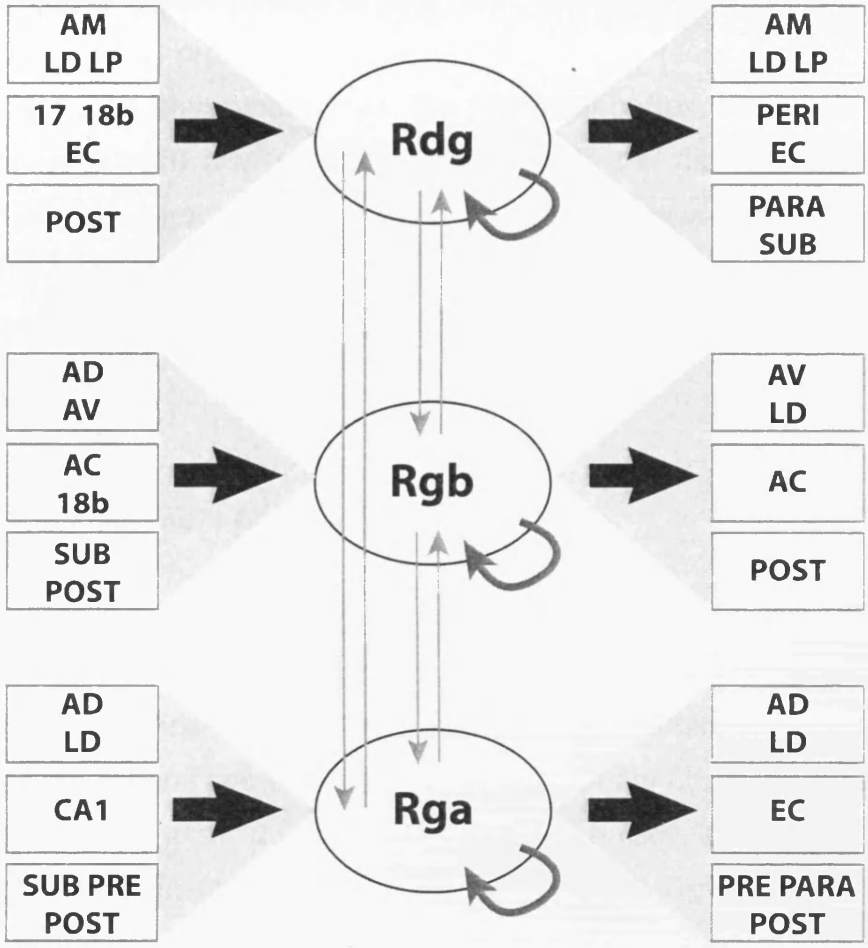

Figure 6. Schematic summary of the main connections of Rdg, Rgb and Rga. Abbreviations: AC, anterior cingulate cortex; AD, anterodorsal nucleus of the thalamus; AM, anteromedial nucleus of the thalamus; AV, anteroventral nucleus of the thalamus; EC, entorhinal cortex; LD, laterodorsal nucleus of the thalamus; LP, lateroposterior nucleus of the thalamus; PARA, parasubiculum; PERI, perirhinal cortex; PRE, presubiculum; POST, postsubiculum; Rdg, retrosplenial dysgranular cortex; Rgb, retrosplenial granular b cortex; Rga, retrosplenial granular a cortex; SUB, subiculum (based on Van Groen and Wyss, 1990c, 1992, 2003; Shibata et al., 2009).

Afferents and efferents of Rdg

Retrograde tracers revealed projections from the three sub-regions (Rdg, Rgb, Rga) of the retrosplenial cortex (see Figure 6). Rdg receives projections from the anteromedial, laterodorsal and lateroposterior nucleus of the thalamus, visual region (areas 17 and 18b), the entorhinal cortex, and the postsubiculum. Rdg projects to other parts of the retrosplenial cortex (only lightly to Rga), the entorhinal cortex, the perirhinal cortex, the parasubiculum and postsubiculum. It also projects ipsilaterally to the caudate nucleus, the laterodorsal and lateroposterior nuclei of the thalamus; bilaterally to the anterior thalamic nuclei. Only neurons in caudal Rdg connect to the visual areas (Van Groen and Wyss, 1990a, 1992; Wyss and Van Groen, 1992; Van Groen et al., 1993).

Afferents and efferents of Rgb

The main cortical afferents of Rgb arise from other parts of the retrosplenial cortex, the anterior cingulate cortex, area 18b as well as the ventral subiculum; the dorsal subiculum and the postsubiculum (Figure 6). Subcortical projections come from a few neurons of the CA1 field of the dorsal hippocampus and from the anterior thalamic nuclei, but only from the anterodorsal and anteroventral nuclei. Efferents of Rgb target the three subdivisions of the retrosplenial cortex, the anterior cingulate cortex, the entorhinal cortex, the anteroventral and laterodorsal nuclei of the thalamus, and the postsubiculum (Van Groen and Wyss, 1990a; Wyss and Van Groen, 1992; Van Groen et al., 1993; Van Groen and Wyss, 2003).

Afferents and efferents of Rga

Subcortical afferents to Rga originate in the anterodorsal and laterodorsal nuclei of the thalamus (Figure 6). Cortical projections to Rga come from the retrosplenial cortex, the subiculum, the presubiculum and postsubiculum. There is also, as for Rgb, a small input from the CA1 field of the dorsal

hippocampus. Rga projects to the retrosplenial cortex, the entorhinal cortex, the anterodorsal and laterodorsal nuclei of the thalamus, the presubiculum, the parasubiculum and the postsubiculum (Van Groen and Wyss, 1990c, a; Wyss and Van Groen, 1992; Van Groen et al., 1993).

Overall

As presented above, the sub-regions of the retrosplenial cortex have different connections with other cortical and subcortical regions. However, these three sub-regions (Rdg, Rgb, Rga) are all connected to each other (see Shibata et al., 2009) and share certain common properties, e.g. reciprocal connections with the anterior thalamic nuclei and the hippocampal formation. Figure 7 presents the organisation of the intrinsic connections of the retrosplenial cortex. To summarise, transverse projections (in a coronal plan) are reciprocal, whereas longitudinal projections (in a sagittal plan) are generally from the rostral part to the caudal part of the retrosplenial cortex.

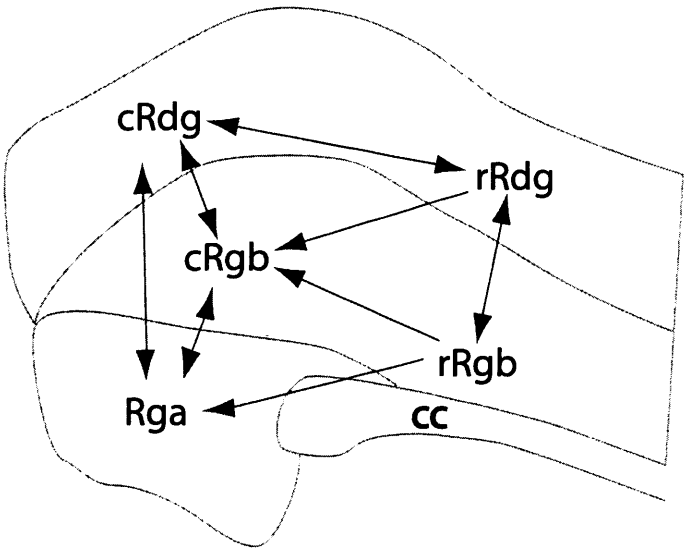

Figure 7. Schematic representation of the organisation of the intrinsic connections of the retrosplenial cortex (Shibata et al., 2009). Abbreviations: r, rostral part of the retrosplenial cortex; c, caudal part of the retrosplenial cortex; CC, Corpus Callosum; Rdg, retrosplenial dysgranular cortex; Rgb, retrosplenial granular b cortex; Rga, retrosplenial granular a cortex.

Analyses of the connections of the retrosplenial cortex highlight its central position and its role as a prominent gateway for information exchange between the hippocampal formation, thalamic nuclei and neocortical areas of the brain. The retrosplenial dysgranular cortex may be particularly important for processing visual spatial cues, while the connection of the retrosplenial granular cortex (Rgb and Rga) could suggest that it is particularly involved with navigation based on internal cues.

The retrosplenial cortex functions

In humans

Positron emission tomography (PET) and other imaging techniques (e.g. fMRI) have made considerable progress in understanding and investigating the role of the retrosplenial cortex in memory processes. First, the retrosplenial cortex has been widely associated with spatial memory. Indeed, it has been discovered that the retrosplenial cortex is activated by most navigation tasks (Maguire, 2001a; Epstein and Higgins, 2007; Iaria et al., 2007). Functional imaging studies have also pointed to an involvement of the retrosplenial cortex in a range of varied memory tasks, such as novel image detection (Tulving et al., 1994), and paired word associate learning (Fletcher et al., 1995). Furthermore, the retrosplenial cortex appears to be implicated in retrieval more than encoding memory (Kondo et al., 2005), as well as more in recollection than familiarity-based processes (Henson et al., 1999).

Patient studies reveal a dysregulation of the retrosplenial cortex in several pathologies related to memory impairments. These disorders include Mild Cognitive Impairments and Alzheimer's disease (Desgranges et al., 1998; Nestor et al., 2003a; Nestor et al., 2003b), vascular dementia (Martinez-Bisbal et al., 2004), Korsakoff syndrome (Reed et al., 2003) (Aupee et al., 2001), hypoxia-induced amnesia (Aupee et al., 2001), and epilepsy (Archer et al., 2003). In addition, it has been found that specific damage to the retrosplenial

cortex can cause anterograde amnesia (Valenstein et al., 1987; Maguire, 2001a) and topographic amnesia (Yasuda et al., 1997; Maguire, 2001a).

In animals

There is plenty of evidence showing that the retrosplenial cortex clearly contributes to memory processing, such as spatial memory. Normal animals trained in a working memory task in a radial-arm maze showed an increase of c-*fos* activity in the retrosplenial cortex (Vann et al., 2000a). Other sites showing increased c-Fos levels included the anterior thalamic nuclei, the presubiculum, the parasubiculum and the postsubiculum (Vann et al., 2000a). Further lesion studies reveal that damage to the retrosplenial cortex impairs animals in several spatial tasks. Retrosplenial cortex lesions induce a deficit in both reference and working memory in the Morris water maze (Sutherland et al., 1988; Harker and Whishaw, 2002; Vann and Aggleton, 2002; Aggleton and Vann, 2004; Lukoyanov et al., 2005), as well as a deficit in the standard working memory task in the radial-arm maze (Vann and Aggleton, 2002). A recent study tested retrosplenial lesion animals in a paradigm using two T-mazes (Pothuizen et al., 2008). The aim of this experiment was to target and isolate different spatial strategies to solve the task. The use of the two T-mazes made it possible to examine alternation around a constant bearing, as a fixed reference (direction alternation). It was found that retrosplenial cortex lesions, only, disrupted the latter (direction alternation) condition (Pothuizen et al., 2008).

Object recognition tasks highlight the importance of the retrosplenial cortex for spatial components. Animals with damage to the retrosplenial cortex performed normally in the object recognition task, but were severely impaired in the object-in place procedure (Vann and Aggleton, 2002; Parron and Save, 2004). Thus, lesioned animals discriminated novel from familiar objects, but were not able to recognise the object that was displaced to a new location.

Recent studies have showed that the retrosplenial cortex is involved in contextual fear conditioning. Animals that received retrosplenial cortex lesions were impaired in signalled (with a tone) and unsignaled fear conditioning (Keene and Bucci, 2008b); lesioned animals froze less compared to the control animals. Another study of Keene and Bucci (2008a) showed as well that the retrosplenial cortex was involved in the processing of multiple conditioned stimuli. Lesioned animals spent less time waiting for the food in the simultaneous compound conditioned stimuli compared to the controls.

Covert pathology

In humans

The term covert pathology is used to refer to an area that appears normal by standard histological means and yet is functionally lesioned. A potential cause of covert pathology is the presence of damage to distal, but connected sites. For instance, in the case of the retrosplenial cortex, the loss of afferents might be sufficient to induce its dysfunctions.

In Alzheimer's disease (AD), the first overt neuropathology symptoms (amyloid plaques and neurofibrillary tangles) are typically found in the entorhinal cortex, the hippocampus and the anterior thalamic nuclei (Braak and Braak, 1991a, 1991b). Nevertheless, the retrosplenial cortex is the first area that consistently exhibits metabolic alterations in the progress of Alzheimer's disease. PET scans revealed hypoactivity of the retrosplenial cortex at early stages of the disease (Minoshima et al., 1997; Nestor et al., 2003b; Liang et al., 2008). Scahill et al. (2002), however, showed that the posterior cingulate cortex may already suffer from atrophy in mildly affected AD patients, but not in pre-symptomatic patients. A consequence of these findings is that the retrosplenial hypoactivity may be a result of extrinsic pathology, intrinsic pathology, or both.

The first possible explanation is that the retrosplenial cortex is sensitive to extrinsic damage. Thus, metabolic changes in the retrosplenial cortex (hypoactivity) may be induced by the neuropathology of the hippocampus and/or the anterior thalamic nuclei at early stages. The strongest evidence for this effect probably comes from studies of temporal lobe and diencephalic amnesia (Fazio et al., 1992; Clarke et al., 1994; Joyce et al., 1994), where there should not be direct retrosplenial damage. However, in a study of semantic amnesia, patients were found to have a severe degree of atrophy of MTL but this was not accompanied by posterior cingulate hypometabolism (Nestor et al., 2006). Such findings are more consistent with the second hypothesis for this retrosplenial hypoactivity, namely that it comes from previously undetected intrinsic damage to the retrosplenial cortex (Scahill et al., 2002; Pengas et al., 2008). Indeed, Pengas and colleagues (2008) directly compared the relative atrophy of the hippocampus and the posterior cingulate cortex in patients with Mild Cognitive Impairments. They found that retrosplenial cortex atrophy was present in incipient AD and concluded that the hypometabolism of the retrosplenial cortex was a consequence of local, specific, neurodegeneration in the retrosplenial cortex.

In animals

In animal studies, when a lesion is made the consequences are often explained by the loss of the specific lesion. However, it is important to remember that the lesion also has effects and consequences on other brain regions of the same network. Distal dysfunctions can be caused by anatomical disconnections somewhere in the system (Aggleton, 2008). Any lesion will affect at least two other regions by a loss of afferent information and the loss of an efferent target.

Covert pathology is by definition hidden by traditional histological methods. Thus, it is necessary to look to a neuronal marker that could reveal a dysregulation of activity. Once again, the use of IEGs mapping may prove insightful. In practice, a lesion can be made, then after several weeks of

recovery, IEG mapping can be processed. Based on anatomical connections, neural activity of different brain regions can be assessed.

Jenkins et al. (2004a) showed that anterior thalamic damage can disrupt the function of the retrosplenial cortex as defined by IEG expression. c-Fos and Zif268 counts in the retrosplenial cortex were significantly lower following lesions in the anterior thalamic nuclei. The hypoactivity of the retrosplenial cortex was particularly striking in the retrosplenial granular cortex but not the dysgranular Cortex. Within Rgb, the c-Fos decrease was especially prominent in the superficial layers (II and III) compared to the deeper layers. However, the analyses of Nissl staining did not find differences in the actual number of cells (Jenkins et al., 2004a). This result is consistent with the idea of covert pathology; the tissue looks intact but has severe immediate-early gene expression alterations. Another study interested in the covert pathology hypothesis examined retrosplenial cortex activity after unilateral lesions of the hippocampus (Jenkins et al., 2006). Because it was a unilateral lesion, the comparison of c-*fos* activity was within the animal, between the two hemispheres (one lesioned, one control). It was found that unilateral hippocampal lesions induced hypoactivity in several brain regions of the same network, such as the anterior thalamic nuclei, the entorhinal cortex, the perirhinal cortex, and parahippocampal regions. However, retrosplenial cortex activity was not measured. For this reason, Chapter 2 will focus on the effect of different hippocampal lesions on the activity of the retrosplenial cortex as measured by IEG expression. A last example was a study looking at distal effects of unilateral fornix lesions (Vann et al., 2000). IEG hypometabolism was found in many regions, including many parts of the extended hippocampal memory system, such as the hippocampus, the anterior and the posterior cingulate cortex, the entorhinal cortex and parahippocampal cortex. Retrosplenial cortex activity was only measured overall, as a single structure, i.e. there was no distinction between the three sub-regions or the layers (Van Groen and Wyss, 1990c, 1992, 2003).That is why Chapter 4 looks at the effects of different fornix lesions on the different sub-regions of the retrosplenial cortex.

Rationale for specific experiments in thesis

This thesis concerns the ways in which different brain regions work in concert to support various aspects of learning and memory. Most of this thesis is focused on the extended hippocampal memory system and on the nature of the anatomical connections between key structures involved in memory. Because the experimental sections in this thesis look at several distinct regions (hippocampus, mammillary bodies, fornix) more detail will be presented about these specific structures in the appropriate Chapters. My research combines behaviour in rats and IEG imaging. IEG expression, as measured by immunohistochemistry, will be used in all experimental chapters in order to map brain activity within the memory system. Of particular interest is the place and role of the retrosplenial cortex in this putative functional network. The retrosplenial cortex will be studied in much more detail compared to previous IEG studies of this region. Lesion techniques will be used to study distal effects and covert pathology, mostly in the retrosplenial cortex.

Two different approaches then become possible, depending on whether the lesion was made in a brain region or a fibre tract. In Chapter 2, lesions of the hippocampus will disconnect *direct* inputs to the retrosplenial cortex. For these experiments, different types of hippocampal lesions are also compared: unilateral and bilateral lesions, along with different behavioural tasks, and different strains of rats.

The next two Chapters (3 and 4) then describe the effect of fibre tract lesions within the putative memory system under investigation on the retrosplenial cortex. Radiofrequency lesions are made in order to damage two main fibre tracts: the mammillothalamic tract (MTT) and the fornix. Both tracts have a critical place in the extended hippocampal memory system. However, the mammillothalamic tract projections are connected to the retrosplenial cortex indirectly, via a third region (the anterior thalamic nuclei). In contrast, the fornix not only has numerous indirect connections with the retrosplenial cortex but also may have direct connections with the retrosplenial cortex (Gage et

al., 1994). Hence, in the case of the mammillothalamic tract lesions, any changes of retrosplenial cortex activity will be a consequence of disruption of the memory system but will not be due to direct deafferentation of the retrosplenial cortex per se. Chapter 3 then looks at activity changes induced by MTT lesions in the retrosplenial cortex. Then, Chapter 4 compares unilateral and bilateral fornix lesion effects on retrosplenial cortex activity.

Chapter 5 uses the same IEG technique but in a different manner. Instead of looking at brain activity in lesioned animals, IEG mapping will be measured in normal animals following the performance of a behavioural task. The aim of this experiment is to extend our knowledge of object recognition by multi-level analyses. First, a new object recognition task has been developed to help animals show robust discrimination of novelty/familiarity. Second, mapping of brain activity was measured in multiple sites at a higher resolution (hippocampus and retrosplenial cortex) compared to previous studies. Third, patterns of interactions within the anatomical memory network were then examined using structural equation modelling. These analyses can examine the direction of effects and so test for qualitative network changes that accompany different forms of learning.

Chapter 2

The Impact of Hippocampal Lesions on Immediate-early Gene Protein Counts in Retrosplenial Cortex

Introduction

Anatomical, behavioural, and neuropsychological studies increasingly reveal the importance of hippocampal interactions with the retrosplenial cortex (areas 29 and 30). The direct projections from the subiculum to the retrosplenial cortex (Van Groen and Wyss, 1990c, 1992; Insausti et al., 1997; Kobayashi and Amaral, 2003; Van Groen and Wyss, 2003) provide a non-fornical route by which the hippocampus can influence many sites, including prefrontal cortex. Lesion studies have not only confirmed that retrosplenial cortex lesions disrupt many spatial tasks that are also dependent on the hippocampus (Cooper and Mizumori, 1999; Vann and Aggleton, 2002, 2004a), but have also shown their interdependence for aspects of spatial memory (Sutherland et al., 1988; Mizumori et al., 2000). Further support comes from studies of patients with focal lesions and from fMRI studies, which link the hippocampus and retrosplenial cortex for spatial navigation and episodic memory (Maguire, 2001a; Iaria et al., 2007). The present study addressed one possible explanation for this interdependence; namely that hippocampal lesions produce permanent dysfunctions in retrosplenial cortex activity.

There is growing evidence that the retrosplenial cortex is vulnerable to the loss of its distal connections. Related studies, based on the dense projections from the anterior thalamic nuclei to retrosplenial cortex, showed that large thalamic lesions reduce levels of cytochrome oxidase and markers for acetyl choline in the retrosplenial cortex, but do not cause retrosplenial cell loss (Van Groen et al., 1993). Subsequent studies of selective anterior thalamic lesions found a dramatic and permanent fall in the expression of the immediate-early genes (IEGs) c-*fos* and *zif*268 in retrosplenial cortex (Jenkins et al., 2004a; Poirier and Aggleton, 2009). This loss was especially marked in the superficial layers (up to 90% loss), and subsequent slice studies revealed a loss of plasticity in the local circuits within the same superficial layers, indicative of covert pathology (Garden et al., 2009). PET studies have also shown that the retrosplenial hypoactivity in various neurological conditions (Korsakoff's disease, Mild Cognitive Impairment, Alzheimer's disease) is characterised both by a loss of memory and prominent pathology in sites connected with the retrosplenial cortex (Braak & Braak, 1991a; Fazio et al., 1992 ; Minoshima et al., 1997; Reed et al., 2003; Nestor et al., 2003a, b). In Alzheimer's disease this hypoactivity is evident at very early stages in the disease, when overt pathology is present in afferent sites (e.g. the hippocampus and entorhinal cortex) but not typically reported in the retrosplenial cortex itself (Braak and Braak, 1991a, b). However, there is recent evidence of retrosplenial cortex atrophy in patients with Mild Cognitive Impairment as well as those with early Alzheimer's disease, suggesting intrinsic as well as extrinsic pathology in the retrosplenial cortex (Scahill et al., 2002; Pengas et al., 2008).

The present study examined whether hippocampal formation lesions, like anterior thalamic lesions, markedly disrupt retrosplenial cortex IEG activity. Levels of c-Fos and Zif268 proteins were compared in different cytoarchitectonic sub-regions within retrosplenial cortex. These IEGs were selected as they have high expression levels in the retrosplenial cortex, both have repeatedly been implicated in plastic processes (Herdegen and Leah, 1998; Tischmeyer and Grimm, 1999, see Chapter 1), and there are no previous reports on the impact of hippocampal lesions upon IEG expression in the retrosplenial cortex. In Experiments 1, 3, and 4 the rats had previously

been used for other behavioural studies. Therefore, all the lesions in this Chapter (Experiments 1-4) were made by colleagues before the beginning of my PhD. The resultant variations in procedure (e.g. lesion method, rat strain) helped to test the generality of the findings.

Materials and Methods

General Methods

Table 1. Summary of procedural differences for Experiments 1 - 4.

Experiment and lesion site	Lesion method	Post-surgery time	Additional task before IEG	IEG induction task
1. bilateral hippocampus	radiofrequency	8 months	T-maze alternation	Radial-arm maze exploration
2. unilateral hippocampus	NMDA	1 month		Paired-viewing
3. bilateral hippocampus	Ibotenic acid	2-2.5 months	Water-maze	Novel environment
4. bilateral entorhinal	Ibotenic acid	3 months	CTA	Novel environment

Abbreviation: CTA, conditioned taste aversion.

In Experiments 1, 3, and 4 tissue was obtained from cohorts of rats involved in separate behavioural experiments that were designed to study the impact of hippocampal or entorhinal cortex lesions (Table 1). These behavioural tests were completed a minimum of 14 days prior to the present IEG study. These cohorts were chosen as they involved different surgical methods (radiofrequency, injection of a cytotoxin, different anaesthetic), the impact of the lesions had been behaviourally confirmed, and overall animal usage could be minimised. The rats in Experiment 2 had unilateral hippocampal lesions and so did not receive prior behavioural tests, apart from those integral to the study. These variations in procedure (Table 1) helped to test the reliability of any findings. At the same time, the methods for visualising and analysing IEG expression were consistent across all experiments. In addition to standard Nissl staining (Experiments 1-4), tissue from the rats in Experiments 3 and 4

was stained for neuronal nuclei protein (NeuN, Jongen-Relo and Feldon, 2002) in order to help detect whether there was any neuronal loss in retrosplenial cortex following either hippocampal or entorhinal cortex lesions.

In all four experiments rats were exposed to either a novel environment or novel visual stimuli 90 minutes prior to perfusion (Table 1). This 90 min interval was selected as it typically corresponds to peak production of the c-Fos protein after a specific event (Bisler et al., 2002; Zangenehpour and Chaudhuri, 2002). These behavioural manipulations ensured that IEG expression in the retrosplenial cortex in control hemispheres was sufficiently high to detect any lesion-induced changes, i.e. floor effects were avoided.

For all surgeries, animals were first anaesthetised and then placed in a stereotaxic head holder (Kopf Instruments, Tujunga, CA). A longitudinal incision was made in the scalp, which was retracted to expose the skull. Craniotomies were made directly above the target regions, and the dura cut to expose the cortex. After every surgery, the skin was sutured, antibiotic powder applied (Acramide: Dales Pharmaceuticals, UK), and the animal placed in a temperature-controlled recovery box. Animals also received 5 ml of glucose saline subcutaneously (s.c.) and the analgesic agent Meloxicam, 1.0 mg/kg (s.c.). Paracetamol was added to the water for three days post-surgery.

The rats were kept in pairs, housed under diurnal conditions (14 h light/10 h dark) and were thoroughly habituated to handling before the study began. All experiments were conducted in accordance with the United Kingdom Animals (Scientific Procedures) Act 1986.

Experiment 1: Bilateral radiofrequency hippocampal lesions

Animals

The subjects were 12 male Dark Agouti (DA) rats (Harlan, UK), a fully pigmented strain. The rats were 12-14 weeks old and weighed 208-257 g at the time of surgery. Animals had previously been trained for six sessions (36 trials) on reinforced T-maze alternation (Table 1). This task, which confirmed the effectiveness of the hippocampal lesions, was completed 3-4 weeks before the immunohistochemistry study.

Surgery

The 12 DA rats were divided into two groups; bilateral lesions of the hippocampus (RF Hpc, n = 6), and surgical controls (RF Hpc Sham, n = 6). The lesions were made by Dr. RJ Kyd. All rats were deeply anaesthetised with a mixture of isoflurane gas (Aerrane liquid; Baxter Healthcare Ltd., UK) and oxygen. The incisor bar of the stereotaxic frame was set at +5.0. Diazepam was administered systemically (2.5 mg/kg, i.p.). Lesions were made by radiofrequency using an RFG4-A Lesion Maker (Radionics, Burlington). The electrode (0.3 mm tip length, 0.25 mm diameter) was lowered vertically, and at each site the temperature at the tip of the probe was raised to 75°C for 60 sec.

Each hippocampal lesion was formed by making 16 lesions per hemisphere (in 14 separate tracts). The stereotaxic coordinates of the lesions (Table 2) correspond to those used by Sanderson et al. (2006). The control surgical procedure was identical to that for hippocampal lesions except the electrode tip was lowered only 1.7 mm from the top of the cortex using the same AP and laterality coordinates (14 times per hemisphere). The temperature at the tip of the electrode was not raised. The IEG expression study was conducted 8 months post-surgery.

Table 2. Stereotaxic coordinates of bilateral radiofrequency hippocampal lesions

injection	AP	LM	DV	injection	AP	LM	DV
1	2.4	±1.0	3.5	9	4.5	±2.6	3.6
2	2.7	±0.7	3.5	10	5.2	±4.6	4.4
3	2.7	±1.8	3.7	11	5.2	±3.0	3.6
4	3.0	±1.1	3.7	12	5.6	±4.9	5.1
5	3.0	±2.6	3.6	13	5.6	±4.9	7.5
6	4.0	±0.8	3.6	14	5.9	±3.8	4.0
7	4.0	±1.5	2.5	15	5.9	±4.8	5.2
8	4.0	±3.8	3.8	16	5.9	±4.8	6.5

Abbreviations: AP, anteroposterior; LM, lateromedial; DV, dorsoventral.

Behavioural procedure to induce IEG expression

Spontaneous exploration of radial-arm maze

Each rat was allowed to explore spontaneously an unfamiliar eight-arm radial maze in an unfamiliar room. The maze consisted of an octagonal central platform (34 cm diameter) and eight equally spaced radial arms (87 cm long, 10 cm wide) with food wells at the end. The floor of the maze was made of wood, while the side walls were clear Perspex (24 cm high). All animals were tested in the same, distinctive rectangular room (295 x 295 x 260 cm).

The rat was first placed in the central platform and then freely allowed to visit every arm for 30 minutes. The eight arms were baited and continually rebaited with sucrose pellets (45 mg; Noyes Purified Rodent Diet, Lancaster, NH, USA). Each animal was placed in a holding box in a quiet, dark room for 30 minutes before and 90 minutes after the single radial-arm maze session. Animals were habituated to this dark room for 2 hours every day for the 7 days prior to radial-arm maze exploration.

Experiment 2: Unilateral NMDA hippocampal lesions

Rats were trained on the 'paired-viewing' task using the behavioural procedure originally described by Zhu et al. (1996). The data in the present study come from an IEG expression experiment solely designed to measure the impact of hippocampal lesions on cortical function. For this procedure, the rats were shown visual images on computer monitors 90 minutes before perfusion. The visual stimuli were selected as they cause c-*fos* activation in either the perirhinal cortex ('novel stimuli') or the hippocampus ('novel arrangements') in normal rats (Wan et al., 1999).

Animals

The study used 11 adult male DA rats (Bantin and Kingman, Hull, UK) weighing between 180 and 200 g at the time of surgery.

Surgery

All rats received unilateral hippocampal lesions by injecting N methyl–d-aspartate (NMDA) The lesions were made by Dr. EC Warburton. All animals were deeply anaesthetised by an intraperitoneal (i.p.) injection (60 mg/kg) of 6% sodium pentobarbital (Sigma Chemical Company Ltd, Poole, UK, freshly dissolved in saline). Unilateral lesions of the hippocampus (NMDA Hpc) were made by injecting 0.15 μl of 0.06 M NMDA (Sigma Chemical Company Ltd., Poole) dissolved in phosphate buffer (pH 7.2) into 12 sites in one hippocampus and 0.1 μl in one further site (see Jarrard, 1989). Each injection was made gradually over a 4 min period through a 1 μl Hamilton syringe, and the needle was left *in situ* for a further 3 min before being withdrawn. Anteroposterior (AP) and lateromedial (LM) stereotaxic co-ordinates were calculated relative to bregma, dorsoventral (DV) co-ordinates were calculated relative to the top of the cortex (Paxinos and Watson, 1997). The incisor bar was set so that the top of the skull was horizontal. The coordinates (AP, LM,

and DV) of the 14 sites correspond to those reported by Jenkins et al. (2006), see Table 3. The left or right hemisphere was targeted in equal numbers of animals.

Table 3. Stereotaxic coordinates of unilateral NMDA hippocampal lesions

injection	AP	LM	DV	Vol	injection	AP	LM	DV	Vol
1	5.4	5.0	6.1	0.08	8	3.9	3.5	2.7	0.1
2	5.4	5.0	5.3	0.08	9	3.9	2.2	3.0	0.1
3	5.4	5.0	4.5	0.09	10	3.9	2.2	1.8	0.1
4	5.4	4.2	3.9	0.1	11	3.1	3.0	2.7	0.1
5	4.7	4.5	6.5	0.05	12	3.1	1.4	3.0	0.1
6	4.7	4.0	7.2	0.1	13	3.1	1.4	2.1	0.1
7	4.7	4.0	3.5	0.05	14	2.4	1.0	3.0	0.05

Abbreviations: AP, anteroposterior; LM, lateromedial; DV, dorsoventral; Vol, volume (in ml).

Behavioural procedure to induce IEG expression

Paired-viewing procedure ('novel stimuli' and 'novel arrangements')

The rats were trained on one of two conditions on the paired-viewing procedure (Wan et al., 1999). One condition ('novel stimuli', n = 3) was chosen as it increases c-Fos in the perirhinal cortex while the other condition ('novel arrangements', n = 8) induces c-Fos changes in the hippocampus (Wan et al., 1999). Each rat was trained in an open-topped viewing chamber (30 x 30 x 35 cm), the front of which was transparent (Perspex) with a central observing hole: 3 cm in diameter, 6 cm above the floor. When the rat's head was positioned in the observing hole, an infrared beam was interrupted so signalling the computer (Viglen P5-100) to start a trial. Pictures could be shown on two computer monitors placed 30 cm in front of the observing hole. A black partition ensured that the rat's left eye could not see the right monitor screen, and its right eye could not see the left screen.

Training began after a 2-week recovery period. During training the rats were allowed *ad libitum* access to water for 2 h each day. Each rat was first trained for 3 days to go to the observing hole for blackcurrant juice reward. For the next 6 days the rats were shown different visual images on the two computer monitors set behind the observer hole. When the rat held its head in the observer hole for a variable interval of 3-4 sec, pictures (each 15 x 12 cm) were displayed for 4.5 sec on the two monitors. After the pictures had been displayed for 4 sec a drop of blackcurrant juice was delivered by a metal tube that the rat could just reach and lick. As the tube was reached through the observer hole the rats remained oriented towards the visual stimuli. Each day consisted of two morning training sessions and one afternoon session. The second morning session followed the first without a delay and in each morning session 30 pictures (the familiar set) were presented to both eyes. Both eyes saw the same 30 pictures, but the order of presentation differed for the two monitors, so that a different picture was seen by each eye on every trial. In the afternoon training session one eye was exposed to the familiar pictures while the other eye was exposed to a set of 30 novel pictures. A different set of 30 novel pictures was shown each afternoon to familiarise the animal with seeing novel and familiar stimuli simultaneously. The different sets of novel and the familiar set of pictures were so presented that by the end of the experiment each eye had seen the same number of novel and familiar stimuli. The final set of novel stimuli was shown with the familiar set on the afternoon of day 6, one eye seeing each set. Each animal was placed in a holding box in a quiet, dark room for 30 minutes before and 90 minutes after daily sessions.

For three rats each monitor only displayed one picture at a time. The 'Novel stimuli' consisted of completely new pictures presented in just one monitor (Wan et al., 1999). 'Novel arrangements' (n = 8) were created by presenting familiar groups of the same three pictures but with rearranged spatial relationships. Once again, only one eye was shown the novel arrangements. Which eye saw the novel stimuli was counterbalanced across animals and side of lesion.

Experiment 3: Bilateral ibotenic acid hippocampal lesions

Animals

The experiment comprised 15 male Lister Hooded rats (Harlan, UK) weighing 280-400 g at the time of surgery. These rats had previously been trained in a water maze, in which animals with hippocampal lesions were impaired in discriminating local geometric features (Table 1). The training, which was completed 2 weeks before the IEG study, confirmed the effectiveness of hippocampal lesions.

Surgery

Each rat was placed in an induction box and anaesthesia was induced with a mixture of isoflurane gas (Aerrane liquid; Baxter Healthcare Ltd., UK) and oxygen, prior to being placed in a stereotaxic apparatus. Nine rats received hippocampal lesions (IBO Hpc, n = 9); the lesions were made by Dr. P Jones. The infusions of ibotenic acid (Biosearch Technologies, San Rafael, CA), which was dissolved in sterile phosphate-buffered saline (PBS, pH 7.4) to produce a 63 mM solution, were made via a 2 µl Hamilton syringe. Volumes of between 0.05 µl and 0.10 µl ibotenic acid were infused in 14 sites per hemisphere. Stereotaxic coordinates and volumes of the injection sites are similar to Experiment 2, except that the lesions were bilateral (see Table 3). Infusions were made at a rate of 0.03 µl/min, and the needle was left *in situ* for 2 min after completing each infusion. Rats in the sham-operated control group (IBO Hpc Sham, n = 6) underwent a similar surgical procedure to those in lesion groups in which the skin was incised, the cortex exposed and the dura perforated with a 25 gauge Microlance3 needle (Becton Dickinson, Drogheda, Ireland), but neither cortical damage nor injection were made. Post-operative procedures matched other studies, and the immediate-early gene analysis followed from 2 to 2.5 months post-surgery.

Behavioural procedure to induce IEG expression

The rats were exposed to a novel environment by placing them individually in a new non-transparent cage with clean sawdust placed on a rack (with limited visibility) in a novel room. Rats were first left for 15 minutes in this novel cage after which they were returned to their home cages for 90 minutes prior to perfusion.

Experiment 4: Bilateral ibotenic acid entorhinal cortex lesions

Animals

The animals were 19 male Lister Hooded rats (Harlan, UK) weighing 280-400 g at the time of surgery. These rats had previously undergone a conditioned taste aversion task (Mundy et al., 2005) that did not confirm the effect of the lesions in this perceptual task. This experiment had been completed two weeks before training for immediate-early gene expression (Table 1).

Surgery

Rats received bilateral lesions of the entorhinal cortex (IBO Ent, n = 11) or sham surgeries (IBO Ent Sham, n = 8). The lesions were made by Dr. M.E. Mundy. Animals were anaesthetised with a mixture of isoflurane gas (Aerrane liquid; Baxter Healthcare Ltd., UK) and oxygen The injections were made in six sites (in total) under a mediolateral angle of 15°. A total of 0.2 µl of ibotenic acid was injected in each of these six sites over a period of 1 min. The cannula was left *in* situ for 1 min after each injection. The stereotaxic coordinates are presented in Table 4 and are based on the study of Coutureau et al. (1999). The immunohistochemistry was carried out approximately 3 months post-surgery.

Table 4. Stereotaxic coordinates of bilateral ibotenic acid entorhinal cortex

injection	AP	LM	DV
1	8.2	±3.5	7.5
2	8.2	±3.5	7.0
3	8.2	±3.5	6.0

Abbreviations: AP, anteroposterior; LM, lateromedial; DV, dorsoventral.

Behavioural procedure to induce IEG expression

The behavioural procedures were identical as in Experiment 3.

IEG immunohistochemistry

c-Fos and Zif268. Ninety minutes after completing the radial arm-maze exploration, the paired-viewing final session, or being placed in a novel cage, rats were deeply anaesthetised by an intraperitoneal (i.p.) injection (60 mg/kg) of 6% sodium pentobarbital (Sigma Chemical Company Ltd, Poole, UK, freshly dissolved in saline), and perfused intracardially with 0.1 M PBS followed by 4% paraformaldehyde in 0.1 M PBS (PFA). The brains were removed and postfixed in PFA for 4 h and then transferred to 25% sucrose overnight at room temperature with rotation. Sections were cut at 40 µm on a freezing microtome in the coronal plane for Experiment 1 and 2 and in the horizontal plane for Experiment 3 and 4. Series of sections were collected in 0.1 M PBS containing 0.2%Triton X-100 (PBST). A peroxidase block was then carried out where the sections were transferred to 0.3% hydrogen peroxide in PBST for 10 minutes to inhibit endogenous peroxidase and then washed several times with PBST. Sections were incubated in PBST containing c-Fos rabbit polyclonal antibody (1:5000; Ab-5, Oncogene Science, UK); Zif268 (also known as Egr-1/Krox-24/NGFI-A) for Experiment 1, (antibody 1:3000; C-19, Santa Cruz Biotechnology, USA), for 48 h at 4°C with periodic rotation. Sections were then washed with PBST and incubated in biotinylated goat anti-rabbit secondary antibody (diluted 1:200 in PBST; Vectastain, Vector

Laboratories, Burlingame, USA) and 1.5% normal goat serum. Sections were then washed and processed with avidin-biotinylated horseradish peroxidase complex in PBST (Elite Kit, Vector Laboratories) for 1 h at room temperature, again with constant rotation. Sections were washed again in PBST and then in 0.05 M Tris buffer. The reaction was then visualised using diaminobenzidine (DAB Substrate Kit, Vector Laboratories) and then stopped by washing in cold PBS. Sections were mounted on gelatine-coated slides, dehydrated through a graded series of alcohols and coverslipped.

IEG cell counts: Experiments 1 - 4

Estimates were made of IEG-positive cells and also of the total numbers of cells present in the retrosplenial cortex by using an automated cell counting procedure. Wherever possible, counting procedures were without knowledge of the group assignments. Images were viewed on a Leica DMRB microscope, photographed using an Olympus DP70 camera, and transferred to a computer. Counts of the stained nuclei were carried out using the program analySIS^D (Soft-Imaging Systems; Olympus, UK). Regions of interest were assessed using counts of nuclei labelled above threshold. The counts were made in a frame area of 0.84 x 0.63 mm, which enabled all laminae to be included in one image.

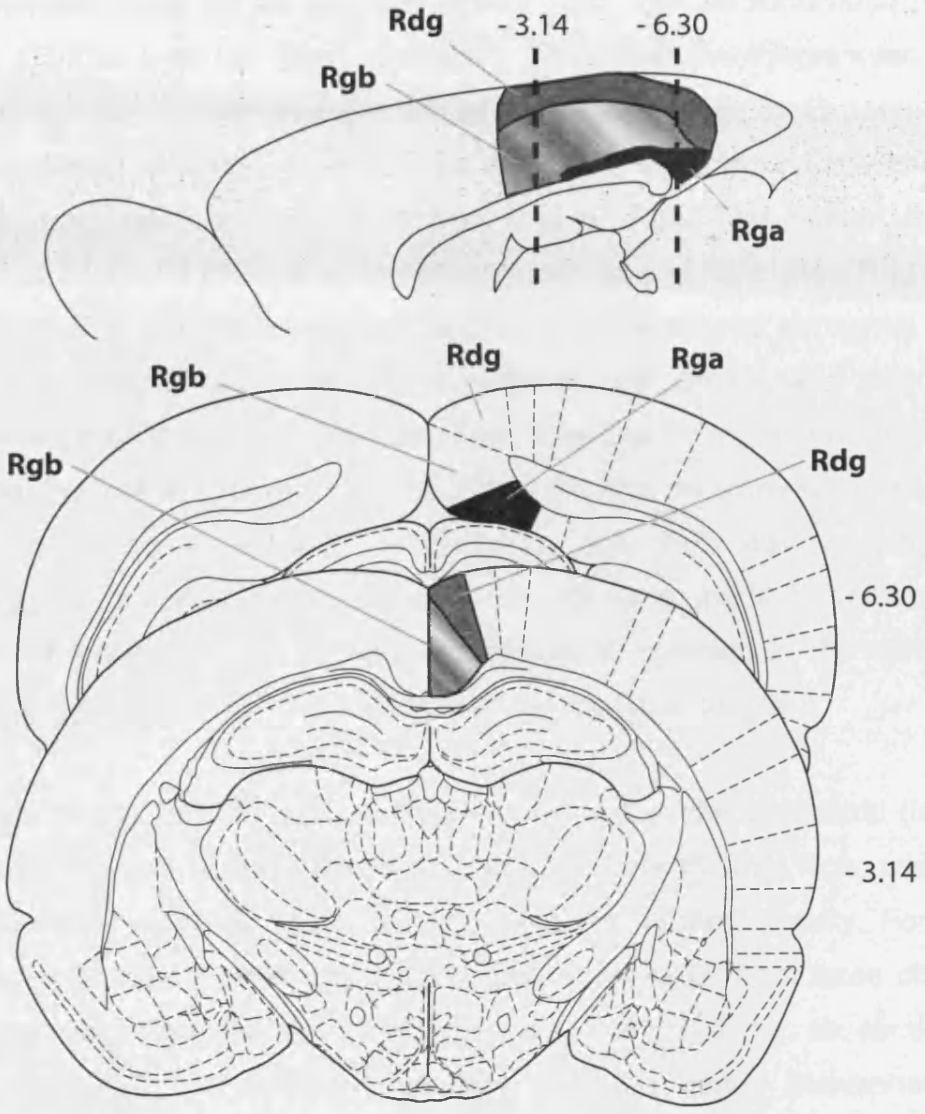

Figure 1. Retrosplenial cortex sub-regions analysed for immediate-early gene levels. The sagital (upper) and coronal (lower) sections show the location of the regions of interest. The numbers refer to the distance (mm) from Bregma according to the atlas of Paxinos and Watson (1997). The shaded areas represent the level of counts. Abbreviations: CC, corpus callosum; Rdg, retrosplenial dysgranular cortex; Rgb, retrosplenial granular b; Rga, retrosplenial granular a.

Retrosplenial cortex (Wyss and Van Groen, 1992) can be subdivided (Figure 1) into granular b cortex (Rgb), granular a (Rga), and the dysgranular cortex (Rdg). Separate counts were made in all three sub-regions for Experiments 1 and 2 (coronal sections). Counts were made only in Rgb for Experiments 3 and 4 (horizontal sections) i.e. not in Rdg or Rga. The reason for this difference concerns the shape and location of Rdg and Rga. Area Rdg spans the dorsal convexity of the cortex, and as a consequence horizontal slices give very unequal amounts of the various cell lamina and can often completely miss the deeper laminae. Area Rga lies more caudal within area 29, and the border between caudal Rgb and Rga is extremely difficult to detect in horizontal sections. Accordingly, only Rgb was examined in Experiments 3 and 4. Here, separate counts were made for rostral Rgb (rostral to splenium) and caudal Rgb (caudal to splenium). The distinctive border between caudal Rgb and Rdg enabled the latter counts.

Separate counts of IEG positive cells were made in the superficial (layer II and upper III) and deep (lower layer III to VI) layers of Rdg, Rgb, and Rga. This border is signalled by an abrupt change in packing density. For each brain area analysed, counts of positive cells were taken from three different sections in each hemisphere for Experiments 1, 3 and 4 (i.e. six sections in total) and from four different sections into the same hemisphere for Experiment 2 (unilateral lesion). These area counts were then averaged to produce a mean for a given animal. The Nissl and NeuN counts were made by the same protocol as that used for IEG positive cells. These counting procedures were not stereological, and so while providing information about relative numbers of cells they do not provide accurate counts of absolute cell numbers.

Nissl and NeuN staining

A one-in-four series of sections was mounted directly onto slides and stained using cresyl violet, a Nissl stain, for Experiments 1-4. In addition, for Experiments 3 and 4 (ibotenate hippocampal and entorhinal lesions

respectively), tissue was stained for a specific neuronal marker, neuronal nuclei protein, NeuN (Jongen-Relo and Feldon, 2002). NeuN was identified using immunohistochemistry. The procedure was very similar as those for c-Fos and Zif268. The NeuN protein was identified using a horse anti-mouse rat adsorbed secondary antibody and 1.5% normal horse serum.

Neuronal cell counts: Experiments 1 - 4

In addition to the relative counts of Nissl-stained cells, several parameters were also analysed using the same software (analySIS^D, Soft-Imaging Systems, Olympus, UK). In order to reduce counts of glial cells and so improve the validity of the neuronal counts, cells were only counted if they had a feret mean between 5 to 20 µm (the feret mean refers to the minimum diameter of a cell). Using this constraint, six parameters were investigated within each region of interest; 1) the mean area of all cells, 2) the mean intensity of the signal (the 'grey value') for all cells, 3) the mean perimeter of all cells, 4) the mean diameter of all cells, 5) the mean of the sphericity values (a measure of how similar the cells are to a sphere) for all cells, 6) the mean convexity value of the cells in an area (a measure of the extent that the cells are infolded or indented).

Parietal cortical damage: Experiment 1

As a control measure, the amount of damage in the overlying cortex was assessed quantitatively in order to determine if it was correlated with c-Fos level changes. Most of this damage was to the parietal cortex, but it often extended caudally to include rostral parts of area 18b. Cortical damage was quantified using the analySIS^D programme. The total size of the cortical lesion (μm^2) was measured from drawings of the extent of parietal and area 18b cell loss on captured images of the Nissl-stained sections. Coronal sections were captured and measured every 40 µm, starting from the first visible damage, thus the number of images depended of the extent of the cortical lesion.

Statistics

Cell counts were compared using an ANOVA with one between-subject factor (group, two levels - control vs. lesion) and one within-subject factor (region: Experiments 1-2, six levels - Rdg superficial, Rdg deep, Rgb superficial, Rgb deep, Rga superficial and Rga deep; Experiments 3-4, four levels - rostral superficial and deep Rgb, caudal superficial and deep Rgb). Because the standard deviations were proportional to the mean, the raw cells counts were subject to logarithmic transformations (Howell, 2002). Simple effects were examined when a significant ($p < 0.05$) interaction was found.

In a final series of analyses designed to compare results across the four experiments the counts for each individual animal for each area were normalised against the mean score of the respective control group for that area. The scores were normalised by dividing the mean number of activated neurons in a lesioned animal by the mean of the appropriate control group, and calculating the proportion score as a percentage. Thus, a score of 100 would correspond to a score that matched that of the appropriate control group, and a score lower than 100 reflects a lower number of cells. Group comparisons used either *t*-tests or one-way ANOVA, and Newmann-Keuls *post-hoc* tests were used as appropriate.

Results

Experiment 1: Radiofrequency bilateral hippocampal lesions

Lesion analysis

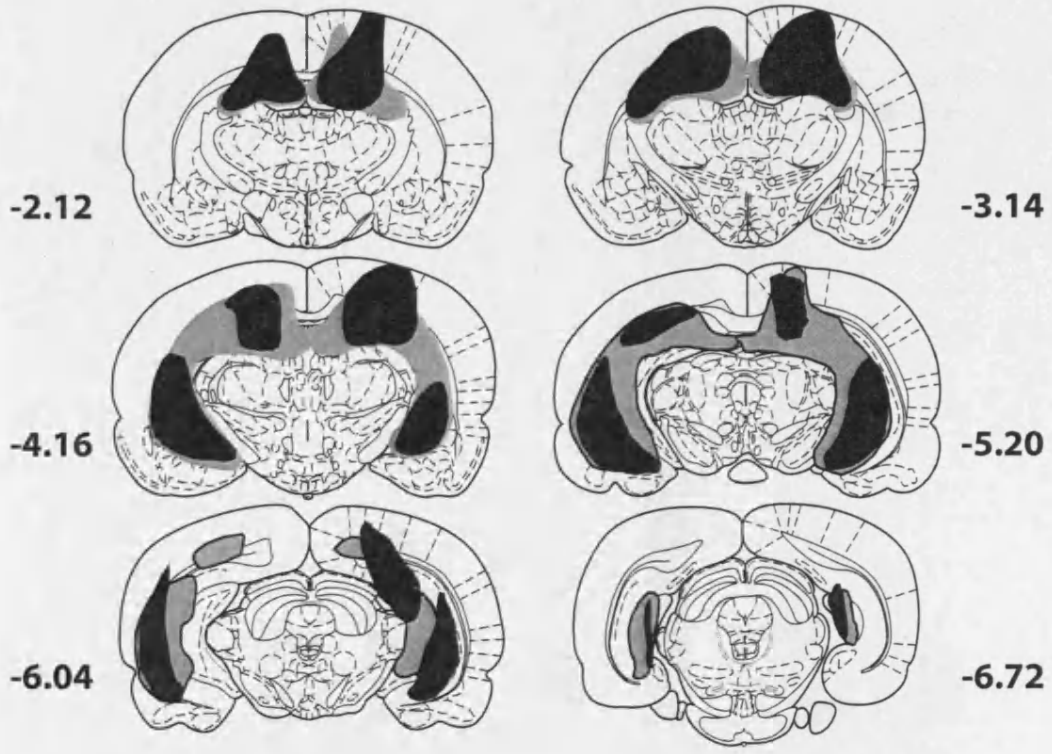

Figure 2. Experiment 1, Radiofrequency hippocampal lesions (RF Hpc) on coronal sections. Diagrammatic reconstructions of the lesions with the largest (grey) and smallest (black) lesions. The numbers refer to the distance (mm) from Bregma (Paxinos and Watson, 1997)

All hippocampal lesions (Figure 2) resulted in substantial damage to the structure. Cell loss was most complete in the dorsal hippocampus, involving areas CA1, CA2, CA3, dentate gyrus and for most cases, the dorsal subiculum. There was consistent partial damage to the fimbria/fornix, which in some cases, was substantial. All rats had damage to the ventral hippocampus, but typically the lesions spared part of the most posterior regions of the ventral hippocampus, which were, nevertheless, markedly

shrunken. In approximately half of RF Hpc cases the damage in the overlying cortex extended beyond the tract marks to involve limited parts of the parietal cortex and rostral 18b (Figure 2).

Immediate-early gene counts

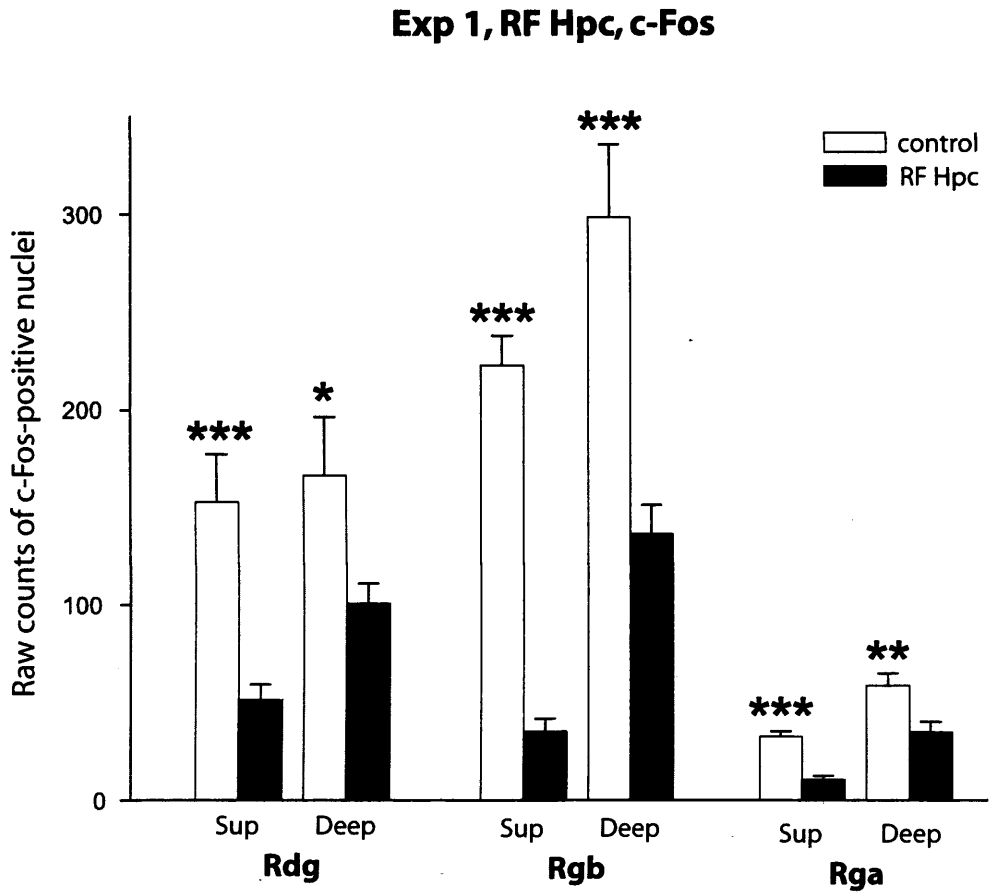

Figure 3. Experiment 1. c-Fos levels after radiofrequency bilateral hippocampal lesions (RF Hpc) and after control surgeries. Raw counts of c-Fos-positive cells are shown for the superficial and deep layers of the dysgranular (Rdg) and the granular (Rgb and Rga) retrosplenial cortex. Data are shown as mean ± SEM. Significance of differences in raw counts: $*p < 0.05$; $**p < 0.01$; $***p < 0.001$.

c-Fos. Counts of c-Fos-positive cells in Rdg, Rgb and Rga, were markedly reduced (70%) following the bilateral, radiofrequency hippocampal lesions (Figures 3, 4). There was a significant decrease in c-Fos counts (group, $F_{(1,10)}$

= 54.8, $p < 0.001$; group x region interaction, $F_{(5,50)} = 11.0$, $p < 0.001$). The interaction reflected the fact that the degree of c-Fos protein loss differed between regions (Figure 3), with the greatest decrease occurring in the superficial layers of Rgb. Subsequent inspection showed that the difference between the two groups was significant in both the superficial layers (II and upper III) and in the deep layers (lower III to VI), as confirmed by the simple effects (Rdg: superficial, $F_{(1,60)} = 29.7$, $p < 0.001$ – deep, $F_{(1,60)} = 5.2$, $p < 0.05$; Rgb: superficial, $F_{(1,60)} = 93.1$, $p < 0.001$ – deep, $F_{(1,60)} = 15.1$, $p < 0.001$; Rga: superficial, $F_{(1,60)} = 32.9$, $p < 0.001$ – deep, $F_{(1,60)} = 7.1$, $p < 0.01$). In addition to the very evident loss of Fos-positive cells in layer II, there also appeared to be a band of cells in layer V that showed abnormally low levels of c-Fos (Figure 4).

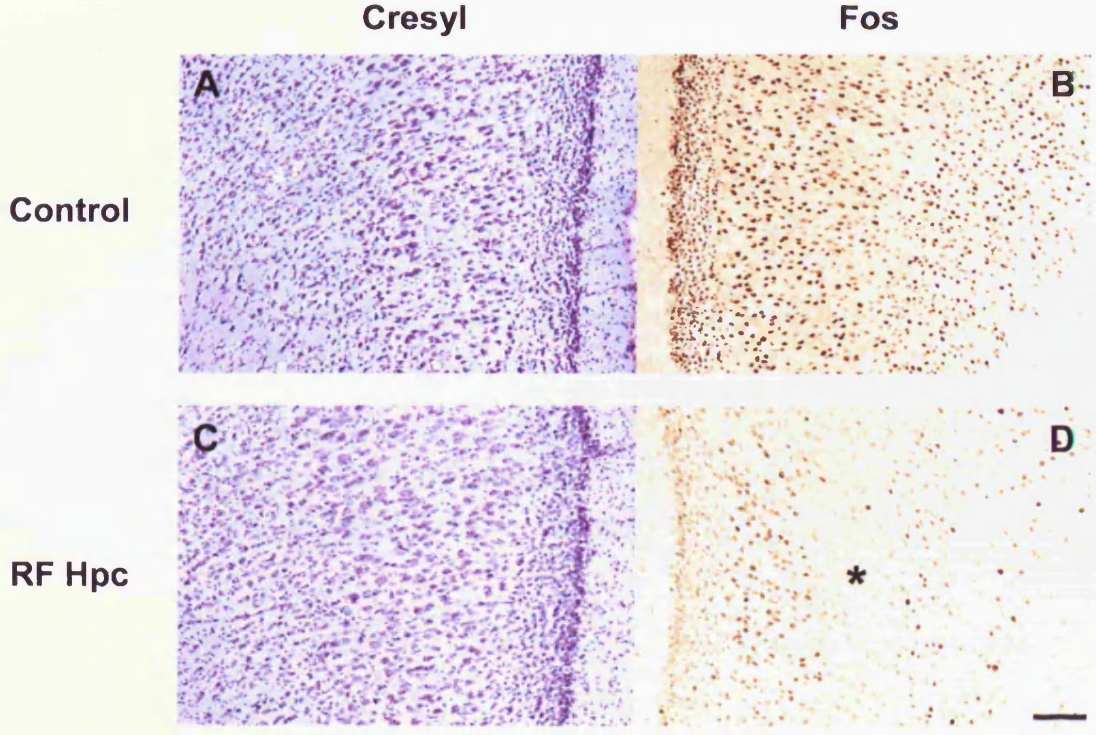

Figure 4. Experiment 1. Photomicrographs comparing Nissl and c-Fos Levels in Rgb in rats with either a bilateral radiofrequency hippocampal lesion (RF Hpc, C, D) or sham surgery (Control, A, B). The brightfield photomicrographs of coronal sections show the comparable appearance of Nissl stained sections (cresyl) in the Rgb (A, C), which contrast with the striking loss of c-Fos-positive cells following hippocampal lesions (D versus B). The asterisk denotes the zone of c-Fos-free cells in layer V. Scale bar, 100 µm.

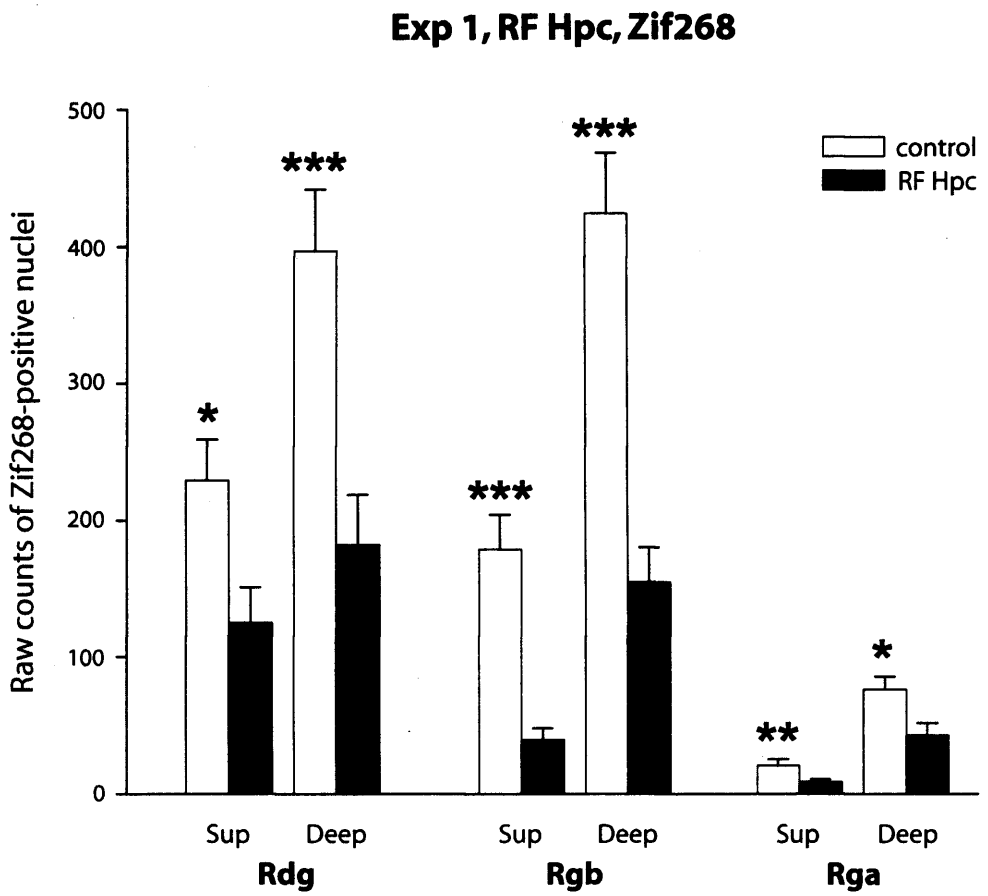

Figure 5. Experiment 1. Zif268 levels after radiofrequency bilateral hippocampal lesions (RF Hpc) and after control surgeries. Raw counts of Zif268-positive cells are shown for the superficial and deep layers of the dysgranular (Rdg) and the granular (Rgb and Rga) retrosplenial cortex. Data are shown as mean ± SEM. Significance of differences in raw counts: *p < 0.05; **p < 0.01; ***p < 0.001.

Zif268. As with c-Fos, a significant reduction of Zif268 cells was observed in the lesion group (group, $F_{(1,10)} = 19.0$, $p < 0.001$; group x region, $F_{(5,50)} = 5.2$, $p < 0.001$; Figure 5). Similarly to c-Fos counts, the interaction reflected a greater decrease in the superficial layers of Rgb (Figure 5). Subsequent analyses revealed that the decrease of Zif268-positive nuclei was found across all sub-regions of the retrosplenial cortex (simple effects; Rdg: superficial, $F_{(1,60)} = 6.9$, $p < 0.05$ – deep, $F_{(1,60)} = 11.3$, $p < 0.001$; Rgb: superficial, $F_{(1,60)} = 38.1$, $p < 0.001$ – deep, $F_{(1,60)} = 17.1$, $p < 0.001$; Rga: superficial, $F_{(1,60)} = 8.6$, $p < 0.01$ – deep, $F_{(1,60)} = 6.0$, $p < 0.05$). The pattern of Zif268 changes was very similar to

that observed for c-Fos, with the most striking losses in layers II, upper III and V.

Experiment 2: NMDA unilateral hippocampal lesions

Lesion analysis

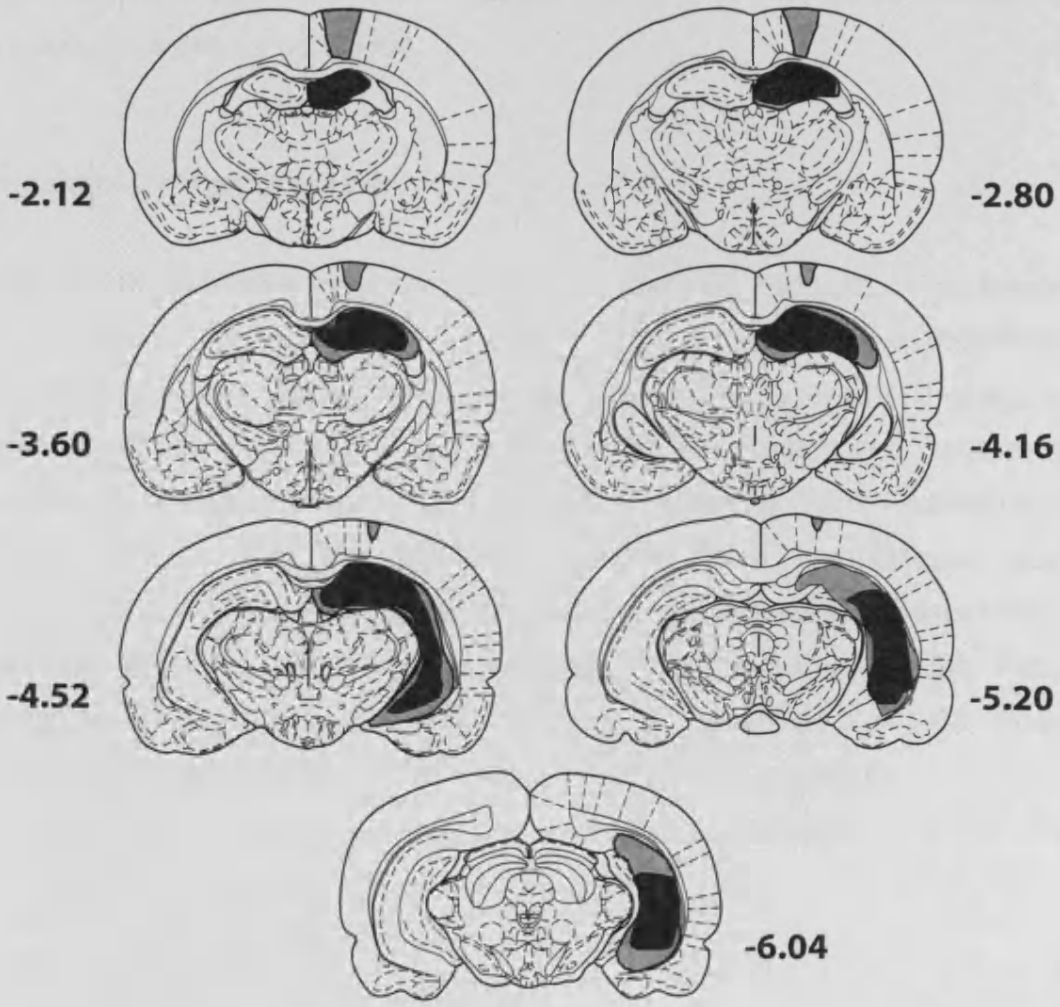

Figure 6. Experiment 2, unilateral NMDA hippocampal lesions (NMDA Hpc) on coronal sections. Diagrammatic reconstructions of the lesions with the largest (grey) and smallest (black) lesions. The numbers refer to the distance (mm) from Bregma (Paxinos and Watson, 1997).

All hippocampal lesions caused near total cell loss in the dorsal hippocampus, with only minor sparing of the ventral horn of the dentate gyrus in one case (Figure 6). The amount of sparing of the ventral hippocampus varied between animals. In eight of the eleven cases there was almost total cell loss, while in three cases there was sparing of the most posterior regions of ventral hippocampus, in particular CA3 and medial blade of the dentate gyrus. Cell loss also occurred in the cortex overlying the dorsal hippocampus. This cortical damage was restricted to the parietal cortex overlying CA1. In all animals the ventral subiculum was partially spared, while the dorsal subiculum was more consistently damaged.

Immediate-early gene counts

c-Fos. Unilateral NMDA hippocampal lesions markedly reduced c-Fos levels (60%) across the retrosplenial cortex (Figure 7). Raw counts were significantly lower in the lesioned hemisphere (group, $F_{(1,20)} = 34.1$, $p < 0.001$; group x region interaction, $F_{(5,100)} = 7.0$, $p < 0.001$), while the interaction showed that this loss was more marked in the superficial layers of Rgb. Subsequent analyses showed that the difference between both hemispheres was significant for all the layers of the three sub-regions (simple effects; Rdg: superficial, $F_{(1,120)} = 8.5$, $p < 0.01$ – deep, $F_{(1,120)} = 4.1$, $p < 0.05$; Rgb: superficial, $F_{(1,120)} = 59.5$, $p < 0.001$ – deep, $F_{(1,120)} = 6.6$, $p < 0.05$; Rga: superficial, $F_{(1,120)} = 26.5$, $p < 0.001$ – deep, $F_{(1,120)} = 6.9$, $p < 0.01$).

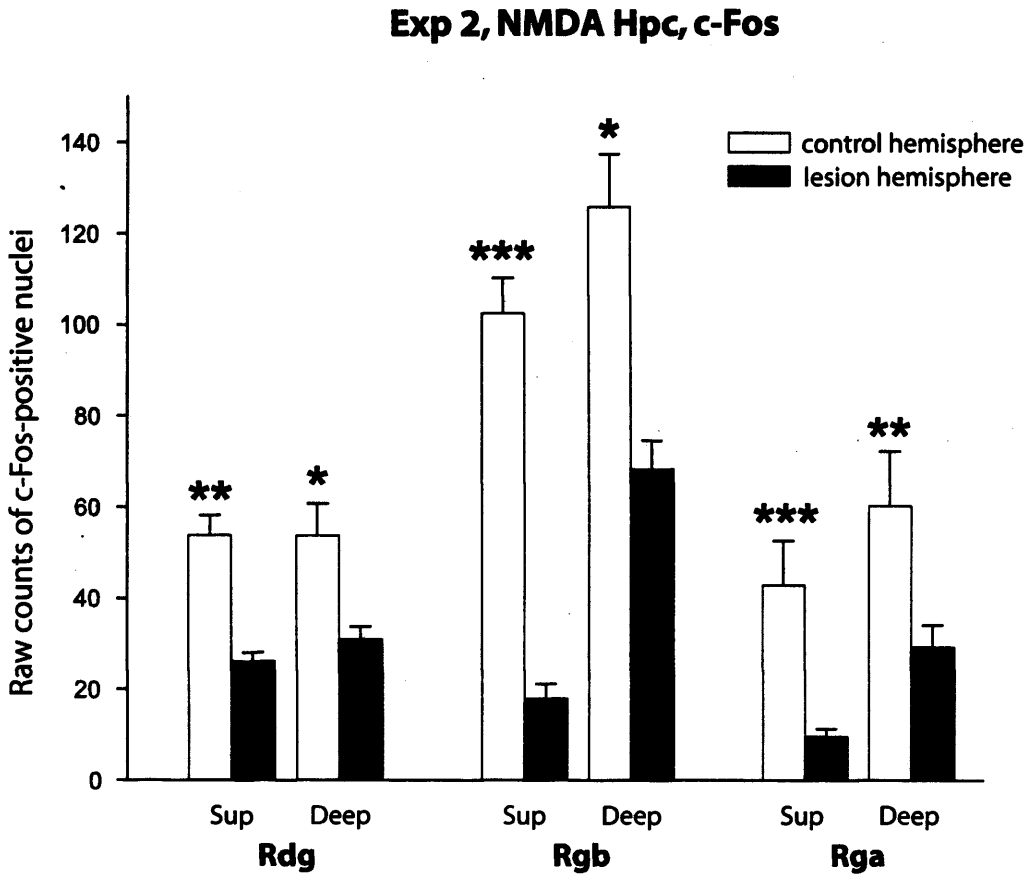

Figure 7. Experiment 2. c-Fos levels after unilateral NMDA hippocampal lesions. Raw counts of c-Fos-positive cells are shown for the superficial and deep layers of the dysgranular (Rdg) and the granular (Rgb and Rga) retrosplenial cortex in the lesion and control hemispheres. Data are shown as mean ± SEM. Significance of differences in raw counts: $*p < 0.05$; $**p < 0.01$; $***p < 0.001$.

Experiment 3: Ibotenic acid bilateral hippocampal lesions

Lesion analyses

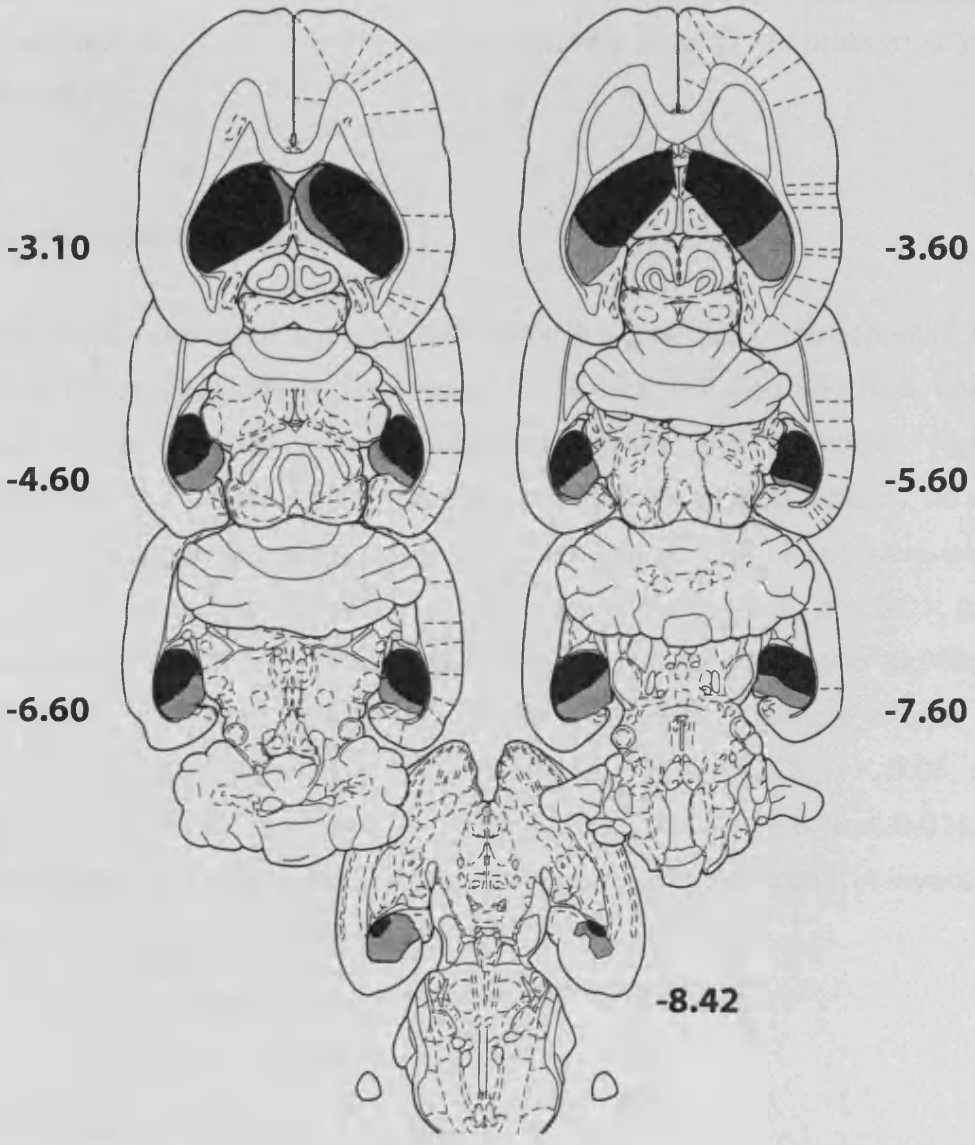

Figure 8. Experiment 3, ibotenic acid hippocampal lesions (IBO Hpc) on horizontal sections. Diagrammatic reconstructions of the lesions with the largest (grey) and smallest (black) lesions. The numbers refer to the distance (mm) from Bregma (Paxinos and Watson, 1997).

All rats with hippocampal lesions sustained bilateral damage to both the dentate gyrus and the CA subfields at all dorsal and ventral levels (Figure 8). The range of cell loss amounted to 65-100% of the intact hippocampus (dentate gyrus, CA1-3). The majority of rats also sustained some cell loss in the subiculum (including the pre- and parasubiculum). This damage was most evident in ventral regions of the subiculum. There was no detectable cell loss in the postsubiculum or in the medial or lateral entorhinal cortex in any of the lesioned rats.

Immediate-early gene counts

c-Fos. Raw counts were taken only from the granular b retrosplenial cortex. Due to horizontal sections, the shape and location of Rdg and Rga, counts in these areas are not consistent (see Materials and Methods). Rgb was subdivided into the rostral and caudal area (pre and post splenium), as well as superficial and deep layers. In the lesioned animals (IBO Hpc) there was a c-Fos decrease across the whole of Rgb (group, $F_{(1,13)} = 9.6$, $p < 0.01$; group x area interaction, $F_{(3,39)} = 0.3$; Figure 9). This lesion effect was significant in both layers and in both rostral and caudal areas of Rgb (simple effects; rostral Rgb: superficial, $F_{(1,52)} = 8.5$, $p < 0.01$ – deep, $F_{(1,52)} = 6.3$, $p < 0.05$; caudal Rgb: superficial, $F_{(1,52)} = 7.0$, $p < 0.05$ – deep, $F_{(1,52)} = 9.6$, $p < 0.01$). Once again, there was a striking loss of c-Fos-positive cells not only in layers II and upper III, but also in layer V (Figure 10).

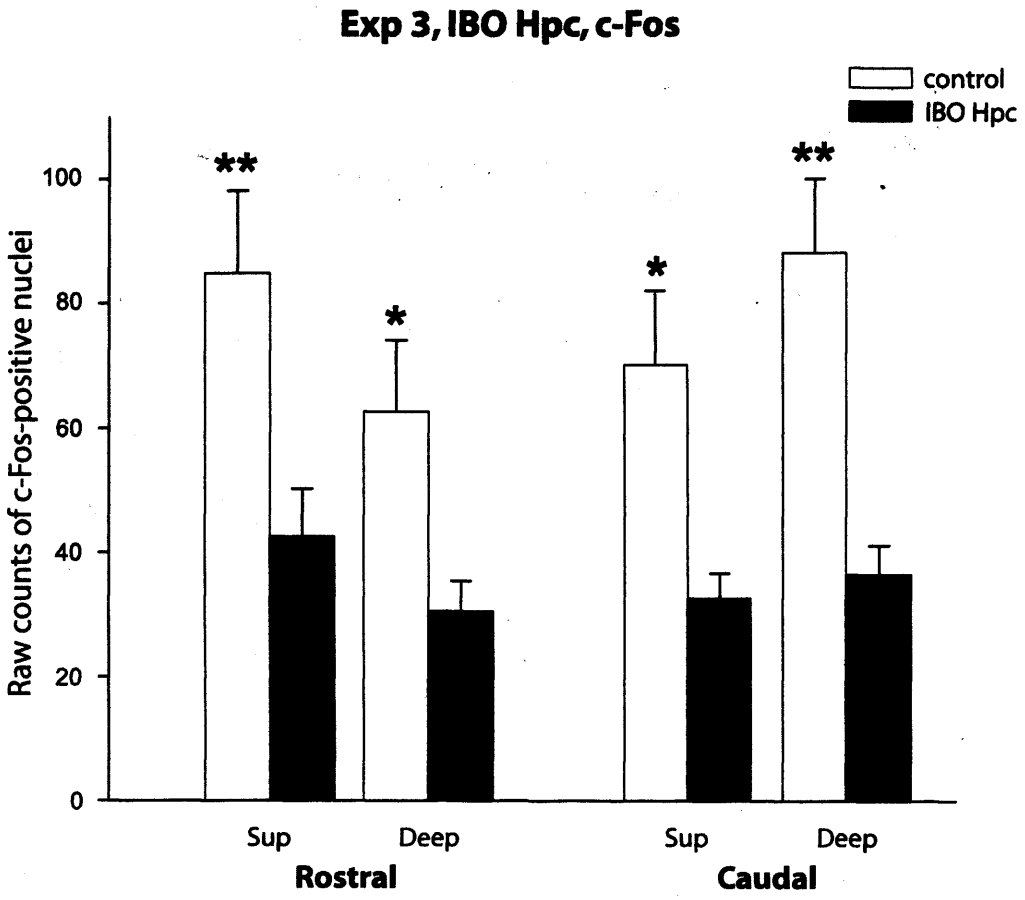

Figure 9. Experiment 3. c-Fos levels after bilateral ibotenic acid hippocampal lesions (IBO Hpc) and after control surgeries (Sham). Raw counts of c-Fos-positive cells are shown for the superficial and deep layers of the rostral and caudal granular b retrosplenial cortex. Data are shown as mean ± SEM. Significance of differences in raw counts: $*p < 0.05$; $**p < 0.01$.

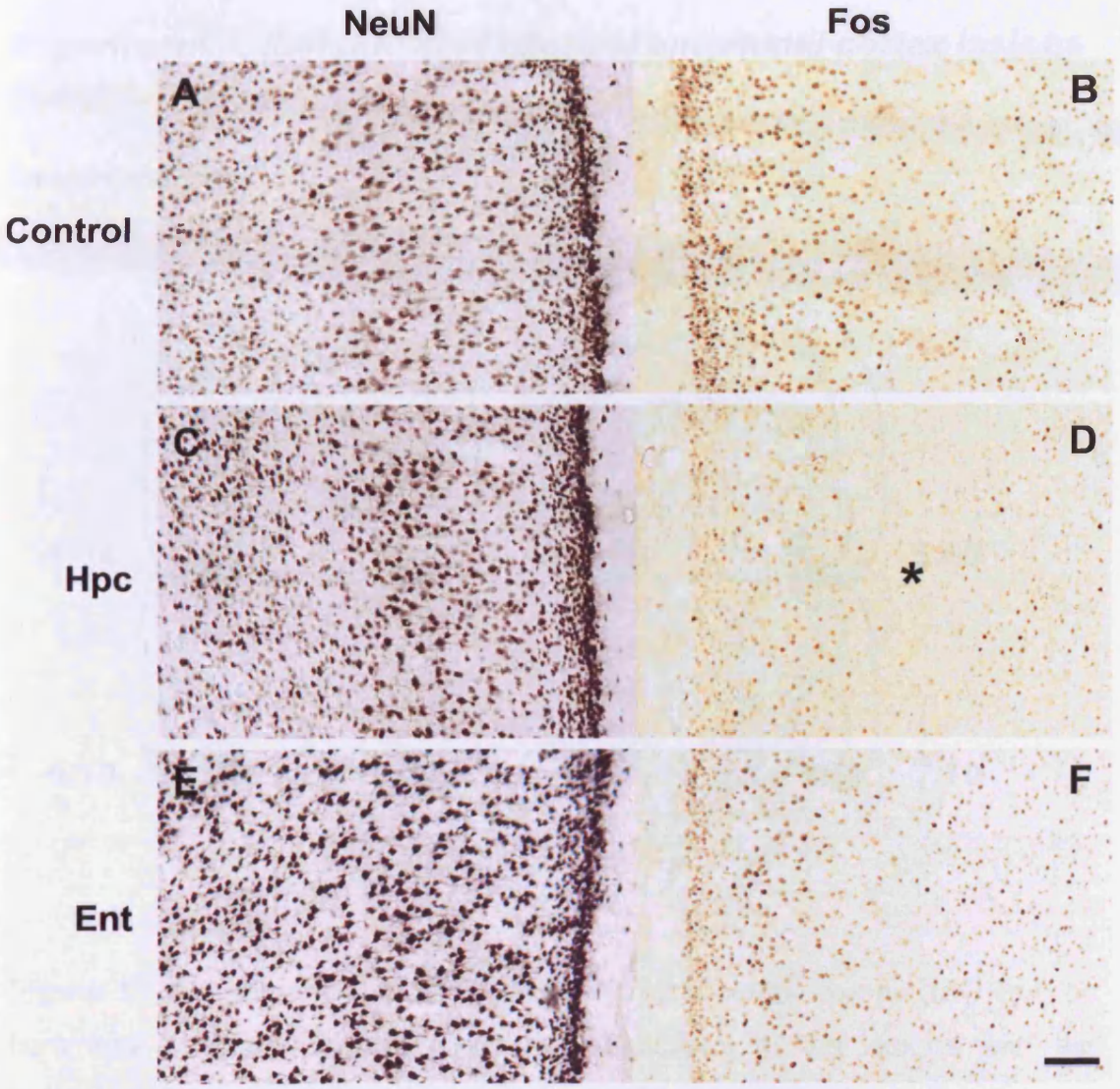

Figure 10. Photomicrographs comparing NeuN and c-Fos Levels in Rgb in rats with either a bilateral ibotenic acid hippocampal lesion (Experiment 3; IBO Hpc, C, D), a bilateral ibotenic acid entorhinal lesion (Experiment 4; IBO Ent, E, F), or a sham surgery (Control, A, B). The brightfield photomicrographs of horizontal sections show the comparable levels of neurons in the retrosplenial cortex (A, C, E), which contrast with the selective, striking loss of c-Fos-positive cells following hippocampal lesions (D versus B and F). The asterisk denotes the zone of c-Fos-free cells in layer V. Scale bar, 100 μm.

Experiment 4: Ibotenic acid bilateral entorhinal cortex lesions

Lesion analyses

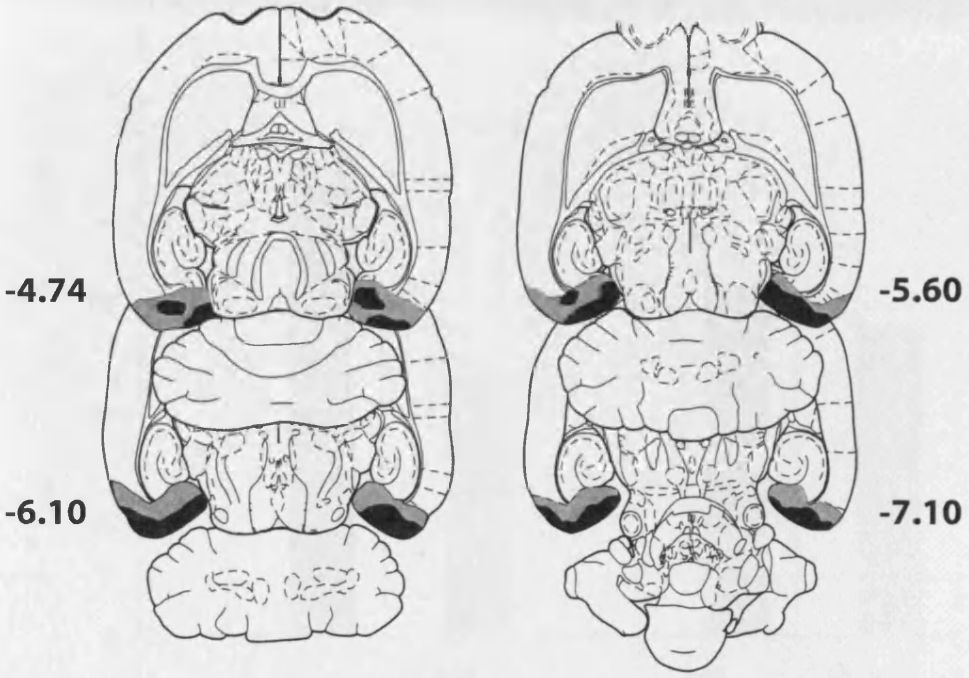

Figure 11. Experiment 4, ibotenic acid entorhinal cortex lesions (IBO Ent) on horizontal sections. Diagrammatic reconstructions of the lesions with the largest (grey) and smallest (black) lesions. The numbers refer to the distance (mm) from Bregma (Paxinos and Watson, 1997).

All lesioned rats sustained substantial cell loss within the medial entorhinal cortex, and cell loss that was more variable in the lateral entorhinal cortex (Figure 11). There was, as intended, substantial sparing of cells in the subicular complex. Typically, the lesion extended from -4.6 to -7.6 mm ventral to the surface of the brain (Paxinos and Watson, 1997).

Immediate-early gene counts

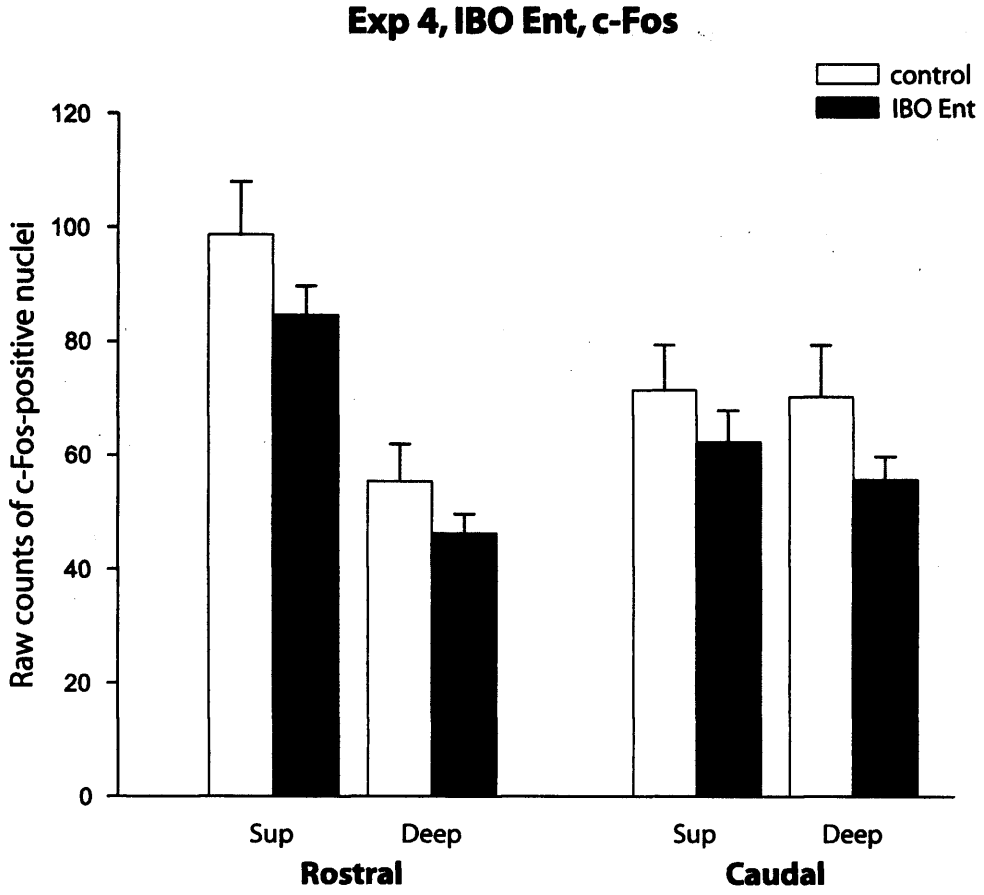

Figure 12. Experiment 4. c-Fos levels after bilateral ibotenic acid entorhinal cortex lesions (IBO Ent) and after surgery controls (Sham). Raw counts of c-Fos-positive cells are shown for the superficial and deep layers of the rostral and caudal granular b retrosplenial cortex. Data are shown as mean ± SEM.

c-Fos. Raw counts were taken only from the granular b retrosplenial cortex. A non-significant reduction in c-Fos levels was found in rostral and caudal Rgb (group, $F_{(1,17)} = 1.7$, $P = 0.2$; group x area interaction, $F < 1$; Figure 12).

Neuronal cell counts: Experiments 1 - 4

Nissl-stained counts

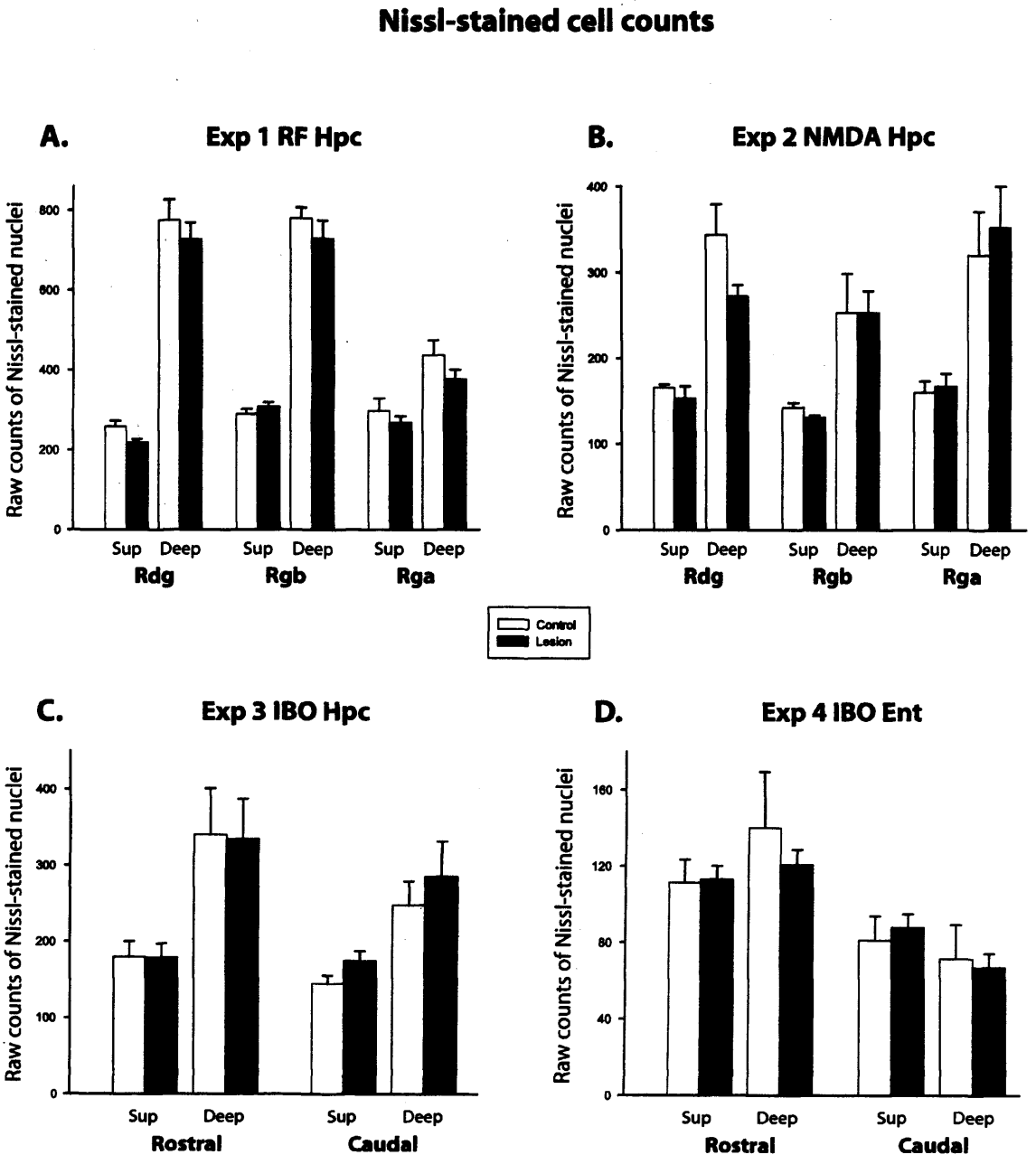

Figure 13. Raw counts of Nissl-stained cells **A.** radiofrequency bilateral hippocampal lesions (RF Hpc), **B.** NMDA hippocampal lesions (NMDA Hpc), **C.** ibotenic acid hippocampal lesions (IBO Hpc). **D.** ibotenic acid entorhinal lesions (IBO Ent). Nissl raw counts are shown for superficial and deep layers of dysgranular (Rdg) and granular (Rgb and Rga) retrosplenial cortex (**A, B**); or for superficial and deep layers of rostral and caudal granular b retrosplenial cortex (**C, D**). Data are shown as mean ± SEM. For clarity, the scale of the Y axis has been changed between.

Nissl-stained cell counts. There were no significant differences between groups in the total Nissl cell counts taken across all layers of the retrosplenial cortex for any of the experiments, see Figure 13 (RF Hpc: group, $F_{(1,10)} = 3.5$, $p = 0.09$, Figure 4; group x region interaction, $F < 1$; NMDA Hpc: group, $F < 1$; group x region interaction, $F < 1$; IBO Hpc: group, $F < 1$; group x area interaction, $F_{(3,36)} = 1.2$, $p = 0.3$; IBO Ent: group, $F < 1$; group x area interaction, $F < 1$).

Nissl-stained cell parameters

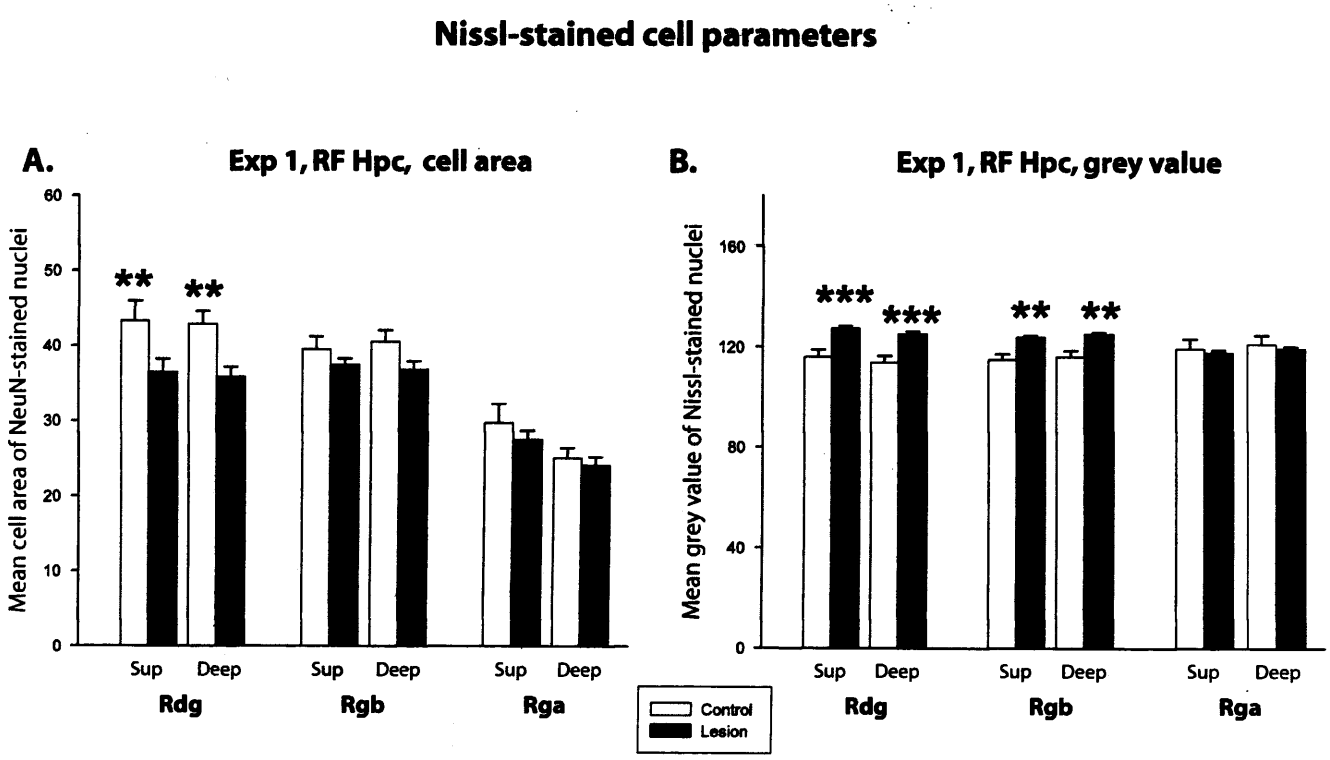

Figure 14. Cell parameters of Nissl-stained cells. Only parameters with significant group differences are presented. Only after radiofrequency hippocampal lesions (RF Hpc) were cell parameter changes noted (two out of six parameters): **A.** cell area, the mean area of all cells, **B.** grey value, the mean intensity of the signal. Data are shown as mean ± SEM. Significance of differences in raw counts: $^{**}p < 0.01$; $^{***}p < 0.001$.

In addition to counting cell numbers, other cell parameters were analysed and compared to help determine whether the lesions caused morphological abnormalities in the retrosplenial cortex. The cell parameters were: cell area, intensity ('grey value') of stain, perimeter, diameter, sphericity, and convexity. In Experiments 2-4, there were no significant changes in any of the six studied parameters ($p > 0.05$) for the areas under investigation in each experiment. In Experiment 1 no group differences were found for perimeter, diameter, sphericity and convexity (see Chapter 2, Materials and Methods). Significant group effects were, however, found for the Nissl-stained mean area of all cells (group, $F_{(1,10)} = 6.09$, $p < 0.05$; group x area interaction, $F_{(5,50)} = 1.84$, $p = 0.12$) and the grey value (group, $F_{(1,10)} = 9.86$, $p < 0.05$; group x area interaction, $F_{(5,50)} = 5.66$, $p < 0.001$). Subsequent analyses showed a decrease of the mean cell area in the lesion group (Figure 14), but only in Rdg (simple effects; Rdg: superficial, $F_{(1,60)} = 8.68$, $p < 0.01$ – deep, $F_{(1,60)} = 9.19$, $p < 0.01$), and an increase of the grey value in the lesion group in Rdg and Rgb (simple effects; Rdg: superficial, $F_{(1,60)} = 13.44$, $p < 0.001$ – deep, $F_{(1,60)} = 13.01$, $p < 0.001$; Rgb: superficial, $F_{(1,60)} = 8.40$, $p < 0.01$ – deep, $F_{(1,60)} = 8.61$, $p < 0.01$).

Counts of NeuN-positive cells in Rgb (Figures 10, 15) failed to find evidence of a change in neuronal number following ibotenic acid lesions of either the hippocampus or entorhinal cortex (IBO Hpc: group, $F_{(1,13)} = 0.1$; group x area interaction, $F_{(3,39)} = 2.3$, $p = 0.09$; IBO Ent: group, $F < 1$; group x area interaction, $F < 1$).

NeuN-positive cell counts (Experiments 3-4)

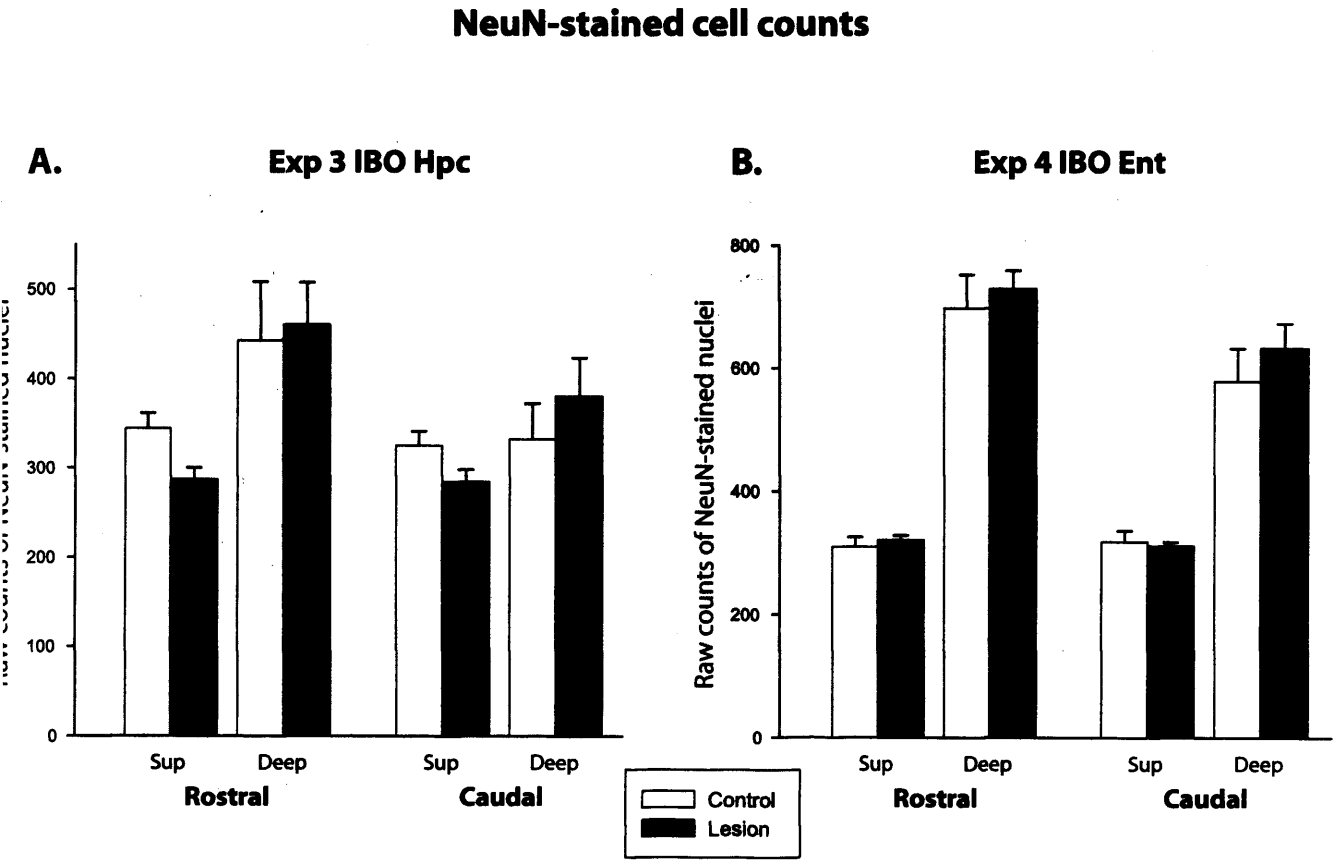

Figure 15. Raw counts of NeuN-stained cells **A.** ibotenic acid hippocampal lesions (IBO Hpc), **B.** ibotenic acid entorhinal lesions (IBO Ent). Raw counts of NeuN-stained cells are shown for the superficial and deep layers of the rostral and caudal granular b retrosplenial cortex. Data are shown as mean ± SEM.

Parietal cortical damage in Experiment 1

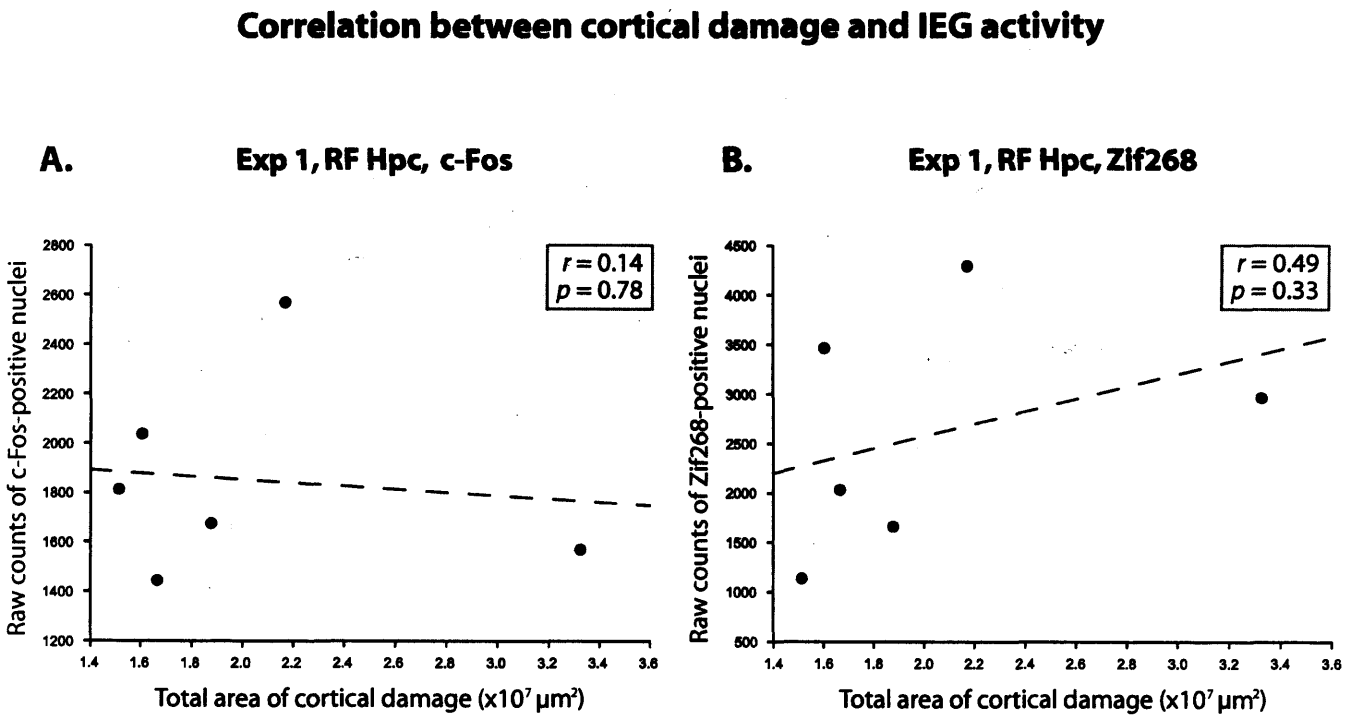

Figure 16. Correlations (Pearson *r*) between total area of cortical damage and IEG-positive cell counts (raw) across the total retrosplenial cortex after radiofrequency hippocampal lesions (RF Hpc). **A.** c-Fos; **B.** Zif268.

For Experiment 1, an additional check was made on the possible impact of damage to the parietal cortex and area 18b (Figure 16). Correlations using the estimates of total, bilateral parietal and area 18b damage against the raw counts of IEG positive cells in the retrosplenial cortex (combined counts from Rgb, Rga, and Rdg) found no significant correlations between these two measure (c-Fos, Spearman's rho, $r = 0.14$, $p = 0.78$; Zif268, Spearman's rho, $r = 0.49$, $p = 0.33$).

Comparisons of IEG findings across Experiments 1 - 4:

For each of the three sub-regions within retrosplenial cortex (Rga, Rgb, Rdg) it was found that hippocampal lesions reduced overall c-Fos-positive cell

counts (superficial and deep laminae combined) by between 49% (Rgb, Experiment 3) and 70% (Rgb Experiments 1 and 2). Thus, for Experiments 1-3 the c-Fos counts were typically less than half of those of the control cases. In order to compare statistically the magnitude of these IEG changes across the different experimental techniques (different lesion method, different rat strain, different behavioural task) the data were first normalised against their respective controls (For Experiment 3 the data were taken from just rostral Rgb to aid comparability with the other experiments). These comparisons (Figure 17) further confirmed how hippocampal lesions, but not entorhinal cortex lesions, consistently reduced retrosplenial cortex activity as measured by c-Fos expression. Zif268 was only visualised in Experiment 1.

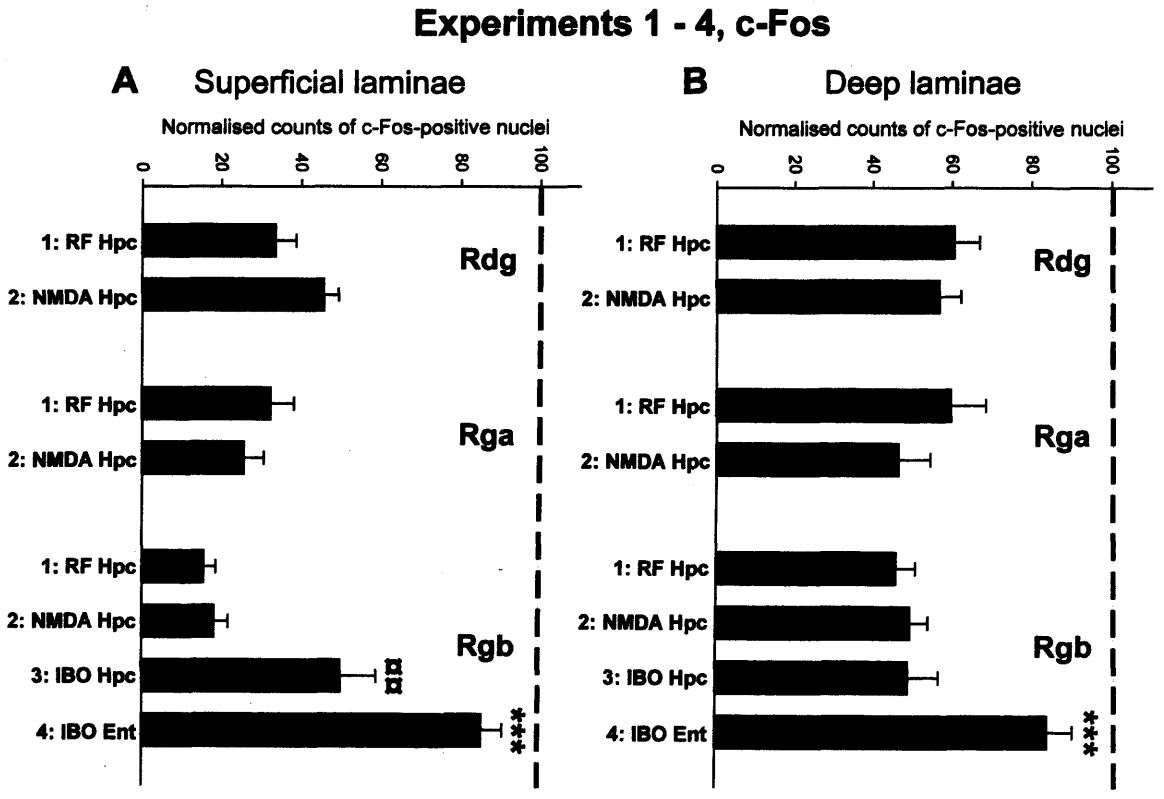

Figure 17. Experiments 1 - 4. Normalised counts of c-Fos-positive cells in the superficial (A) and deep laminae (B) of the retrosplenial cortex. Data are shown as mean ± SEM. Any significance differences in these normalised counts within each sub-region across the various lesion conditions are indicated: ¤¤ p <0.01 (IBO Hpc); ***p < 0.001 (IBO Ent).

Comparisons across the four experiments indicated that the magnitude of the c-Fos loss in Rdg or Rga did not differ significantly when the lesions were made either by radiofrequency or by NMDA (Rdg: superficial, $p = 0.067$, deep, $p = 0.4$; Rga; superficial, $p = 0.67$, deep, $p = 0.3$). There was, however, a significant effect of lesion method for Rgb ($F_{(3,33)} = 38.5$, $p < 0.001$). Of the three lesion methods, the IBO Hpc rats had the least reduction of c-Fos activity in the superficial layers (IBO Hpc vs. RF Hpc, Newman-Keuls, $p < 0.01$; IBO Hpc vs. NMDA Hpc, $p < 0.01$). There were, however, no differences in the deep layers (IBO Hpc vs. RF Hpc, $p = 0.99$; IBO Hpc vs. NMDA Hpc, $p = 0.91$). The RF Hpc and NMDA Hpc rats showed similar c-Fos decreases ($p = 0.99$) in superficial and deep layers. Finally, post-hoc analyses revealed a significant difference between the entorhinal cortex lesions and all three other hippocampal surgeries ($p < 0.001$).

Discussion

The main findings of this study are very clear. Lesions of the rat hippocampus resulted in consistent, striking decreases in the counts of c-Fos-positive cells in the retrosplenial cortex. Typically this reduction was at least 50% of the total IEG counts in the retrosplenial cortex. A very similar result was found for Zif268 in the one experiment in which this IEG was studied. These IEG decreases were found across all three sub-regions of area 29 (Rga, Rgb, Rdg). Furthermore, these IEG reductions were found in both the superficial and deep layers. Although the superficial layers (II and upper III) often displayed the most dramatic decreases in IEG-positive cells, there was an additional band of cells in layer V of the granular retrosplenial cortex that often appeared to be largely devoid of c-Fos-positive cells (Figures 4, 10). In contrast, entorhinal cortex lesions led to little or no change in retrosplenial IEG levels. These novel findings show that hippocampal lesions leave the retrosplenial cortex abnormal, raising the possibility that retrosplenial dysfunction contributes to the impact of hippocampal damage. The entorhinal lesion results show that this hippocampal lesion effect is selective and not simply due to any deafferentation of the subiculum.

The present study deliberately examined a variety of methods to lesion the hippocampus, and also varied the behavioural methods used to raise IEG levels above their resting baseline levels in the retrosplenial cortex. In spite of the many procedural changes (table 1) the findings were remarkably consistent (Figure 14) and all hippocampal lesions led to significant reductions in c-Fos-positive cells across the retrosplenial cortex. These IEG depletions, which were found across both superficial and deep layers, were of comparable magnitude across experiments in spite of the variations in procedure. The only minor exception was the evidence of a relatively smaller c-Fos decrease in Rgb in Experiment 3 (Figure 17). While this subtle difference might reflect the change in rat strain, it is more likely due to the differential involvement of the dorsal and ventral subiculum in Experiments 1-3. In Experiment 3 there was the most sparing of the dorsal subiculum, which projects to Rgb (Van Groen and Wyss, 2003), so potentially limiting the IEG disruption.

Assessments of the numbers of retrosplenial cells and the physical parameters of these same cells showed that the region appeared grossly normal in spite of the reductions in both IEGs. The hippocampal lesions did not alter significantly the numbers of Nissl-stained cells in any of the sub-regions within the retrosplenial cortex. Likewise, there were no changes in the numbers of NeuN-positive cells in Experiment 3, both results showing the lack of cortical atrophy following the various hippocampal lesions. More detailed measurements of the physical properties of the Nissl-stained material in Rdg, Rgb, and Rga again found no evidence of robust changes in volume, staining intensity, or shape. No changes were found in Experiments 2 - 3. The only exception was for Nissl staining in Experiment 1 (radiofrequency lesions) where a decrease in cell area was found just in Rdg, and an increase in staining intensity was noted in Rdg and Rgb. These selective changes may be associated with the use of radiofrequency in Experiment 1, and the inevitable greater damage to white matter. This damage also often included parts of the overlying parietal cortex and area 18b, and it may be relevant that area 18b projects directly to Rdg and Rgb (Van Groen and Wyss, 1992, 2003) but not

to Rga (Van Groen and Wyss, 1990c). It is, therefore, plausible that the loss of white matter would have resulted in slightly greater cell packing.

Studies into the impact of retrosplenial cortex dysregulation in rats have shown how lesions in this area consistently impair tests of spatial memory (Sutherland et al., 1988; Mizumori et al., 2000; Alexinsky, 2001; Cooper et al., 2001; Whishaw et al., 2001; Vann and Aggleton, 2002, 2004a). These same spatial tests are also sensitive to hippocampal lesions. Furthermore, there are dense, reciprocal connections between the two structures (Wyss and Van Groen, 1992), with hippocampal efferents from CA1, the subiculum and postsubiculum projecting directly to Rdg, Rgb and Rga. This arrangement suggests that the two areas work conjointly to support spatial memory (Mizumori et al., 2000). This notion was tested directly by Sutherland and Hoesing (1993) who examined the effects of crossed, unilateral lesions in the hippocampus and retrosplenial cortex. The subsequent deficits in the Morris water maze (Sutherland and Hoesing, 1993) showed that the hippocampus and the retrosplenial cortex have interdependent functions. The present findings help to explain this relationship as the interdependence may arise, in part, from the changes in retrosplenial activity caused by hippocampal damage i.e. the retrosplenial cortex becomes functionally lesioned.

The present study cannot confirm whether the retrosplenial IEG changes reflect 'covert pathology' or whether the retrosplenial IEG changes are simply due to the disconnection of a major afferent, i.e. whether they reflect a permanent malfunction in some retrosplenial neurons or whether the neurons remain functionally intact and normal but are relatively unresponsive due to the lack of one set of excitatory afferents. In order to demonstrate the former (covert pathology) it would be necessary to show that the responsiveness of some retrosplenial neurons to all other (intact) inputs is permanently abnormal. There are, in fact, several reasons to believe this 'covert pathology' account. First, the IEG depletions were very marked (especially in Rgb) and were found across both the superficial and deep lamina in retrosplenial cortex. This global effect on area 29 can be contrasted to the innervations from the hippocampal region, which appear more restricted as they terminate in

laminae I-III (Wyss and Van Groen, 1992). Second, the surgeries would have left intact the other numerous afferents to area 29 e.g. from the anterior thalamic nuclei, the lateral dorsal thalamic nucleus, the anterior cingulate cortex, contralateral area 29, and areas 17 and 18b (Van Groen et al., 1993), yet these inputs were not sufficient to compensate for the lost hippocampal afferents. Third, there is growing evidence that the retrosplenial cortex shows covert pathology following anterior thalamic nuclei lesions. Not only do all three sub-areas (Rdg, Rgb, Rga) show very marked decreases in c-Fos and Zif268 counts (Jenkins et al., 2004a) but electrophysiological studies using retrosplenial cortex slices taken from rats with unilateral anterior thalamic lesions reveal a loss of synaptic plasticity in superficial Rgb on the same side as the anterior thalamic nuclei lesion (Garden et al., 2009). This loss of plasticity is revealing as it cannot be a mere deafferentation effect as the stimulated microcircuits are still present in the slice (Garden et al., 2009). Given that the IEG losses in the superficial laminae appear similar after hippocampal lesions to those observed after anterior thalamic nuclei lesions (Jenkins et al., 2004) it becomes increasingly likely that the present lesions might also be sufficient to disrupt plasticity. Fourth, the retrosplenial cortex is abnormally sensitive to systemic NMDA receptor modulation (Olney et al., 1993; 1998) highlighting its potential sensitivity to the loss of these glutamatergic inputs. Finally, the growing evidence that the activity of *c-fos* and *zif*268 is integral to many neuronal functions, including neuronal plasticity (Herdegen and Leah, 1998; Hughes et al., 1999; Tischmeyer and Grimm, 1999, see Chapter 1), makes it increasingly unlikely that tissue showing chronically low IEG levels could contribute normally to tests of learning and memory.

The lack of any marked changes in retrosplenial c-Fos levels after entorhinal cortex lesions provides evidence for the specificity of the response to hippocampal damage. This region provides an ideal control as the lesion methodology was identical to that used in Experiment 3 and the lesion placement was immediately adjacent to the hippocampus. Not only does the entorhinal cortex have some direct projections to the retrosplenial cortex (Van Groen and Wyss, 1992; Insausti et al., 1997) but the granular retrosplenial

cortex is also innervated by the subiculum (Van Groen and Wyss, 1990, 1992) which, in turn, is innervated by the entorhinal cortex. The surprising lack of a clear change in retrosplenial cortex accords with the report that aspiration lateral entorhinal cortex lesions need not decrease, and can indeed increase, c-*fos* in the hippocampus, parietal cortex and piriform cortex (Bernabeu et al., 2006). The present null result can also be added to that seen after postrhinal cortex lesions (Jenkins *et al.*, 2004), and so highlights the specificity of the hippocampal lesion effects on retrosplenial cortex.

The patterns of c-Fos and Zif268 changes following hippocampal lesions can be compared with those seen after anterior thalamic lesions. Like the hippocampus, the anterior thalamic nuclei have dense, reciprocal connections with area 29. While lesions in both the hippocampus and anterior thalamic nuclei produce a dramatic fall in retrosplenial c-Fos and Zif268 levels (Jenkins et al., 2004a; Poirier and Aggleton, 2009), there is at least one clear difference. The IEG changes following anterior thalamic lesions are extremely evident in the superficial laminae of the retrosplenial granular b cortex but not in the deeper laminae (Jenkins et al., 2004a). This laminae selectivity was not seen in the present study (Figure 14, there was a decrease of c-Fos activity across the three sub-regions of the retrosplenial cortex) as in addition to the striking loss of superficial label there was also a clear loss of deeper IEG label, sometimes seen as a cell-free band in layer V (Figures 4, 8). The difference presumably reflects the fact that hippocampal inputs to the retrosplenial cortex are focused in lamina I-III (especially II), while the anterior thalamic inputs terminate in I, III, IV with much lighter terminations in lamina II (Van Groen and Wyss, 1990c, 1992, 2003). Nevertheless, it is striking that lesions in both the anterior thalamic nuclei and the hippocampus both have such remarkable effects on IEG levels in the retrosplenial cortex, and this common effect adds weight to other evidence from rats showing that these three regions (the hippocampus, anterior thalamic nuclei, retrosplenial cortex) function together to support aspects of memory (Sutherland and Hoesing, 1993; Warburton et al., 2001).

The importance of retrosplenial dysfunction to various neurological conditions is only gradually emerging. Of especial, potential relevance to the present study are the findings of retrosplenial hypoactivity in Alzheimer's disease, Mild Cognitive Impairment, Korsakoff's disease, and other forms of diencephalic amnesia (Fazio et al., 1992; Aupee et al., 2001; Reed et al., 2003; Nestor et al., 2003b). The retrosplenial cortex is one of the first brain sites to show metabolic hypoactivity in Alzheimer's disease (Minoshima et al., 1997; Nestor et al., 2003a). In the early stages of this disease, three of the very earliest sites to show overt pathology (amyloid plaques and neurofibrillary tangles) are the entorhinal cortex, the hippocampus and the anterior thalamic nuclei (Braak and Braak, 1991a, 1991b). Thus, it has been suggested that retrosplenial hypoactivity is a response to deafferentation from such sites (Fazio et al., 1992; Meguro et al., 1999; Hirao et al., 2006). In addition to extrinsic pathology, recent studies have found evidence of intrinsic pathology within the retrosplenial cortex in patients with Mild Cognitive Impairment and early Alzheimer's disease (Scahill et al., 2002; Pengas et al., 2008). It is striking, therefore, that when two of these three sites (hippocampus, anterior thalamus) are damaged a very marked IEG hypoactivity is found in retrospienial cortex. These findings support the notion that the retrosplenial hypoactivity seen in Alzheimer's disease is a secondary response to distal damage in these limbic sites.

Chapter 3

The Effects of Mammillothalamic Tract Lesions on the Extended Hippocampal Memory System Activity, as Measured by Immediate-Early Gene Expression

Introduction

The mammillothalamic tract (MTT) offers a uniquely informative target for the study of diencephalic memory mechanisms as it is the only diencephalic structure consistently associated with amnesia after strokes (von Cramon et al., 1985; Graff-Radford et al., 1990; Clarke et al., 1994; Van der Werf et al., 2003; Yoneoka et al., 2004; Carlesimo et al., 2007). At present, most accounts describing the role of the medial diencephalon in memory emphasize the importance of the hippocampal inputs to the region; indeed the mammillary bodies and anterior thalamus are often referred to as an "extended-hippocampal memory system" (Delay and Brion, 1969; Gaffan, 1992; Aggleton and Brown, 1999; Gaffan, 2001). While the hippocampus-fornix-mammillary body pathway has repeatedly been implicated in episodic memory, we still lack consensus on why diencephalic damage, and damage to the MTT in particular, might disrupt memory.

One of the first accounts was that the mammillary bodies and anterior thalamus formed part of a system by which information from the hippocampus reaches the cingulate cortex (Barbizet, 1963; Delay and Brion, 1969). According to this account, MTT lesions would indirectly prevent the hippocampal outputs reaching the anterior thalamus and, hence, the cingulate cortex, thus impairing memory formation. A second hypothesis is that the medial diencephalon, including the MTT, serves as a critical, indirect link connecting the hippocampus to the prefrontal cortex (Warrington and Weiskrantz, 1982). A third hypothesis combines the previous two hypotheses by proposing that diencephalic damage causes widespread cortical dysfunction, again due to a loss of hippocampal inputs, and this is responsible for subsequent memory impairment (Mair et al., 1979; Paller, 1997; Vann and Aggleton, 2004b). These three hypotheses can all accommodate the finding that MTT lesions impair spatial tasks that depend on the integrity of the hippocampus and anterior thalamic nuclei (Field et al., 1978; Vann et al., 2003a) and all emphasize the importance of hippocampal inputs to the medial diencephalon. However, because the hippocampus also directly projects to both the prefrontal cortex and cingulate cortex, the mammillary bodies and/or anterior thalamus would need to provide additional information or these indirect pathways would seem redundant. A fourth hypothesis is that diencephalic and medial temporal lobe amnesias are largely independent (Parkin, 1984). The prediction is that the effects of damage to the MTT and hippocampus should be very different, and that MTT damage would not affect normal hippocampal function.

To determine how MTT damage might result in memory impairments, the impact of MTT lesions on behaviourally-induced activity was measured in three key regions: the retrosplenial cortex, the prefrontal cortex and the hippocampus. The MTT appears unique amongst fibre tracts linked to episodic memory as it only carries connections that comprise the putative memory system (Delay and Brion, 1969; Aggleton and Brown, 1999), i.e., it does not project to additional structures (Cruce, 1975). Furthermore, the MTT is only indirectly connected to the three key regions under investigation. Consequently, any observed activity changes in these three regions cannot be due to direct

deafferentation, nor can they be predicted with any certainty from standard neuroanatomical analyses.

The functional effects of MTT lesions on target brain structures were assessed by the expression of an immediate-early gene, c-*fos*. While Fos has low basal levels its expression has repeatedly been linked to increased neural activity (Sagar et al., 1988; Dragunow and Faull, 1989) and has been implicated in learning and memory (e.g. Tischmeyer and Grimm, 1999; Guzowski, 2002); blocking Fos expression by use of antisense oligodeoxynucleotides can disrupt performance on tasks that normally increase c-*fos* activity (e.g. Morrow et al., 1999; He et al., 2002; Seoane and Brown, 2007). In addition, c-Fos increases in the three target regions (retrosplenial cortex, prefrontal cortex, hippocampus) are associated with the performance of spatial memory tasks by normal rats (Vann et al., 2000a; Vann et al., 2000c). Finally, to determine the specificity of any observed c-Fos changes, comparisons were made with the effects of amygdala lesions. This limbic structure was selected as it has direct connections with the hippocampus and prefrontal cortex, but damage to the amygdala does not result in amnesia nor typically impairs spatial memory.

To induce c-Fos activation, all animals were given forced-runs in a radial-arm maze in a novel room (Vann et al., 2000a; Vann et al., 2000c; Jenkins et al., 2002b). The forced-run version of the radial-arm maze was used as rats with MTT lesions are impaired on standard version of the radial-arm maze task (Vann et al., 2003a). Therefore in the standard version, MTT lesioned animals would be expected to make more errors than the surgery control group and so the two groups would not be behaviourally matched for the immediate-early gene experiment. For this reason, access to individual arms was controlled by the experimenter to avoid abnormal arm choices by the MTT group. Moreover, this task has been shown to increase c-Fos expression in a number of sites (hippocampus, retrosplenial cortex, prelimbic cortex, postrhinal cortex, perirhinal cortex, and parasubiculum) compared to animals performing the same task in a familiar room (Jenkins et al., 2002).

The present study revealed that MTT and amygdala lesions produce very different patterns of c-Fos expression, the former pattern clearly distinguishing between the four hypotheses under investigation.

Materials and Methods

Animals

The study involved 36 naïve, male, pigmented rats (DA strain, Harlan. Bicester, UK) weighing between 215 g and 250 g at the time of surgery. After a post-surgery recovery period of at least 10 days, the rats were deprived to 85% of their free-feeding body weight and were maintained at this level or above throughout the experiment. Water was available *ad libitum.* Rats were housed in pairs under diurnal conditions (14 h light, 10 h dark), and testing occurred at a regular time during the light period. Animals were thoroughly habituated to handling before the study began. All experiments were performed in accordance with the UK Animals (Scientific Procedures) Act (1986) and associated guidelines.

Surgical procedure

First, twenty rats were divided into two cohorts: bilateral mammillothalamic tract lesions (MTTx, n = 10) and surgical controls (n = 10). The surgeries were made by Dr. SD Vann. Animals were deeply anesthetised by intraperitoneal injection of sodium pentobarbital (60 mg/kg). Each animal was then placed in a stereotaxic headholder (David Kopf instruments, Tujunga, CA). A longitudinal incision was made in the scalp, which was retracted to expose the skull. The skull was drilled at the point of the lesion. The MTT lesions were made by radiofrequency using a Radionics TCZ (Radionics, Burlington, VT) electrode (0.7 mm tip length, 0.25 mm diameter). The electrode was lowered vertically and the tip temperature was raised to 60°C for 15 sec using an RFG4-A Lesion Maker (Radionics). The stereotaxic coordinates were: anteroposterior (AP)

+4.2, lateral-medial (LM) ±0.9 (both relative to bregma), and dorsoventral (DV), -6.9 mm from top of cortex; the incisor bar was set at +5.0. For the MTT surgical controls the probe was positioned at the same AP and LM but was only lowered to DV -5.9 to avoid damaging the tract, and the temperature was not raised.

The remaining 16 rats were divided into two groups: bilateral amygdala lesions (n = 8) and surgical controls (n = 8). Bilateral amygdala lesions were made by injecting 0.42 µL of 0.9M N-methyl-D-aspartate (NMDA; Sigma Chemical Company Ltd., UK) dissolved in phosphate buffer (pH 7.2) into one site in each hemisphere using a 1-µL Hamilton syringe (Bonaduz, Switzerland). Each injection was made gradually over a 5-min period and the needle was left *in situ* for a further 5 min before being withdrawn. The stereotaxic coordinates relative to bregma were: AP -0.8, LM ±4.0, DV -9.7 with the incisor bar again being set at +5.0. The surgical controls underwent the same procedure with the needle being lowered, but without the injection of NMDA.

After every surgery, the skin was sutured, antibiotic powder applied (Acramide: Dales Pharmaceuticals, UK), and the animal placed in a temperature-controlled recovery box. Animals also received 5 ml of glucose saline subcutaneously; Paracetamol and sucrose were added to the rats' drinking water for three days post-surgery.

Behavioural testing

Apparatus

Testing was carried out in an eight-arm radial maze. The maze consisted of an octagonal central platform (34 cm diameter) and eight equally spaced radial arms (87cm long, 10cm wide). The base of the central platform and the arms were made of wood, whereas panels of clear Perspex (24 cm high) formed the

walls of the arms. At the start of each arm was a clear Perspex guillotine door (12 cm high) attached to a pulley.

Two identical radial-arm mazes placed in two different rooms were used for the experiment. The two rooms (295 x 295 x 260 cm and 255 x 330 x 260 cm) were markedly different (i.e., size, shape, lighting) and contained distinct, salient, visual cues such as geometric shapes and high-contrast stimuli on the walls.

Behavioural training

Animals were allowed to recover for a minimum of three weeks before maze training began. All animals were first thoroughly habituated to handling and then matched pairs (one lesion, one control) were trained for 11 days to run down pre-selected arms of an eight-arm radial maze in order to retrieve sucrose reward pellets (45 mg; Noyes Purified Rodent Diet, Lancaster, NH, USA) from the end of the arm. On the final test day (day 12) the animals performed the same task but in a novel room. At the beginning of each trial all arms were baited (a trial comprises a visit to all eight arms); the experimenter controlled each arm the animals visited by using a pulley system to open the guillotine door at the start of the arm. When all eight arms had been visited (i.e. the trial had been completed) the rat was contained in a holding box for approximately 2 min whilst all arms were rebaited. Each session consisted of multiple trials in the radial-arm maze, one after the other, and lasted 20 min. Different, randomised arm sequences were used on successive trials. Matched pairs of animals both completed the same number of trials and visited the same arms in the same order. Each animal was placed in a holding box in a quiet, dark room for 30 min before and 90 min after each radial-arm maze session. This time window was chosen as peak levels of the c-Fos protein are found approximately 90 min after activation (e.g. Sharp et al., 1993; Bisler et al., 2002; Zangenehpour and Chaudhuri, 2002).

IEG immunohistochemistry

c-Fos. Ninety minutes after completing the final radial-arm maze session in the novel room, rats were deeply anesthetised with sodium pentobarbital (60 mg/kg, Euthatal, Rhone Merieux, UK) and transcardially perfused with 0.1 M phosphate buffer saline (PBS) followed by 4% paraformaldehyde in 0.1 M PBS (PFA). The brains were removed and postfixed in PFA for 4 h and then transferred to 25% sucrose overnight at room temperature with rotation. Sections were cut at 40 µm on a freezing microtome in the coronal plane. One series (one-in-three sections) was collected in PBS. Sections were transferred to 10 mM citrate buffer (pH=6) dissolved in deionised H_2O. Sections were incubated in a water bath at 70°C for 30 min. Endogenous peroxidase was blocked by incubating the sections in 0.3% hydrogen peroxide in PBST for 10 min, before rinsing several times with PBST. Sections were next incubated in PBST containing c-Fos rabbit polyclonal antibody (1:5000; Ab-5, Oncogene Science, UK), for 48 h at 4°C with periodic rotation. Sections were then washed with PBST and incubated for c-Fos in biotinylated goat anti-rabbit secondary antibody (diluted 1:200 in PBST; Vectastain, Vector Laboratories, Burlingame, USA) and 1.5% normal goat serum. Sections were then washed and processed with avidin-biotinylated horseradish peroxidase complex in PBST (Elite Kit, Vector Laboratories) for 1 h at room temperature, again with constant rotation. Sections were washed again in PBST and then in 0.05 M Tris buffer. The reaction was then visualized using diaminobenzidine (DAB Substrate Kit, Vector Laboratories) and finally stopped by washing in cold PBS. Sections were mounted on gelatine-coated slides, dehydrated through a graded series of alcohols and cover-slipped. The tissue from each behaviourally matched pair of animals was processed simultaneously. A second one-in-three series was mounted directly onto gelatine-coated slides and stained using cresyl violet, a Nissl stain, for verification of the lesion and histological identification of specific brain regions.

IEG cell counts

Estimates were made of IEG-positive cells by using an automated cell counting procedure. Counting procedures were carried out without knowledge of the group assignments. Images were viewed on a Leica DMRB microscope and photographed using an Olympus DP70 camera. The program analySIS^D (Soft-Imaging Systems; Olympus, UK) was used to count the number of nuclei above threshold. The counts were made in a frame area of 0.84 x 0.63 mm, which enabled all laminae to be included in one image. For all hippocampal counts (dorsal, ventral, dentate gyrus, CA3, and CA1), the entire extent of the target region within the selected coronal sections was assessed. These counting procedures were not stereological, and so while providing information about relative numbers of cells they do not provide accurate counts of absolute cell numbers.

For all brain areas analysed (Figure 1), counts were taken from at least four consecutive sections from each hemisphere and these counts were averaged to produce a mean. Scores were normalised to reduce variability in levels of c-Fos counts across matched pairs of animals (one lesion and one surgical control). The scores were normalised by dividing the mean number of activated neurons in a given animal for a given site by the combined mean of the two animals in each matched pair and expressing the result as a percentage. This normalisation procedure also equates the cell counts from different regions, which would otherwise vary considerably. However, as normalisation can make interactions difficult to interpret, raw cell-counts were also analysed for comparison purposes.

Regions of interest

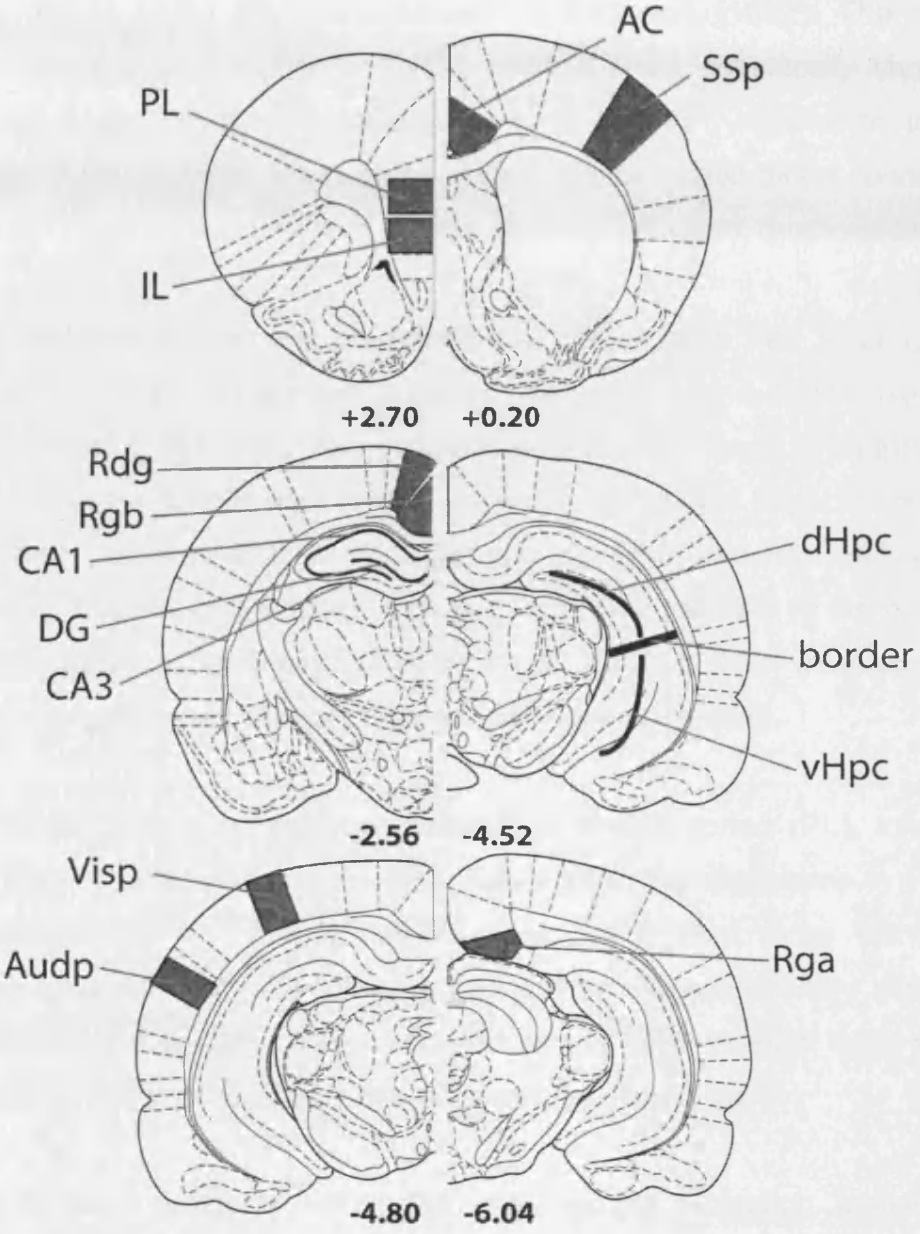

Figure 1. Diagrams of coronal sections indicating regions of interest investigated: anterior cingulate cortex (AC), primary auditory cortex (Audp), CA1, CA3, dentate gyrus (DG), dorsal hippocampus (dHpc), ventral hippocampus (vHpc), infralimbic cortex (IL), prelimbic cortex (PL), presubiculum (Pre), retrosplenial dysgranular cortex (Rdg), retrosplenial granular a (Rga), retrosplenial granular b (Rgb), primary somatosensory cortex (SSp), primary visual cortex (Visp). The numbers refer to the distance (mm) from bregma according to the atlas of Paxinos and Watson (1997).

Cytoarchitectonic subfields were identified from coronal sections (Paxinos and Watson, 1997), using the nomenclature of Swanson (1992). The regions sampled are depicted in Figure 1. The regions were specifically chosen to either test three potential hypotheses or were "control" regions to test the specificity of any findings. None of the chosen regions have direct connections with the MTT and as such none of the results reflected direct deafferentation.

The retrosplenial cortex can be subdivided (Wyss and Van Groen, 1992; Shibata et al., 2009) into granular b cortex (Rgb), granular a cortex (Rga), and the dysgranular cortex (Rdg) and separate counts were made in all three sub-regions. Separate counts were also made in the superficial (layer II and upper III) and deep (lower layer III to VI) layers of Rdg, Rgb, and Rga as lesions of the anterior thalamic nuclei have been shown to affect activity in the deep and superficial layers differentially (Jenkins et al., 2002b). This deep/superficial border is signalled by an abrupt change in cell packing density.

Three frontal regions were also examined: prelimbic cortex (PL), infralimbic cortex (IL) and anterior cingulate (AC) cortex (using designations in Paxinos and Watson, 1997). Finally, counts were taken from three comparison sensorimotor areas (primary visual area, primary somatosensory area, and primary auditory area) which were selected as any differences in these regions might reflect abnormal sensorimotor patterns following surgery.

Cytoarchitectonic subfields within the hippocampal formation consisted of dentate gyrus (DG), CA3, and CA1. The "dorsal" and "ventral" hippocampal division corresponded to DV level -5.0 from bregma. This "dorsal/ventral" distinction was used as it maps directly onto borders used for lesion studies (e.g. Moser et al., 1993; Bannerman et al., 1999) and previous IEG studies (e.g. Vann et al., 2000c); the "dorsal" (dHPC) distinction used in the present study has also been categorised as "intermediate" hippocampus and "ventral" (vHPC) is equivalent to "temporal" hippocampus (Bast, 2007; Bast et al., 2009). The dorsal (intermediate) and ventral (temporal) hippocampal counts involved just the DG and fields CA1 and CA3, i.e., not the subiculum complex. At this level the dentate gyrus is present in both the dorsal (intermediate) and ventral

(temporal) hippocampus. c-Fos-positive cells in the hippocampal formation were counted by Dr. SD Vann but it was decided to retain these counts for comparison purposes (Vann and Albasser, 2009).

Statistics

The data from the hippocampus, frontal cortex, retrosplenial cortex, and control areas were grouped separately before being investigated in separate analyses of variance. When significant interactions were found the simple effects for each brain region were analysed as recommended by Winer (1971); on occasions when there was a significant main effect but no group x region interaction the simple effects were examined so that regions which significantly differed between groups could be identified (Howell, 1987). The probability level of 0.05 was taken as being statistically significant. Raw counts were also analyzed but due to the high level of variation in cell counts across pairs of animals but high correlation within the matched pairs, the raw scores were analyzed using a within-subject design. For the direct amygdala/MTT comparisons, a 2x2x6, 2x2x3 and 2x2x2 design were used for retrosplenial cortex, frontal cortices, and dorsal/ventral hippocampus, respectively; each analysis comprised one between- and two within-subject factors.

Results

Histological analysis

Mammillothalamic tract lesions (MTTx)

Ten rats received lesions of the MTT while a further ten underwent sham surgery to act as controls. Nine of the ten MTTx rats had complete, bilateral lesions of the MTT whilst one rat had minor sparing in the left MTT. In this one case, cell counts were only taken from the right hemisphere. All lesions were discrete and so only produced very limited damage to the medial-most part of

the zona incerta immediately adjacent to the tract (Figure 2A); this comprised only a very small amount of the total volume of the zona incerta, which extends rostral and caudal to the level of the lesion.

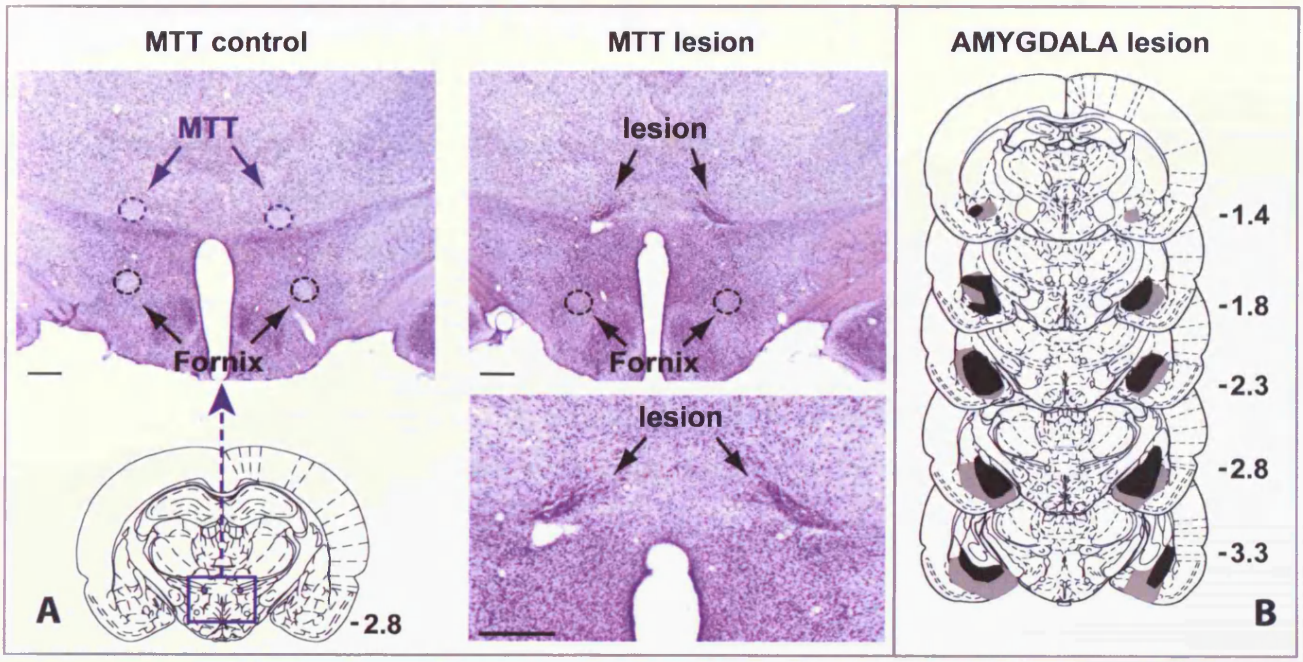

Figure 2. A. Photomicrograph of coronal sections showing a surgical control on the left and a typical MTT lesion on the right. Scale bar, 100 µm. **B.** Diagrammatic reconstructions of the amygdala lesions showing the cases with the largest (grey) and smallest (black) lesions. The numbers refer to the distance (mm) from bregma according to the atlas of Paxinos and Watson (1997).

Amygdala lesions

Eight animals received bilateral lesions of the amygdala with a further eight undergoing sham surgery to act as controls. The lesions were placed centrally within the amygdala (Figure 2B). All major nuclei were included, and any sparing tended to be in the most lateral aspect of this structure. The lesions did not encroach into the piriform or entorhinal cortices, although in all animals

there was a very small amount of cell loss to that part of the ventral striatum directly above the central nucleus.

Behavioural test

On the final test day, matched pairs of animals performed a forced-run version of the eight-arm radial maze task in a novel room. After 20 min testing the animals completed a mean of 4.1 ±0.5 trials (a trial comprises a visit to all eight arms). This number was fewer than that completed on the last day of training in the familiar room (4.6 ± 0.8; Wilcoxon $T = 247$, $p < 0.01$), presumably reflecting the animals' reaction to the new environment. There was no difference between the number of trials completed by the amygdala lesion or MTTx groups (Mann-Whitney $U = 68$, $p > 0.5$), which were both matched to their controls in terms of number of trials.

Immediate-early gene cell counts: c-Fos-positive cells

To test the hypotheses under investigation, three brain regions were assessed: retrosplenial cortex, frontal cortices and hippocampal formation. In addition, immediate-early gene activity was assessed in three control sites to determine the specificity of any findings. The areas analysed were identified from coronal sections; the areas sampled are depicted in Figure 1. For completeness, analyses of both normalised (Figure 3) and raw counts (Figure 4) of nuclei are presented.

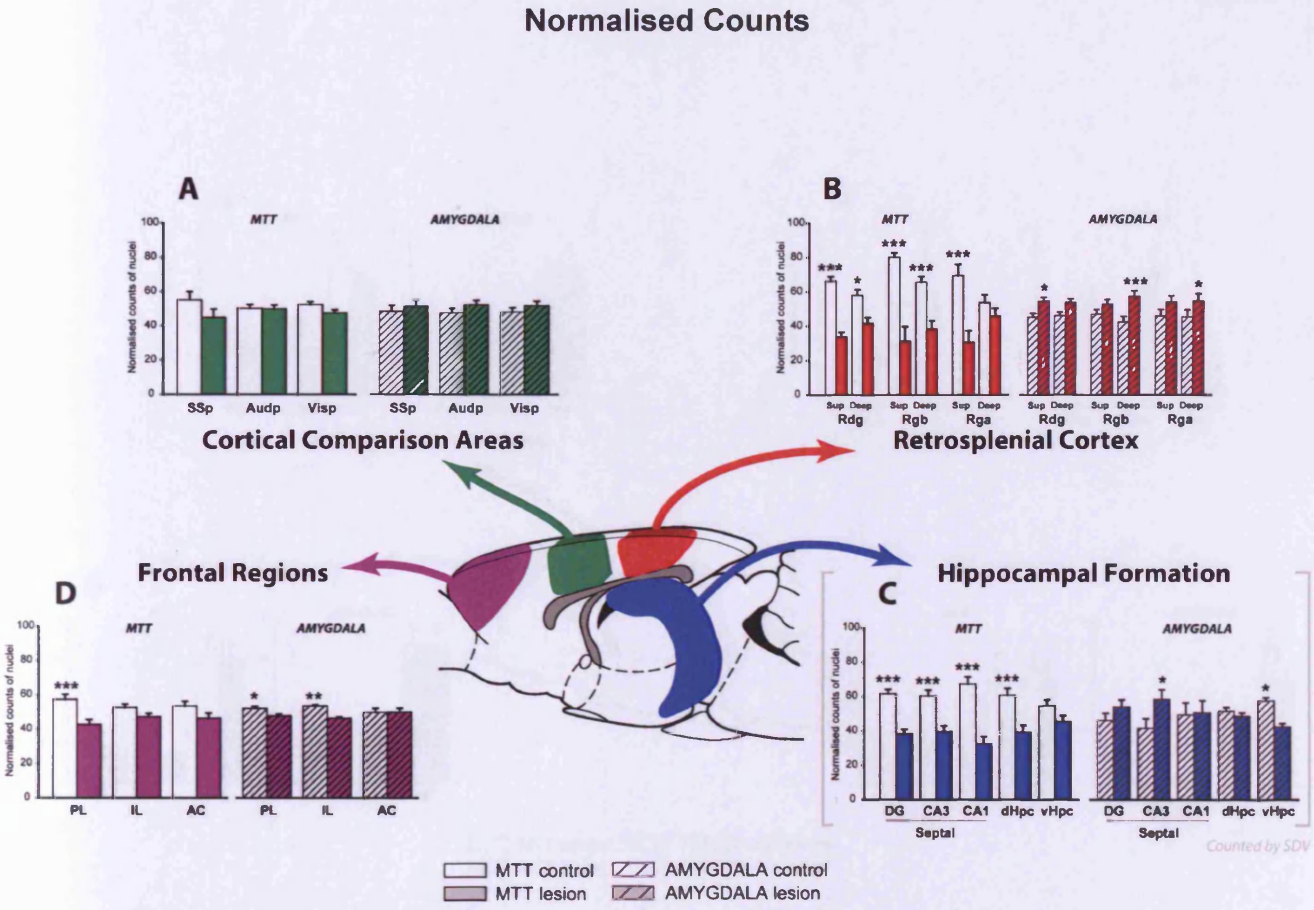

Figure 3. Overview of the *normalised* counts of c-Fos-positive cells following bilateral MTT and bilateral amygdala lesions in the four main regions counted. **A**. *Cortical Comparison Areas:* primary somatosensory cortex (SSp), primary auditory cortex (Audp), primary visual cortex (Visp). **B.** *Retrosplenial Cortex*: superficial and deep layers of the dysgranular (Rdg) and the granular (Rgb and Rga) retrosplenial cortex **C**. *Hippocampal Formation*: dentate gyrus (DG), CA3, CA1, dorsal (dHpc) and ventral (vHpc) hippocampus. **D.** *Frontal Regions*: prelimbic (PL), infralimbic (IL) and anterior cingulate (AC) cortices. Normalised counts of c-Fos-positive cells are presented as mean ± SEM. Significance levels: *$p < 0.05$; **$p < 0.01$; ***$p < 0.001$.

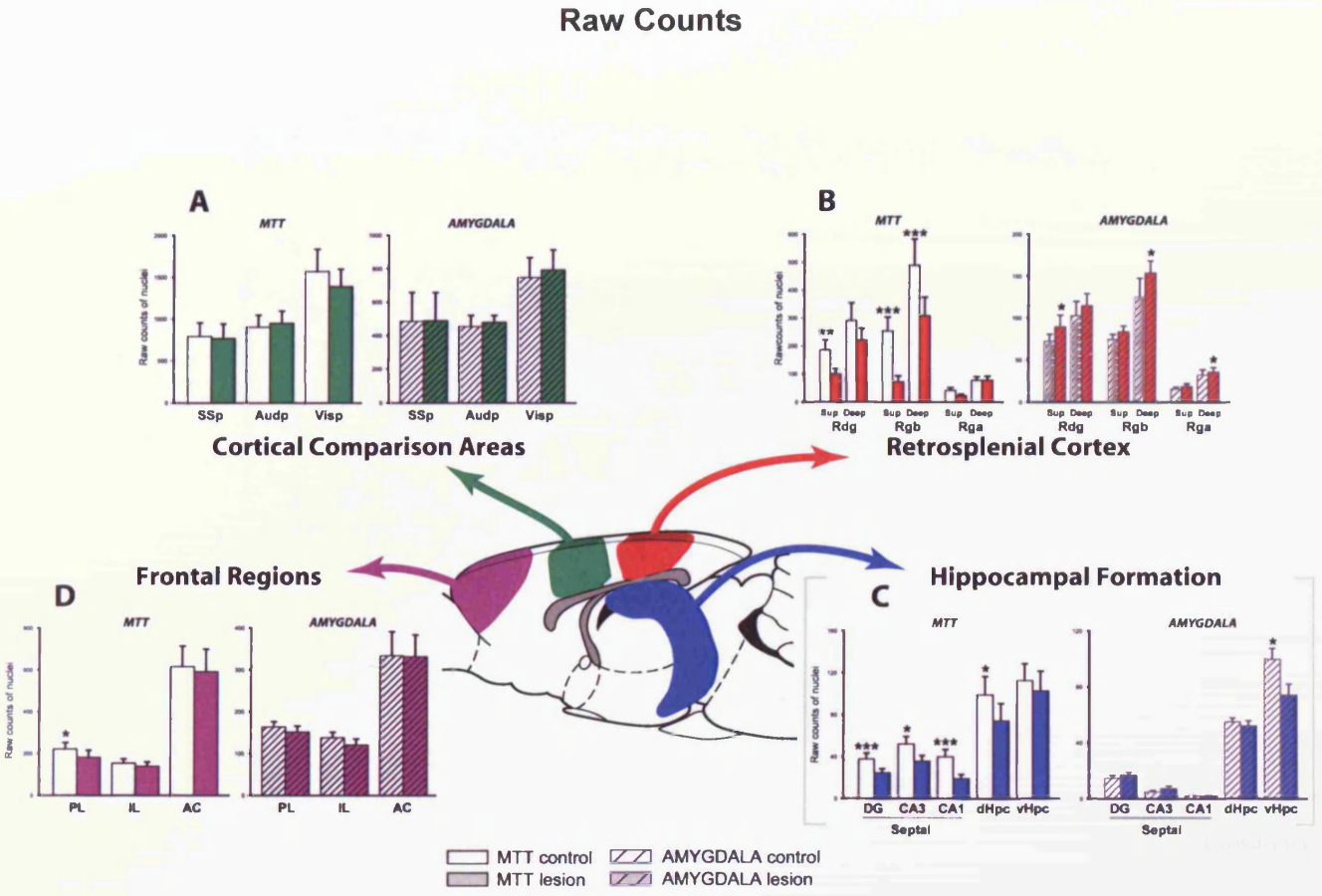

Figure 4. Overview of the *raw* counts of c-Fos-positive cells following bilateral MTT and bilateral amygdala lesions in the four main regions counted. **A**. *Cortical Comparison Areas:* primary somatosensory cortex (SSp), primary auditory cortex (Audp), primary visual cortex (Visp). **B.** *Retrosplenial Cortex*: superficial and deep layers of the dysgranular (Rdg) and the granular (Rgb and Rga) retrosplenial cortex. **C**. *Hippocampal Formation*: dentate gyrus (DG), CA3, CA1, dorsal (dHpc) and ventral (vHpc) hippocampus. **D.** *Frontal Regions*: prelimbic (PL), infralimbic (IL) and anterior cingulate (AC) cortices. Raw counts of c-Fos-positive cells are presented as mean ± SEM. Significance levels: **p* < 0.05; **p < 0.01; ****p* < 0.001.

Retrosplenial cortex

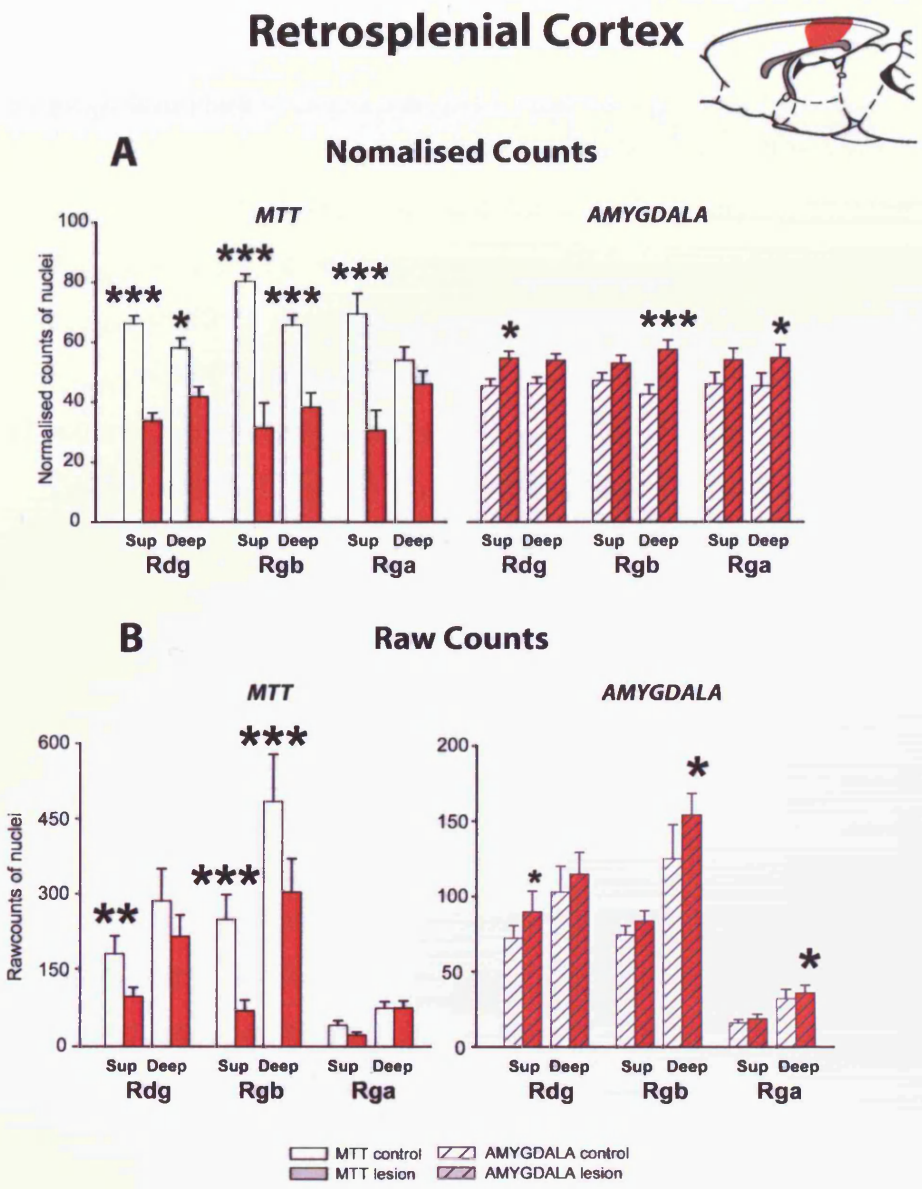

Figure 5. c-Fos levels in the retrosplenial cortex following bilateral MTT lesions and their controls (left-hand side histograms) and bilateral amygdala lesions and their controls (right-hand side histograms). **A.** Normalised counts and **B.** raw counts of c-Fos-positive cells are presented as mean ± SEM. Significance levels: *$p < 0.05$; **$p < 0.01$; ***$p < 0.001$. Abbreviations: *Retrosplenial Cortex*: superficial and deep layers of the dysgranular (Rdg) and the granular (Rgb and Rga) retrosplenial cortex.

MTT lesions resulted in highly significant c-Fos decreases in the retrosplenial cortex (group, $F_{(1,18)} = 32.2$, $p < 0.001$; group x region interaction, $F_{(5,90)} = 9.3$, $p < 0.001$; Figure 6). The significant interaction reflected the fact that the greatest c-Fos decrease was in the superficial layers of the retrosplenial cortex (Figure 5A). Subsequent analyses showed that MTT lesions significantly reduced c-Fos both in the superficial (II and upper III) and in the deep (lower III to VI) layers for all three retrosplenial sub-regions, except for the deep layers of Rga (Rdg: superficial, $F_{(1,108)} = 23.2$, $p < 0.001$, deep, $F_{(1,108)} = 5.8$, $p < 0.05$; Rgb: superficial, $F_{(1,108)} = 52.7$, $p < 0.001$, deep, $F_{(1,108)} = 16.5$, $p < 0.001$; Rga: superficial, $F_{(1,108)} = 33.0$, $p < 0.001$, deep , $F_{(1,108)} = 1.38$, $p = 0.24$). As with the normalised scores, analyses of raw cell counts (Figure 5B) revealed a significant effect of lesion ($F_{(1,9)} = 22.5$, $p < 0.01$) and lesion x region interaction ($F_{(5,45)} = 14.1$, $p < 0.001$). The interaction was due to significant decreases in cell counts in superficial Rdg ($F_{1,9} = 17.8$, $p = 0.01$), and superficial and deep layers of Rgb ($F_{(1,9)} = 23.3$, $p < 0.001$ and $F_{(1,9)} = 27.4$, $p < 0.001$, respectively). There were borderline decreases in the deep layers of Rdg ($F_{(1,9)} = 4.70$, $p = 0.058$) and the superficial layers of Rga ($F_{(1,9)} = 4.73$, $p = 0.058$) but as with the normalised data there was no difference in the deep cell layers of Rga ($F < 1$).

The amygdala lesions also altered cumulative c-Fos-positive cell counts taken across all layers of the retrosplenial cortex ($F_{(1,14)} = 11.5$, $p < 0.01$) but in this case it was due to an *increase* in cell counts in the lesion group (Figure 5A). Although no group x region interaction was found ($F < 1$) the only sub-regions that showed significant differences were superficial layers of Rdg ($F_{(1,84)} = 4.4$, $p < 0.05$), deep layers of Rga ($F_{(1,84)} = 11.3$, $p < 0.001$) and deep layers of Rgb ($F_{(1,84)} = 4.5$, $p < 0.05$), all of which were due to an *increase* in c-Fos-stained nuclei level in the amygdala-lesion group. Analyses using raw scores (Figure 5B) resulted in a significant effect of lesion ($F_{(1,7)} = 6.0$, $p < 0.05$) due to increased cell counts following the amygdala lesion, but none of the simple effects reached significance [highest F value for deep layers of Rgb: ($F_{(1,7)} = 4.1$, $p = 0.08$)].

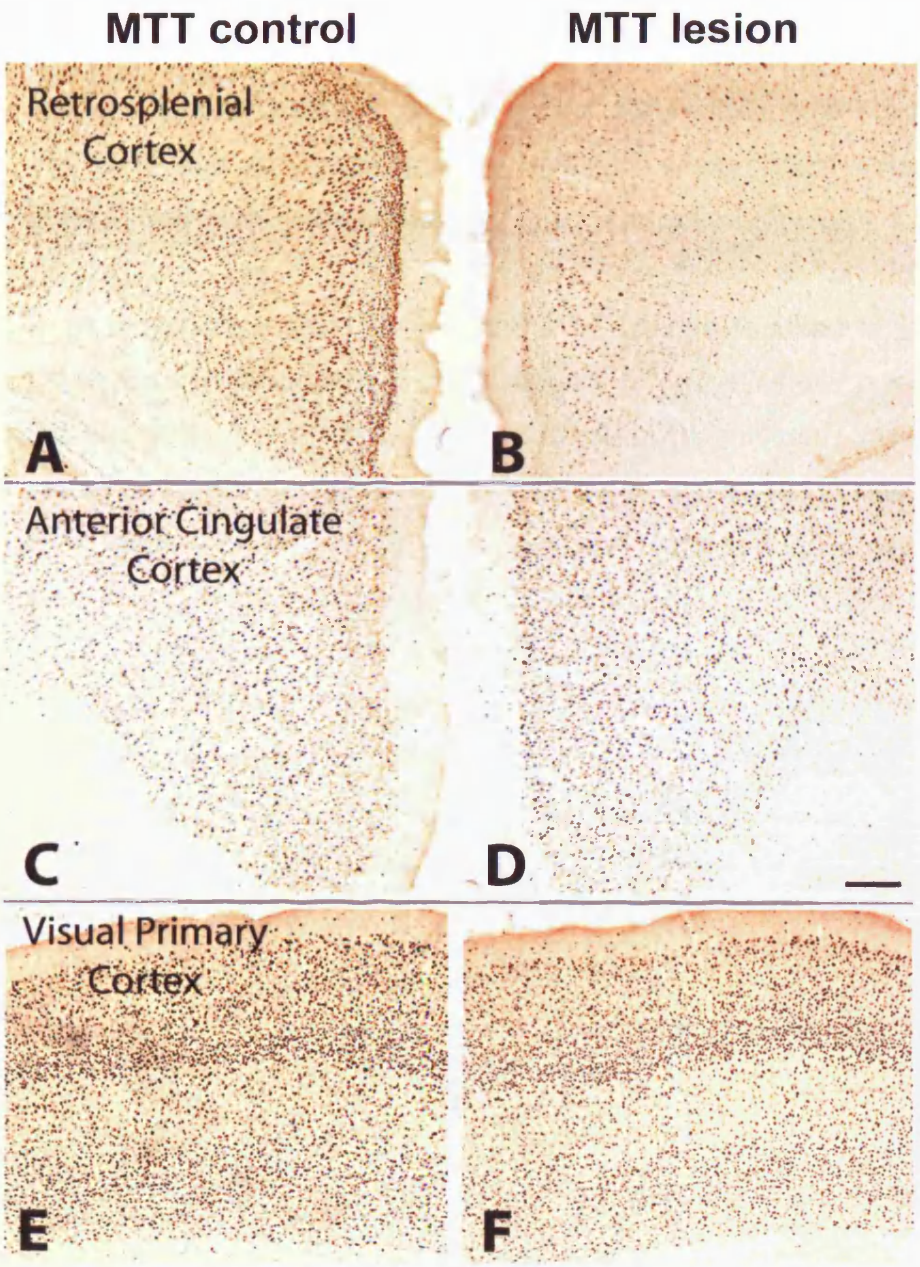

Figure 6. Photomicrographs comparing c-Fos levels in retrosplenial cortex (**A, B**), anterior cingulate cortex (**C, D**) and visual primary cortex (**E, F**) in rats with a control surgery (**A, C, E**) or bilateral MTT lesion (**B, D, F**). The photomicrographs are taken from behaviourally-matched pairs of animals where tissue was processed simultaneously to reduce variation. The brightfield photomicrographs of coronal sections show the comparable c-Fos levels in the anterior cingulate cortex which contrasts with the specific, striking loss of c-Fos-positive cells following MTT lesions in the retrosplenial cortex (**B** versus **A, C** versus **D**). Scale bar, 100 μm.

Direct comparisons of MTT/Amygdala lesion retrosplenial effects

Analyses using normalised scores for Rga cortex, Rgb cortex, and Rdg cortex for both the MTT and Amygdala groups revealed a significant experiment (MTT/Amygdala) x group (lesion/control) x region interaction ($F_{(5,160)} = 9.34$, $p < 0.001$) reflecting the very different pattern in retrosplenial activity following either MTT or amygdala lesion. Overall, the MTT lesions resulted in a highly significant decrease in retrosplenial c-Fos counts ($F_{(1,32)} = 74.84$, $p < 0.001$) whereas the amygdala lesions resulted in a small, but significant, *increase* in retrosplenial c-Fos counts ($F_{(1,32)} = 5.18$, $p < 0.05$). Analyses using raw scores resulted in a similar pattern of findings as there was a highly significant experiment x group x region interaction ($F_{(5,80)} = 12.1$, $p < 0.001$) and a significant experiment x group interaction ($F_{(1,16)} = 22.1$, $p < 0.001$). This was due to a significant difference between the c-Fos-positive cell counts in the MTT and amygdala lesion groups ($F_{(1,18)} = 13.86$, $p < 0.01$) but not control groups ($F_{(1,18)} = 1.52$, $p = 0.27$). In addition, there was a lesion effect in the MTT group ($F_{(1,16)} = 6.39$, $p < 0.05$) as there were fewer c-Fos-positive cells in the MTT group compared to the controls; there was no significant differences in c-Fos-positive counts in the retrosplenial cortex between the amygdala lesion and control groups ($F < 1$) .

Frontal Regions

Overall, there was a significant c-Fos reduction in frontal regions (prelimbic, infralimbic, and anterior cingulate; Figure. 7A) after MTT lesions (group, $F_{(1,18)} = 18.36$, $p < 0.001$). While there was no group x region interaction ($F_{(2,36)} = 1.71$, $p = 0.19$), the simple effects revealed that only the prelimbic counts significantly decreased after MTT lesions ($F_{(1,54)} = 15.29$, $p = 0.001$). With the raw cell counts (Figure 6B), there was only a borderline lesion effect for the frontal regions ($F_{(1,9)} = 4.5$, $p = 0.06$) and no lesion effect for any of the regions individually (prelimbic, $p = 0.11$; infralimbic, $p = 0.3$; anterior cingulate, $F < 1$).

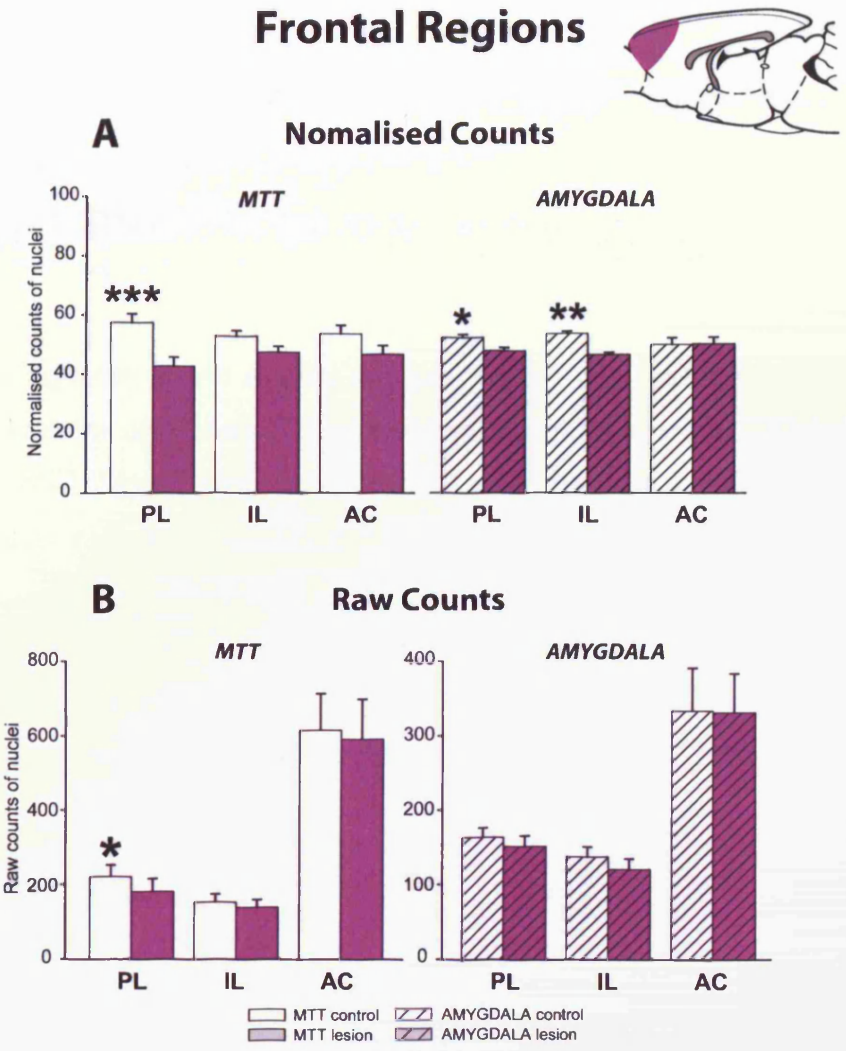

Figure 7. c-Fos levels in the frontal regions following bilateral MTT lesions and their controls (left-hand side histograms) and bilateral amygdala lesions and their controls (right-hand side histograms). **A.** Normalised counts and **B.** raw counts of c-Fos-positive cells are presented as mean ± SEM. Significance levels: *p < 0.05; **p < 0.01; ***p < 0.001. Abbreviations: *Frontal Regions*: prelimbic (PL), infralimbic (IL) and anterior cingulate (AC) cortices.

As with the MTT lesions, the amygdala lesions produced a significant group effect (Figure 7A; $F_{(1,14)} = 7.15$, $p < 0.05$) and a group x region interaction ($F_{(2,28)} = 3.7$, $p < 0.05$). This interaction reflected significant lesion-induced c-Fos reduction in both prelimbic ($F_{(1,40)} = 4.4$, $p < 0.05$) and infralimbic ($F_{(1,40)} = 11.4$, $p < 0.01$) cortices but not in the anterior cingulate cortex ($F < 1$). Analyses using raw scores (Figure 7B) also revealed a significant effect of lesion ($F_{(1,7)} =$

10.5, $p < 0.05$), but while the amygdala lesion-induced decrease in infralimbic cortex was highly significant ($F_{(1,7)} = 6.8$, $p < 0.05$) the decrease in prelimbic cortex was only borderline ($F_{(1,7)} = 5.1$, $p = 0.059$). Again, there was no difference in cell counts in the anterior cingulate cortex ($F < 1$; Figure 6).

Direct comparisons of MTT/Amygdala lesion frontal cortex effects

Analyses using normalised scores for the infralimbic, prelimbic and anterior cingulate cortex for both the MTT and Amygdala groups showed no significant experiment (MTT/Amygdala) x group (lesion/control) x region interaction ($F_{(2,64)} = 1.81$, $p = 0.1$), reflecting the similarity in lesion-induced effects in these frontal regions. In addition, there was no experiment (MTT/Amygdala) x group (lesion/control) effect ($F_{(1,32)} = 3.76$, $p = 0.061$). The same pattern was found using raw scores as there was no experiment x group x region interaction ($F < 1$) and no experiment x group interaction ($F_{(1,16)} = 3.69$, $p = 0.073$).

Hippocampal formation

The hippocampal formation data were counted by Dr. SD Vann. They remain in the Chapter for the purpose of comparison with the remaining findings (Vann and Albasser, 2009). MTT lesions caused a highly significant reduction in c-Fos-stained nuclei in the hippocampus proper ($F_{(1,18)} = 68.7$, $p < 0.001$; Figure 8A), with varying degrees of reduction in different sub-regions. c-Fos hypoactivity was seen in all sub-regions of the septal pole of the hippocampus (DG, $F_{(1,90)} = 21.3$, $p < 0.001$; CA3, $F_{(1,90)} = 17.0$, $p < 0.001$; CA1, $F_{(1,90)} = 47.5$, $p < 0.001$) as well as the more caudal, dorsal (intermediate) hippocampus (dHpc, $F_{(1,90)} = 18.1$, $p < 0.001$). The lack of a significant c-Fos decrease in the ventral (temporal) hippocampus (vHpc, $F_{(1,90)} = 3.4$, $p > 0.05$) reflected a dorsal/ventral hippocampal difference, and accounted for the group x region interaction ($F_{(4,72)} = 3.6$, $p < 0.01$). Exactly the same pattern of results was found with the raw cell counts (Figure 8B: MTT lesions resulted in a significant overall reduction in c-Fos-stained nuclei in the hippocampus proper ($F_{(1,9)} = 15.73$, $p < 0.01$). Simple effects revealed significant decreases in all sub-

regions counted apart from the ventral (temporal) hippocampus (DG, $F_{(1,9)}$ = 16.3, $p < 0.001$; CA3, $F_{(1,9)}$ = 17.0, $p < 0.05$; CA1, $F_{(1,9)}$ = 34.3, $p < 0.001$; dHPC, $F_{(1,9)}$ = 8.0, $p < 0.05$; vHPC, $F < 1$).

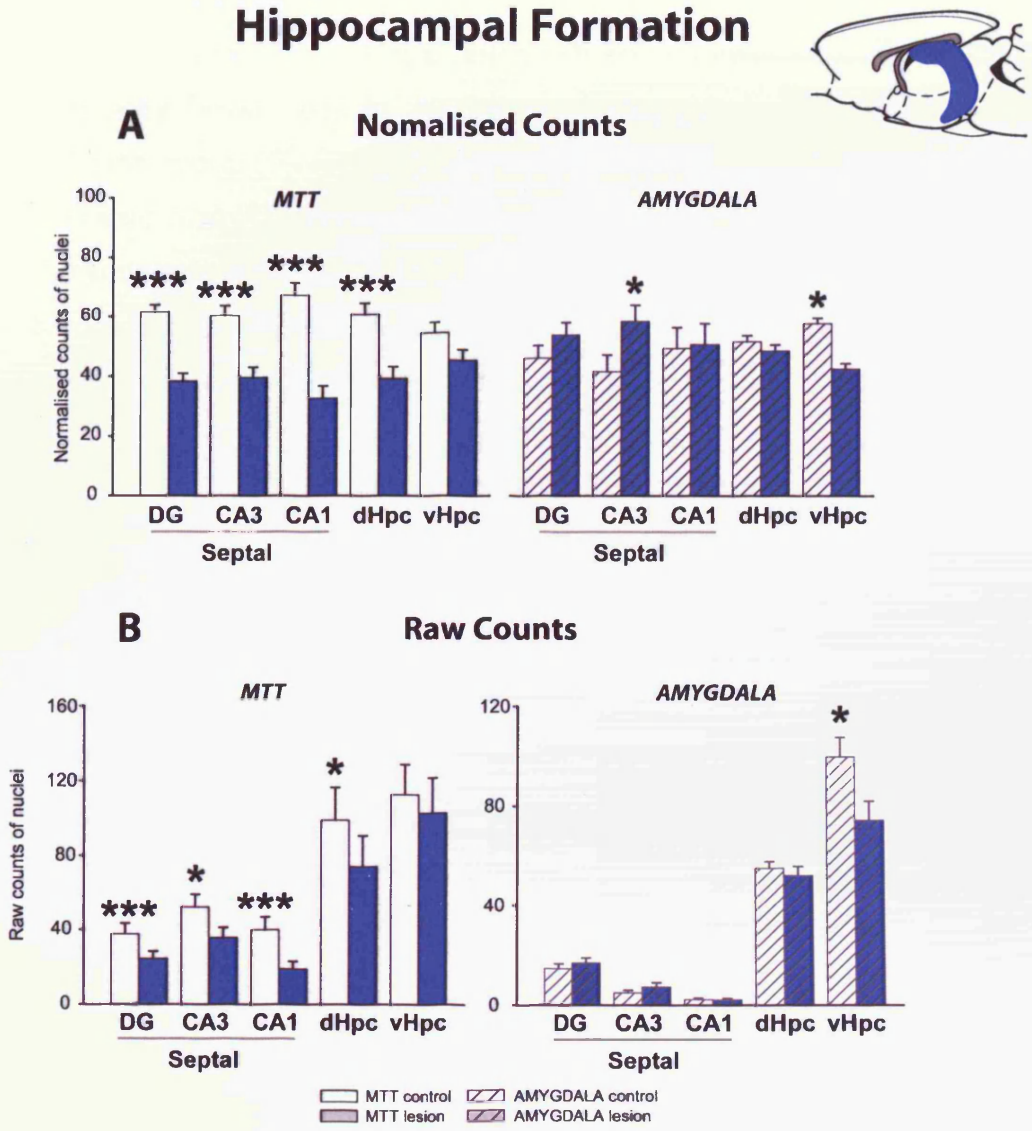

Figure 8. c-Fos levels in the hippocampal formation following bilateral MTT lesions and their controls (left-hand side histograms) and bilateral amygdala lesions and their controls (right-hand side histograms). **A.** Normalised counts and **B.** raw counts of c-Fos-positive cells are presented as mean ± SEM. Significance levels: *$p < 0.05$; **p < 0.01; ***$p < 0.001$. Abbreviations: dentate gyrus (DG), CA3, CA1, dorsal (dHpc) and ventral (vHpc) hippocampus.

The amygdala lesions did not significantly alter overall hippocampal c-Fos-positive cell counts (Figure 8A; group, $F < 1$) although there was a group x region interaction ($F_{(4,56)} = 4.9$, $p < 0.01$). This was due to a significant *increase* in cell counts in the amygdala lesion group in CA3 of the septal pole ($F_{(1,51)} = 6.7$, $p < 0.05$) while none of the other sub-regions in the septal pole showed lesion-induced changes. In addition, while there was no lesion-induced difference in cell counts in the dorsal (intermediate) hippocampus ($F < 1$) there were significantly fewer cells in the ventral (temporal) hippocampus in the amygdala lesion group ($F_{(1,51)} = 5.5$, $p < 0.05$). Again, analyses using the raw scores produced a similar pattern of results (Figure 8B): there was no overall effect of amygdala lesion ($F_{(1,7)} = 4.6$, $p = 0.069$) but there was a group x region interaction ($F_{(4,28)} = 12.1$, $p < 0.001$) due to a significant decrease in cell counts in the ventral (temporal) hippocampus ($F_{(1,7)} = 14.0$, $p < 0.01$) but not in any other region.

Direct comparisons of MTT/Amygdala lesion hippocampal effects

Analyses using normalised scores for the dorsal (intermediate) and ventral (temporal) hippocampus for both the MTT and Amygdala groups revealed a significant experiment (MTT/Amygdala) x group (lesion/control) x region interaction ($F_{(1,32)} = 20.94$, $p < 0.001$). This interaction was due to a significant decrease in c-Fos-positive cells in the dorsal (intermediate) hippocampus in the MTT lesion group ($F_{(1,23)} = 16.48$, $p < 0.001$), contrasting with the significant decrease in c-Fos-positive cells in the ventral (temporal) hippocampus following amygdala lesions ($F_{(1,27)} = 30.38$, $p < 0.001$). None of the other comparisons was significant. The analyses using the raw scores gave exactly the same pattern of results. There was a significant experiment x group x region interaction ($F_{(1,16)} = 9.3$, $p < 0.01$) which was due to a significant decrease in c-Fos-positive cells in the dorsal (intermediate) hippocampus in the MTT-lesion group compared to their matched controls ($F_{(1,16)} = 12.6$, $p < 0.01$; amygdala group, $F < 1$). In contrast, there was a significant decrease in cell counts in the ventral (temporal) hippocampus in the amygdala lesion group compared to their matched controls ($F_{(1,16)} = 5.8$, $p < 0.05$; MTT group, $F_{(1,16)} = 1.80$, $p = 0.32$).

Cortical comparison areas

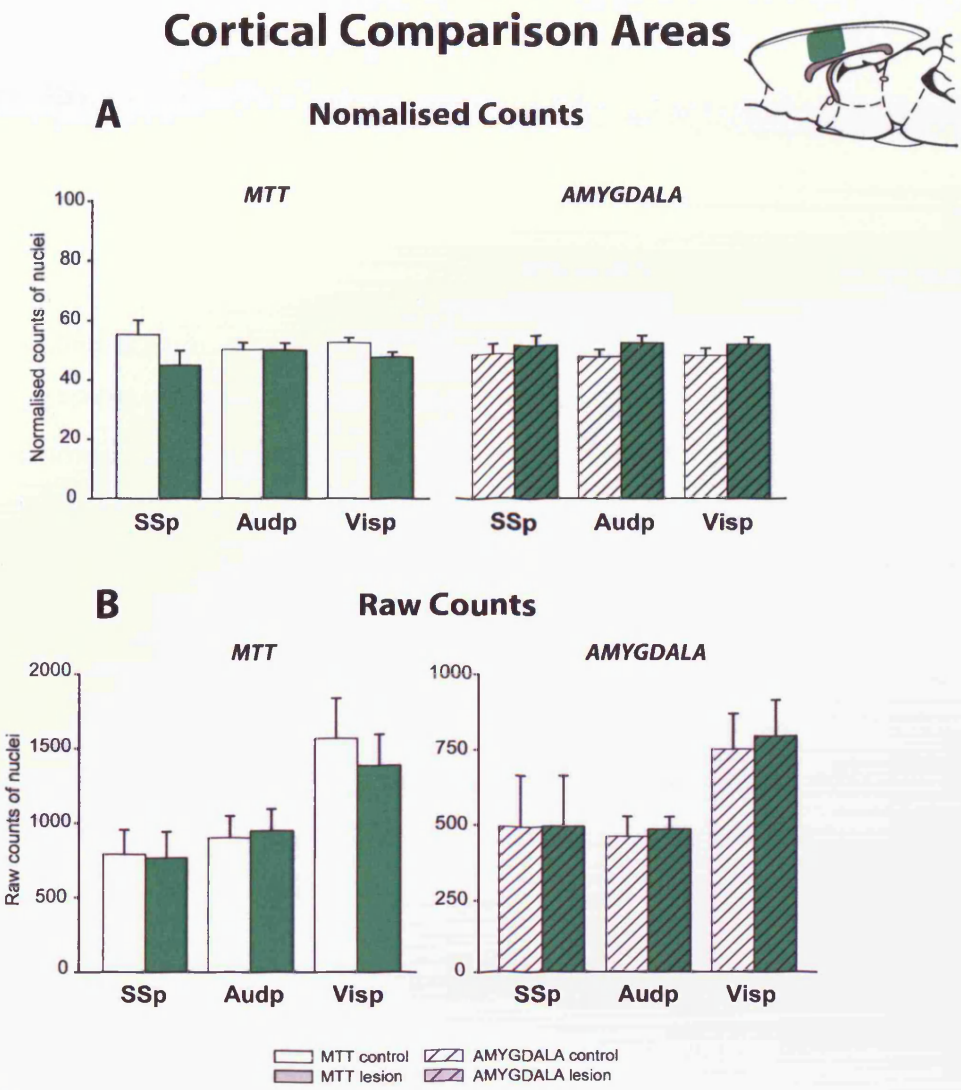

Figure 9. c-Fos levels in the cortical comparison areas following bilateral MTT lesions and their controls (left-hand side histograms) and bilateral amygdala lesions and their controls (right-hand side histograms). **A.** Normalised counts and **B.** raw counts of c-Fos-positive cells are presented as mean ± SEM. Significance levels: *$p < 0.05$; **$p < 0.01$; ***$p < 0.001$. Abbreviations: *Cortical Comparison Areas:* primary somatosensory cortex (SSp), primary auditory cortex (Audp), primary visual cortex (Visp).

There were no significant, overall changes in c-Fos counts after either MTT or amygdala lesions in the three primary cortices that were analysed

(somatosensory, auditory, visual Figure 6; MTT, $F < 1$; Amygdala, $F_{(1,14)} = 2.7$, $p = 0.13$; Figure. 9A). Likewise, there was no group x region interaction (MTT, $F_{(2,36)} = 3.05$, $p = 0.31$; Amygdala $F < 1$). Similarly, there was no effect of lesion on the raw cell counts in the three primary cortices (Amygdala and MTT both $F < 1$; Figure 9B).

Discussion

The mammillothalamic tract (MTT) and amygdala were both included in MacLean's (1949) revised version of the Papez' circuit (1937) and, as such, were considered to support similar functions. However, the present study revealed fundamentally different patterns of distal, neuronal dysfunction following lesions in the MTT or the amygdala. While both structures have repeatedly been implicated in learning and memory, there is a clear consensus that the forms of memory (spatial and emotional) are qualitatively different. The double dissociations found in hippocampal and retrosplenial c-*fos* activity following lesions of the MTT and amygdala underline the distinct roles of these two structures; the similarity of MTT and amygdala lesion effects upon the prelimbic cortex reveals this structure as a potential convergence point for the effects of these structures on learning.

The reason why episodic memory fails after medial diencephalic pathology remains unresolved. Since the 1960s, the mammillary bodies and anterior thalamic nuclei have typically been seen as part of a memory circuit by which hippocampal information is relayed to key, cortical sites via the medial diencephalon (Delay and Brion, 1969). The present study sought to test four current theories of diencephalic amnesia: 1) medial diencephalic damage disrupts indirect temporal lobe efferents acting upon the cingulate cortex (Delay and Brion, 1969; Aggleton and Brown, 1999); 2) medial diencephalic damage disconnects indirect hippocampal-frontal interactions (Warrington and Weiskrantz, 1982); and 3) diencephalic damage causes widespread cortical dysfunctions (Mair et al., 1979; Paller, 1997; Vann and Aggleton, 2004b). A fourth hypothesis is that diencephalic damage causes memory impairments

that are independent of the hippocampus as diencephalic and temporal amnesias are distinct syndromes (Parkin, 1984). The present study compared these hypotheses by looking at a measure of functional activity (c-*fos*) in the retrosplenial cortex, the frontal cortex and the hippocampus, following lesions of the MTT or amygdala. The MTT was targeted as lesions to this structure produce substantial, spatial memory impairments in rats (Vann et al., 2003a), and result in amnesia in humans (von Cramon et al., 1985; Graff-Radford et al., 1990; Clarke et al., 1994; Van der Werf et al., 2003; Yoneoka et al., 2004; Carlesimo et al., 2007). The task chosen in the present study has previously been shown to increase c-Fos expression in a number of sites of interests (e.g. hippocampus, retrosplenial cortex, prelimbic cortex; Jenkins et al., 2002).

The MTT lesions in the present study were very discrete and resulted in complete disconnection of the projections from the medial mammillary nuclei to the anterior thalamic nuclei, whereas, the projections from the lateral mammillary nuclei remained largely intact (data not shown, but see Vann and Albasser, 2009). As it is the medial mammillary nucleus, and its thalamic projections, that are most strongly implicated in Korsakoff's syndrome and other memory disturbances (see Vann and Aggleton, 2004b) this feature adds to the specificity of the present study with regards to mnemonic processing and amnesia. The observed pattern of c-Fos hypoactivity supports a combination of hypotheses 1-3, as there is both frontal and cingulate dysfunction by way of the prelimbic cortex and retrosplenial cortex, respectively. However, as the flow of information in these models is proposed to go *from* the hippocampus, it would not necessarily be predicted that the functional status of the hippocampus would itself be compromised. Instead, the hippocampal hypoactivity emphasizes the role of projections *from* the anterior thalamic nuclei to the hippocampus (Shibata, 1993; Amaral and Witter, 1995) with the implication that the medial diencephalon is providing additional information to the circuit, possibly from the tegmental nuclei of Gudden. However, a clear implication is that meaningful distinctions between diencephalic and temporal lobe amnesia cannot be made if both cause dysfunctions within the same network of areas.

All sub-regions of the septal hippocampus (dentate gyrus, CA3 and CA1) and of the dorsal hippocampus were hypoactive following MTT lesions, which contrasts with a lack of effect in the ventral hippocampus. These changes reveal how a selective loss of indirect medial diencephalic inputs impact upon the medial temporal activity. The dorsal/ventral hippocampal dissociation is especially illuminating as the dorsal (septal/intermediate), rather than the ventral (temporal), hippocampus is most closely associated with spatial memory in animals (Moser et al., 1993; Jung et al., 1994; Vann et al., 2000c). This dorsal hippocampal hypoactivity following MTT lesions would, therefore, help to explain why rats with MTT lesions show impairments when spatial encoding is at a premium (Vann et al., 2003a). In contrast, while the amygdala is thought to interact with the hippocampus to enhance episodic memory (Cahill and McGaugh, 1998; LaBar and Cabeza, 2006), amygdala lesions do not cause amnesia. In accordance with these findings, the amygdala lesions resulted in hypoactivity in the ventral hippocampus; consistent with the dense connections between the amygdala and temporal pole of the hippocampus and their complementary roles in emotional memory (e.g. Mackiewicz et al., 2006). These data, therefore, provide further support for the current views of functional dissociation in dorsal versus ventral hippocampus (Moser et al., 1993; Bannerman et al., 2003; Bast, 2007). The present results also show that a loss of MTT fibres, brought about by mammillary body atrophy, may be sufficient to explain the reduction in hippocampal functional activity both in Korsakoff amnesics and also patient BJ who suffered mammillary damage following an intranasal penetration injury (e.g. Kapur et al., 1994; Reed et al., 2003; Caulo et al., 2005). The route by which MTT lesions disrupt hippocampal activity could be via direct projections from the anterior thalamic nuclei (Amaral and Cowan, 1980) or via the retrosplenial cortex, which was also hypoactive.

The MTT lesions also reduced c-Fos expression in prelimbic cortex, the prefrontal region in the rat that receives most inputs from the hippocampus (Jay et al., 1989; Witter et al., 1989). This extension of the impact of MTT damage to prefrontal cortex shows that discrete medial diencephalic damage can have a dual impact upon both hippocampal and frontal activity. In this way, MTT damage has selective effects upon multiple regions thought to be critical for the

encoding and recall of episodic memory. The prelimbic cortex was the only region where both the MTT and amygdala lesions reduced c-Fos expression, so providing a convergence point for spatial and emotional memory information. Although the clear differences in effects of either amygdala or MTT lesions highlight their different roles in memory, the ventral hippocampal and prefrontal hypoactivity following amygdala lesions could potentially exacerbate effects of diencephalic (or temporal lobe) amnesia resulting in a more global impairment (Gaffan, 2001; Gaffan et al., 2001). As MTT lesions result in prelimbic cortex hypoactivity, it suggests that frontal dysfunction could be a key part of episodic memory impairment, even when there is no direct damage. In the past there have been problems dissociating involvement of the frontal lobe in diencephalic amnesia as additional damage to the mediodorsal thalamus would result in a loss of frontal projections as well as direct damage to the frontal cortex in cases of Korsakoff's syndrome. The present results show that prelimbic hypoactivity can occur in a model of diencephalic amnesia without direct deafferentation or damage. Although comparisons between rat and primate frontal cortices can be limited due to cross-species differences, the prelimbic, infralimbic and anterior cingulate cortices in the rat are thought to be homologous to those cortices in the primate (Preuss, 1995).

Within this revised framework, where diencephalic damage results in disruptions of hippocampal and prefrontal activity, the striking decrease of *c-fos* activity in the retrosplenial cortex may prove to be critical. Retrosplenial pathology is sufficient to induce human amnesia (Valenstein et al., 1987; Maguire, 2001a) and retrosplenial hypoactivity is also seen in the amnesic Korsakoff's syndrome (Joyce et al., 1994; Reed et al., 2003). This cortical area has dense connections with the anterior thalamic nuclei, the hippocampus, and the prefrontal cortex (Wyss and Van Groen, 1992; Shibata, 1998; Shibata et al., 2004). Consequently, the retrosplenial cortex is seen as a key link for temporal-diencephalic, temporal-frontal, and thalamic-hippocampal interactions (Kobayashi and Amaral, 2003). Consistent with this view, retrosplenial c-Fos expression was markedly reduced by lesions of the anterior thalamic (Jenkins et al., 2002a; Jenkins et al., 2002b; Poirier and Aggleton, 2009) nuclei and the hippocampus (see Chapter 2, Albasser et al., 2007), indeed, this is the only

clear site of hypoactivity in home-cage control animals after anterior thalamic lesions (Jenkins et al., 2002a). However, in these studies the c-*fos* hypoactivity followed the loss of a direct input, but in the present study c-*fos* hypoactivity followed the loss of an indirect input and so could not be predicted *a priori*. The striking decrease in c-Fos in the retrosplenial cortex following either anterior thalamic or MTT lesions is in contrast to the much smaller effects following fornix lesions (see Chapter 4 and Vann et al., 2000b). The implication from this result is that the retrosplenial hypoactivity resulting from loss of mammillary body efferents cannot solely be explained in terms of an indirect loss of hippocampal/fornical inputs, but that the mammillary bodies have an additional, independent contribution.

The quantitative and qualitative similarities in retrosplenial, prefrontal and hippocampal hypoactivity following either MTT lesions or anterior thalamic lesions (Jenkins et al., 2002a; Jenkins et al., 2004a; Poirier and Aggleton, 2009) suggest that the anterior thalamic lesion effects are due, in the main part, to their loss of their mammillary body inputs. By the same logic, it seems unlikely that any additional damage to zona incerta in the MTT lesion animals is responsible for the pattern of c-*fos* hypoactivity. Further, it becomes clear that hypoactivity in hippocampus and/or retrosplenial cortex can occur without direct deafferentation; instead, it appears that the hypoactivity is brought about by a functional disruption of this memory circuit. The present results are consistent with findings from the pyrithiamine-induced thiamine deficiency (PTD) model of diencephalic amnesia, where disruption of acetylcholine was found in the rat hippocampus and cortex (Pires et al., 2005; Savage et al., 2003; Roland and Savage, 2007). However, in the same way as patients with Korsakoff's syndrome, the pathology in the PTD rat model is diffuse and, in addition to diencephalic damage, there is widespread cortical and thalamic damage as well as damage to major white matter tracts including the corpus callosum and internal capsule (Langlais et al., 1996). The present finding, that disconnection of the MTT is sufficient to induce hippocampal and cortical hypoactivity, suggests that the acetylcholine dysfunction in the same areas in the PTD model are also most likely attributable to the loss of mammillary body efferents.

The present study used a combination of lesions and immediate-early gene imaging to investigate current models of diencephalic amnesia and in doing so provide a more complete explanation for memory disruptions resulting from damage to the diencephalon. The results revealed that MTT damage has pervasive effects on the retrosplenial cortex, the prelimbic cortex and the hippocampus, target sites critically linked to the encoding and recall of episodic memory. As MTT lesions produce severe, persistent deficits on tasks such as delayed-matching-to-position in the water-maze (Vann and Aggleton, 2003), a task that is also sensitive to hippocampal (Bannerman et al., 2002) and retrosplenial cortex lesions (Vann et al., 2003b), it is possible that the MTT lesion effects reflect functional disturbances in this network of structures. Together, the findings from the present study unify accounts of the core memory deficits in temporal lobe and diencephalic amnesias by strongly indicating that both syndromes are associated with dysfunctions in common networks of regions

Chapter 4

Effects of Fornix Lesions on Retrosplenial Cortex Activity and Beyond

Introduction

The fornix is one of the principal fibre tracts in the brain and provides one of the major routes between the temporal lobe and the diencephalon. It, therefore, occupies a central position within the extended hippocampal memory system (Delay and Brion, 1969; Aggleton and Brown, 2006). The projections within the fornix that arise from the hippocampal formation originate in the CA fields of the hippocampus and the subiculum (Adelmann et al., 2004; Saunders and Aggleton, 2007). The fornix divides into two separate tracts around the anterior commissure: (1) the precommissural fornix innervates frontal and septal regions; (2) the postcommissural fornix projects to the mammillary bodies and the anterior thalamic nuclei (Figure 1). Both divisions innervate other hypothalamic nuclei. It is also important to appreciate that the fornix also conveys projections to the hippocampal formation, most notably from the septum, diagonal band, and supramammillary nucleus.

Animal studies show that the fornix is necessary for memory. First, bilateral fornix lesions (combining the precommissural and the postcommissural fornix) impair spatial memory tasks, such as the Morris water maze and the radial-arm maze (Olton et al., 1978; Olton et al., 1982; Markowska et al., 1989; Cassel et al., 1998). In a disconnection study of the fornix and the anterior thalamic nuclei (ATN), Warburton et al. (2000) reported that lesioned animals

were impaired in learning object location, but not object recognition. Second, In addition to memory impairments, fornix lesions alter locomotor activity and produce hyperactivity in rats (Cassel et al., 1998; Bannerman et al., 2001).

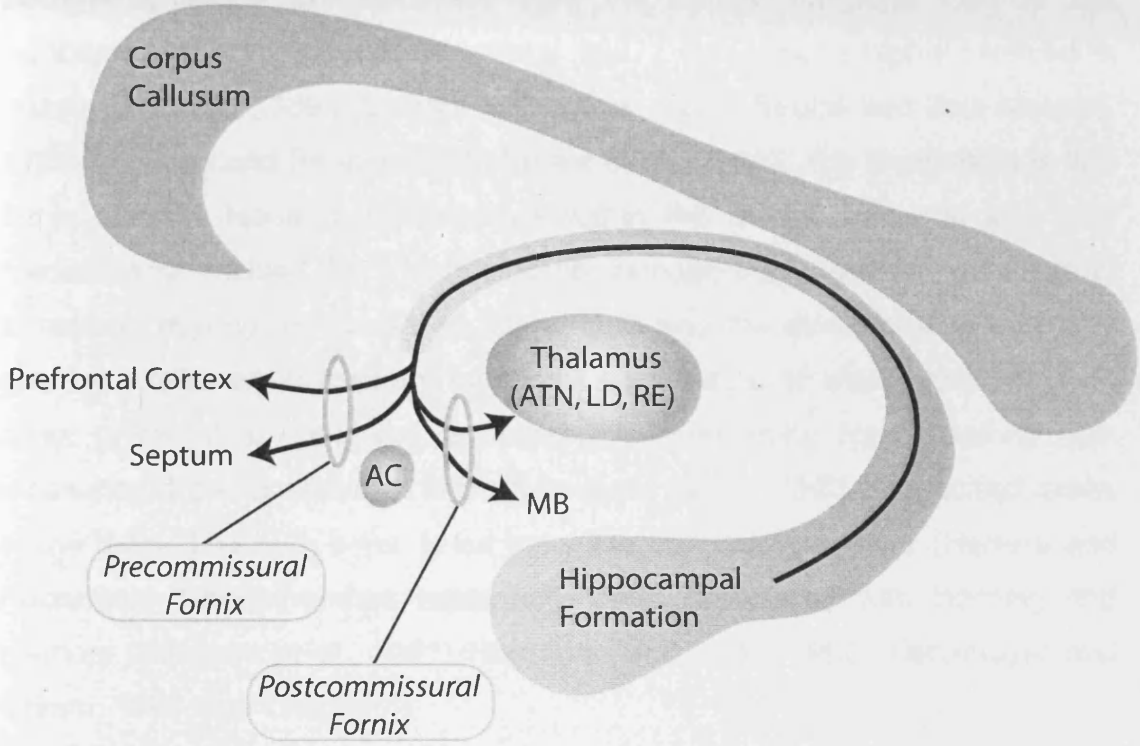

Figure 1. Diagrammatic representation of the location of the fornix and its divisions. The arrows show the connections from the hippocampal formation (based on Aggleton, 2008). Abbreviations: AC, anterior commissure; ATN, anterior thalamic nuclei; LD, laterodorsal nucleus of the thalamus; MB, mammillary bodies; RE, nucleus reuniens.

Single case human studies have typically reported that the fornix is vital for memory (Gaffan and Gaffan, 1991; Hodges and Carpenter, 1991; D'Esposito et al., 1995; McMackin et al., 1995; Renou et al., 2008; Vann et al., 2009). Recently, additional evidence comes from studies of cohorts of patients with colloid cysts, a benign tumour that develops in the third ventricle adjacent to the fornix. During surgical removal of the colloid cyst, the whole tumour will be removed, but surrounding normal tissue, including the fornix, may be compromised. Surgical removal of colloid cysts associated with fornix damage

resulted in poor memory performance, such as in learning and recall tests (Hodges and Carpenter, 1991; Aggleton et al., 2000; Tsivilis et al., 2008).

As mentioned earlier, the fornix is assumed to be important for memory because it is the primary route from the medial temporal lobe to the diencephalon (Aggleton and Saunders, 1997), two regions highly involved in memory (Gudden, 1896; Scoville and Milner, 1957; Squire and Zola-Morgan, 1991; Aggleton and Sahgal, 1993; Spiers et al., 2001). The implication is that fornix damage leads to dysfunctions within the medial temporal lobe and medial diencephalon. The impact of fornix damage may, however, also extend to regions beyond the medial temporal lobe and the diencephalon that may also be implicated in memory functions. This issue, of where fornix lesions might prove disruptive, was addressed by combining fornix lesions with measuring the expression of immediate-early genes (IEG) in specified areas of the brain. The IEG, c-*fos*, is an inducible transcription factor (Herrera and Robertson, 1996) that has repeatedly been associated with learning and memory (Nikolaev et al., 1991; Herdegen and Leah, 1998; Tischmeyer and Grimm, 1999, see Chapter 1).

Vann et al. (2000b) assessed the impact of fornix loss upon the activity of multiple brain areas, as measured by immediate-early gene activity. It was found that fornix lesions induced hypoactivity in multiple sub-regions within the extended hippocampal memory system, such as the hippocampus, the anterior thalamic nuclei and the retrosplenial cortex. For example, fornix lesions led to a significant c-Fos reduction in all hippocampal subfields that were examined, i.e. dentate gyrus, CA1, and CA3 (Vann et al., 2000b). This study supports the notion of an extended hippocampal memory system as all these regions are involved in spatial memory, and damage to each of them results in poorer performance in spatial memory tasks (Olton et al., 1979; Byatt and Dalrymple-Alford, 1996; Vann and Aggleton, 2002). In the study of Vann et al. (2000b), the c-*fos* activity of the retrosplenial cortex was treated as a whole, presumably reflecting the fact that the study sought to compare c-*fos* activity across a wide range of diverse regions (39 in total). However, there are some anatomical and behavioural evidences that the sub-regions of the

retrosplenial cortex have different roles and that the retrosplenial cortex should not be treated as a uniform structure.

First, it is standard to divide the retrosplenial cortex into different cytoarchitectonic sub-regions. In the rat, the major subdivision is between the dysgranular cortex (Rdg, Van Groen and Wyss, 1992) and the granular cortex. The retrosplenial granular cortex is then subdivided into two sub-regions: the retrosplenial granular b (Rgb, Van Groen and Wyss, 2003) and the retrosplenial granular a (Rga). These three retrosplenial sub-regions (Rdg, Rgb, Rga) have different connectivity (e.g. Rdg receives most of the visual inputs), but also share reciprocal connections with each other (Van Groen and Wyss, 1990c, 1992, 2003). Second, a lesion study of the retrosplenial cortex found that damage to Rgb but not Rga impaired animals in spatial learning in the water maze task (Van Groen et al., 2004). Third, it was found that selective lesions of the dysgranular retrosplenial cortex (Rdg) were sufficient to impair animals in a spatial memory task by biasing their strategy to solve the task (Vann and Aggleton, 2005). Initially, there was no group difference when animals were first learning a standard version of the radial-arm maze task. However, when the radial-arm maze was rotated after the first four arm choices, animals with Rdg lesions were impaired in the task. The maze rotation prevents the animals from using intra-maze cues or an egocentric strategy. This study indicates that animals with Rdg lesions are poor at using distal cues. Fourth, the retrosplenial cortex is vulnerable to anterior thalamic lesions (Jenkins et al., 2002a; Jenkins et al., 2004a). Indeed, anterior thalamic lesions induce a very marked hypoactivity in the superficial layers (layer II and upper layer III) of the retrosplenial granular (Rgb and Rga) cortex; but not in the deep layers (lower III to VI) of the granular cortex. In a recent follow-up study (Poirier and Aggleton, 2009), it was shown that over time the disruption caused by anterior thalamic nuclei lesions to retrosplenial immediate-early gene expression expanded from the superficial laminae to the deep laminae of granular b cortex and to the dysgranular sub-region. One of the goals of this Chapter was to examine in more detail (sub-regions, layers and rostro-caudal axis) the nature of the retrosplenial cortex hypoactivity found after fornix lesions.

From the previous Chapters and previous studies, it is known that the retrosplenial cortex is unusually sensitive to damage to the extended hippocampal network. A further aim of this study was, therefore, to assess whether fornix lesions would produce similar effects on the retrosplenial cortex compared to (1) hippocampal lesions (Chapter 2, Albasser et al., 2007); (2) anterior thalamic nuclei lesions (Jenkins et al., 2004a); or mammillothalamic track lesions (Chapter 3, Vann and Albasser, 2009). All of these experiments used bilateral lesions. To be able to compare this study with the previous ones, bilateral lesions of the fornix were made.

The aim of this study was to determine the effects of fornix lesions on retrosplenial activity, as measured by the expression of the immediate-early gene c-*fos*. The initial experiment led to three other experiments as it emerged that the indirect impact of fornix damage on the retrosplenial cortex varied depending on experimental parameters. These extra experiments will be described and explained throughout this Chapter.

Materials and Methods

Four related experiments were conducted in order to study the effects of fornix lesions on retrosplenial cortex IEG activity. These experiments were very similar to each other, but differed in three specific aspects: 1) lesion: bilateral versus unilateral, 2) the anaesthetic: gas or injectable, and 3) the behavioural test immediately prior to IEG analysis: spontaneous exploration versus working memory.

Experiment 1: gas anaesthetic, bilateral fornix lesion, spontaneous exploration in radial-arm maze (c-Fos)

Animals

The study involved 16 naïve, male, pigmented rats (DA strain, Harlan. Bicester, UK) weighing between 225 g and 258 g at the time of surgery. Animals were divided into two groups: bilateral lesions of the fornix (n = 8) and surgical controls (n = 8). After a post-surgery recovery period of at least 10 days, the rats were deprived to 85% of their free-feeding body weight and were maintained at this level or above throughout the experiment. Water was available *ad libitum.* Rats were housed in pairs under diurnal conditions (14 h light, 10 h dark), and testing occurred at a regular time during the light period. Animals were thoroughly habituated to handling before the study began. All experiments were performed in accordance with the UK Animals (Scientific Procedures) Act (1986) and associated guidelines.

Surgical procedure

Animals were deeply anaesthetised with a mixture of isoflurane gas (Aerrane liquid; Baxter Healthcare Ltd., UK) and oxygen. Each animal was then placed in a stereotaxic headholder (David Kopf instruments, Tujunga, CA) and the incisor bar was set at +5.0. A longitudinal incision was made in the scalp, which was retracted to expose the skull. A craniotomy directly above the lesion area was drilled. The fornix lesions were made by radiofrequency using a Radionics TCZ (Radionics, Burlington, VT) electrode (0.7 mm tip length, 0.25 mm diameter). Two lesions were made per hemisphere. The stereotaxic coordinates of the lesion relative to ear-bar zero were: anteroposterior (AP) +5.3, dorsoventral (DV) +7.1, lateromedial (LM) ±0.7, and AP +5.3, DV +7.0, and LM ±1.7. For each coordinate, the electrode was lowered vertically into the fornix and the tip temperature was raised to 75 °C using an RFG4-A Lesion Maker (Radionics). After every surgery, the skin was sutured, antibiotic

powder applied (Acramide: Dales Pharmaceuticals, UK), and the animal placed in a temperature-controlled recovery box. Animals also received 5 ml of glucose saline subcutaneously; Paracetamol and sucrose were added to the rats' drinking water for three days post-surgery.

Behavioural testing

Prior to this experiment, the animals were involved in separate behavioural experiments such as a conditioning task in operant chambers and a T-maze alternation task in which fornix lesioned animals were impaired confirming the effect of the lesion. These behavioural tests were completed a minimum of 14 days prior to the start of the present IEG study. The animals were tested in the present study 4 months after surgery.

Apparatus

Testing was carried out in an eight-arm radial maze. The maze consisted of an octagonal central platform (34 cm diameter) and eight equally spaced radial arms (87 cm long, 10 cm wide). The base of the central platform and the arms were made of wood, whereas panels of clear Perspex (24 cm high) formed the walls of the arms. At the start of each arm was a clear Perspex guillotine door (12 cm high) attached to a pulley. All animals were tested in the same distinctive rectangular room (295 x 295 x 260 cm). The room contained distinct, salient, visual cues such as geometric shapes and high-contrast stimuli on the walls.

Spontaneous exploration

Each rat was allowed to freely explore an unfamiliar eight-arm radial arm maze in an unfamiliar room for 20 min. The rat was first placed in the central platform and then freely allowed to visit all eight arms. Each arm was baited and continually rebaited with sucrose pellets (45 mg; Noyes Purified Rodent Diet, Lancaster, NH, USA). Each animal was placed in a holding box in a

quiet, dark room for 30 min before and 90 min after the single radial-arm maze session. Animals were habituated to this dark room for 2 h every day for the 7 days prior to radial-arm maze exploration.

IEG immunohistochemistry: c-Fos

Ninety minutes after completing the final radial arm-maze session, rats were deeply anaesthetised with sodium pentobarbital (60 mg/kg; Euthatal; Rhone Merieux, UK) and perfused intracardially with 0.1 M PBS followed by 4% paraformaldehyde in 0.1 M PBS (PFA). This procedure was identical to the previous Chapters 2 and 3 (see Materials and methods).

A second one-in-four series was mounted directly onto gelatine-coated slides and stained using cresyl violet, a Nissl stain, for verification of the lesion and histological identification of specific brain regions.

IEG-positive cell counts

Estimates were made of IEG-positive cells by using an automated cell counting procedure. Counting procedures were carried out without knowledge of the group assignments. Images were viewed on a Leica DMRB microscope and photographed using an Olympus DP70 camera. The program analySIS^D (Soft-Imaging Systems; Olympus, UK) was used to count the number of nuclei above threshold. The threshold was set up by the experimenter, and remained the same for the matched sections (between the two hemispheres of an animal or between the two animals of the same matched pair). The counts were made in a frame area of 0.84 x 0.63 mm, which enabled all laminae to be included in one image. These counting procedures were not stereological, and so while providing information about relative numbers of cells they do not provide accurate counts of absolute cell numbers.

For all brain areas analysed, counts were taken from four consecutive sections from each hemisphere (so eight images in total per region per animal). These

counts were averaged to produce a mean. Scores were normalised to reduce variability in levels of IEG counts between animal. The scores were normalised by dividing the mean number of positive cells of one animal by the combined mean of the two paired animals (one lesion, one surgical control). The result was expressed as a percentage. This normalisation procedure also equates the cell counts from different regions, which would otherwise vary considerably. Raw counts were also analysed between animals (for bilateral fornix lesions) or within animals (for unilateral fornix lesions).

Regions of interest

Cytoarchitectonic subfields were identified from coronal sections (Paxinos and Watson, 1997) and were based on previous studies (Chapter 2, Jenkins et al., 2002a; Albasser et al., 2007). For Experiment 1, the regions sampled are depicted in Figure 2.

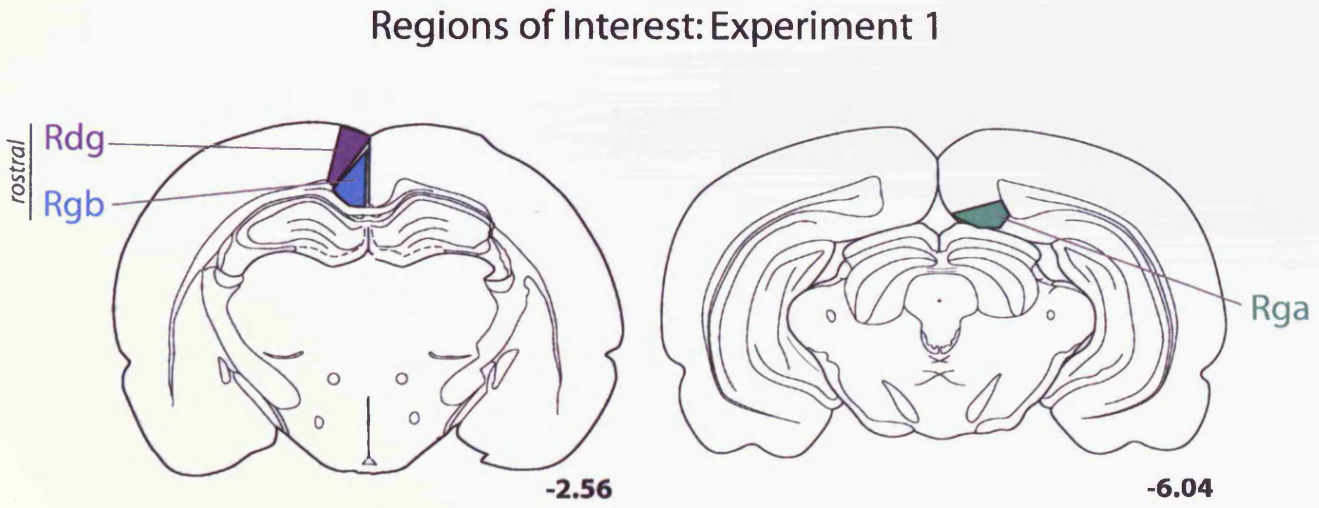

Figure 2. Diagrams of coronal sections indicating areas sampled in Experiment 1. The numbers indicate the distance (in millimetres) of the sections from bregma (Paxinos and Watson, 1997). Abbreviations: Rdg, retrosplenial dysgranular cortex; Rgb, retrosplenial granular b cortex; Rga, retrosplenial granular a cortex.

The retrosplenial cortex can be subdivided (Wyss and Van Groen, 1992) into granular b cortex (Rgb), granular a cortex (Rga), and the dysgranular cortex (Rdg) and separate counts were made in all three sub-regions. Separate counts were also made in the superficial (layer II and upper III) and deep (lower layer III to VI) layers of Rdg, Rgb, and Rga as lesions of the anterior thalamic nuclei have been shown to affect activity in the superficial and deep layers differentially (Jenkins et al., 2002b; Jenkins et al., 2004a). This superficial/deep border is signalled by an abrupt change in cell packing density.

Experiment 2: gas anaesthetic, bilateral fornix lesion, spontaneous exploration in radial-arm maze (c-Fos)

This experiment was a replication of Experiment 1, where the three main parameters (lesion, anaesthetic and behaviour) were kept the same. In addition, the retrosplenial cortex was counted in more detail, by dividing Rdg and Rgb into rostral and caudal.

Animals

Animals were 12 DA rats divided into two groups (lesion, n = 6; surgical controls, n = 6) weighing between 218 g and 243 g at the time of surgery.

Behavioural testing

These rats had previously undergone a conditioning task in operant chambers (Kyd et al., 2008) that had been completed 2 weeks before the beginning of the training for the present IEG study. The animals were tested in the present IEG study 4 months after surgery.

Region of interest

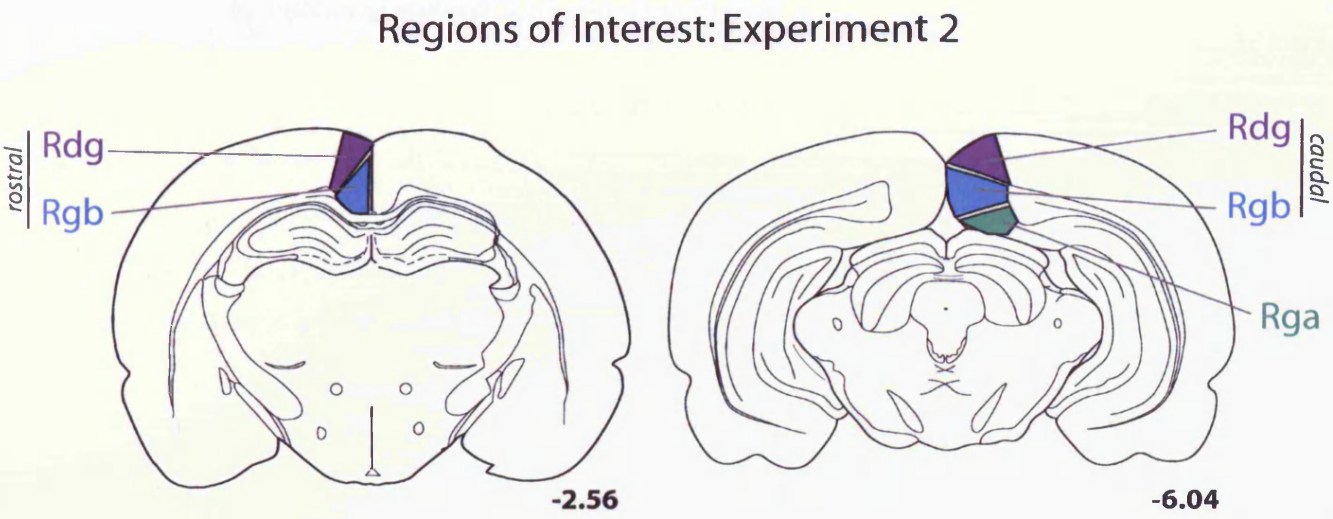

Figure 3. Diagrams of coronal sections indicating areas sampled. **A.** The rostral retrosplenial cortex. **B.** The caudal retrosplenial cortex. The numbers indicate the distance (in millimetres) of the sections from bregma (Paxinos and Watson, 1997). Abbreviations: Rdg, retrosplenial dysgranular cortex; Rgb, retrosplenial granular b cortex; Rga, retrosplenial granular a cortex.

In addition to the rostral retrosplenial cortex, the caudal parts of Rdg and Rgb were also counted (see Figure 3). This separation was made because of the different rostro-caudal connections and functional specialisation within the retrosplenial cortex (Van Groen et al., 2004; Vann and Aggleton, 2005; Pothuizen et al., 2009; Shibata et al., 2009).

Experiment 3: gas anaesthetic, unilateral fornix lesion

A. spontaneous exploration in radial-arm maze (c-Fos)

B. working memory in radial-arm maze (c-Fos and Zif268)

The three main differences in this experiment were that (1) the fornix lesion was unilateral and not bilateral; (2) two different behavioural tasks in the radial-arm maze were compared; (3) The additional IEG, *zif*268, was assessed in Experiment 3B. Only the protocol changes compared to Experiment 1 or 2 will be presented.

Animals

Animals were 13 male DA rats weighing between 215 g and 253 g at the time of surgery. Animals were separated in two groups: spontaneous exploration in the radial-arm maze (Experiment 3A, n = 7) and working memory in the radial-arm maze (Experiment 3B, n = 6).

Surgical procedure

The procedure was similar to the one used for Experiments 1 and 2, except that all the animals received unilateral fornix lesions. The lesions were made only in one hemisphere and the coordinates were identical to those in the previous Experiments 1-2. Approximately equal numbers of animals received lesions to the left or right hemisphere. The beginning of the test started four months after surgery.

Behavioural training

Experiment 3A. Six animals were tested in the same spontaneous exploration version of the radial-arm maze used in Experiments 1 and 2.

Experiment 3B. The seven other animals were trained in the working memory version of the radial-arm maze, as described below.

Habituation

Animals were trained to run in a radial-arm maze. Habituation consisted of 4 consecutive days. For the first 2 days, the animals were allowed to explore freely the maze. In the arms and at their ends, several food sucrose pellets (45 mg; Noyes Purified Rodent Diet, Lancaster, NH, USA) were scattered to motivate the animal's exploration. Each arm was baited with food rewards, and the wells were constantly rebaited. From day 3, the use of the guillotine door was introduced. From this stage, no more than one single pellet was placed in each well.

Training

Animals were trained (12 sessions) to run in the radial-arm maze using a standard working memory procedure (Olton et al., 1978). At the start of a trial, all eight arms were baited with a single food pellet. The rat was placed in the central platform and all the doors to the arms were then raised. The animal was allowed to make a choice and run down an arm to get its reward. When the rat returned to the central platform, all doors were closed for 10 sec before they were again opened, permitting the animal to make another choice. This continued until all eight arms had been visited. Retrieving all eight pellets constituted a single trial, and was composed of a minimum of eight arm runs. The only unusual aspect of the training was that each session consisted of multiple trials in the radial-arm maze, one after the other, so that each session lasted for 20 min to prolong exposure to task demands. Therefore, after

entering all eight arms the animal was removed from the maze while it was rebaited, and then the rat returned to the maze to perform a new trial. This procedure was repeated for 20 min. The delay between each trial (2 min) was the time it took to rebait all of the arms. During this period, animals were placed in a travelling box that had an aluminium top, base, and sides (10 x 10 x 26 cm). Each animal was placed in a holding box in a quiet, dark room for 30 min before and 90 min after each radial-arm maze session.

IEG immunohistochemistry: c-Fos and Zif268

For Experiment 3B only, in addition to c-*fos*, another IEG, *zif*268, was assessed to determine the retrosplenial cortex activation. The immunohistochemical methods were identical to the previous experiments, except that the c-Fos antibody was replaced by the Zif268 antibody (1 : 5000; C-19, Santa Cruz Biotechnology, USA).

IEG-positive cell counts

Unlike Experiments 1 and 2, unilateral fornix lesions were made in Experiment 3. For this reason, the cell count methods changed in two aspects: (1) area counts were taken from six consecutive sections from each hemisphere (instead of four consecutive sections from both hemisphere with bilateral fornix lesion; Experiments 1 and 2). These counts were averaged to produce a mean. (2) Scores were normalised to reduce variability in levels of IEG counts between animals. The normalisation was obtained by dividing the mean number of activated neurons in one hemisphere (e.g. lesion) by the combined mean of the two hemispheres (one lesion, one control). The result was expressed as a percentage. This normalisation procedure also equates the cell counts from different regions, which would otherwise vary considerably.

Regions of interest

Like in Experiment 2, both rostral and caudal retrosplenial cortex sub-regions (see Figure 3) were analysed.

Experiment 4: injectable anaesthetic, unilateral fornix lesion, working memory in the radial-arm maze (c-Fos and Zif268)

Animals

Ten DA rats received unilateral fornix lesions just as the animals of Experiment 3. The animals weighed between 217 g and 264 g at the time of the surgery.

Surgical procedure

Contrary to the previous experiments, Animals were deeply anaesthetised by an intraperitoneal (i.p.) injection (60 mg/kg) of 6% sodium pentobarbital (Sigma Chemical Company Ltd, Poole, UK, freshly dissolved in saline). The rest of the surgical technique was identical as that used in Experiment 3. Like in Experiment 1-3, the animals were tested in the present study 4 months after surgery.

Behavioural training

Animals were trained in the same working memory task of the radial-arm maze as used in Experiment 3B.

As in Experiments 2 and 3, both the rostral and caudal retrosplenial cortex sub-regions were analysed. In addition, two comparison sensorimotor areas (motor cortex and primary somatosensory area) were also selected as any differences

in these regions might reflect abnormal sensorimotor patterns following surgery (Figure 4).

Regions of interest

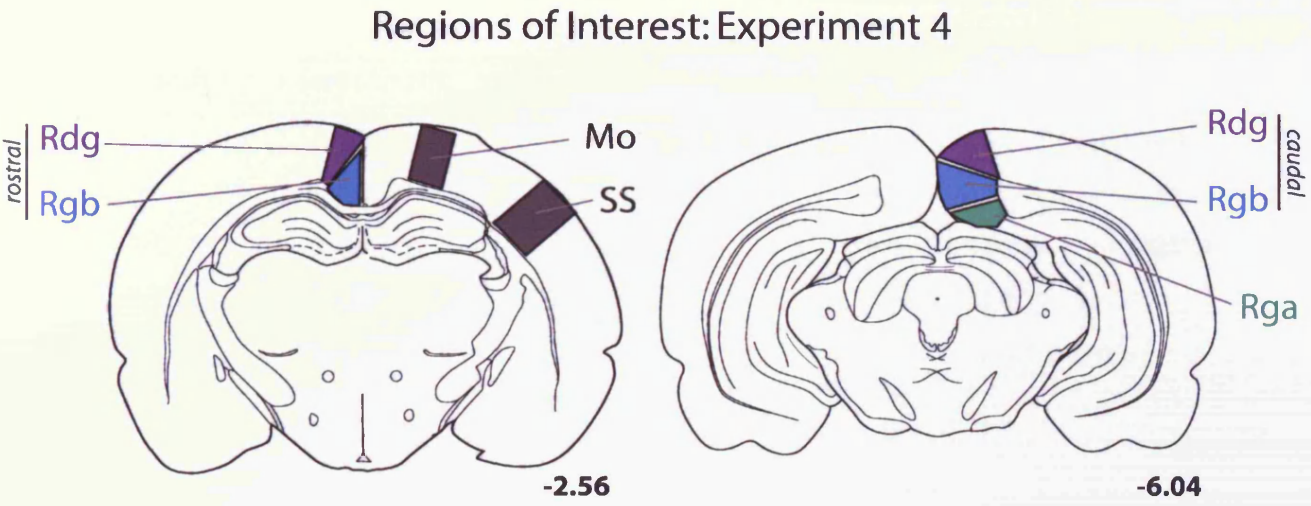

Figure 4. Diagrams of coronal sections indicating areas sampled in Experiment 4. **A.** The rostral retrosplenial cortex and control comparison areas. **B.** The caudal retrosplenial cortex. The numbers indicate the distance (in millimetres) of the sections from bregma (Paxinos and Watson, 1997). Abbreviations: Mo, primary motor; cortex. Rdg, retrosplenial dysgranular cortex; Rgb, retrosplenial granular b cortex; Rga, retrosplenial granular a cortex; SS primary somatosensory cortex.

Experiments 1 to 4

Table 1 summarises the main parameters that changed between the four experiments.

Table 1. Overview of the four experiments

Experiment	Anaesthetic	Fornix Lesion	Behaviour in radial-arm maze
1	gas	bilateral	spontaneous exploration
2	gas	bilateral	spontaneous exploration
3A	gas	unilateral	spontaneous exploration
3B	gas	unilateral	working memory
4	injectable	unilateral	working memory

Statistics

The data from the various retrosplenial cortex and control areas were grouped separately before being investigated in separate analyses of variance. When significant interactions were found the simple effects for each brain region were analysed as recommended by Winer (1971). The probability level of 0.05 was taken as being statistically significant. Normalised counts were analysed using a one between- (groups) x one within-subject (sub-regions) design. The normalisation helps to reduce the variation of the cell counts in two ways: (1) it reduces the variance between two different brain regions that have highly different number of cells; (2) the normalisation is based on pairs of animals (one control, one lesion) that have been processed together for the behaviour and the immunohistochemistry, therefore it reduces the variation of cell counts from two different batches (i.e. immediate-early gene staining can differ between two batches, biasing the results if the brains are not paired). However, the normalisation leads to a caveat. The normalisation expresses the data for one group as a proportion of the total for both groups, thereby restricting the number of degrees of freedom. Even though for comparing across sites the normalisation procedure is still optimal, only the differences between groups and not the individual group statistics may be determined. For these reasons, raw counts were further analysed. Due to the high level of variation in cell counts across pairs of animals but the high correlation within each matched pairs, the raw scores were analysed using a within-subject design.

Results

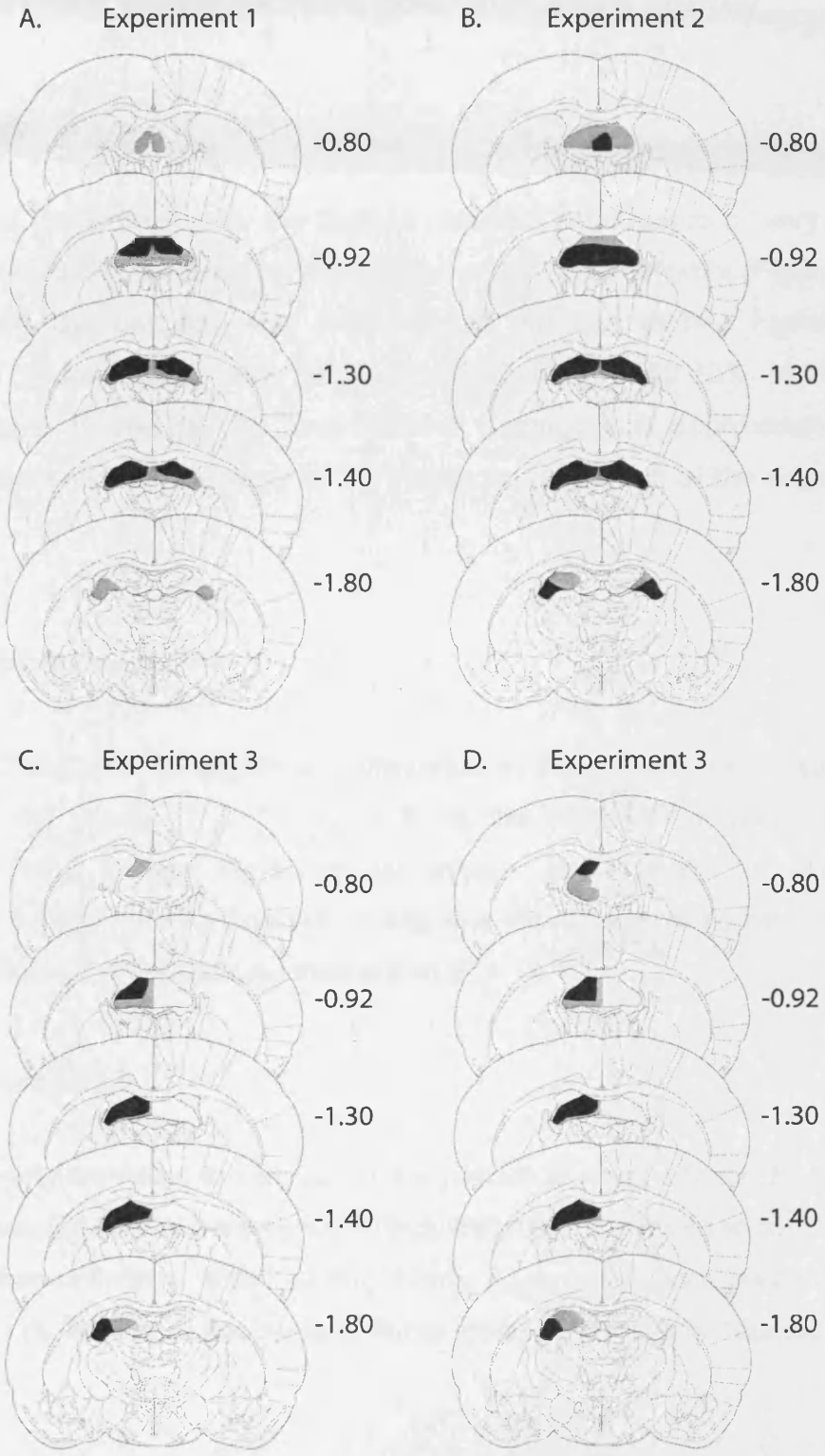

Figure 5. Coronal sections illustrating the extent of the largest (*gray*) and smallest (*black*) fornix lesions in the four experiments. The numbers indicate the distance (in millimetres) of the sections from bregma (Paxinos and Watson, 1997).

Experiment 1: gas anaesthetic, bilateral fornix lesion, spontaneous exploration in radial-arm maze (c-Fos)

Histology

In four of the eight cases, the lesions resulted in complete or very close to complete (90–100%) bilateral transection of the fimbria/fornix (Figure 5A). In three rats, the damage was asymmetrical, so that in one hemisphere it involved approximately 80 -100% of the tract and 60-70% in the other hemisphere. In one rat, the total bilateral damage was approximately 70%. There was restricted damage to the most caudal portion of the septum in all rats.

IEG-positive cell counts

c-Fos. There was no significant difference in the overall normalised c-Fos-positive cell counts ($F < 1$; Figure 6) in the retrosplenial cortex following bilateral fornix lesions. Moreover, no group x region interaction was found ($F_{(5,70)} = 1.66$, $p = 0.15$). Analyses using raw scores confirmed the absence of lesion effect ($F < 1$) and of an interaction ($F < 1$).

Interim conclusion:

This experiment failed to reproduce the pattern of results found by Vann and colleagues (2000b), where *c-Fos* hypoactivity of the retrosplenial cortex was found after unilateral lesion of the fornix. Due to the inconsistency of the results, a replication of the bilateral fornix lesion study was conducted.

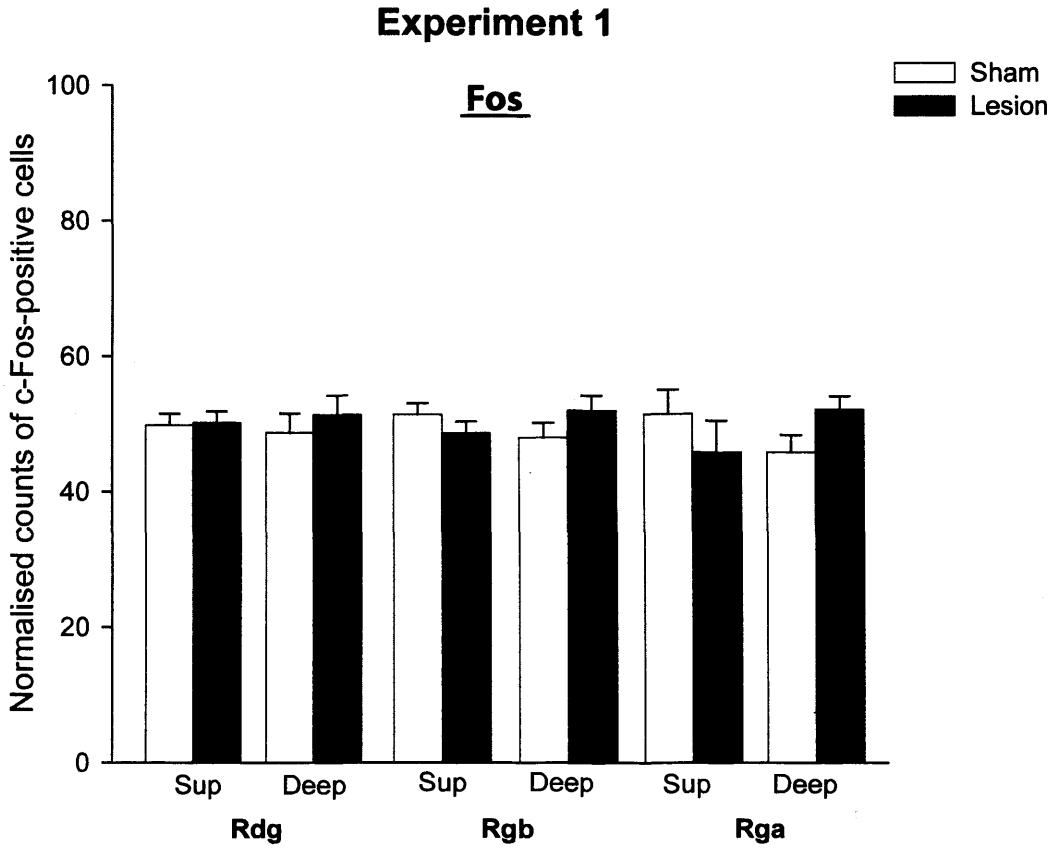

Figure 6. Experiment 1, c-Fos levels after bilateral fornix lesions (black) and their sham controls (white). Normalised counts of c-Fos-positive cells are presented as mean ± standard error of mean (SEM). Abbreviations: Deep, deep layers; Rdg, retrosplenial dysgranular cortex; Rga, retrosplenial granular a cortex; Rgb, retrosplenial granular b cortex; Sup, superficial layers.

Experiment 2: gas anaesthetic, bilateral fornix lesion, spontaneous exploration in radial-arm maze (c-Fos)

Histology

The lesions were complete in 4 out of 6 cases. The percentage of the bilateral fimbria/fornix that was removed was estimated at 90-100% (Figure 5B). This fornix damage was typically accompanied by damage to the caudal portion of

the septum. In one rat, the damage extended to the most rostral part of the left hippocampus.

IEG-positive cell counts

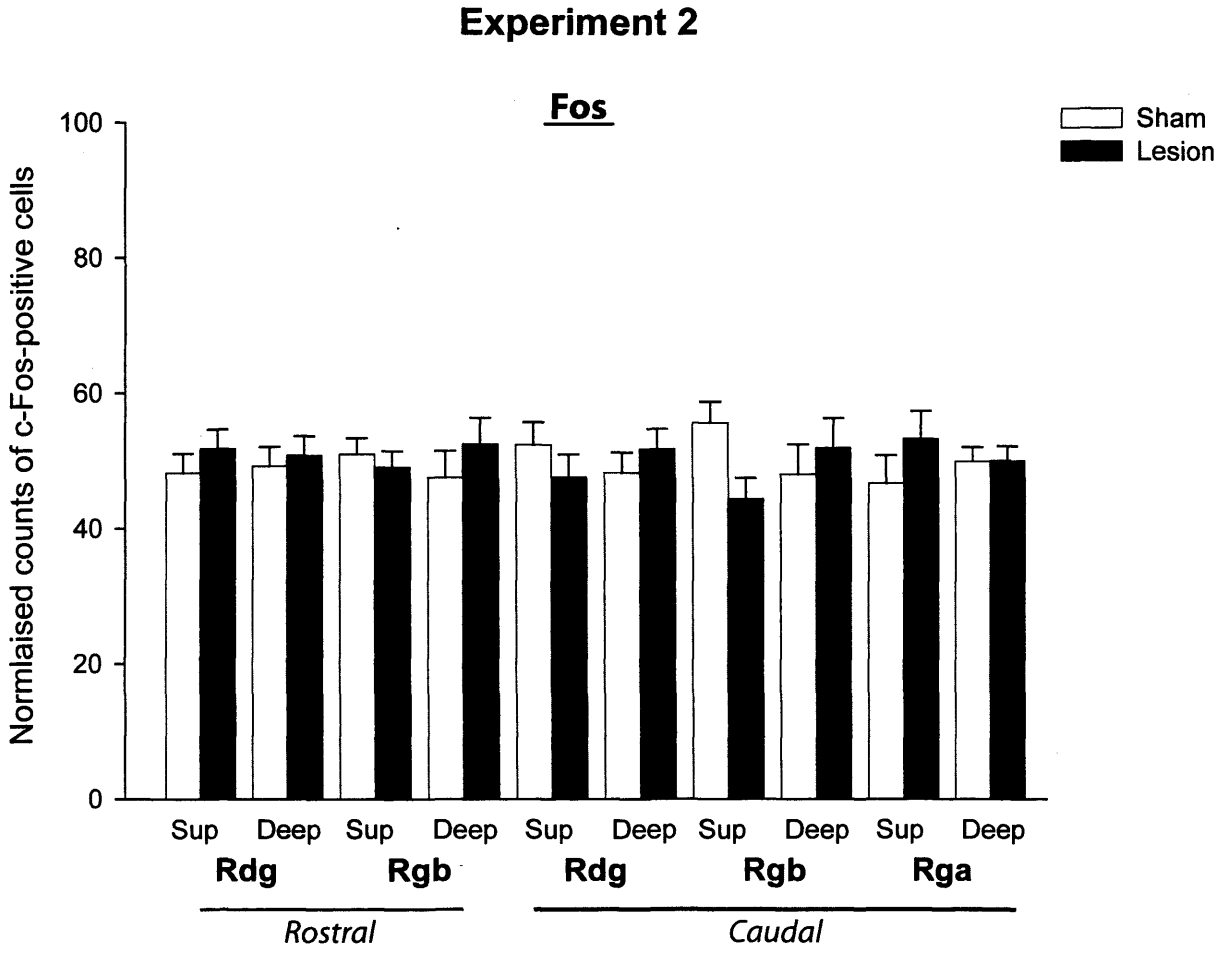

Figure 7. Experiment 2, c-Fos levels after bilateral fornix lesions (black) and their sham controls (white). Normalised counts of c-Fos-positive cells are presented as mean ± standard error of mean (SEM). Abbreviations: Deep, deep layers; Rdg, retrosplenial dysgranular cortex; Rga, retrosplenial granular a cortex; Rgb, retrosplenial granular b cortex; Sup, superficial layers.

c-Fos. In this experiment, the retrosplenial cortex activity was analysed in more detail (rostral and caudal; Figure 7). However, similar to the previous experiment, no overall effect of lesion was found in the retrosplenial cortex (*F*

< 1). Likewise, there was no group x region interaction ($F_{(9,90)}$ = 1.66, p = 0.15). As with the normalised scores, neither a significant lesion (F < 1) nor an interaction (F < 1) was found with the c-Fos raw counts.

Interim conclusion:

This replication study confirmed the absence of lesion effects on c-*fos* activity in the retrosplenial cortex, and so failed to resolve the discrepancy with the findings of Vann *et al.* (2000b) following unilateral fornix lesions. The first possible explanation could be that bilateral fornix lesions do not have the same effect as a unilateral fornix lesion on retrosplenial cortex. Other brain regions might compensate for the complete loss of the fornix and help maintain a 'normal' retrosplenial cortex activity. Another possible reason for this null result may be due to the different behavioural task used to increase c-Fos expression. In the study of Vann *et al.* (2000b), animals were trained in the working memory version of the radial-arm maze task as they had unilateral fornix lesions, whereas animals in Experiments 1 and 2 were trained in a spontaneous exploration version of the radial-arm maze task. In order to get a better understanding of the effect of fornix lesion, the next experiment involved *unilateral* fornix lesions in two different behavioural versions of the radial-arm maze: spontaneous exploration (Experiment 3A) and working memory (Experiment 3B). The latter (Experiment 3B) was designed to match the conditions used by Vann et al. (2000b).

Experiment 3: gas anaesthetic, unilateral fornix lesion

A. spontaneous exploration in radial-arm maze (c-Fos)

B. working memory in radial-arm maze (c-Fos and Zif268)

Histology

The extent of the 13 unilateral fornix lesions is shown in Figure 5C. The lesions included both the fornix and the fimbria. None of the lesions encroached into the intact hemisphere. In 10 out of 13 cases, the unilateral fornix lesions were essentially complete (in one hemisphere only). The percentage of the fimbria/fornix that was removed was estimated to range from 80 to 100%. In 10 cases, the lesion extended to the caudal part of the septum. For 2 cases, there was extra damage to the very rostral part of the hippocampus.

IEG-positive cell counts

A. Spontaneous exploration in radial-arm maze (c-Fos)

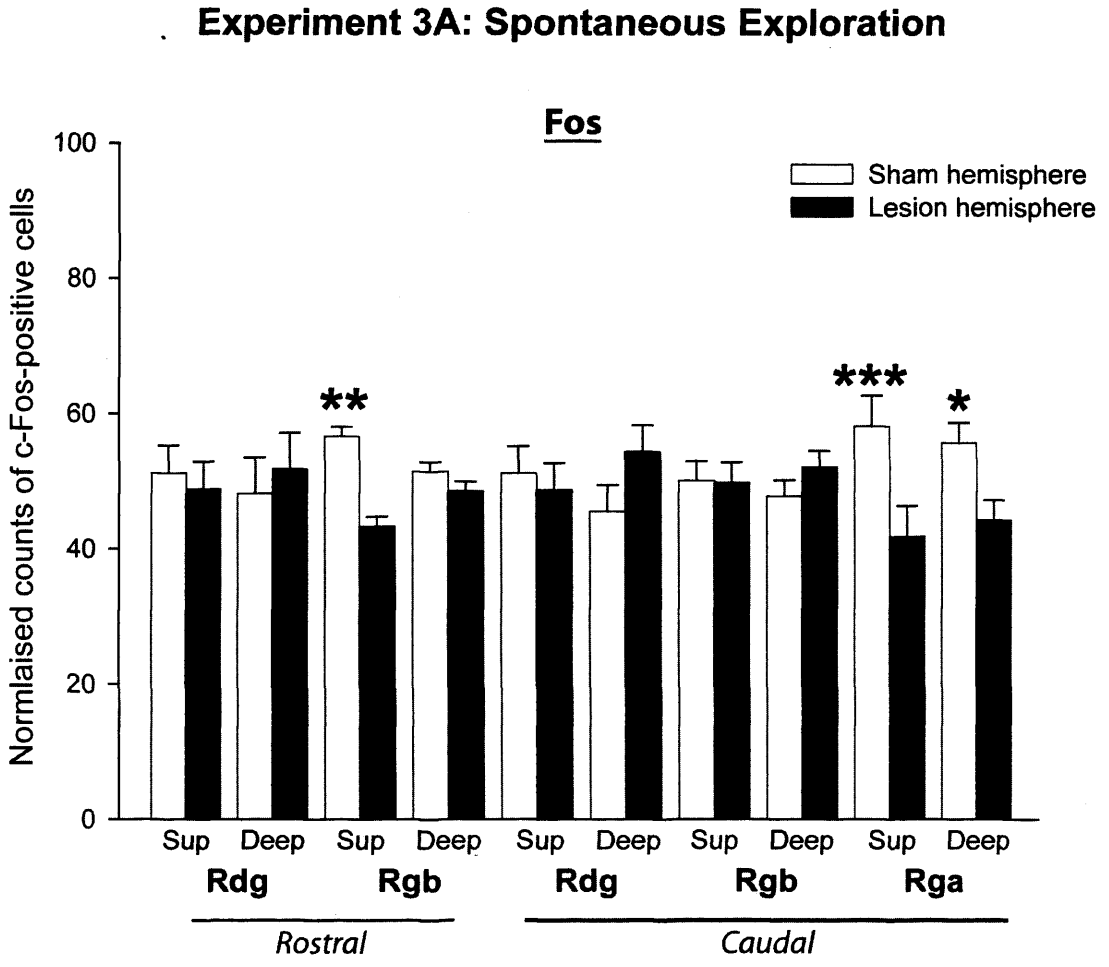

Figure 8. Experiment 3A, spontaneous exploration in radial-arm maze. Normalised c-Fos counts in the retrosplenial cortex in the fornix lesion (black) and control (white) hemispheres after spontaneous exploration. All normalised percentages sum to 100. Errors bars refer to ± SEM of the corresponding mean values. *** $p < 0.001$; ** $p < 0.01$; * $p < 0.05$. Abbreviations: Deep, deep layers; Rdg, retrosplenial dysgranular cortex; Rga, retrosplenial granular a cortex; Rgb, retrosplenial granular b cortex; Sup, superficial layers.

c-Fos. Retrosplenial cortex activity was measured after spontaneous exploration in the radial-arm maze. There was no overall effect of the

unilateral lesions ($F_{(1,10)}$ = 2.11, p = 0.18; Figure 8). However a group x region interaction was found ($F_{(9,90)}$ = 3.05, p < 0.01). Inspection of the simple effects showed that the interaction was caused by reduced counts in the fornix lesion hemisphere in specific sub-regions (Figure 8): superficial layers of rostral Rgb; superficial and deep layers of Rga. All the simple effects are presented in Table 2. Analyses of the raw counts revealed that there was no significant effect of lesions ($F_{(1,5)}$ = 3.88, p = 0.11). Moreover, no interaction was found F < 1).

Table 2. Simple effects after unilateral fornix lesions (Experiment 3A, c-Fos only)

AP	Sub-regions	layers	$F_{(1,100)}$	p
Rostral	Rdg	Superficial	< 1	
		Deep	< 1	
	Rgb	Superficial	**7.19**	**< 0.01****
		Deep	< 1	
Caudal	Rdg	Superficial	< 1	
		Deep	3.18	0.078
	Rgb	Superficial	< 1	
		Deep	< 1	
	Rga	Superficial	**10.81**	**< 0.001*****
		Deep	**5.30**	**< 0.05***

Significant simple effects are highlighted in grey and bold. *** p < 0.001; ** p < 0.01; * p < 0.05. Abbreviations: Rdg, retrosplenial dysgranular cortex; Rga, retrosplenial granular a cortex; Rgb, retrosplenial granular b cortex.

B. working memory in radial-arm maze (c-Fos and Zif268)

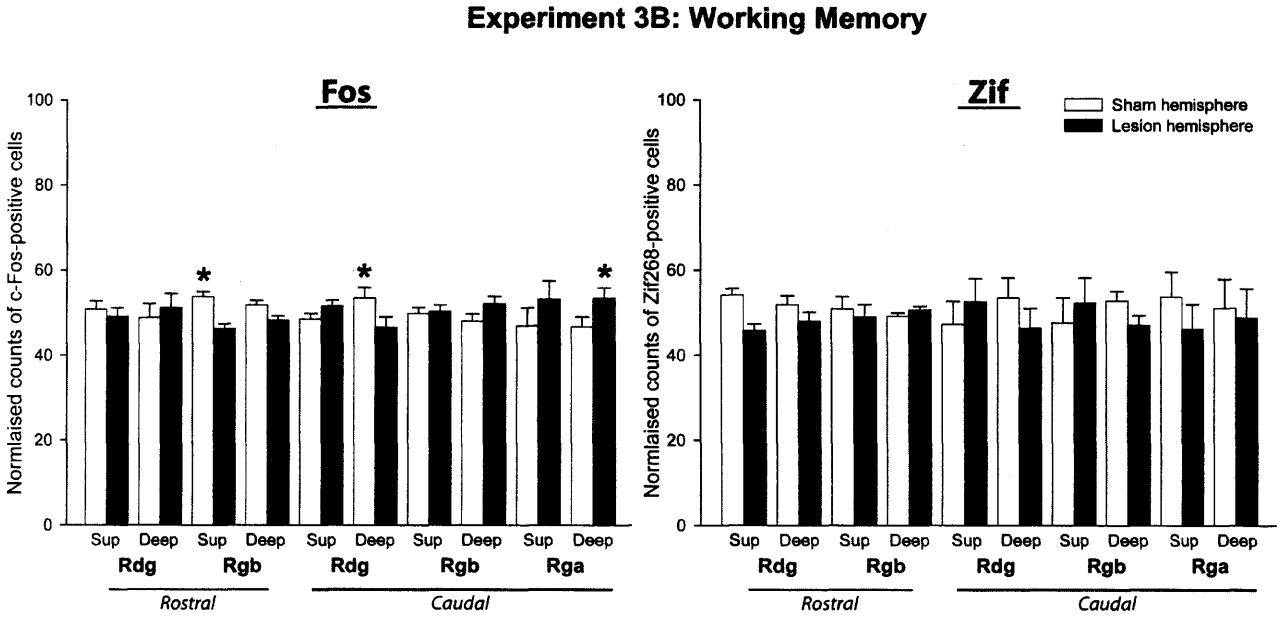

Figure 9. Experiment 3B, working memory in radial-arm maze. Normalised c-Fos counts (left) and Zif268 counts (right) in the retrosplenial cortex in the lesion (black) and control (white) hemisphere after the working memory task. All normalised percentages sum to 100. Errors bars refer to ± SEM of the corresponding mean values. * $p < 0.05$. Abbreviations: Deep, deep layers; Rdg, retrosplenial dysgranular cortex; Rga, retrosplenial granular a cortex; Rgb, retrosplenial granular b cortex; Sup, superficial layers.

c-Fos. For this group, animals were trained in the working memory version of the radial-arm maze task. The lesion did not affect overall retrosplenial cortex activity ($F < 1$, Figure 9, left). But as in the previous experiment, there was a group x region interaction ($F_{(9,108)} = 2.97$, $p < 0.01$). Subsequent analyses (see Table 3) revealed c-Fos changes in three specific sub-regions: superficial layers of rostral Rgb, deep layers of caudal Rdg and deep layers of Rga. In two of these three sites, the fornix lesion hemisphere had reduced counts. The raw counts did not show a significant lesion effect ($F_{(1,6)} = 1.08$, $p = 0.348$). Likewise, no group x region was found ($F_{(9,54)} = 1.46$, $p = 0.19$).

Table 3. Simple effects after unilateral fornix lesions (Experiment 3B, c-Fos)

AP	Sub-regions	layers	$F_{(1,120)}$	*p*
Rostral	Rdg	Superficial	< 1	
		Deep	< 1	
	Rgb	Superficial	**5.36**	**< 0.05***
		Deep	1.24	0.27
Caudal	Rdg	Superficial	< 1	
		Deep	**4.39**	**< 0.05***
	Rgb	Superficial	< 1	
		Deep	1.60	0.21
	Rga	Superficial	3.70	0.057
		Deep	**4.34**	**< 0.05***

Only c-Fos simple effects analysis is presented as there was no group effect or interaction for Zif268. Significant simple effects for c-Fos are highlighted in grey and bold. * $p < 0.05$. Abbreviations: Rdg, retrosplenial dysgranular cortex; Rga, retrosplenial granular a cortex; Rgb, retrosplenial granular b cortex.

Zif268. Similar to c-*fos* activity, there was no overall effect of the lesion on *zif*268 retrosplenial cortex activity ($F < 1$, Figure 9, right). But unlike c-Fos counts, no group x region interaction was found with Zif268 counts ($F < 1$). Accordingly to the normalised counts, the raw counts did not show an effect of lesions ($F_{(1,6)} = 1.03$, $p = 0.35$). No group x region interaction was found ($F < 1$).

Interim conclusion:

Experiments 3A and 3B showed similar results, in that there was no overall IEG difference, with only inconsistent effects in retrosplenial cortex sub-regions after unilateral fornix lesions. Thus it can be concluded that the different behavioural tasks are not responsible for changes in the retrosplenial

cortex activity following unilateral fornix lesions. So even by training unilateral fornix animals in the same working memory version of the radial-arm maze task used by that Vann et al. (2000b), our results did not match their data. Moreover, the extra analysis of another IEG, *zif*268, which has showed similar activation compared to c-*fos* in the retrosplenial cortex in previous studies (Jenkins et al., 2004a; Albasser et al., 2007), failed to replicate the fornix lesion effect on the retrosplenial cortex.

In summary, changing the lesion (bilateral to unilateral), the behavioural task or the IEG did little to resolve the inconsistencies with Vann et al. (2000b). While a small number of retrosplenial sites now showed modest IEG changes, this effect was sporadic. After having re-examined the original experiment, it was noted that the only difference remaining between Vann's study and the experiments of this chapter was the anaesthetic used for the surgery. In this Chapter (Experiments 1-3), all the animals were anaesthetised with a mixture of isoflurane gas and oxygen, whereas intraperitoneal injection of sodium pentobarbital (60 mg/kg, Euthatal, Rhone Merieux, UK) was used in the study of Vann et al. (2000b).

Experiment 4: injectable anaesthetic, unilateral fornix lesion, working memory in the radial-arm maze (c-Fos and Zif268)

Histology

The unilateral fornix lesions were complete (in one hemisphere only) in 8 out of 10 cases. The estimated damage to the fornix ranged between 90 and 100%, as shown in Figure 5D, whereas the other hemisphere remained intact. In all cases, the lesion extended to the caudal part of the septum. For 3 cases, the rostral part of the hippocampus was also damaged.

IEG-positive cell counts

The retrosplenial cortex

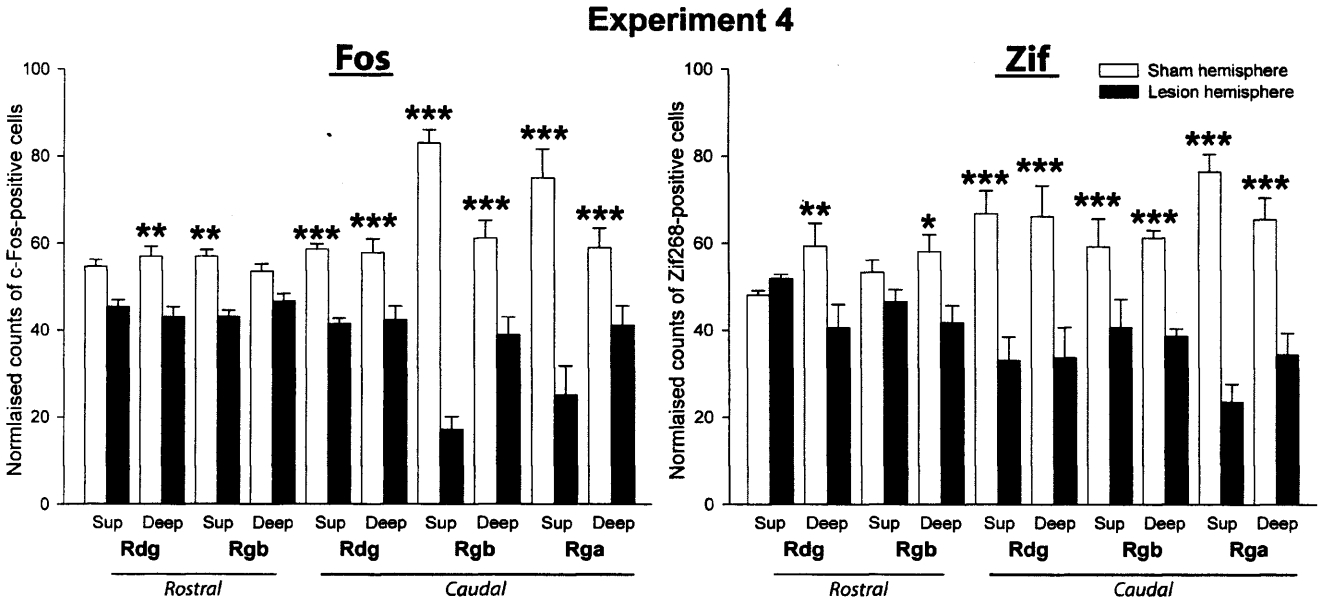

Figure 10. Experiment 4, working memory in radial-arm maze. c-Fos (Left) and Zif268 (Right) levels after unilateral fornix lesions after working memory task in radial-arm maze. Normalised counts of IEG-positive cells in the retrosplenial cortex are shown for the sham control hemisphere (white) and the fornix lesion hemisphere (black). Data are shown as mean + SEM. Significance of differences in counts: * $p < 0.05$, ** $p < 0.01$, *** $p < 0.001$. Abbreviations: Deep, deep layers; Rdg, retrosplenial dysgranular cortex; Rga, retrosplenial granular a cortex; Rgb, retrosplenial granular b cortex; Sup, superficial layers.

c-Fos. In contrast to the previous Experiments 1-3, there was a widespread fall in c-Fos-positive cell counts across the retrosplenial cortex on the side of the fornix lesions (Figure 10). For the first time in this study, an overall effect of the lesions was found ($F_{(1,18)} = 84.5$, $p < 0.001$). In addition, there was a group x region interaction ($F_{(9,162)} = 20.1$, $p < 0.001$), showing changes in c-Fos counts across sub-regions. The impact of the fornix lesions was most evident in the caudal retrosplenial cortex. Simple effects are presented in

Table 4. Similar to the normalised counts, raw counts revealed a significant lesion effect ($F_{(1,9)}$ = 23.46, p < 0.001) as well as an interaction ($F_{(9,81)}$ = 6.65, p < 0.001). Subsequent analyses showed that the c-Fos decrease was found in most of the retrosplenial sub-regions (simple effects; rostral Rdg: superficial, $F_{(1,90)}$ = 3.87, p = 0.052 – deep, $F_{(1,90)}$ = 14.26, p < 0.001; rostral Rgb: superficial, $F_{(1,90)}$ = 9.60, p < 0.003 – deep, $F_{(1,90)}$ = 8.26, p < 0.005; caudal Rdg: superficial, $F_{(1,90)}$ = 2.55, p = 0.11 – deep, $F_{(1,90)}$ = 8.17, p < 0.005; caudal Rgb: superficial, $F_{(1,90)}$ = 66.05, p < 0.001 – deep, $F_{(1,90)}$ = 19.42, p < 0.001; Rga: superficial, F < 1 – deep, $F_{(1,90)}$ = 1.61, p = 0.21).

Zif268. Counts of Zif268-positive cells in Rdg, Rgb and Rga were markedly reduced following unilateral fornix lesions (see Figure 10, right) when animals were anaesthetised with an injection of sodium pentobarbital ($F_{(1,18)}$ = 25.90, p < 0.01). As for c-Fos, there was a group x region interaction ($F_{(9,162)}$ = 20.1, p < 0.001), reflecting different degrees of Zif268 hypoactivity between sub-regions, with a greater decrease occurring in the caudal part of the retrosplenial cortex. Subsequent inspection showed that the differences between the two groups were significant in most of the sub-regions, as confirmed by the simple effects (see Table 4). Moreover, the raw counts confirmed the significant lesion effect ($F_{(1,9)}$ = 30.22, p < 0.001) as well as the interaction ($F_{(9,81)}$ = 11.41, p < 0.001). Subsequent analyses confirmed the widespread Zif decrease throughout the retrosplenial sub-regions (simple effects; rostral Rdg: superficial, F < 1 – deep, $F_{(1,90)}$ = 9.45, p < 0.003; rostral Rgb: superficial, $F_{(1,90)}$ = 1.24, p = 0.27 – deep, $F_{(1,90)}$ = 7.22, p < 0.009; caudal Rdg: superficial, $F_{(1,90)}$ = 30.69, p < 0.001 – deep, $F_{(1,90)}$ = 28.69, p < 0.001; caudal Rgb: superficial, $F_{(1,90)}$ = 9.31, p < 0.003 – deep, $F_{(1,90)}$ = 13.91, p < 0.001; Rga: superficial, $F_{(1,90)}$ = 75.79, p < 0.001 – deep, $F_{(1,90)}$ = 26.18, p < 0.001).

Table 4. Simple effects after unilateral fornix lesions (Experiment 4, c-Fos and Zif268)

	c-Fos	Zif268

AP	sub-regions	layers	$F_{(1,180)}$	p	$F_{(1,180)}$	p
Rostral	Rdg	Superficial	3.77	0.054	< 1	
		Deep	**8.42**	**< 0.01****	**8.10**	**< 0.01****
	Rgb	Superficial	**8.52**	**< 0.01****	1.06	0.31
		Deep	2.09	0.151	**6.19**	**< 0.05***
Caudal	Rdg	Superficial	**12.85**	**< 0.001*****	**26.30**	**< 0.001*****
		Deep	**10.49**	**< 0.001*****	**24.59**	**< 0.001*****
	Rgb	Superficial	**190.6**	**< 0.001*****	**7.98**	**< 0.01****
		Deep	**21.61**	**< 0.001*****	**11.92**	**< 0.001*****
	Rga	Superficial	**109.1**	**< 0.001*****	**64.97**	**< 0.001*****
		Deep	**13.98**	**< 0.001*****	**22.44**	**< 0.001*****

Significant simple effects are highlighted in grey and bold. *** $p < 0.001$; ** $p < 0.01$; * $p < 0.05$. Abbreviations: Rdg, retrosplenial dysgranular cortex; Rga, retrosplenial granular a cortex; Rgb, retrosplenial granular b cortex.

Cortical comparison areas (Experiment 4)

c-Fos. There was no significant, overall change in c-Fos counts after unilateral fornix lesions in the two cortical regions that were analysed (motor cortex and somatosensory cortex; $F < 1$, Figure 11, left). Likewise, there was no group x region interaction ($F < 1$). The raw counts did not show a lesion effects ($F < 1$), and no interaction was found ($F < 1$).

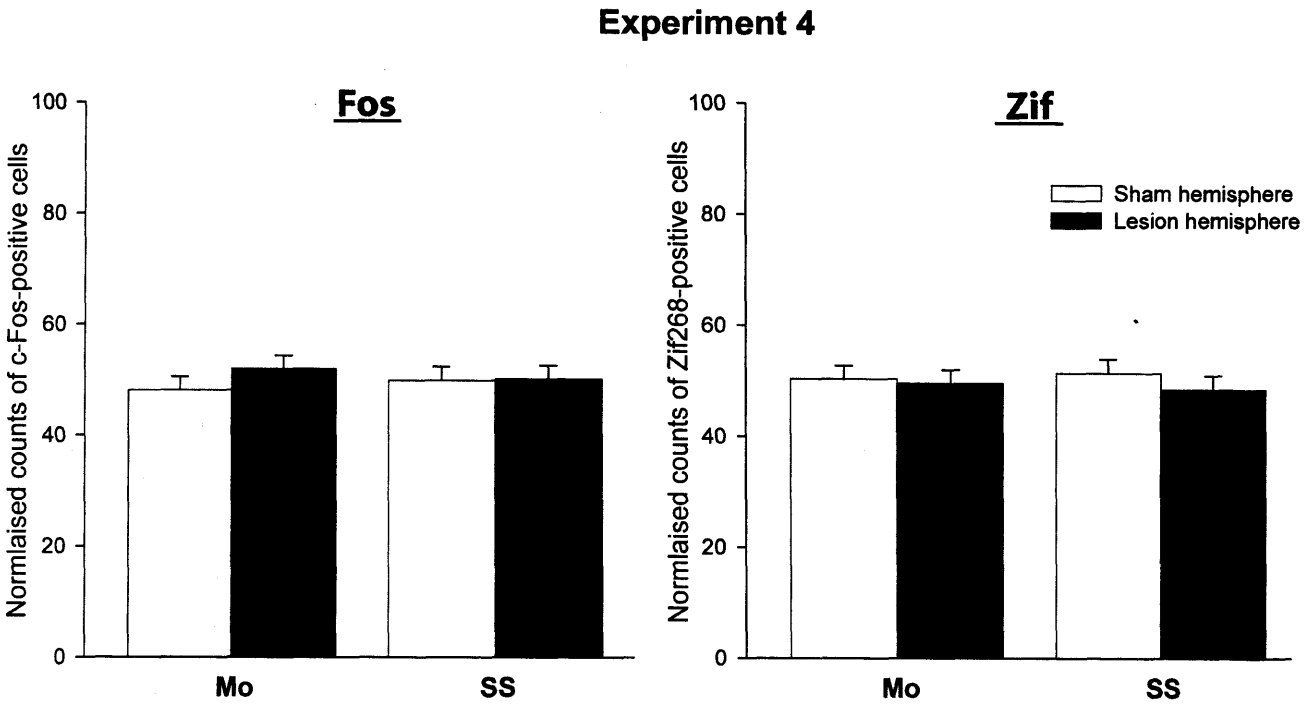

Figure 11. Cortical comparison for Experiment 4, working memory in radial-arm maze. c-Fos (Left) and Zif268 (Right) counts following the working memory test in the radial-arm maze. Normalised counts of IEG-positive cells are shown for the cortical comparison areas. Data are shown as mean + SEM. Abbreviations: Mo, primary motor cortex; SS, primary somatosensory area.

Zif268. Similar to c-Fos counts, unilateral fornix lesions did not induce significant changes in Zif268 counts in either motor cortex or somatosensory cortex ($F < 1$, Figure 11, right). No group x region interaction was found ($F < 1$). With the raw counts, there was no effect of the lesions on the Zif268 counts ($F < 1$), and no interaction was found either ($F < 1$).

Comparison between anaesthetics: gas versus injectable.

In order to test whether the anaesthetic used for unilateral fornix lesions may have an impact on the retrosplenial cortex activity, a direct comparison was made between the effect of gas (Experiment 3B) and of injectable (Experiment 4). Here except for the anaesthetic used, all the other features of

the protocol, such as the behaviour, the immunohistochemistry and the counting, were rigorously matched between Experiments 3B and 4. Normalised counts in the retrosplenial cortex of the lesion hemisphere were then compared.

Comparison between gas and injectable: Experiment 3B versus Experiment 4

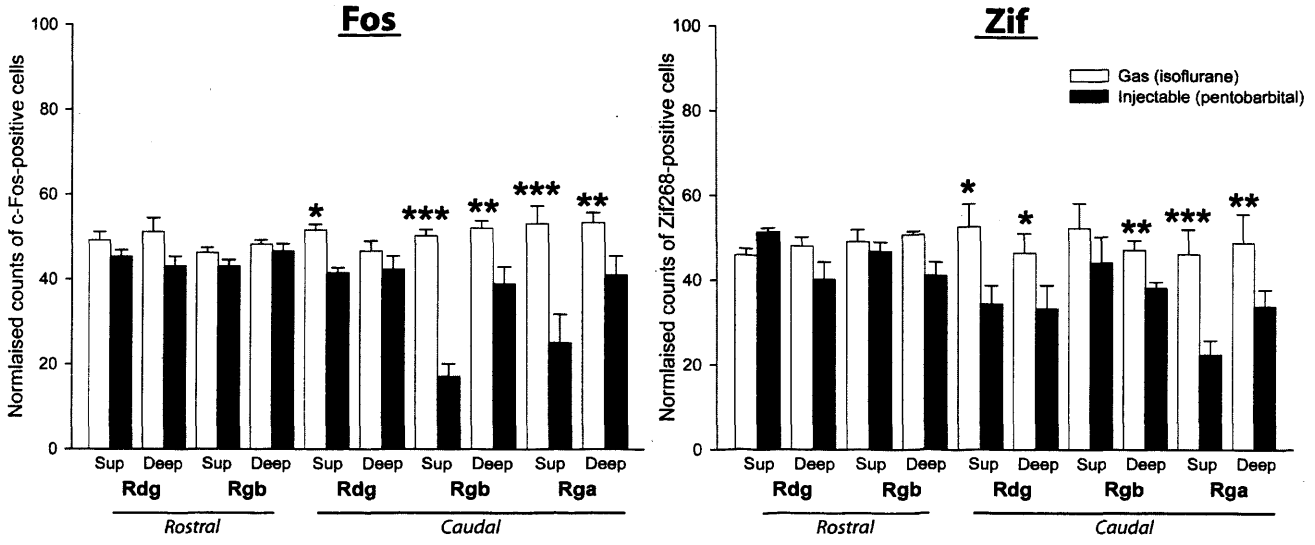

Figure 12. Comparison between Experiment 3B and 4. c-Fos (Left) and Zif268 (Right) counts in the retrosplenial cortex levels after unilateral fornix lesions made with gas (white) or pentobarbital (black). The bar chart represents normalised counts of IEG-positive cells in the retrosplenial cortex. Data are shown as mean + SEM. Significance of differences in counts: * $p <$ 0.05, ** $p < 0.01$, *** $p < 0.001$. Abbreviations: Deep, deep layers; Rdg, retrosplenial dysgranular cortex; Rga, retrosplenial granular a cortex; Rgb, retrosplenial granular b cortex; Sup, superficial layers.

c-Fos. The counts of c-Fos-positive cells were significantly lower after fornix lesions when anaesthesia was induced by an injection of pentobarbital compared to the mixture of isoflurane gas and oxygen ($F_{(1,15)} = 24.97$, $p <$ 0.001, see Figure 12, left). A group x region interaction was found ($F_{(9,15)} =$ 7.08, $p < 0.001$), revealing a greater decrease of activity in the caudal part of the retrosplenial cortex, as shown by the simple effects analysis (see Table 5).

Zif268. There was a significant effect of the anaesthetic used during surgery, with a greater decrease of Zif268-positive cells with injectable anaesthetic, sodium pentobarbital ($F_{(1,15)}$ = 16.34, p < 0.001, Figure 12, right). A group x sub-region interaction was found ($F_{(9,15)}$ = 4.52, p < 0.001), showing that caudal sub-regions were more sensitive to the effects of the lesions made with pentobarbital, as presented in Table 5.

Table 5. Simple effects: Comparison between anaesthetics (Experiment 3B & 4)

			c-Fos		Zif268	
AP	**sub-regions**	**layers**	$F_{(1,150)}$	p	$F_{(1,150)}$	p
Rostral	Rdg	Superficial	< 1		1.64	0.25
		Deep	3.25	0.074	3.25	0.12
	Rgb	Superficial	< 1		< 1	
		Deep	< 1		**4.68**	**< 0.05***
Caudal	Rdg	Superficial	**5.04**	**< 0.05***	**5.04**	**< 0.05***
		Deep	< 1		3.98	0.082
	Rgb	Superficial	**54.46**	**< 0.001*****	< 1	
		Deep	**8.56**	**< 0.01****	**7.33**	**< 0.01****
	Rga	Superficial	**38.95**	**< 0.001*****	**38.95**	**< 0.001*****
		Deep	**7.51**	**< 0.01****	**7.81**	**< 0.01****

Significant simple effects are highlighted in grey and bold. *** p < 0.001; ** p < 0.01; * p < 0.05. Abbreviations: Rdg, retrosplenial dysgranular cortex; Rga, retrosplenial granular a cortex; Rgb, retrosplenial granular b cortex.

Discussion

Lesions centred in the fornix do not always reduce c-*fos* activity in the retrosplenial cortex. In Experiments 1 and 2, animals received bilateral lesions of the fornix, using isoflurane gas for the surgery and were tested in spontaneous exploration in radial-arm maze. There was no evidence of activity changes in the retrosplenial cortex. In Experiment 3, animals were also anaesthetised with isoflurane gas, and had unilateral fornix lesions. Two different behavioural tasks (3A, spontaneous exploration; 3B working memory) were performed by the animals. Once again, no clear effect of the fornix lesions on retrosplenial cortex activity was found in the two different behavioural tests. The results do not appear to be task specific. Even though there were changes in the protocol in these three experiments, the conclusion remained consistent with no clear effect of the fornix lesions on retrosplenial cortex activity. In the final Experiment 4, the anaesthetic was changed for the first time compared to the other three experiments. The animals were anaesthetised with injection of pentobarbital (i. v.), and unilateral lesions of the fornix were made. The animals were trained in the working memory task in the radial-arm maze (identical to Experiment 3B). In the present study, it was only in Experiment 4 that fornix lesions induced a consistent IEG hypoactivity in the retrosplenial cortex. This hypoactivity was most evident in the caudal part of the retrosplenial cortex.

Fornix lesions consistently impair performance of the working memory task in the radial-arm maze (Olton et al., 1979; Aggleton et al., 1992; Cassel et al., 1998). Animals with retrosplenial cortex lesions are also impaired in spatial tasks, such as the working memory task in the radial-arm maze (used in the present study) or the reference memory task in the water maze (Vann and Aggleton, 2002). Moreover, performing the working memory task in the radial-arm maze produced significant c-Fos increases in both rostral and caudal parts of the retrosplenial cortex compared to rats running up and down a single arm in the same maze (Vann et al., 2000a). Vann et al. (2000b) showed in an IEG study, that fornix lesions induce c-*fos* hypoactivity in the

retrosplenial cortex. However, in that study, the retrosplenial cortex was treated as a single, uniform structure and was not divided into its three sub-regions Rdg, Rgb and Rga (Van Groen and Wyss, 1990c, 1992, 2003). In addition, there was no differentiation in the c-Fos counts between the superficial and deep layers of the retrosplenial cortex. The aim of the present study was to assess in more detail the effect of fornix lesions upon retrosplenial cortex activity. However, this study revealed an unexpected feature.

Table 6. Results of the four experiments

Experiment	Anaesthetic	Fornix Lesion	Behaviour in radial-arm maze	IEG changes in retrosplenial cortex
1	gas	bilateral	spontaneous exploration	-
2	gas	bilateral	spontaneous exploration	-
3A	gas	unilateral	spontaneous exploration	occasional
3B	gas	unilateral	working memory	occasional
4	injectable	unilateral	working memory	constant ↓

IEG changes in the retrosplenial cortex: -, no changes; occasional, changes in specific sub-regions, but no group effect; ↓ changes in most of the sub-regions accompanied with a lesion effect.

It is clear from Table 6 that of our manipulations one critical factor was needed to replicate the findings of Vann et al. (2000b), the anaesthetic. Indeed, retrosplenial cortex hypoactivity following fornix lesions occurred only when the animals were deeply anaesthetised with pentobarbital injection. Variations in the fornix lesions (unilateral and bilateral) or behaviour (spontaneous exploration and working memory) had little or no effect on IEG levels in the retrosplenial cortex (see Table 2). The last experiment of the present study not only replicated previous data, but also revealed that this retrosplenial cortex hypoactivity found after fornix lesions was greater in the caudal part of the retrosplenial cortex. The hypoactivity was neither layer-specific nor c-Fos-specific, i.e. like hippocampal lesions induce overall

changes (Chapter 2, Albasser et al., 2007). In addition, the present study highlights the implication of different anaesthetic on normal activity of the retrosplenial cortex. Therefore, isoflurane gas may have a "protecting effect" following fornix lesions. From this study, it remains unclear whether this gas anaesthetic protection constrains to IEG levels or whether it could prevent behavioural impairments compared to the pentobarbital anaesthetic.

During anaesthesia, the physiology and neurochemistry of the brain are changed. For example, brain electrical activity, blood flow, energy metabolism, neurotransmission, intracellular cascades, gene and protein expressions are all affected during anaesthesia (Hemmings et al., 2005). In animal studies, it was demonstrated that desflurane anaesthesia changed the expression of twenty different proteins in the brain; changes that could persist up to 72 h after anaesthesia (Futterer et al., 2004). In a more recent study, Culley et al. (2006) identified 297 genes, as measured by microarray analysis, that were up- or down-regulated in the rat hippocampus 2 days after general anaesthesia with a mixture of isoflurane and nitrous oxide. These affected genes are known to participate in a wide array of processes including cell survival, signal transduction and synaptic plasticity, transcriptional regulation, metabolism, cell cycle, protein biosynthesis, and structural and vesicular processes, implying that multiple molecular processes are still altered 2 days after general anaesthesia (Culley et al., 2006).

In addition, clinical studies indicate that anaesthesia and surgery are associated with early cognitive impairments in both middle-aged and aged patients, but these deficits were not related to either hypoxemia or hypotension (Moller et al., 1998; Johnson et al., 2002). There is more evidence that anaesthetics, on their own, can have an impact on behavioural performance of the animals. For example, 2 h of isoflurane-nitrous oxide anaesthesia impairs acquisition of a hippocampal-dependent spatial memory task 48 h after cessation of anaesthesia in young rats and at least 2 weeks after cessation of anaesthesia in aged rats (Culley et al., 2004b; Culley et al., 2004a; Crosby et al., 2005). In a recent study, Baxter and colleagues compared the effects of two different anaesthetics, isoflurane and propofol on

rats' behaviour (Baxter et al., 2008). The anaesthesia was used to make neurotoxic lesions of the dorsal hippocampus of the rats. Then animals were tested in a 3/6 reference/working memory task in the radial-arm maze, where the same three arms were baited on each test session, but not rebaited within a trial (Schmitt et al., 2003). This protocol was chosen because it was expected that even animals with severe spatial impairments (dorsal hippocampal lesion) should be able to complete this task (Bannerman et al., 1999). That study of Baxter et al. (2008) found that both lesion groups were impaired, but not in the same way. In early training and overall, the group anaesthetised with propofol (compared to the group anaesthetised with isoflurane) was more impaired. However, at the end of the training, the impairment became larger in the group anaesthetised with isoflurane (relative to the group anaesthetised with propofol). There was no clear evidence of histo-pathological effects between the two groups, except a small increase of body temperature of the rats with the propofol anaesthesia. In addition, no behavioural difference was found between isoflurane and propofol in the two surgery controls (sham). The different lesion effects of the two anaesthetics may be explained by their interactions with the N-methyl-D-aspartate (NMDA) neurotoxin used to make the dorsal hippocampal lesions. It is also possible that the interactions between anaesthetic and lesion can change the extent of the lesion. One way to limit this anaesthetic-neurotoxin effect is to change the lesion technique. In this Chapter, lesions were made with radiofrequency, which by increasing the temperature of the tip of the probe damages the fornix. Thus, chemical interactions between the radiofrequency lesion method and the anaesthetics are reduced (the anaesthetic could, however, affect blood perfusion or post-injury repair processes, and so still affect lesion extent). Furthermore, the extent of the fornix damage was similar between the four Experiments of this Chapter (see Figure 5).

The nature of anaesthetics is to interact with brain physiology, leading to favourable and adverse effects. In order to improve animal welfare, anaesthetic and surgical procedures are evolving constantly. It appears that this factor should be considered carefully in experiment design, and especially when comparisons of lesion effects on behaviour are made with other studies.

It is now accepted that different anaesthetics can have different effects on the organism. For example, it was found that in rats anaesthetised with isoflurane, cerebral blood flow and cerebral blood volume were greater compared to animals anaesthetised with pentobarbital (Todd and Weeks, 1996). Evidence indicates that volatile anaesthetics, such as isoflurane, can have a protection effect, by reducing cerebral infarct volumes, on cerebral injury produced by focal ischemia in animal models (Soonthon-Brant et al., 1999). Nevertheless, it is important to remember that these different anaesthetic effects are specific. For example, in a study of Tung and colleagues (2008), the effects of prolonged different anaesthetics on adult hippocampal cell proliferation were assessed. It was found that prolonged anaesthesia did not alter neural cell proliferation, and by extension, that anaesthetic-induced inhibition of cell proliferation may not explain postoperative cognitive impairments.

As mentioned earlier, there is a possibility that different lesion effects in different groups may relate to interactions between the anaesthetics and the NMDA system. Indeed, it has been found that administration of isoflurane maintained at a specific concentration reduces NMDA-mediated cortical injury *in vitro* and *in vivo* (Yang and Zorumski, 1991; Harada et al., 1999). Volatile anaesthetics, such as isoflurane can reduce neural injury by attenuating NMDA excitotoxicity: this effect was found in several studies showing that isoflurane reduces calcium influx (Miao et al., 1995), reduces glutamate release (Schlame and Hemmings, 1995; Ratnakumari and Hemmings, 1998) and increases the rate of uptake of excitatory of neurotransmitters (Larsen et al., 1997). However, pentobarbital and other intravenous anaesthetics have been shown to be more effective on inhibitory pathways in area CA1 of the rat hippocampus *in vitro* (Wakasugi et al., 1999; Asahi et al., 2006). The findings indicate that intravenous anaesthetics do not modulate NMDA receptors, but produce inhibitory actions due to enhancement in the γ-aminobutyric acid type A ($GABA_A$) receptor-mediated responses in the rat hippocampal CA1. These results provide further support that the mechanisms of anaesthetic actions produce distinctive effects on different pathways in the central nervous system. Thus, the protective effect of isoflurane found in the present study

may be explained by its ability to reduce the NMDA excitotoxicity following the fornix lesions. In a recent electrophysiological study, Wang et al. (2009) compared the effects of desflurane (a volatile anaesthetic) and propofol on hippocampal slice CA1 pyramidal cells after hypoxia in rat. Desflurane, but not propofol, improved the resting and action potentials in the pyramidal cells after hypoxia. These electrophysiological changes improve the recovery of the cells and, therefore, may be part of the protective effect found with volatile anaesthetic.

The changes in IEG expression in the retrosplenial cortex following fornix lesions are also interesting in comparison with previous IEG/lesion studies. In the present experiment, a c-Fos reduction of around 20% was found in the retrosplenial cortex, whereas (radiofrequency, NMDA and ibotenic acid) lesions of the hippocampus halved the number of positive cells in the retrosplenial cortex (see Chapter 2 and Albasser et al., 2007). This difference is striking as the fornix carries fibres that travel to and from the hippocampal formation (Saunders and Aggleton, 2007). It is, however, known that the hippocampus has direct connections with the retrosplenial cortex (Van Groen and Wyss, 1990b; Wyss and Van Groen, 1992). In contrast, only one study has reported direct connections from the fornix to the retrosplenial cortex via a cholinergic pathway (Gage et al., 1994). Given that other anatomical studies have failed to find this pathway (Valenstein et al., 1987; Van Groen and Wyss, 1990c, 1992, 2003), it should be treated with caution. Even if there may exist connections between fornix and retrosplenial cortex, it does not explain why retrosplenial cortex hypoactivity was found only in Experiment 4. In all the experiments (1-4) of this Chapter, the fornix was damaged, so interrupting only direct connections between those two structures.

Fornix lesions are often considered to have similar effects on behaviour compared to hippocampal lesions (Aggleton and Brown, 1999; Galani et al., 2002). However, fornix lesions seem to be, sometimes, not as severe as hippocampal lesions (Eichenbaum et al., 1990; Whishaw and Jarrard, 1995). For example, on reference memory tests in the Morris water maze, rats with fornix lesions are slower than normal animals, but they are still able to learn

about the approximate location of the hidden platform (Whishaw and Jarrard, 1995; Warburton and Aggleton, 1999). In contrast, animals with hippocampal lesions require considerable overtraining to show a place preference in the water maze (Morris et al., 1990). As a consequence, some but not all behavioural studies predict a similar impact of both fornix and hippocampal lesions, yet the IEG studies (Chapters 2 and 4) revealed that these two lesions produce very different patterns of c-*fos* activity in the retrosplenial cortex. Clearly, the two forms of lesion should not be seen as directly comparable.

A separate IEG study focused on the effects of anterior thalamic nuclei lesions on retrosplenial cortex activity. It was found that anterior thalamic nuclei lesions cause massive reductions in c-Fos levels (80% or more), which are localised in the superficial layers of the granular retrosplenial cortex (Jenkins et al., 2004a). Once again, the pattern of c-Fos counts was very different from the one obtained after fornix lesions, as c-Fos changes were not as severe and more evident in the caudal part of the retrosplenial cortex. The fornix is one of the major input routes to the anterior thalamic nuclei (Aggleton et al., 1986), which, in turn, have direct projections to the retrosplenial cortex (Van Groen et al., 1993). The fornix is, however, not the only input to the anterior thalamic nuclei, as these nuclei receive dense afferent connections from the mammillary bodies (Vann and Aggleton, 2004b; Vann et al., 2007). These latter projections are unidirectional; they originate in the mammillary bodies, form the mammillothalamic tract and terminate in the anterior thalamic nuclei. The mammillothalamic tract does not contain direct inputs to the retrosplenial cortex and so can have only indirect effects on the retrosplenial cortex. However, it has been shown that radiofrequency mammillothalamic tract lesions markedly reduce the activity of the retrosplenial cortex (see Chapter 3, Vann and Albasser, 2009). This anatomical property raises an unresolved question as mammillothalamic tract lesions have much more profound effects upon retrosplenial IEG levels than fornix lesions. Nevertheless, both tracts densely innervate the anterior thalamic nuclei and only the fornix is thought to possess a few fibres that reach the retrosplenial cortex directly (see Gage et al., 1994). These IEG findings suggest that the

anterior thalamic nuclei are more gated by the mammillary bodies than by the fornix; and so might explain the discrepancies between the two IEG/lesion studies.

To conclude, this study highlights the potential importance of the fornix in the extended hippocampal memory system (Delay and Brion, 1969; Aggleton and Brown, 2006). Fornix lesions reduce IEG activity in the retrosplenial cortex, especially in its caudal part. This greater hypoactivity of the caudal retrosplenial cortex is, however, specific to the fornix lesions and differs to other previous IEG/lesion studies (Jenkins et al., 2004a; Albasser et al., 2007; Vann and Albasser, 2009). In addition, this study draws attention to the need of choosing the appropriate anaesthesia and its consequences. This factor should be considered carefully in experimental design, in cross-study comparisons and study replications of lesion effects on behaviour. Finally, in order to conclude more precisely on the protective effect of the isoflurane anaesthesia, a final experiment is needed (and planned), where both behaviour and IEG expression will be assessed. Two groups of animals will be anaesthetised by either isoflurane gas or pentobarbital injection, while physiological parameters, such as temperature and blood pressure will be measured. The rats will have bilateral fornix lesions made by radiofrequency. Animals will then be tested on different spatial tasks sensitive to fornix lesions to determine if the severity of the deficit is modulated by anaesthetic. Finally, several markers will be assessed to compare the effects of the two anaesthetics at a cellular and molecular level: NeuN and Nissl staining for cytoarchitectural differences; markers of NMDA and GABA receptors for anaesthetic interactions; IEG levels for neuronal activity.

Chapter 5

Combining a New Behavioural Paradigm With Immediate-Early Gene Expression to Investigate Object Recognition

Introduction

In order to understand how novel events are learnt it is necessary to uncover the patterns of interactions between key temporal lobe structures. Studies of rats and monkeys have repeatedly shown that the perirhinal cortex is necessary for identifying visual novelty (Zola-Morgan et al., 1989; Brown and Aggleton, 2001), though the functional significance of its links with the hippocampus for learning remain highly contentious (Eichenbaum et al., 2007; Squire et al., 2007). A recent model, largely derived from in-depth recordings in the human temporal lobe, states that the rhinal cortex serves as a 'gatekeeper' for memory via its ability to regulate hippocampal activity (Fernandez and Tendolkar, 2006). In this model, Fernandez and Tendolkar (2006) suggest a rhinal processing stage that optimises the declarative memory system by fully integrating encoding and retrieval operations before transfering more efficiently the information to the hippocampus (Figure 1). When a new item is perceived, a large number of rhinal neurons is required to process this item, leading to the feeling that the item is unknown. This recruitment leads to effective encoding and effective information transfer to the hippocampus for further encoding. In contrast, when a familiar item is perceived, smaller numbers of rhinal neurons are necessary to process this

item, leading to a less vigorous encoding and reduced information transfer to the hippocampus (see Figure 1). As a consequence, novel stimuli evoke greater hippocampal resources. The present study sought to examine this model and, in particular, test the hypothesis that the 'gatekeeper' function involves effective changes in the activity of the two major pathways from the parahippocampal cortices to the hippocampus, the perforant pathway (to the dentate gyrus) and the temporo-ammonic pathway (to the CA fields).

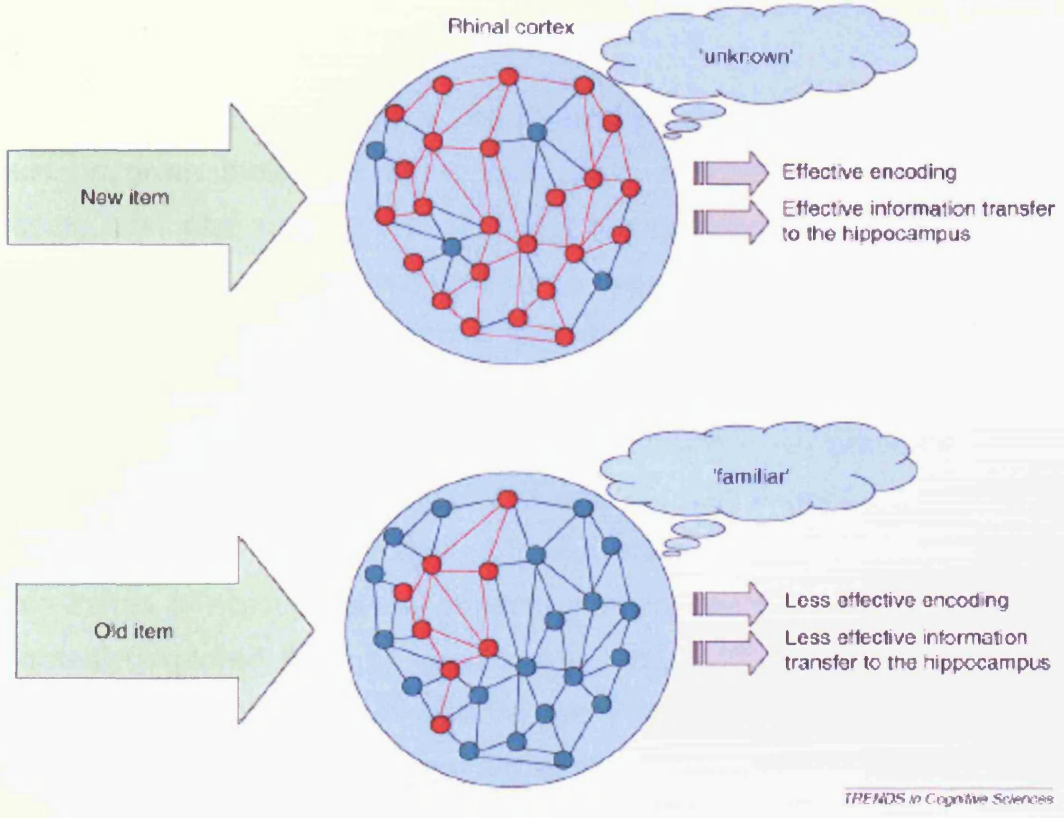

Figure 1. The gatekeeper of the declarative memory system: schematic depiction of the integrated operation executed by the rhinal cortex and its consequences for recognition, encoding and information transfer to the hippocampus (Fernandez and Tendolkar, 2006).

Testing these proposals requires the measurement of simultaneous activity across multiple temporal lobe sites. To achieve this goal the present study compared immediate-early gene (IEG) expression in normal rats. The IEG c-*fos* was selected as it is rapidly induced following exposure to novel visual stimuli (Zhu et al., 1996; Wan et al., 1999; Van Elzakker et al., 2008). While

there are other potential activity markers, c-*fos* has the particular advantage that its role as an inducible transcription factor links it strongly with neuronal plasticity and learning dependent on the temporal lobe (Tischmeyer and Grimm, 1999; Wan et al., 1999; Fleischmann et al., 2003). To induce c-*fos* activity rats were trained on an object recognition task. This category of tasks is ideal as not only the perirhinal cortex is vital for normal recognition, but there is evidence from antisense infusions that c-*fos* activity in the perirhinal cortex is required for stable recognition memory in rats (Seoane and Brown, 2007).

The first task was to devise a behavioural procedure where individual rats could be given multiple trials to help yield a signal detectable to activity imaging, and also display robust object recognition. Rats were accordingly trained on a new shuttle-box (the bow-tie maze) task that combines features of delayed nonmatching-to-sample (Mishkin and Delacour, 1975; Aggleton, 1985) with spontaneous exploration (Ennaceur and Delacour, 1988). For Group Novel every trial consisted of being simultaneously presented with two objects for exploration, one novel and one familiar. A control group ('Group Familiar') provided baseline levels of c-*fos* activity as these rats explored the same series of objects, but all objects were highly familiar as the rats had repeatedly explored them on previous sessions. All objects were baited so that both sets of rats would explore every stimulus, but Group Novel rats should spend disproportionately more time with novel objects. Structural equation modelling was then applied to the c-Fos results to test for changes in the direction of effects within the temporal lobe when rats changed from familiar to novel objects. Indeed, pathways starting in the caudal perirhinal cortex display a dynamic switch in their direction of effects from entorhinal cortex → dentate gyrus (perforant pathway) engagement with novel objects, compared with entorhinal cortex → CA field engagement (temporo-ammonic pathway) with familiar objects. This entorhinal switch not only substantiates the 'gatekeeper' hypothesis, whereby, rhinal cortex moderates hippocampal processing but also indicates that the mechanism involves a change from temporo-ammonic to perforant pathway influences.

Materials and Methods

Animals

Subjects were 20 naïve male rats (Dark Agouti strain, Harlan, UK). The rats were 12-14 weeks old at the beginning of the experiment. Animals were food-deprived to 85% of their free-feeding body weight and were maintained at this level. Water was available *ad libitum*. Rats were housed in pairs under diurnal conditions (14 h light, 10 h dark), and testing occurred at a regular time during the light period. Animals were thoroughly habituated to handling before the study began. All experiments were performed in accordance with the UK Animals (Scientific Procedures) Act (1986) and associated guidelines.

Apparatus

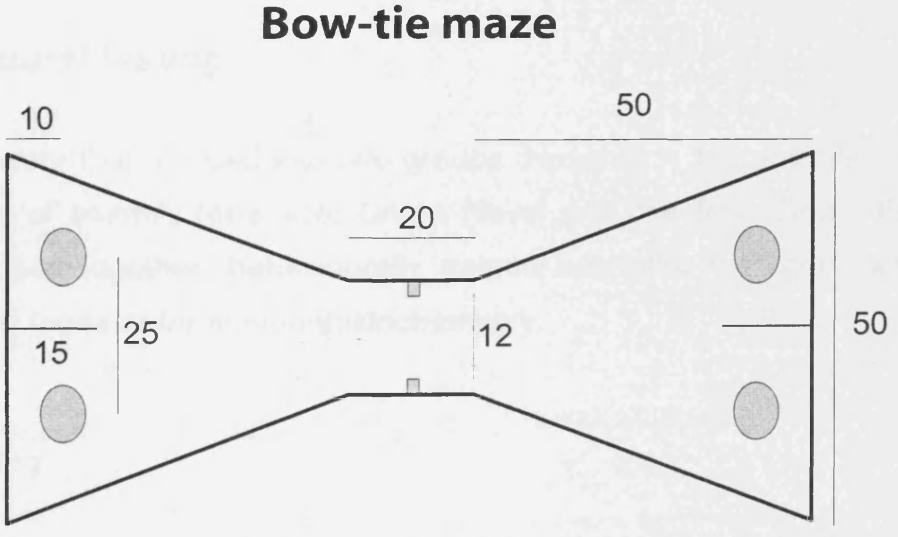

Figure 2. Schematic of the Bow-tie maze, with dimensions in centimetres. Dark circles represent the food well. The guillotine door fits in the centre of the maze.

The animals were tested in a bow-tie shaped maze made of opaque Perspex (Figure 2). The apparatus was 120 cm long, 50 cm wide and 50 cm high.

Each end of the apparatus was triangular, the apices of which were joined by a narrow corridor (12 cm wide). There was an opaque guillotine door in the middle of the corridor that could be raised by the experimenter. The far wall of each triangle contained two recessed food wells, 3.5 cm in diameter and 2 cm deep. The food wells were separated by a short, opaque dividing wall, which protruded 15 cm from the middle of the end wall. These food wells were covered by objects in the experiment proper.

Objects

The study used 147 pairs of different junk objects with various shapes, textures, sizes, and colours. Each object was large enough to cover a food well (3.5 cm diameter) but light enough to be displaced. Any object with obvious scents was excluded. The objects were divided into seven sets of 21 objects.

Behavioural testing

Animals were then divided into two groups: Novel (n = 10) and Familiar (n = 10). Pairs of animals (one from Group Novel and one from Group Familiar) were housed together, behaviourally trained one after the other, and then processed together for immunohistochemistry.

Pretraining

Pretaining, which lasted 7 days, involved training all rats to run from one side of the maze to the other, and to displace any object positioned over the two food wells in order to reach food rewards. On day 1, pairs of rats were placed in the apparatus for 30 minutes where they explored the maze freely and ate sucrose pellets (45mg; Noyes Purified Rodent Diet, Lancaster, NH, USA) scattered on the floor and in the food wells. On days 2 and 3, rats were pretrained singly in the maze for 20 minutes, where they were rewarded for

shuttling between the two goal areas. From day 4, the central guillotine door was used to control the movement of the rat from one side of the maze to the other. From day 6, up to three pairs of different objects were introduced in the maze. By the end of pretraining (day 7) all rats would readily push these same three objects, which covered the food wells, to access the food rewards. These three pairs of objects were not used in the experiment proper.

Training Protocol for Group 'Novel'

Animals received 12 training sessions over 6 days (2 sessions per day: morning and afternoon). For Group Novel, new objects were used throughout Sessions 1-6. Those same objects were then repeated just once over the next 6 sessions (Sessions 7-12), but their order changed (Figure 3). Completely novel objects were used for the final test session (Session 13). This extended training was solely to help the control Group Familiar to become fully familiar with every object, and was not required to improve recognition by Group Novel.

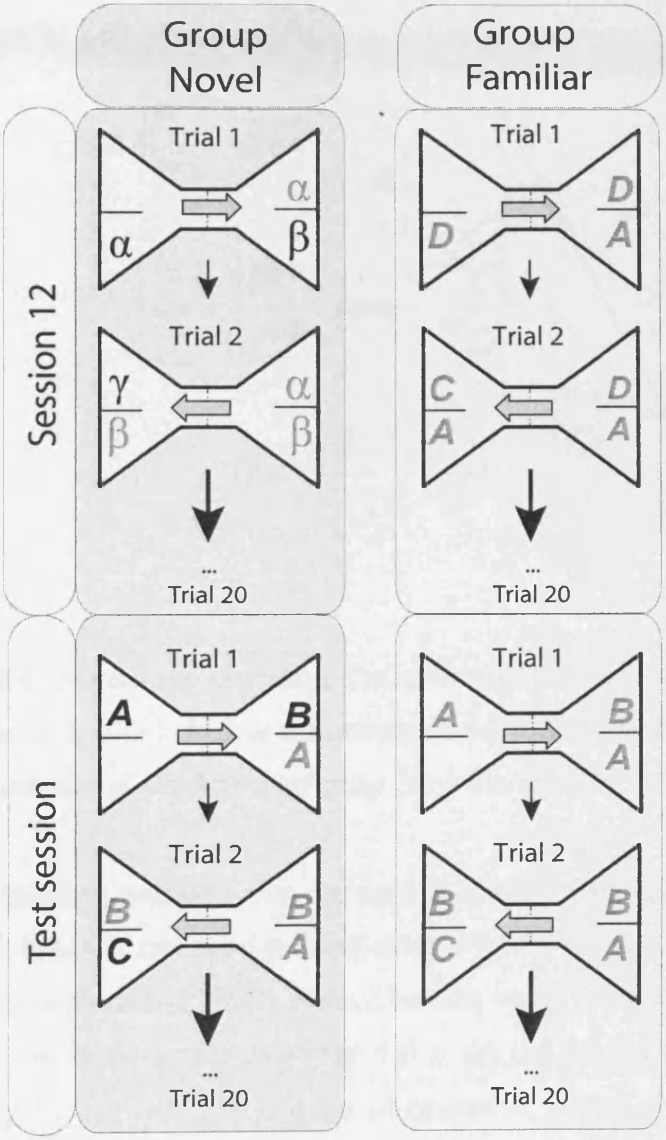

Figure 3. Specific procedure for Group Novel (left) and Group Familiar (right) during session 12 (top) and the test session (bottom). The letters α, β, γ represent a novel set of objects, whereas objects A, B, C are only new for Group Novel.

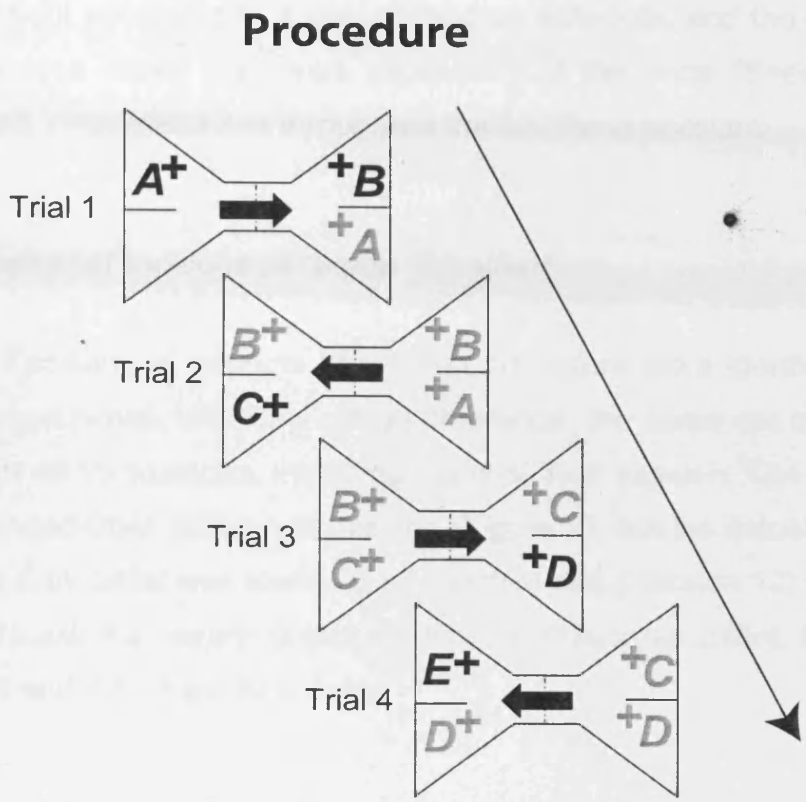

Figure 4. General procedure showing the presentation order of the objects. All objects are rewarded (+). Arrow shows rat movements. Group Novel: Black print represents the novel objects and gray print the familiar objects.

At the start of a training session the rat was placed on one side of the maze, where only one object A covered a food well (Figure 4). A single food pellet was placed in the well under each object before each trial. After one minute the central guillotine door was raised, and the rat ran to the opposite side of the maze. There, the rat had the choice of object A, which was now familiar, and a novel object B (trial 1). Both objects A and B covered baited food wells and were concurrently available to the rat for a total of 1 min. As there were duplicates of each object the rat could not mark an object for the next trial (Figure 4). The guillotine door was then raised to reveal objects B (familiar) and C (novel). Each session contained 20 trials and, hence, 21 sets of objects. Baiting of both the novel and familiar objects ensured the continued exploration of the objects, but did not affect the validity of the behavioural test as it relied on *differential* exploration. The placement of the novel object varied

from left to right according to a pseudorandom schedule, and the order of the objects changed when they were repeated just the once (Sessions 7-12). Animals were video-recorded throughout the last three sessions.

Training Protocol for control Group 'Familiar'

For Group Familiar, all aspects of the test procedure were identical to those used for Group Novel, with one critical difference: the same set of 21 objects was used for all 13 sessions, including the final 'test' session. The order of the objects changed from session to session (Figure 3), but the actual 21 pairs of objects and their order was identical on the final test (Session 13) to that used for Group Novel. As every object covered one sucrose pellet, both groups approached and displaced all objects.

Analysis of behaviour

Novelty discrimination

Exploration of novel and familiar objects was defined as directing the nose at a distance < 1 cm to the object and/or touching it with the nose or the paws. Turning around or sitting on the object was not counted.

Spatial attribute discrimination

Here, analysis was based on the exploration times as before. However, the exploration times just considered when an object was shown the second time within a session. Total exploration times were measured for when the object was either in the 'same' or a 'displaced' spatial configuration from the preceding trial with respect to the most salient room landmarks (Figure 5).

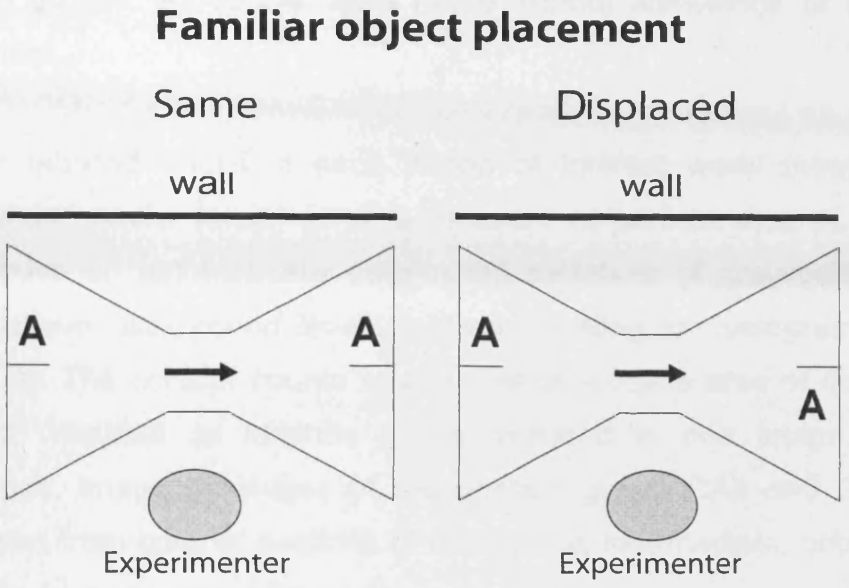

Figure 5. Spatial placement of a now familiar object compared to its previous trial location. Two possible configurations are possible: *same* (left) or *displaced* (right)

c-Fos analysis

On the final testing day, animals were processed using previously described immunohistochemical methods for c-Fos protein (see Chapters 2 and 3).

c-Fos positive cell counts

Estimates of c-Fos-activated cells were made using an automated cell counting procedure. Images were viewed on a Leica DMRB microscope, photographed using an Olympus DP70 camera, and stored digitally. Stained nuclei were counted using the program analySIS^D (Soft-Imaging Systems; Olympus, UK). Although this programme is not stereological, the resulting counts provide accurate information about *relative* numbers of cells, assuming that there are no systematic changes in the volume or packing of the neurons

in the two groups. All counts were made without knowledge of the group assignments.

Counts of labelled nuclei in each region of interest were determined by counting those nuclei (mean feret, a measure of particle size, of 4-20 μm) stained above an automatically determined threshold of grayscale intensity that was above background levels (software setting for histogram intensity phases = 3). The cortical counts were made in a frame area of 0.84 x 0.63 mm, which enabled all laminae to be included in one image. For the hippocampus, image montages of the dentate gyrus, CA3 and CA1 fields were created from coronal sections at the septal, intermediate, and temporal levels of the hippocampus (Figure 6).

For all brain areas analysed, counts were taken from four consecutive sections (i.e. sections 120 μm apart) from each hemisphere. For statistical analyses of regional c-Fos, counts were then normalised according to matched pairs of animals (one Novel, one Familiar) to reduce the contribution of staining variability. Normalisation involved dividing the mean number of activated neurons in a given animal for a given site by the combined mean of the two animals in each matched pair, and expressing this result as a percentage. Thus, all normalised scores across pairs sum to 100. These normalised data were then used for the statistical analyses of active cells.

Regions of interest

Cytoarchitectonic sub-regions were identified from coronal sections. All of the regions sampled are depicted in Figure 6.

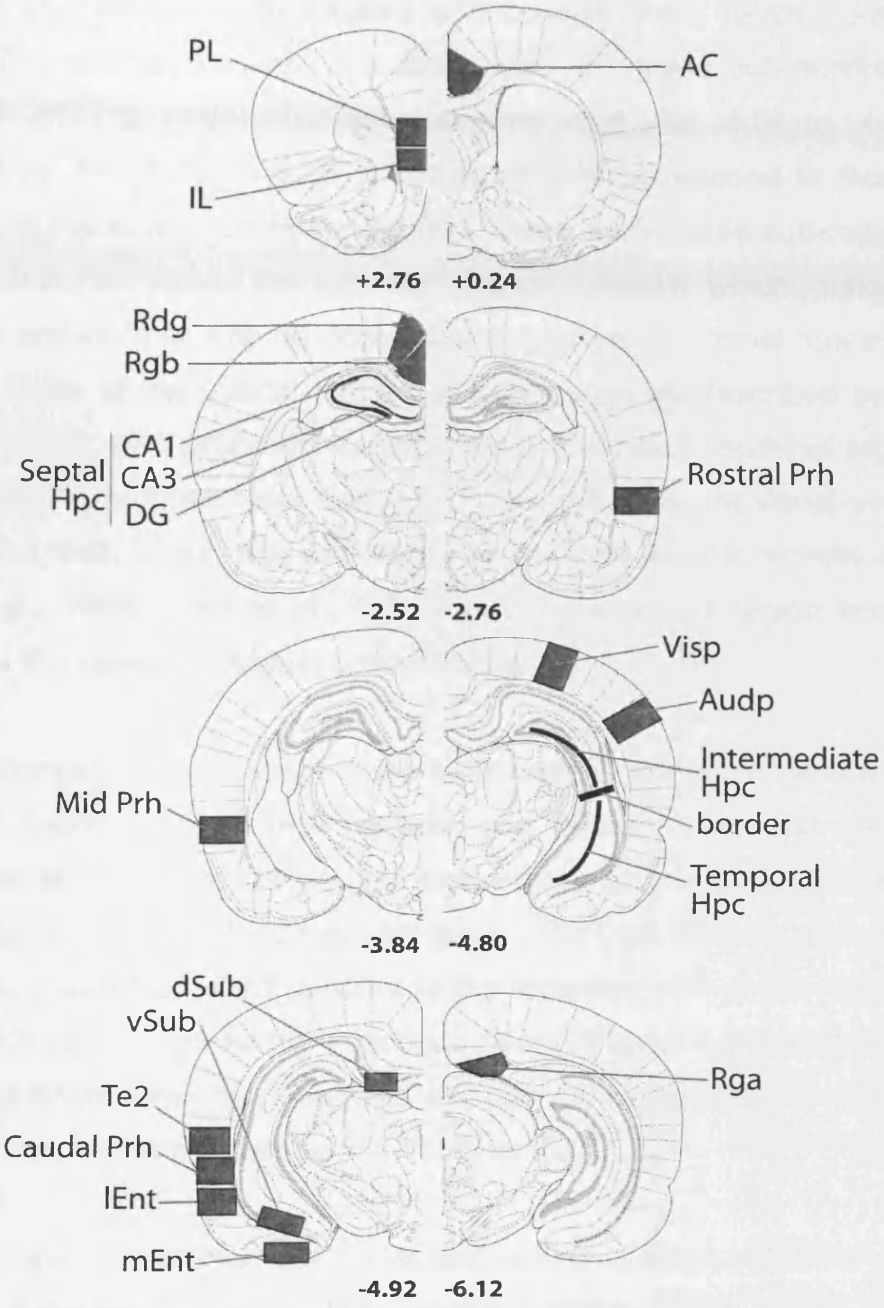

Figure 6. Coronal sections indicating regions of interest: anterior cingulate cortex (AC), areas 35 and 36 for the rostral, mid and caudal perirhinal cortex, area Te2, primary auditory cortex (Audp), CA1, CA3, dentate gyrus (DG) for the septal, intermediate and temporal hippocampus, lateral entorhinal cortex (lEnt), medial entorhinal cortex (mEnt), infralimbic cortex (IL), prelimbic cortex (PL), retrosplenial dysgranular cortex (Rdg), retrosplenial granular a (Rga), retrosplenial granular b (Rgb), dorsal subiculum (d Sub), ventral subiculum (v Sub), primary visual cortex (Visp). The numbers refer to the distance (mm) from bregma according to the atlas of Paxinos and Watson (2005).

The perirhinal cortex nomenclature and borders were taken from Burwell (2001). The perirhinal cortex was subdivided into three sub-regions: rostral (from AP -2.76 to -3.84 relative to bregma), mid (AP -3.84 to -4.80), and caudal (from AP- 4.80 to -6.30). These borders correspond to those levels depicted by Paxinos and Watson (2005). These same three sub-regions were also divided into areas 35 and 36 (Burwell, 2001), which make up the perirhinal cortex. It should be noted that our rostral perirhinal measurements included much of the caudal parietal insular cortex as described by Shi and Cassell (1999), who proposed a much more restricted perirhinal region than Burwell (2001). Counts were also taken from the adjacent visual association cortex area Te2, which has previously been implicated in novelty detection (Zhu et al., 1996; Wan et al., 1999) and is the visual region immediately dorsaly to the caudal perirhinal cortex (Figure 6).

Cytoarchitectonic subfields within the hippocampal formation were subdivided into their septal (dorsal), intermediate, and temporal (ventral) parts (Bast, 2007; Bast et al., 2009). The septal hippocampus counts (DG, CA3, and CA1) were obtained from sections near AP level -2.52 from bregma. Counts for the intermediate part (DG, CA1, CA3) and the temporal pole of the hippocampus (CA1, CA3) were obtained from sections near AP level -4.8 from bregma. The intermediate/temporal hippocampal division corresponded to -5.0 dorso-ventrally from bregma (Paxinos and Watson, 2005).

Adjacent regions included the dorsal and ventral subiculum (dSub, vSub; AP -4.92) and the lateral and medial entorhinal cortices (lEnt, mEnt; AP -4.92). The various layers of the entorhinal could not be counted separately, as the relatively low level of c-Fos counts in this region, combined with the modest intensity of staining, meant that these distinctions could not be made with sufficient confidence.

Three frontal regions were also examined, the prelimbic (PL; AP +2.76), infralimbic (IL; AP +2.76), and anterior cingulate (AC; AP +0.24) cortices. More caudally, the retrosplenial cortex was examined.

The retrosplenial cortex can be subdivided into granular b (Rgb), granular a (Rga), and dysgranular cortex (Rdg). Separate counts were made in all three sub-regions. Furthermore, the superficial (layer II and upper III) and deep (lower layer III to VI) layers of Rdg, Rgb, and Rga were counted separately as there is evidence of their differential involvement in learning tasks (Gabriel et al., 1983).

Finally, counts were also taken from two cortical areas: primary visual area (Visp), primary auditory area (Audp). These two areas were used as control regions; any group differences in these regions might reflect different sensory demands across conditions despite attempts to match task demands.

Statistics

Regional c-fos activation

The c-Fos-positive cell counts were initially analysed in six separate regional groupings; 1) perirhinal cortex, 2) hippocampal subfields, 3) parahippocampal regions, 4) retrosplenial cortex, 5) frontal cortex, and 6) primary sensory cortical areas. These groupings served to reduce Type 1 errors. When there was a group x region interaction, simple effects were examined (Howell, 1982). The probability level of 0.05 was taken as being statistically significant. Normalised counts were analysed using a 2 x 2 between-subject design. Bivariate correlations were calculated using the Pearson product-moment correlation coefficient for regional IEG activity and performance metrics. Because of the flaws of the normalisation discussed previously (see Chapter 4 – Statistics) the raw counts were also analysed.

Structural equation modelling

Structural equation modelling is an integrative approach to assess inter-relationships among correlated (or incorrelated) variables comprising an

underlying theoretical structure. Structural equation models are multiple-equation regression models representing putative causal (and hence *structural*) relationships amoung a number of variables, some of which may affect one another mutually. In the present study, structural equation modelling of c-Fos counts offers a potentially useful way to help correlate the activity of the regions of interest to each other. In addition, the process makes it possible to test the direction of putative effects so allowing one to evaluate the feasibility of network (or model) dynamics (McIntosh and Gonzalez-Lima, 1991; Friston et al., 1993; Jenkins et al., 2003; Poirier et al., 2008).

Using the same network, based on known temporal lobe connections, it was possible to compare statistical models derived for each group (Group Novel and Group Familiar). Path analyses of different network models could also be derived from the covariance matrices representing the relationships between the c-Fos counts in the various regions of interest. Data investigation used the specialized SEM analysis program Amos 6.0 (SPSS, Chicago). The term 'fit' refers to the ability of a model to reproduce the data i.e., usually the variance-covariance matrix.

The models considered six variables (structures), which corresponded to six temporal lobe areas that have been at the center of debates about the neural basis of visual recognition (Brown and Aggleton, 2001; Eichenbaum et al., 2007; Squire et al., 2007). Numerous fit indices exist, each being more or less sensitive to various model parameters (Fan et al., 1997; Hu and Bentler, 1998), and thus it is recommended to report several indices. These fit indices aim to test statistically the explanatory power of the models (similar to the F-test for an ANOVA). Three measures of goodness of fit are reported. Goodness of fit was first indicated by a nonsignificant chi-square (χ^2), the only binary fit/no-fit decision of a model. Two additional measures provided an index of the degree of discrepancy of fit of a model to the data. The comparative fit index (CFI) is an index of the proportion of variance accounted, based on the comparison of a proposed model to an independent model, in which no regions are connected. Such independent models have the least fit, and a high index value means that the tested model is opposite to

the independent model, i.e. thus exhibiting good fit. Alternatively, the root mean square error of approximation (RMSEA) provides an index of absolute fit by determining the average lack of fit per degree of freedom. A 90% confidence interval (CI) around the RMSEA demonstrates the precision of the estimate, and the RMSEA *p* value is for testing the null hypothesis that the population RMSEA is no greater than 0.05.

An important factor in choosing the CFI and RMSEA is that they are both also recommended for their good performance with small sample sizes (Fan et al., 1997; Hu and Bentler, 1998), thus each countering this limitation of the current study. In addition to a nonsignificant χ^2 with a ratio of the χ^2 to the degrees of freedom < 2, a good-fitting model that is a plausible representation of the underlying data structure was considered to either have a CFI = 0.90-0.95 or RMSEA = 0.05, good; < 0.08, acceptable (Tabachnik and Fidell, 1996).

The present models were based on established connections within the medial temporal lobe e.g. perirhinal cortex with lateral entorhinal cortex, the tri-synaptic hippocampal pathway, and the monosynaptic temporo-ammonic connections of the entorhinal cortex with the CA subfields (Steward and Scoville, 1976; Witter et al., 2000). In the case of the reciprocal projections between the lateral entorhinal cortex and CA1 as well as the perirhinal cortex (Witter et al., 2000), paths were tested in both directions, and the strongest one is presented. It is appreciated that these models are anatomically very simplistic and cannot capture the complex interplay that has been revealed between these sites (Van Strien et al., 2009). In addition, the squared multiple correlation (R^2 or coefficient of determination) is also presented for each dependent brain region in the models. This value represents a measure of the proportion of the variance of the dependent variable that is explained by the independent variable(s). A directed (single-headed) arrow represents a direct effect of one variable on another. A bidirectional (two-headed) arrow represents a covariance, between variables, that is not given causal interpretation.

Results

Behavioural measures of object recognition

Initial analyses confirmed that Group Novel could discriminate novel from familiar objects.

First choice

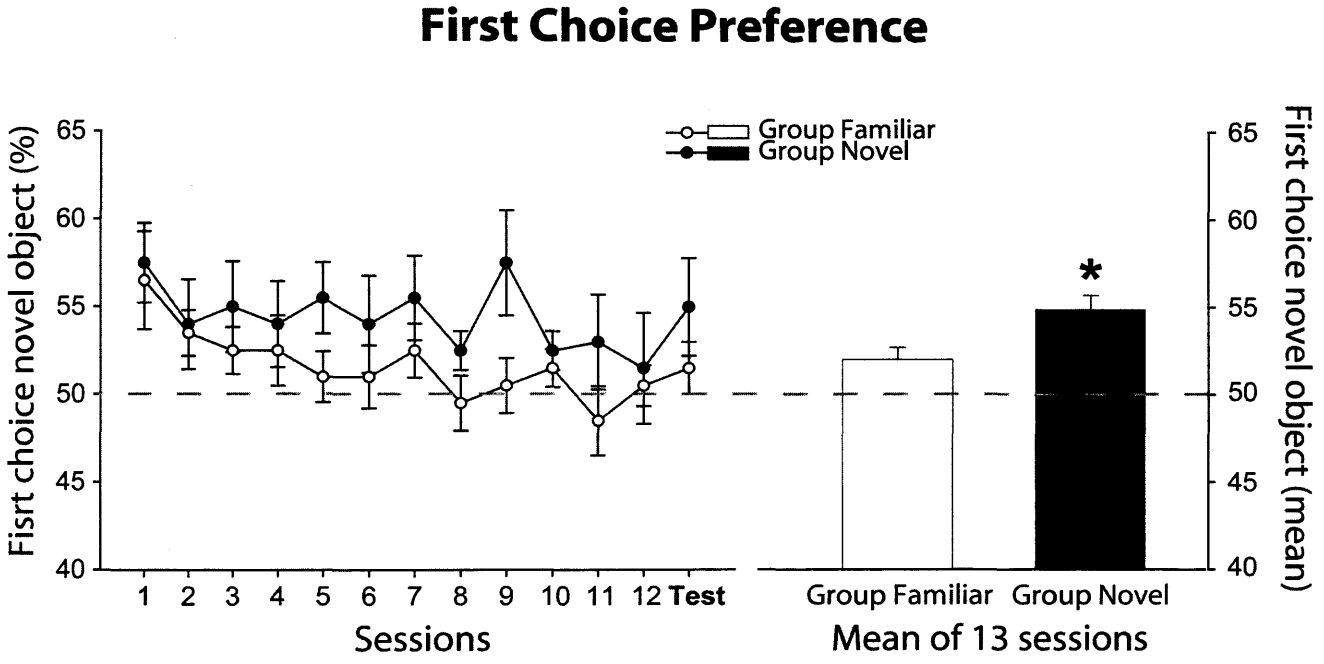

Figure 7. First choice preference of novel objects. The line plot graph shows the scores during the 13 sessions (left). The bar chart represents mean scores of the 13 sessions (right).

The first object selected from each pair was noted for each trial of the object recognition task (Figure 2). Group Novel rats chose between a novel object and a familiar (just explored) object. Group Familiar rats chose between two highly familiar objects (one just explored). Over the 13 sessions, Group Novel consistently selected the novel object significantly more times than Group Familiar selected the less recently explored object ($F_{(1,18)}$ = 7.15, p < 0.05;

Figure 7). Inspection of Figure 7 shows that at the very beginning of training the choice behavior of Groups Novel and Familiar appeared indistinguishable. This pattern is to be expected as at the outset of training (Session 1) the objects were novel for both groups, but became increasingly familiar for Group Familiar only.

Object Recognition D1 (final test session)

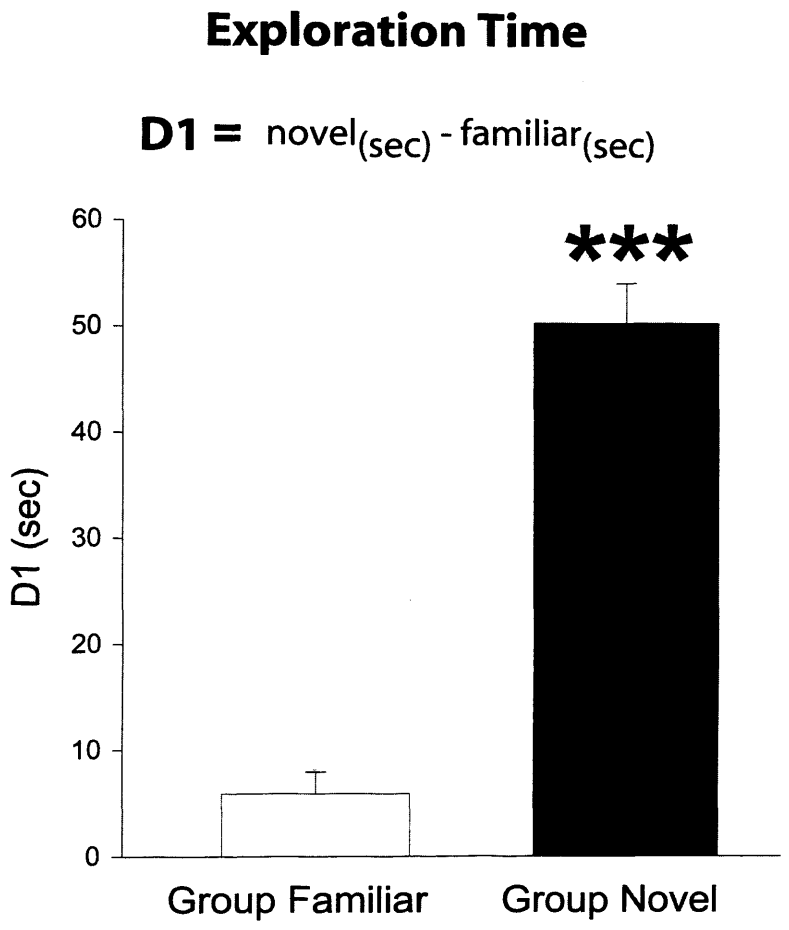

Figure 7. Exploration time as a measure of novelty discrimination by Group Novel and Group Familiar for final test session. Mean D1 scores ($novel_{(sec)}$-$familiar_{(sec)}$) in seconds. Data are shown as mean ± SEM. *** $p < 0.001$.

Group Novel spent disproportionately more time in the final test session (i.e. immediately prior to IEG analysis) spontaneously exploring the novel objects compared to the familiar objects than Group Familiar, as measured by D1 (*t*-

test, $t_{(18)}$ = 10.4, p < 0.001; Figure 7). Further analyses showed that both groups could discriminate between the objects in the test session as they both spent more time exploring the novel (Group Novel) or less recent (Group Familiar) object compared to the most familiar (just seen) object (one-sample *t*-test; D1: Group Familiar, $t_{(9)}$ = 2.9, p < 0.05; Group Novel, $t_{(9)}$ = 13.4, p < 0.001). An indication of the potential robustness of this behavioral task is that every rat in Group Novel had a positive D1 score (lowest = 33 sec, highest = 77 sec).

Total exploration (final test session)

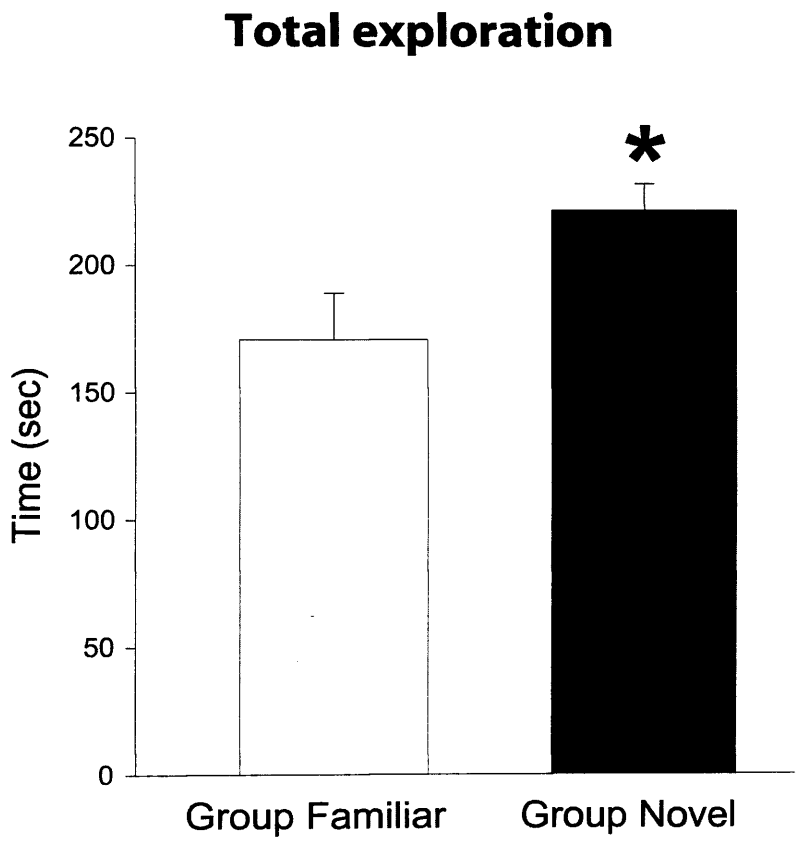

Figure 8. Final test session, mean overall exploration in seconds of both novel and familiar objects. Data are shown as mean ± SEM. * p < 0.05

The combined amount of active sampling of both novel and familiar objects (Figure 8) in the test session was greater for Group Novel than Group Familiar (*t*-test; $t_{(18)} = 2.4$, $p < 0.05$).

Object Recognition Index D2 (final test session)

The total amount of object exploration (Figure 8) in the final test session was different for Group Novel than Group Familiar (*t*-test; $t_{(18)} = 2.4$, $p < 0.05$). Consequently, a second index of recognition performance was used, the Discrimination Ratio, D2 (Ennaceur and Delacour, 1988), which compensates for individual differences in overall exploration. D2 is the difference in time spent exploring the novel objects from the familiar objects (index D1, Figure 7) divided by the total time spent exploring all objects (Figure 8). For Group Novel, D2 reflects novelty discrimination, while for Group Familiar, D2 reflects recency discrimination.

Group Novel had significantly higher D2 scores in the final session than Group Familiar (Figure 9, *t*-test, $t_{(18)} = 9.4$, $p < 0.001$). Although both groups discriminated between the objects in the final test session as they spent more time exploring the novel (Group Novel) or less recent (Group Familiar) object compared to the most familiar (just seen) object (one-sample *t*-test; D2: Group Novel, $t_{(9)} = 13.2$, $p < 0.001$; Group Familiar, $t_{(9)} = 3.1$, $p < 0.05$), this difference was much more robust in Group Novel. For example, every rat in Group Novel had a positive D2 score in the final session.

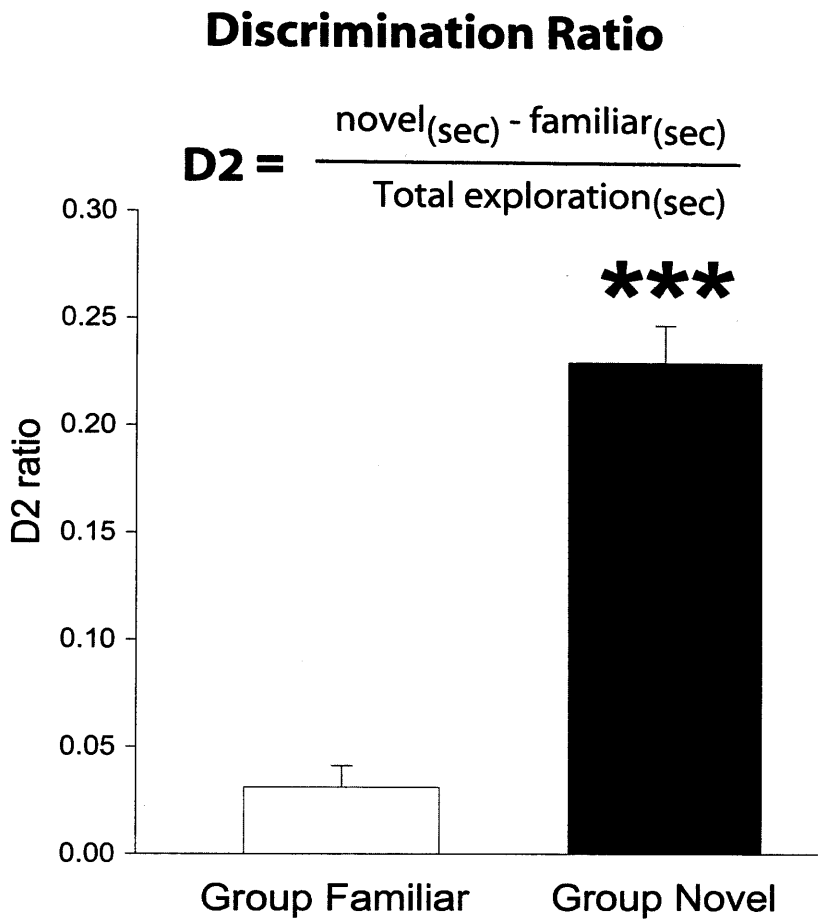

Figure 9. Mean discrimination ratio D2 = [(novel$_{(sec)}$ -familiar$_{(sec)}$) / total exploration$_{(sec)}$] for final test session. Data shown are mean ± SEM. Group differences: *** $p < 0.001$.

Object placement (final test session)

On every test both objects occupied new locations (as initial and repeat object exposures were at opposite ends of the maze), so reducing spatial influences. Even so, we tested for sensitivity to whether the familiar object was in the 'same' or 'displaced' arrangement with respect to the long axis of the maze (Figure 5). There was a significant object placement effect (Figure 10); the two groups spent more time exploring an object when it was 'displaced' ($F_{(1,18)} = 4.5$, $p < 0.05$). A group effect was also found ($F_{(1,18)} = 6.5$, $p < 0.05$), as this difference was more pronounced in Group Familiar, but no interaction was

found ($F < 1$). The larger effect in Group Familiar presumably arose because object exploration by Group Novel rats is predominantly controlled by object novelty, i.e. spatial effects would be attenuated.

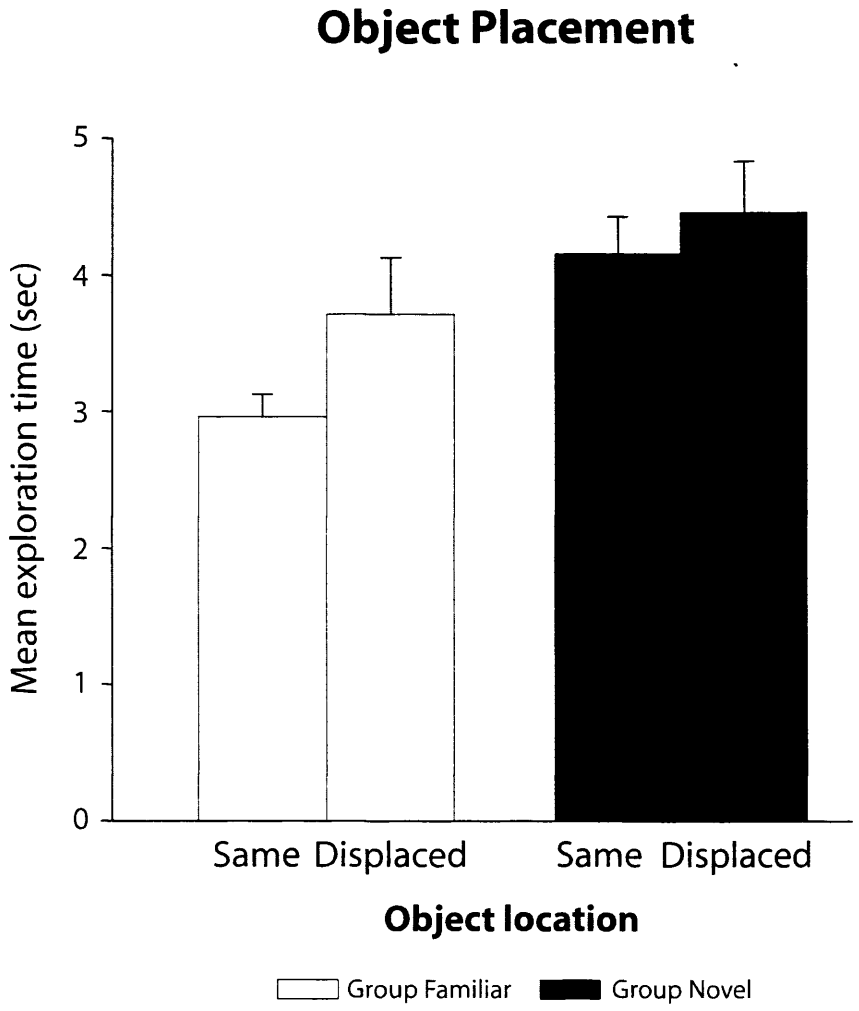

Figure 10. Mean exploration time of a now familiar object compared to its previous trial location. Two possible spatial configurations are possible: *same* or *displaced* (see Figure 4). Data are shown as mean ± SEM.

Immediate-early gene results following the final test session

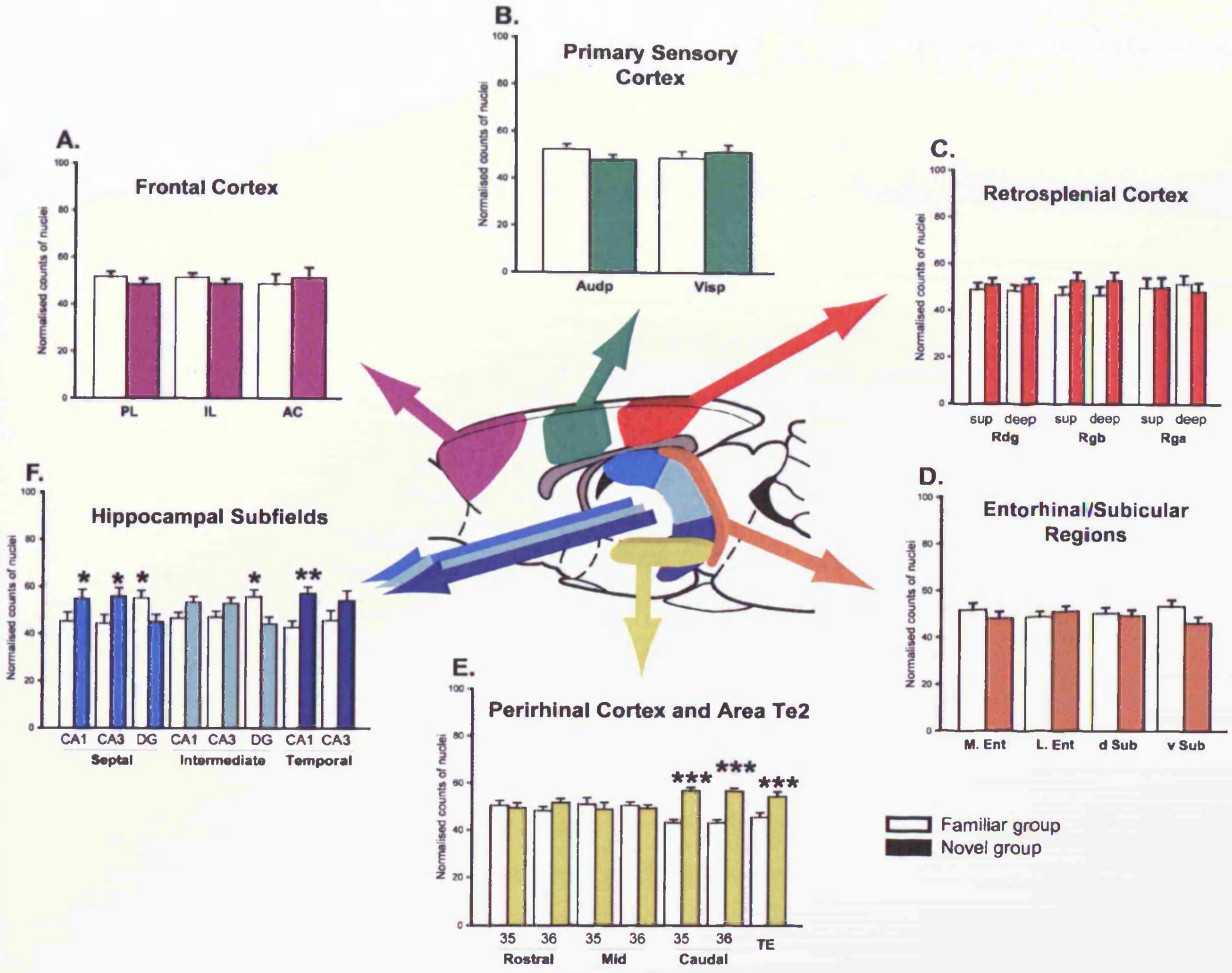

Figure 11. Overview of the c-Fos levels in the 6 main areas of interest following familiar (white) or novel (black) object exposure in the final test session. **A**. *Frontal Cortex*: prelimbic (PL), infralimbic (IL) and anterior cingulate (AC) cortices. **B**. *Primary Sensory Cortex:* primary auditory cortex (Audp), primary visual cortex (Vis). **C**. *Retrosplenial Cortex*: superficial and deep layers of the dysgranular (Rdg) and granular (Rgb and Rga) retrosplenial cortex **D.** *Entorhinal/Subicular Regions*: lateral entorhinal (lEnt) cortex, medial entorhinal (mEnt) cortex, dorsal subiculum (d Sub) and ventral subiculum (v Sub). **E.** *Perirhinal cortex and Area Te2:* areas 35 and 36 of the rostral, mid and caudal perirhinal cortex and area Te2. **F.** *Hippocampal Subfields*: dentate gyrus (DG), CA3, CA1, for septal, intermediate and temporal hippocampus. Normalised counts of c-Fos-positive cells are presented as mean ± SEM. Significance of group differences: * $p < 0.05$; ** $p < 0.01$; *** $p < 0.001$.

Perirhinal Cortex and area Te2

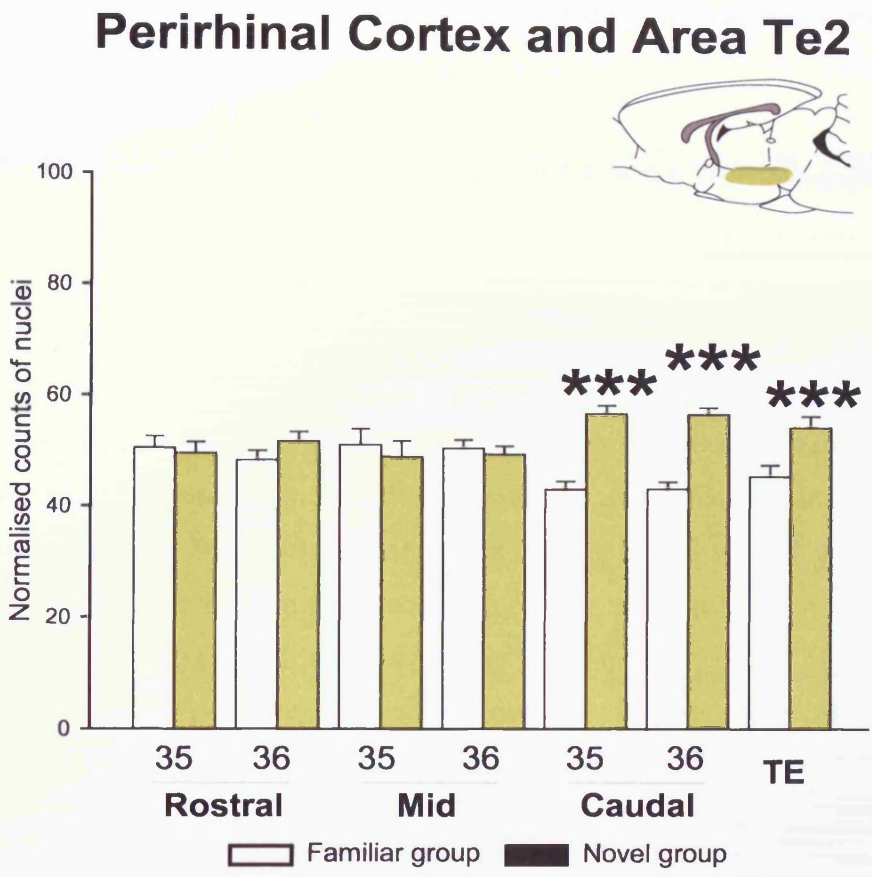

Figure 12. c-Fos levels following familiar (white) or novel (yellow) object exposure. *Perirhinal cortex and Area Te2:* areas 35 and 36 of the rostral, mid and caudal perirhinal cortex and area Te2. Normalised counts of c-Fos-positive cells are presented as mean ± SEM. Significance of group differences: *** $p < 0.001$.

Exposure to novel as opposed to familiar objects (Group Novel versus Group Familiar) increased c-Fos counts in the perirhinal cortex and area Te2 ($F_{(1,18)} = 13.8$, $p < 0.01$; Figure 12). These c-Fos increases were not, however, uniform (group x sub-region interaction, $F_{(6,108)} = 7.4$, $p < 0.001$), and only the caudal parts (c-Fos photomicrograph; Figure 13A) of perirhinal areas 35 and 36 showed significant c-Fos increases (simple effects; rostral: area 35, $F < 1$, area 36, $F_{(1,126)} = 1.6$, $p = 0.21$; mid: area 35, $F < 1$, area 36, $F < 1$; caudal: area 35, $F_{(1,126)} = 25.4$, $p < 0.001$, area 36, $F_{(1,126)} = 24.3$, $p < 0.001$), along

with area Te2 ($F_{(1,126)}$ = 10.6, p < 0.001). Raw counts failed to show a significant group effect ($F_{(1,18)}$ = 2.09, p = 0.166). However, a group x sub-region interaction was found. Subsequent analyses that the c-Fos increase induced by novelty was only significant in area Te2 (simple effects; rostral: area 35, F < 1, area 36, F < 1; mid: area 35, F < 1, area 36, F < 1; caudal: area 35, F < 1, area 36, $F_{(1,126)}$ = 2.62, p = 0.11; area Te2, $F_{(1,126)}$ = 22.83, p < 0.001).

The discrepancy between the normalised counts and the raw counts can be explained by a higher variance in the case of the raw counts. Indeed, the number of positive cells varies a lot between different brain regions. For example, the mean number of positive cells in area 35 was 23 (per section), whereas the mean number of positive cells in area 36 was 114 (per section). In the simple effect analyses, the same mean standard error is used for all comparisons. It is therefore not surprising to lose some of the significant c-Fos changes by looking at the raw counts. However, the same significant changes are still present using the raw counts when a paired t-test was used to compare the sub-regions where a significant difference was found with the normalised counts. Again, an increase of c-Fos activity was found in caudal area 35 (t-test, t = 4.54, df = 9, p < 0.001), caudal area 36 (t-test, t = 3.95, df = 9, p < 0.01)and area Te2 (t-test, t = 5.66, df = 9, p < 0.001).

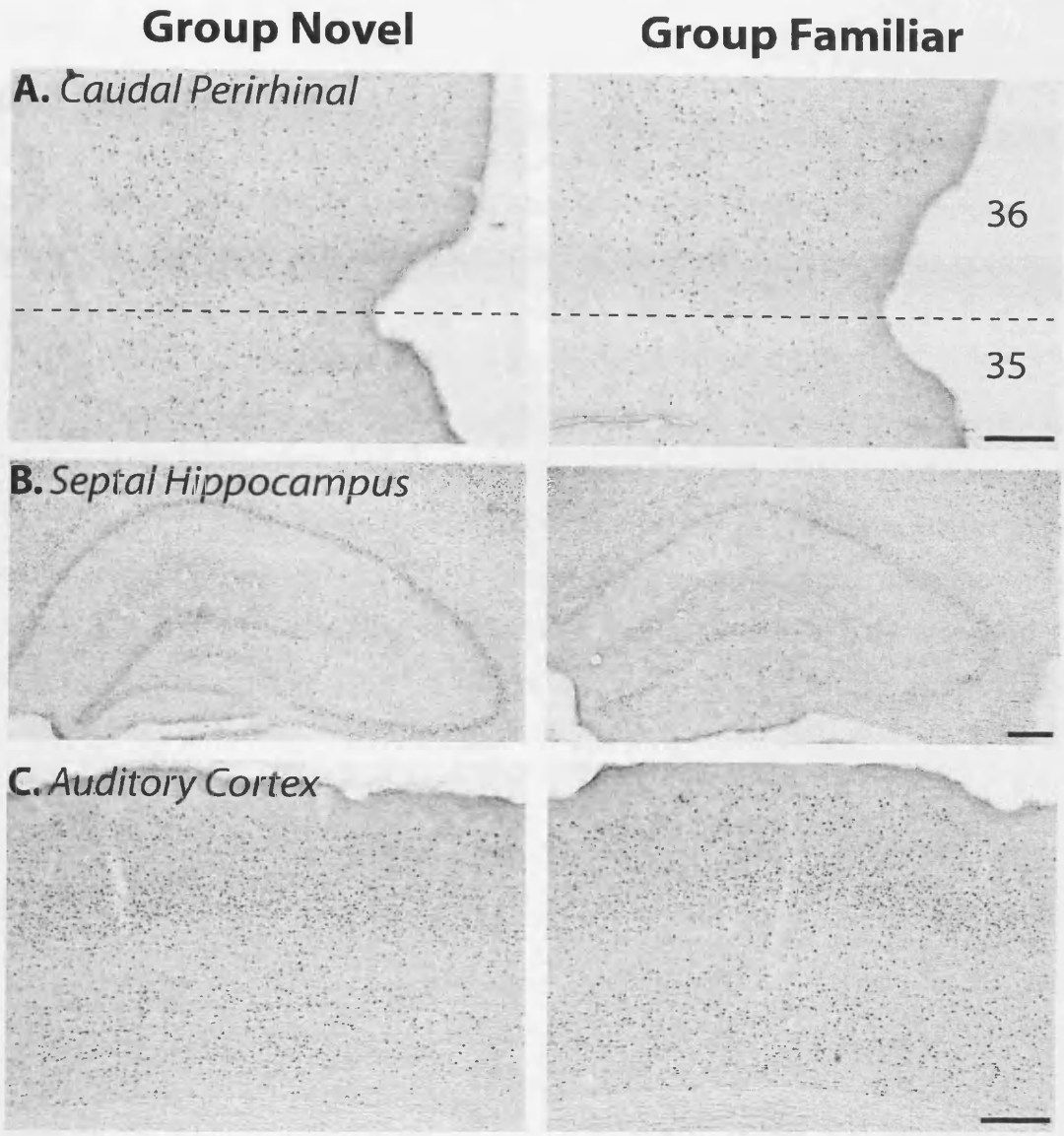

Figure 13. Photomicrographs comparing c-Fos levels between Group Novel (left-hand side) and Group Familiar (right-hand side). **A.** Caudal perirhinal cortex. **B.** Septal hippocampus. **C.** Primary auditory cortex. The photomicrographs are taken from behaviourally-matched pairs of animals where tissue was processed simultaneously to reduce variation. The brightfield photomicrographs of coronal sections show the comparable c-Fos levels in the primary auditory cortex, which contrasts, with the specific increase of c-Fos positive cells following novelty in the caudal perirhinal cortex. Scale bar, 100 µm.

Hippocampal Subfields

For the initial comparison, the three sets (septal, intermediate, temporal) of c-Fos counts for each subfield (CA1, CA3, DG) were summed and compared. While there was a lack of an overall group effect (Novel versus Familiar, $F_{(1,18)} = 2.07$, $p = 0.17$), there was a group x sub-region interaction ($F_{(2,36)} = 21.0$, $p < 0.001$). Simple effect analyses confirmed overall c-Fos increases in CA1 ($F_{(1,54)} = 9.58$, $p < 0.01$) and CA3 ($F_{(1,54)} = 10.26$, $p < 0.01$), but decreases in DG ($F_{(1,54)} = 8.62$, $p < 0.01$) in Group Novel. Raw counts showed similar results with no group effect ($F < 1$), but a group x sub-region interaction ($F_{(2,36)} = 8.22$, $p < 0.001$). Subsequent analyses using simple effects revealed that the only significant changes of c-Fos raw counts was found in CA1 (CA1, $F_{(1,54)} = 4.45$, $p < 0.01$; CA3, $F_{(1,54)} = 1.72$, $p = 0.19$; DG, $F_{(1,54)} = 1.15$, $p = 0.29$).

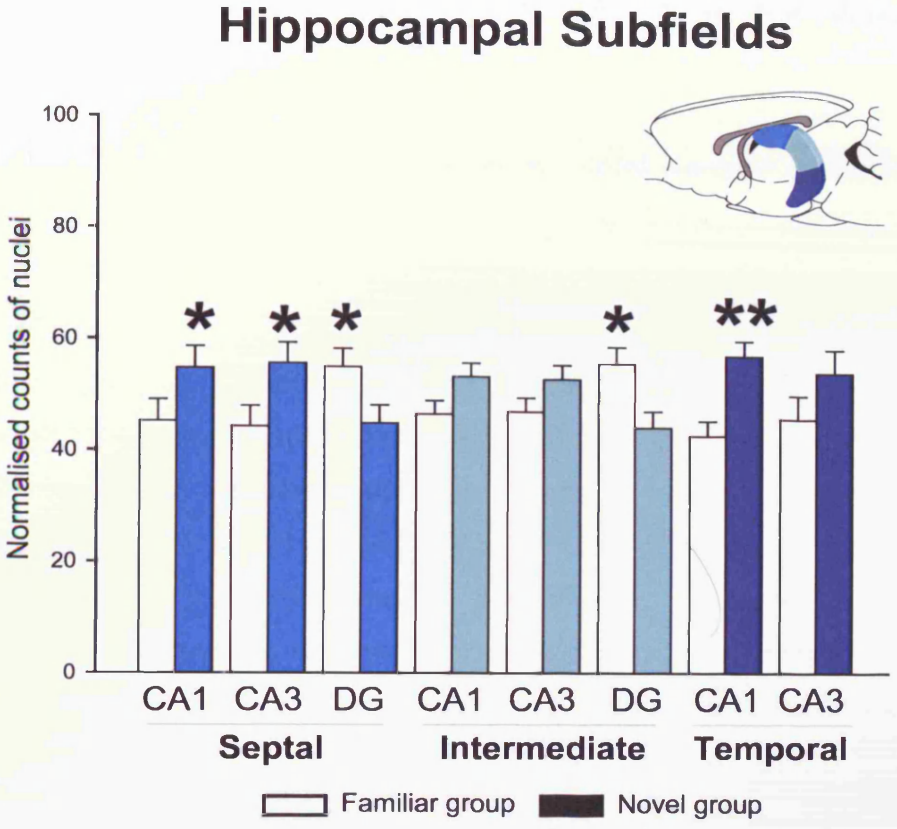

Figure 14. c-Fos levels following familiar (white) or novel (blue) object exposure. *Hippocampal Subfields*: dentate gyrus (DG), CA3, CA1, for septal, intermediate and temporal hippocampus. Normalised counts of c-Fos-positive cells are presented as mean ± SEM. Significance of group differences: * $p < 0.05$; ** $p < 0.01$.

This same pattern of result was repeated when the septal, intermediate, and temporal counts were treated separately, as there was no overall group difference across the entire hippocampal formation ($F_{(1,18)} = 1.63$, $p = 0.22$; Figure 14), but there were consistent changes within specific subfields (group x subregion interaction $F_{(7,126)} = 8.36$, $p < 0.001$). The same pattern of c-Fos changes (Figure 14) was found for each of the three rostro-caudal levels (septal, intermediate, temporal) of the hippocampus i.e. Group Novel displayed a relative c-Fos increase in fields CA1 and CA3, but a decrease in

the dentate gyrus (for septal hippocampus see Figure 13B). Subsequent analyses showed a significant increase in Group Novel c-Fos cell counts in septal CA1 ($F_{(1,144)} = 4.25$, $p < 0.05$), temporal CA1 ($F_{(1,144)} = 9.70$, $p < 0.01$), and septal CA3 ($F_{(1,144)} = 6.04$, $p < 0.05$), as well as a marginal increase in temporal CA3 ($F_{(1,144)} = 3.24$, $p = 0.074$). These increases contrasted with the significant c-Fos decrease in Group Novel in septal dentate gyrus ($F_{(1,144)} = 4.77$, $p < 0.05$) and in intermediate dentate gyrus ($F_{(1,144)} = 6.20$, $p < 0.05$). Looking at the raw counts, there was no group effect ($F < 1$), but there was a group x sub-region interaction ($F_{(7, 144)} = 4.54$, $p < 0.001$). Simple effects confirmed a significant effect only in the temporal CA1 ($F_{(1, 144)} = 9.33$, $p < 0.003$) and a border line effect in the septal DG ($F_{(1, 144)} = 3.52$, $p = 0.062$). All other sub-regions of the hippocampus failed to show significant c-Fos changes (septal CA1, $F < 1$; septal CA3, $F < 1$; intermediate CA1, $F < 1$; intermediate CA3, $F < 1$; intermediate DG, $F < 1$; temporal CA3, $F < 1$). Analyses of *t*-test showed a significant increase of c-Fos-positive cells in the temporal CA1 ($t = 3.05$, df = 9, $p = 0.014$) and a similar trend in the septal CA3 ($t = 2.05$, df = 9, $p = 0.071$). The c-Fos changes in the remaining hippocampal sub-regions did not reach significant differences (septal CA1, $t = 1.49$, df = 9, $p = 0.17$; septal DG, $t = 1.47$, df = 9, $p = 0.17$; intermediate CA1, $t = 1.50$, df = 9, $p = 0.17$; intermediate CA3, $t = 1.02$, df = 9, $p = 0.34$; intermediate DG, $t = 1.68$, df = 9, $p = 0.13$; temporal CA3, $t = 1.67$, df = 9, $p = 0.13$). Raw count analyses failed to confirm all the significant changes found with the normalised counts; mostly due to higher variance in the raw counts between hippocampal sub-regions.

Entorhinal/Subicular Regions

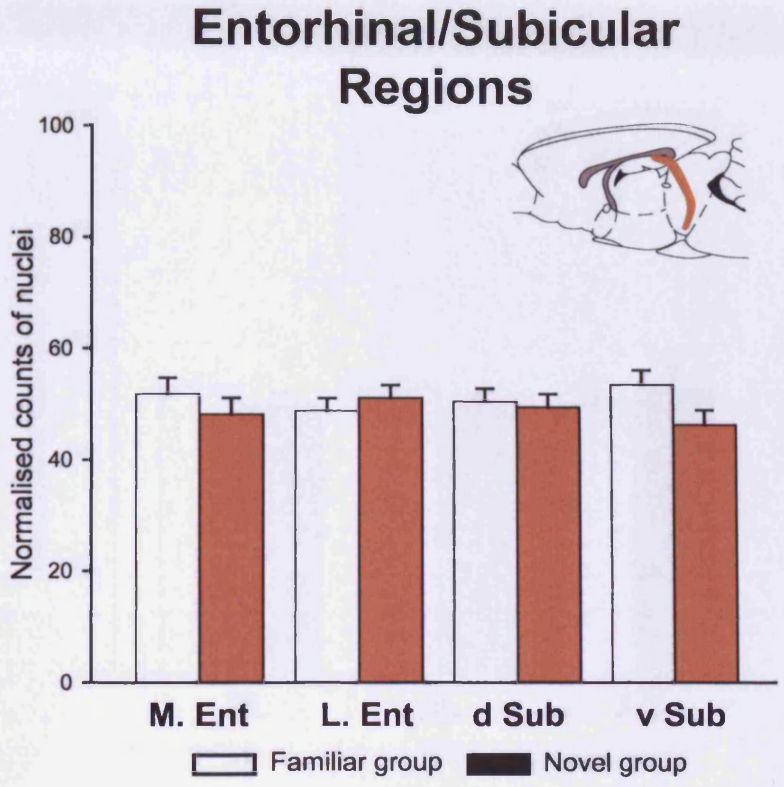

Figure 15. c-Fos levels following familiar (white) or novel (orange) object exposure. *Entorhinal/Subicular Regions*: lateral entorhinal (lEnt) cortex, medial entorhinal (mEnt) cortex, dorsal subiculum (d Sub) and ventral subiculum (v Sub).

No overall changes in c-Fos-positive cell counts were found in the four regions tested (medial and lateral entorhinal cortex, dorsal and ventral subiculum; group, $F < 1$; Figure 15). Likewise, there was no group x sub-region interaction ($F_{(3,54)} = 1.7$, $p = 0.18$). Similar results were obtained with the raw counts (group effect, $F < 1$; interaction, $F_{(3,54)} = 1.21$, $p = 0.32$).

Frontal Cortex

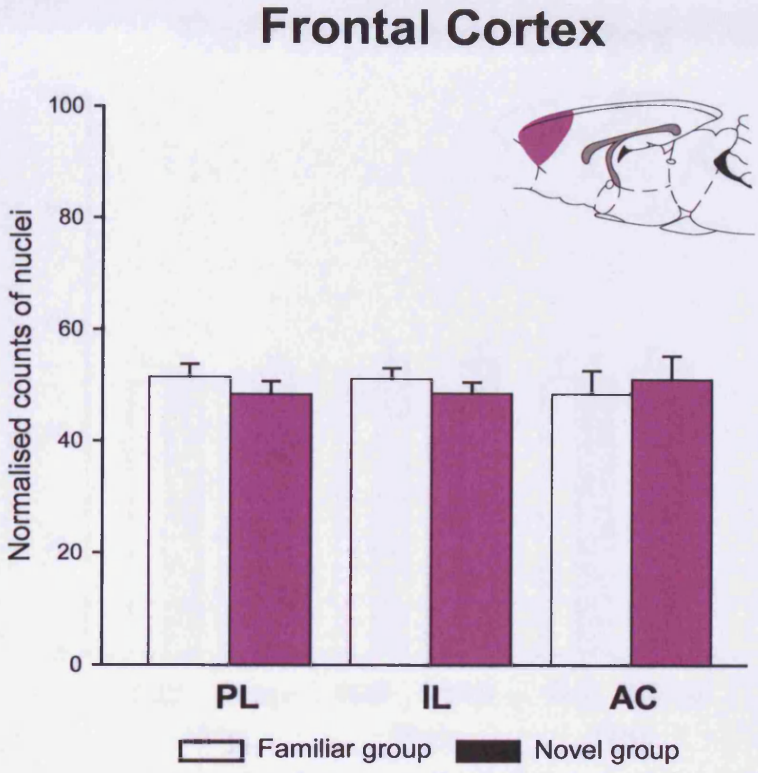

Figure 16. c-Fos levels following familiar (white) or novel (purple) object exposure. *Frontal Cortex*: prelimbic (PL), infralimbic (IL) and anterior cingulate (AC) cortices.

No significant c-Fos group differences ($F < 1$) were found for the three frontal regions (prelimbic, infralimbic, and anterior cingulate; Figure 16) that were analysed. Likewise, there was no group x sub-region interaction ($F < 1$). The analyses of raw counts confirmed the absence of significant c-Fos changes in the frontal cortex ($F < 1$). Moreover; no interaction was found ($F < 1$).

Retrosplenial Cortex

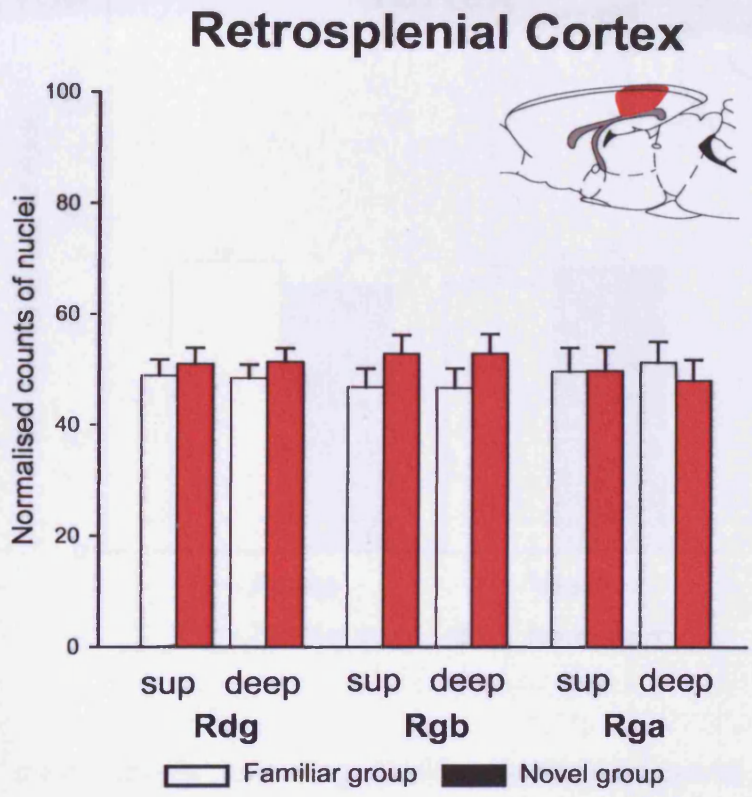

Figure 17. c-Fos levels following familiar (white) or novel (red) object exposure. *Retrosplenial Cortex*: superficial and deep layers of the dysgranular (Rdg) and granular (Rgb and Rga) retrosplenial cortex.

No significant c-Fos group differences ($F < 1$) were found for the three retrosplenial sub-regions (Rdg, Rgb, Rga, $F < 1$; Figure 17) that were analysed. As with the frontal cortex, there was no group x sub-region interaction ($F < 1$). Using the raw counts, no changes of c-Fos-positive cells were found in the retrosplenial cortex ($F < 1$). Likewise there was no group x sub-region interaction ($F < 1$).

Primary Sensory Cortex

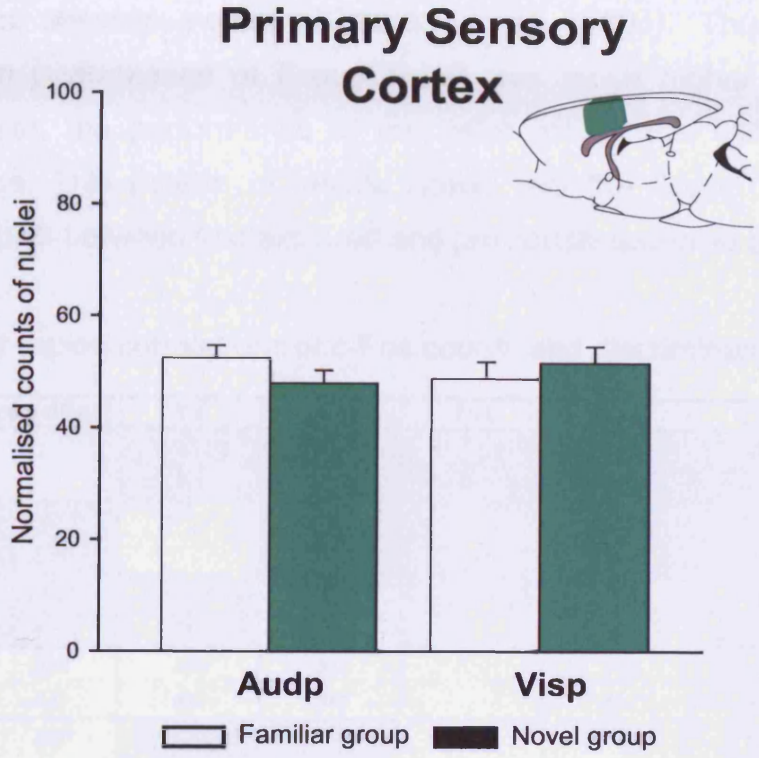

Figure 18. c-Fos levels following familiar (white) or novel (green) object exposure. *Primary Sensory Cortex:* primary auditory cortex (Audp), primary visual cortex (Vis).

To help determine how well matched Group Novel was with its control Group Familiar, c-Fos counts were made in primary sensory areas. No group differences were found in the primary auditory and primary visual (group, $F < 1$, Figures 13C, 18) cortices. These non-results were confirmed by the analyses of the raw counts (group, $F < 1$; group x sub-region interaction, $F < 1$).

Correlations with recognition index D2

The correlations are presented across all brain areas with D2 (table 1). The only significant correlation was between c-Fos absolute counts in CA3 and the

degree of recency discrimination (D2) by Group Familiar rats ($r = 0.87$, $p < 0.001$). This significant correlation (Group Familiar) is consistent with evidence that the hippocampus is more critical for judgments of recency ('when') than absolute novelty (Charles et al., 2004). Thus, while the discrimination performance of Group Novel was much higher than that of Group Familiar, the performance of the latter group was still significantly above chance. This pattern of results shows that the Group Familiar rats could distinguish between just explored and previously explored objects.

Table 1. Inter region correlations of c-Fos counts and discrimination ratio (D2)

		caudPeri	TE	lEnt	DG	CA3	CA1	D2
caudPeri	*r*		**.933****	.769**	.771**	.748*	.832**	-.416
	p		*.001*	*.009*	*.009*	*.013*	*.003*	*.232*
TE	*r*	**.961****		**.878****	**.861****	**.758***	**.781****	-.249
	p	*.001*		*.001*	*.001*	*.011*	*.008*	*.488*
lEnt	*r*	**.872****	**.913****		**.886****	.538	**.633***	.048
	p	*.001*	*.001*		*.001*	*.108*	*.050*	*.895*
DG	*r*	.233	.259	.062		.566	**.633***	.061
	p	*.517*	*.470*	*.865*		*.088*	*.049*	*.868*
CA3	*r*	.580	**.729***	**.763***	.059		**.733***	-.605
	p	*.079*	*.017*	*.010*	*.872*		*.016*	*.064*
CA1	*r*	**.720***	**.676***	**.661***	.424	.582		-.468
	p	*.019*	*.032*	*.038*	*.222*	*.078*		*.173*
D2	*r*	.353	.487	.440	.196	**.867****	.560	
	p	*.317*	*.153*	*.203*	*.587*	*.001*	*.092*	

Group Novel

Group Familiar

Table 1. The bottom left diagonal matrix concerns data from Group Familiar; the top right diagonal matrix concerns data from Group Novel. r, Pearson coefficient, and correlations (two-tailed) that are significant at the 0.05(*) or 0.01(**) are shaded. caudPeri, caudal perirhinal cortex; lEnt, lateral entorhinal cortex; dentate gyrus, DG; CA3 and CA1.

Structural equation modelling

Models for Group Novel and Group Familiar were derived from the correlations across each brain region for the mean, absolute c-Fos counts (Table 1). Models were rejected if they were not based on established

neuronal connectivity within the temporal lobe and if they did not have statistically significant pathways interlinking structures across the model.

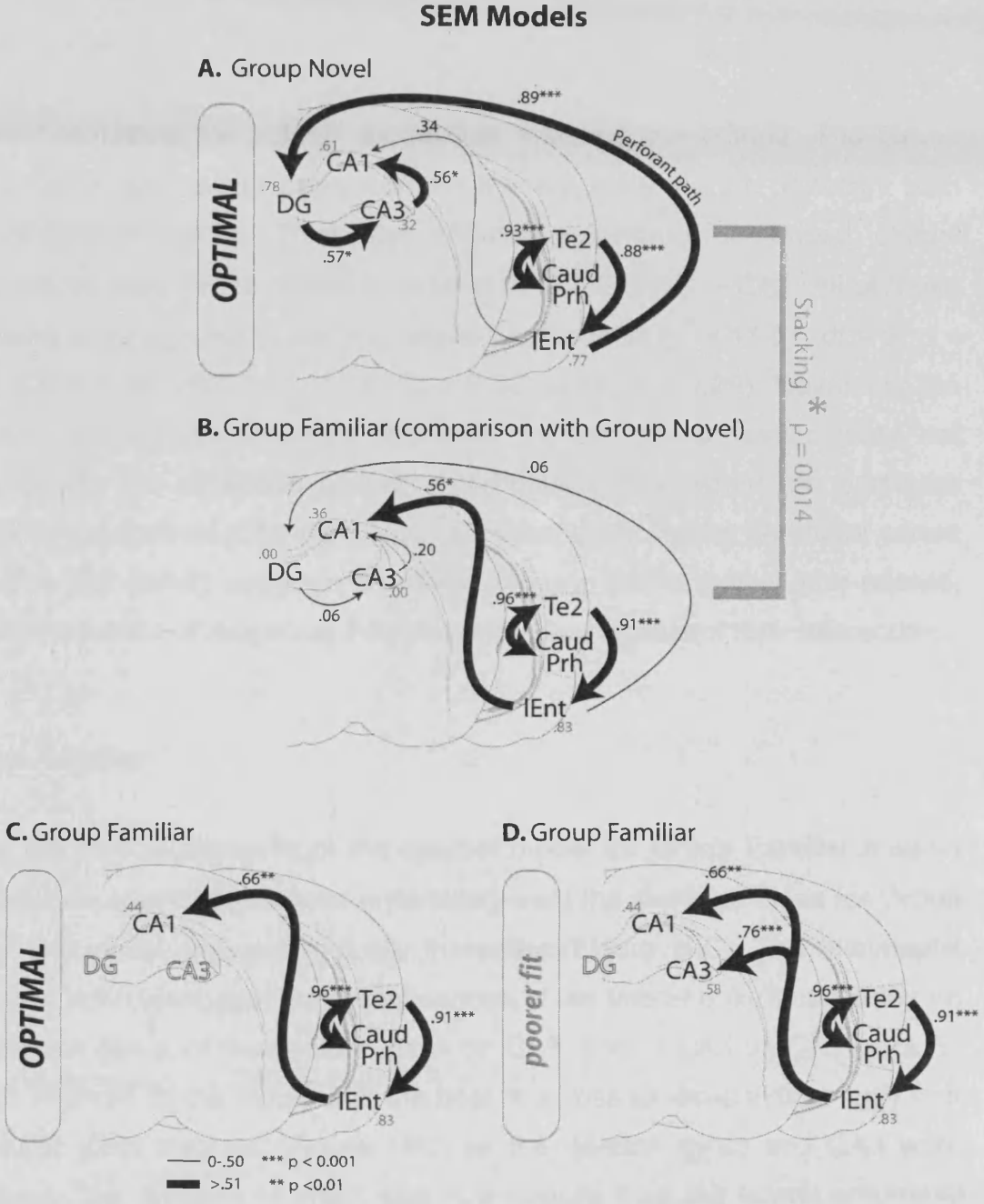

Figure 19. Temporal lobe interactions derived from structural equation modelling. Notice the engagement of the tri-synaptic circuit induced by novelty. **A.** Optimal Group Novel model, **B.** Fitting Group Familiar data into the optimal model of Group Novel (used for stacked comparison between groups) and **C.** Optimal Group Familiar model. **D.** Valid Group Familiar model (poorer fit). The squared multiple correlations (*R* 2) are in gray. The strength of the causal influences is in black. Sites depicted: area Te2, dentate gyrus (DG),

CA1, CA3, lateral entorhinal cortex (lEnt), caudal perirhinal cortex (caudPrh). *$p < 0.05$; ***$p < 0.001$.

Group Novel

Figure 19A shows the optimal model that matched our criteria. The Group Novel model was heavily dependent on a linear route via the perforant path and tri-synaptic circuit. Thus, the network essentially comprised caudal perirhinal ↔ area Te2 → lateral entorhinal → DG → CA3 → CA1. All of these pathways were significant, and the model had good fit ($\chi^2 = 11.01$, df = 9, p = 0.28; CFI = 0.96; RMSEA = 0.16, CI = 0.001-0.42, p = 0.29). Reversing the direction of the paths between structures yielded poorer results (data not shown), with the exception of Te2 - perirhinal cortex, where no particular direction was optimal. The high covariance between caudal perirhinal cortex and area Te2 activity suggests that these regions are intimately inter-related, and that a pattern of reciprocal influence may best represent their interaction.

Group Familiar

While the cortical elements of the optimal model for Group Familiar (caudal perirhinal ↔ area Te2 → lateral entorhinal) were the same as those for Group Novel, the model changed radically thereafter (Figure 19C). The tri-synaptic path was now disengaged as the influences of the lateral entorhinal cortex on the dentate gyrus, of the dentate gyrus on CA3, and of CA3 on CA1 were no longer involved. In the model with the best fit across all three indices only four structures were involved (Figure 19C) as the dentate gyrus and CA3 were removed. The direction of effect was now directly from the lateral entorhinal cortex to CA1 i.e. the temporo-ammonic projection was now engaged rather than the perforant pathway. This model for Group Familiar (Figure 19C) had good fit ($\chi^2 = 1.8$, df = 3, p = 0.62; CFI = 1.00; RMSEA < 0.001, CI = 0.001-0.46, p = 0.63).

It should be added that a model incorporating CA3 could also be derived for Group Familiar (Figure 19D). In this model, which is identical in all other

respects to that depicted in Figure 19C, there are parallel routes from lateral entorhinal cortex to CA3 and CA1, both of which are significant (lEnt - CA1: strength path = 0.76 $p < 0.01$; lEnt CA3: strength path = 0.66, $p < 0.001$). This model has an acceptable level of fit for most indices ($\chi^2 = 10.3$, df = 6, $p = 0.12$; CFI = 0.92; RMSEA = 0.281, CI = 0.001-0.57, $p = 0.12$), but there is no significant pathway from CA3 to CA1. This alternate model also highlights the dominance of the temporo-ammonic pathway over the perforant pathway in Group Familiar, though it has poorer fit than the model depicted in Figure 19C.

Table 2. Stacking of the novel and familiar optimal model

	Model fit					*Group comparisons*		
Stacked model constraints	χ^2	df	*p*	CFI	RMSEA	df	χ^2	*p*
Unconstrained	38.87	18	0.003	0.81	0.25			
All paths	50.64	23	0.001	0.75	0.26	5	11.77	**0.038***
lEnt - DG	47.45	20	0.001	0.75	0.28	2	8.59	**0.014***
DG - CA3	41.80	20	0.003	0.80	0.25	2	2.93	0.23
CA3 - CA1	39.42	20	0.006	0.83	0.23	2	0.55	0.76
lEnt - CA1	39.08	20	0.007	0.83	0.23	2	0.22	0.90

Table 2. Results of the multiple-sample structural equation model analyses in which stacked groups Novel and Familiar were evaluated with specific path constraints; df, degrees of freedom; lEnt, lateral entorhinal cortex; DG, dentate gyrus. Statistical significance < 0.05 level (*) is indicated in bold.

Group Novel versus Group Familiar

The c-Fos results for Group Familiar were next set within the optimal model derived for Group Novel (Figure 19B). Not surprisingly, Group Familiar exhibited poor fit to this model ($\chi^2 = 27.9$, df = 9, $p = 0.001$; CFI = 0.67; RMSEA = 0.48, CI = 0.28-0.69, $p < 0.001$). Because both groups were tested on the same model it was possible to compare them formally by stacking Group Novel and Group Familiar (see Figures 19A, B and Table 2). When both groups were combined the resultant model exhibited poorer fit on all measures ($\chi^2 = 38.7$, df = 18, $p = 0.003$; CFI = 0.81), consistent with the

deleterious impact of Group Familiar. Overall comparison of the unconstrained stacked model and another model, in which each path was simultaneously constrained (structural weights) to be equivalent between the conditions, revealed that the overall structure of the two groups was significantly different (χ^2 = 11.77, df = 5, p = 0.038). This group difference was tested by constraining those individual paths exhibiting a relatively substantial difference in strength, = 0.05. Group differences included the reduction in the effective linear connectivity of the lateral entorhinal cortex to the dentate gyrus (χ^2 = 8.59, df = 2, p = 0.014).

Discussion

Using a new behavioural protocol, rats were shown novel objects and compared to those shown identical, yet familiar objects. The active discrimination of novel objects was strongly associated with c-Fos increases in perirhinal cortex and area Te2. While previous studies have reported c-Fos increases in these areas when rats are exposed to novel objects, this is the first study where the rats' behaviour simultaneously confirms their ability to distinguish novel from familiar. A more complex pattern of c-Fos changes occurred in the hippocampus as there was no overall activity change with novelty, yet different subfields either increased (CA1, CA3) or decreased (dentate gyrus) activity levels. Structural equation modelling highlighted the difference in patterns of c-*fos* activation within the temporal lobe for novel versus familiar stimuli. Especially striking was the switch in parahippocampal – hippocampal effective connectivity from the temporo-ammonic pathway in Group Familiar to the perforant (dentate gyrus) pathway in Group Novel. An important caveat is that like most imaging findings, the results are correlative and so it is misleading to draw causal inferences. It should, however, be noted that there is evidence from antisense infusion experiments to show that c-*fos* activity in the perirhinal cortex is a critical requirement for effective, stable object recognition memory in rats (Seoane and Brown, 2007). Thus, the present study used a marker that may have a causal role for long-term

recognition memory, though the study could only examine short retention periods in Group Novel.

Standard spontaneous exploration tasks typically comprise one trial (two objects) per session. This feature leaves such tasks prone to null results if cellular correlates of novelty for a given object are restricted to a small subpopulation of cells or if the signal itself is small. The very small number of stimuli can also introduce biases associated with specific objects. The present study, therefore, used a new behavioural protocol that combined features of delayed nonmatching-to-sample, e.g. multiple trials, with spontaneous recognition. Very clear exploration differences emerged in every Group Novel animal for novel versus familiar objects, indicative of the robustness of this new test and its potential for examining the neural basis of recognition memory.

Exposure to familiar stimuli was associated with a relative decrease of c-*fos* activity in the perirhinal cortex. This pattern has parallels with the decreases in neuronal activity (Brown and Aggleton, 2001) and the decreases in the BOLD signal (Gonsalves et al., 2005; Henson et al., 2003; Montaldi et al., 2006) found, respectively, in the perirhinal region of monkeys and people when presented with familiar stimuli. Within the perirhinal cortex, *caudal* areas 35 and 36 appeared to show the clearest distinction between novel and familiar objects, as measured by c-Fos. While previous IEG studies have also found changed c-Fos counts in caudal perirhinal cortex associated with familiarity (Zhu et al., 1996; Wan et al., 1999), none has tested for rostro-caudal differences. Similarly, while electrophysiological recordings in rats indicate that caudal areas 35 and 36 can signal novelty (Zhu et al., 1995a), sub-regions within these areas have not been compared. For similar reasons the present findings accord with studies disrupting recognition following perirhinal injections (Griffiths et al., 2008; e.g. Winters and Bussey, 2005) as all of these studies primarily targeted caudal perirhinal cortex. The most likely explanation for this prior focus on caudal perirhinal cortex is that it is a reaction to the uncertainty over the placement of the rostral border of this area (Burwell, 2001; Shi and Cassell, 1999).

The present finding that caudal perirhinal cortex (both areas 35 and 36) has particular importance for identifying object novelty agrees with the recent finding of a significant correlation between object recognition deficits and the amount of perirhinal tissue loss in the caudal, but not the mid or rostral portions of areas 35 and 36 (Albasser et al., 2009). This convergent evidence for a rostro-caudal functional difference has anatomical support as the caudal perirhinal cortex is more closely linked to visual inputs (Furtak et al., 2007), including those from area Te2 (Shi and Cassell, 1999) and from the occipital cortex (Furtak et al., 2007). The inputs from the dorsal (especially midline) thalamus also preferentially target caudal perirhinal cortex (Furtak et al., 2007). Caudal perirhinal cortex is also noteworthy as it is a major source of projections to the other parts of the perirhinal cortex, along with the postrhinal and entorhinal cortices (Furtak et al., 2007). Area Te2 consistently shows c-Fos increases with visual novelty (Zhu et al., 1996; Wan et al., 1999) and is thought to function in tandem with caudal perirhinal cortex (Zhu et al., 1995a).

In addition to the caudal perirhinal cortex c-Fos changes, hippocampal c-Fos changes (increases and decreases) were also associated with novel object exploration. These c-Fos changes in the hippocampus are notable as they suggest a more complex pattern of hippocampal activity changes in response to novelty than suggested by the 'gatekeeper' model (Fernandez and Tendolkar, 2006) and also that this structure is potentially involved in the detection of novel objects i.e. for object recognition. This latter proposal is however, highly contentious (Aggleton and Brown, 1999; Mumby, 2001; Squire et al., 2007). It is, therefore, helpful to note that all previous c-Fos studies that passively exposed rats to sets of novel objects (versus familiar objects) have found no significant hippocampal activity changes (Zhu et al., 1995b; Zhu et al., 1996, 1997; Wan et al., 1999; Warburton et al., 2003; Wan et al., 2004; Aggleton and Brown, 2005). For this reason, the present study stands out.

In view of these consistent null results, where there is no c-Fos hippocampal activity change, it is crucial to examine the procedural differences between the

present study and these previous studies. The most notable difference is that the rats in the present study could investigate the objects in their various locations. It is known that rats automatically learn the spatial disposition of objects explored in an arena (Poucet, 1989; Dix and Aggleton, 1999), and evidence for spontaneous spatial learning was found in the present study. It is, therefore, possible that this spatial learning element contributed to the hippocampal activity changes. This interpretation receives further support from studies which have found that the spatial re-arrangement of familiar room cues (Jenkins et al., 2004b), as well as the introduction of novel spatial cues (Van Elzakker et al., 2008; Vann et al., 2000), consistently changes hippocampal c-*fos* activity. Particularly strong support for this view comes from the fact that the hippocampal results in the present study (increased c-Fos in CA1 and CA3, decreased c-Fos in dentate gyrus) precisely match the c-Fos patterns elicited by the passive presentation of novel spatial arrays of highly familiar visual stimuli (Wan et al., 1999). Indeed, the similarity in these patterns points to a specific mode of hippocampal function when novel object-spatial conjunctions are detected and acquired. Consequently, the hippocampal IEG activations in the present study are most likely to include those spatial processes that are inherent in any study involving object investigation. At the same time, the results in the current study cannot preclude a role in novelty detection.

There remains much debate over how the perirhinal cortex and hippocampus contribute to recognition memory (Brown and Aggleton, 2001; Eichenbaum et al., 2007; Squire et al., 2007). Recent rat studies, based on receiver operating characteristics, point to different but complementary roles for the perirhinal cortex and hippocampus (Fortin et al., 2004). The perirhinal cortex can detect stimulus novelty while the hippocampus helps detect changes in associative aspects of the stimuli, e.g. 'where' and 'when'. This model readily fits the present findings. It has already been noted that the present hippocampal activations in Group Novel match patterns associated with learning spatial dispositions ('where') of stimuli (Wan et al., 1999; Vann et al., 2000). A potential criticism with this account is that both the Novel and Familiar groups showed spatial disposition learning, and so differential hippocampal activation

might not initially be predicted in Group Novel, i.e. the groups should be similar. In fact, a second possible explanation of the present findings is predicted by the 'gatekeeper' hypothesis of perirhinal function (Fernandez and Tendolkar, 2006). In the Fernandez and Tendolkar model (2006), the role of the rhinal cortex is to make rapid and efficient judgments of the nature of the presented item (novel or familiar). The rhinal cortex provides an optimal output for declarative memory by assigning limited encoding resources away from already familiar information and towards novel information before sending the information to the hippocampus for further encoding. By this hypothesis, changes in c-Fos hippocampal activity reflect novelty discrimination by the perirhinal/Te2 cortices, a view supported by the present network analyses.

The optimal models derived by structural equation modelling underline the qualitative differences in the patterns of temporal connectivity evoked by novelty versus familiarity. While novel stimuli engaged the tri-synaptic path via the perforant pathway (lateral entorhinal→DG→CA3→CA1), familiar stimuli (recency) engaged the temporo-ammonic route (lateral entorhinal directly to CA1). This temporal direction of effects in Group Novel (rhinal cortex to hippocampus) matches that found with in-depth electrodes in human patients learning word lists (Fernandez et al., 1999), where event related potentials in the rhinal cortex occurred first (300-500 ms after stimulus onset), followed by a hippocampal subsequent memory effect (500-2000 ms after stimulus onset). At the same time, it should be noted that such analyses can only present a highly simplified account of the multitude of potential medial temporal interconnections (Van Strien et al., 2009). Such limitations do not, however, detract from one the core findings of the present study: that qualitatively different patterns of network effects were found in Groups Novel and Familiar.

It is also striking that a remarkably similar network pattern involving a loss of dentate gyrus influence, reliance of CA1 on temporo-ammonic input, and CA1/CA3 uncoupling occurred in a previous network analysis of Zif268 expression when spatial learning relied on increasingly familiar room cues (Poirier et al., 2008). Similarly, 'place' versus 'landmark' learning in a water

maze resulted in qualitatively different patterns of c-*fos* activation between perirhinal cortex, lateral entorhinal cortex and dentate gyrus, with only new place learning engaging all three in a linear model (Jenkins et al., 2003). The emergence of these similar network patterns across different studies reveal a general switch in hippocampal function from a temporo-dentate mode to a temporo-ammonic mode as behaviour involves highly familiar cues or established spatial arrangements (Van Elzakker et al., 2008).

This switch in dominant routes both supports and extends the 'gatekeeper' hypothesis of perirhinal cortex function (Fernandez and Tendolkar, 2006), in which signals from perirhinal cortex induced by stimulus novelty raise the likelihood of subsequent learning about stimulus attributes via primed hippocampal interactions. As predicted, the patterns of c-Fos activation found in perirhinal cortex/area Te2 in response to novel stimuli are associated with changes in hippocampal engagement. To be specific, the present study now suggests that the priming mechanism is via an entorhinal cortex switch that regulates the preferential roles of the either the perforant pathway (novel stimuli) or the temporo-ammonic pathway (familiar stimuli). The engagement of the perforant pathway route would then enable the hippocampal learning of novel object attributes (Hunsaker et al., 2007; Staresina and Davachi, 2008) including learning their spatial or temporal context (Hoge and Kesner, 2007; Wan et al., 1999).

Chapter 6

General Discussion

What can IEG/lesion studies tell about memory?

Overview

Memory can be defined as the mental ability to store, retain and recall information. Almost 40 years ago, Tulving (1972) proposed the concept of episodic and semantic memory centred on different kinds of information and their sources. He defined episodic memory as the memory of autobiographical events, opposite to semantic memory as the memory of meanings, understandings, and other concept-based knowledge unrelated to specific experiences (general facts). In addition, Tulving (1972) regarded episodic memory as the ability to mentally travel back to recollect specific episodes from the past and stated that only humans may have this "mental time travel" ability. Later, Squire and Zola-Morgan (1991) proposed a classification of memory (see Figure 1), where episodic and semantic memory form declarative memory, which refers to conscious recollection of facts and events.

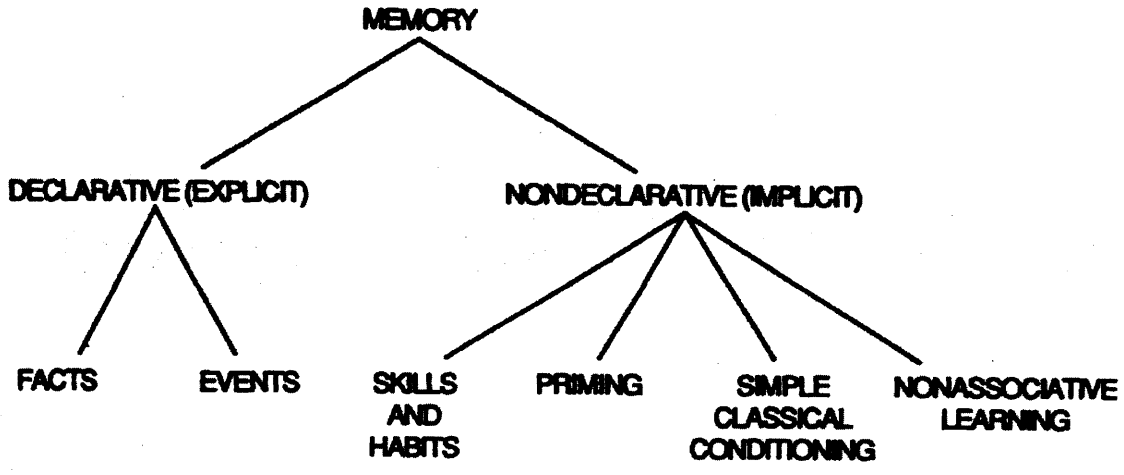

Figure 1. The classification of memory by Squire and Zola-Morgan (1991)

Patients who suffer from amnesia, which particularly affects episodic memory, have had a key role in the investigation of the brain structures necessary for memory. From single case and group studies, two distinct brain regions, associated with anterograde amnesia, emerged. Over 100 years ago, the first organic amnesia was described, highlighting the likely involvement of the diencephalon in memory (Korsakoff, 1887; Gudden, 1896). Almost half a century later, a report by Scoville and Milner (1957) described a profound and selective memory impairment in the patient H.M., after surgical removal of the medial temporal lobe. As a consequence, attention was drawn to the region of the hippocampus. Such findings have led to the goal of uncovering networks of brain regions that may underlie various cognitive processes, including episodic memory (Delay and Brion, 1969; Horel, 1978; Tulving and Markowitsch, 1997; Aggleton and Brown, 1999). To this goal has been added at least one additional brain structure, the retrosplenial cortex, as damage to this region appears sufficient to cause amnesia (Valenstein et al., 1987; Maguire, 2001a). In the next section I will consider network models of declarative memory and examine the findings in this thesis related to these models.

Two different memory models?

The first model, "the medial temporal memory system" (Figure 2), was originally proposed by Squire and Zola-Morgan (1991). In this model, the hippocampus has the highest place above entorhinal cortex, perirhinal cortex and parahippocampal cortices. This model suggests that all these structures are interdependent, and that these structures work together in a cooperative and complementary way (e.g. familiarity and recollection, see Squire et al., 2007). The extent to which these areas specialise in handling specific forms of information remains poorly specified, though it is acknowledged that this model has a unitary process to treat what are subjectively perceived as different forms of memory.

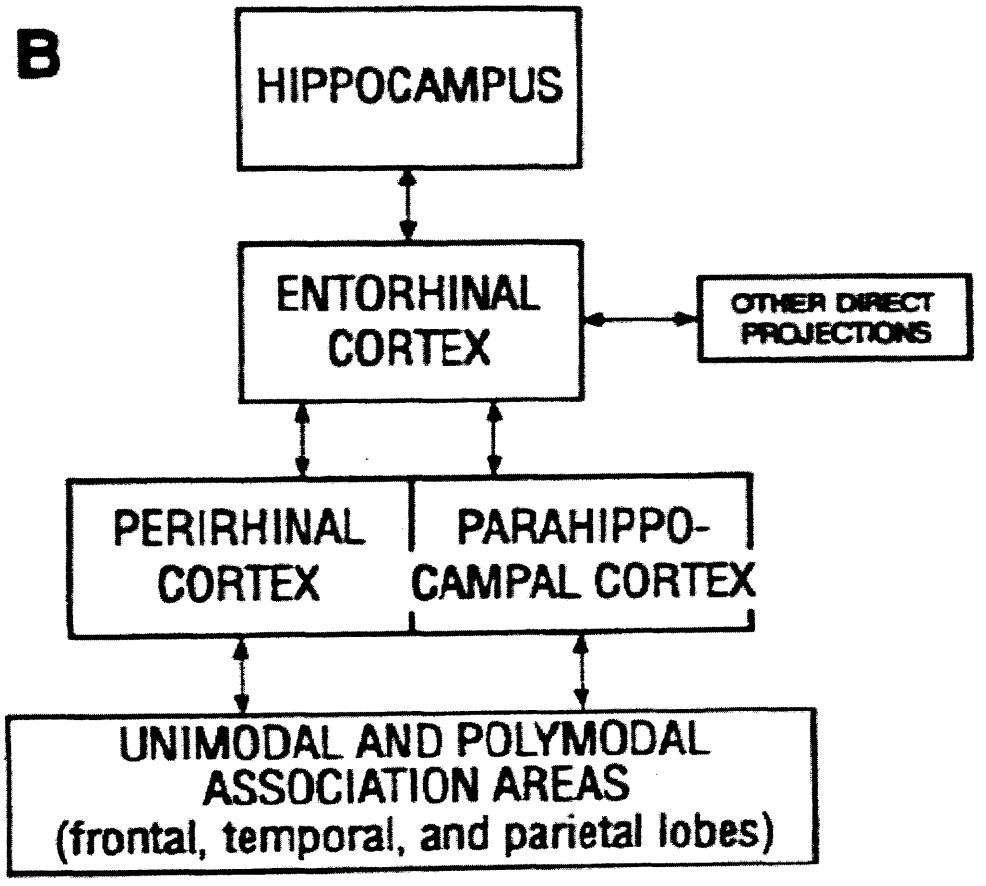

Figure 2. Schematic view of the medial temporal lobe memory system by Squire and Zola-Morgan (1991)

An alternative model, "the extended hippocampal memory system" was proposed by Aggleton and Brown (1999). The medial temporal lobe was extended to the diencephalon to form a larger model including the hippocampus, the fornix, the anterior thalamic nuclei, the mammillary bodies and, later, the retrosplenial cortex (Aggleton and Brown, 2006). The key element of this model begins with the premise that qualitatively different forms of memory may be treated by different components within the medial temporal lobe (e.g. familiarity by the perirhinal cortex versus recollection by the hippocampus). Consequently, this model assumes a dual process view of recognition.

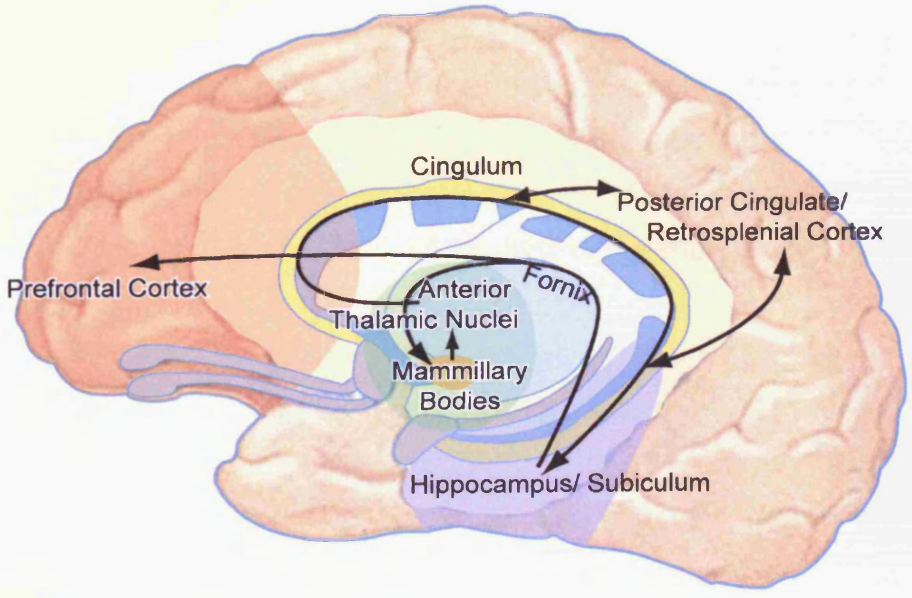

Figure 3. Schematic view of the extended hippocampal memory system by Aggleton and Brown (1999; 2006)

Implications of the findings in this thesis for different memory models

In the course of this thesis, I have provided additional evidence that supports and further extends "the extended hippocampal memory system". Chapters 2 and 4 support the idea of an extended model where damaging one region may induce hidden or "covert" pathology. Combining imaging and lesion techniques, it was found respectively that lesions of the hippocampus (Chapter 2) and the fornix (Chapter 4) induce metabolic hypoactivity in the retrosplenial cortex, whereas this region still appears normal by standard histological means. Our immediate-early gene findings are consistent with previous experiments where lesions of a particular brain structure can disrupt activity of other brain regions within the same extended hippocampal memory system (Vann et al., 2000b; Jenkins et al., 2004a; Jenkins et al., 2006). Table 1 summarises the effects of various lesions on IEG activity across the brain (based on Chapters 2-4 and Vann et al., 2000b; Jenkins et al., 2004a; Jenkins et al., 2006).

Taken together, these studies highlight the importance of remembering that lesion studies do not just investigate the functions of a removed structure, but rather examine how in the absence of that structure, the brain can best compensate, and its impact upon related structures.

A further question is the extent to which temporal lobe amnesia and diencephalic amnesia are linked, i.e. are the medial temporal lobe and the diencephalon part of common integrated, interdependent system? Table 1 clearly shows that there is a potential domino effect in this extended hippocampal memory system. Indeed, damage to one of the structures within this network induces a widespread disruption of the rest of the system. For example, all lesions of the hippocampus cause a decrease of c-*fos* activity in the anterior thalamic nuclei and the retrosplenial cortex. The same is true for the dorsal hippocampus, which shows hypoactivity after lesions of the anterior

Counted areas		Lesioned structures: ATN[1]	FNX[2]	MTT[3]	AMYG[3]	HPC[4]	RSC[5]
Frontal Cx	PL	↘	↗	↘	↘	-	
	IL			-	↘	-	
	AC	↘	↘	-	-	-	
ATN		↘	↘			↘	
RSC		↘	↘	↘	↗	↘	↘
HPC	ventral	↘	↘	-	↘		
	dorsal	↘	↘	↘	-		
Subicular Cx	v SUB	-	↘	-	-	-	
	d SUB	-	-	-	↗		
	Pre SUB	-	↘	-	↗	↘	
	Para SUB	↘	↘	↗	-	-	
	Post SUB	-	↘	↘	-	↘	
Para HPC	PERI		-	-	↗	↘	
	ENT		↘	-	-	↘	
	PostRH		↘			↘	
Sensory Cx	MO	↗	-				
	SS	↗	-	-	-		
	VISp	-	-	-	-	-	↘
	AUDp	-		-	-	-	↘

Table 1. Summary of lesion studies within the extended hippocampal memory system on the IEG activity of different brain areas. Abbreviations: AC, Anterior cingulate; ATN, anterior thalamic nuclei; AUDp, auditory primary cortex; Cx, cortex; ENT, entorhinal cortex; HPC, hippocampus; IL, infralimbic; MO, motor cortex; PostRH, postrhinal; SS, somatosensory cortex; SUB, subiculum; VISp, visual primary cortex. ↘, decrease of IEG; ↗ increase of IEG; - no changes of IEG. Shaded boxes represent areas that have not been counted. Table based on: [1] (Jenkins et al., 2002a; Jenkins et al., 2002b; Jenkins et al., 2004a); [2] (Chapter 4 and Vann et al., 2000b); [3] (Chapter 3); [4] (Chapter 2 and Jenkins et al., 2006); [5] (see Chapter 6)

thalamic nuclei, the fornix, and the mammillothalamic tract. All the studied lesions (see Table 1) induce a reduction of c-Fos counts in the retrosplenial cortex. At a more crude level, these findings show that damage to the diencephalon selectively affects the medial temporal lobe and vice versa. Not surprisingly, fornix damage can reduce c-*fos* activity in multiple sites in the medial temporal lobe and the medial diencephalon. At the same time, this particular result may interact with anaesthetic agent (Chapter 4).

In a recent review, Aggleton (2008) discusses and supports evidence towards an integrated system of temporal lobe and diencephalic amnesia, based on neuroanatomical, neuropsychological, neuroimaging findings. Animal studies can be used to target specific brain lesions and their effects. In Chapter 3, lesions were made in the rat mammillothalamic tract, which carries the projections from the mammillary bodies to the anterior thalamic nuclei in the diencephalon (Vann and Aggleton, 2004b). Mammillothalamic tract lesions resulted in decreases of metabolic activity, as measured by immediate-early gene expression (c-*fos*), in widespread key areas: the hippocampus, the prefrontal cortex, the retrosplenial cortex. These findings unify substrates linked to diencephalic and temporal lobe amnesia; thereby supporting a new account of diencephalic amnesia that emphasizes multiple dysfunctions across hippocampal, retrosplenial and prefrontal areas. In addition, these findings draw attention to the retrosplenial cortex. Indeed, it seems likely that both diencephalic and temporal lobe amnesia cause dysfunctions in a third common region. The retrosplenial cortex may be a perfect candidate. Within this extended system, the retrosplenial cortex has a specific place, as it has dense reciprocal connections with both the anterior thalamic nuclei and the hippocampal formation (Wyss and Van Groen, 1992; Van Groen et al., 1993). Moreover, damage to the retrosplenial cortex is sufficient to produce anterograde amnesia (Valenstein et al., 1987; Maguire, 2001a). Finally, this thesis amongst other studies provides further evidence that the retrosplenial cortex is particularly sensitive to distal damage in structures within the extended hippocampal memory system. Thus, hippocampal (Chapter 2, Albasser et al., 2007), anterior thalamic nuclei (Jenkins et al., 2004a; Poirier and Aggleton, 2009), fornix (Vann et al., 2000b, but see Chapter 4) and

mammillothalamic tract (Chapter 3, Vann and Albasser, 2009) lesions can all disrupt retrosplenial cortex activity. These lesion studies highlight that the retrosplenial cortex, compared to other regions (e.g. parahippocampal regions or subicular cortices), is more sensitive to distal lesions; and that hippocampal and mammillothalamic tract lesions induce the most severe hypoactivity in the retrosplenial cortex (Chapters 2 and 3).

The importance of controls in IEG experiments: evidence from a unilateral retrosplenial cortex lesion study

Lesion studies have revealed a vital role for the retrosplenial cortex in learning and memory by rats, more precisely for spatial memory (Sutherland and Hoesing, 1993; Cooper et al., 2001; Whishaw et al., 2001; Van Groen et al., 2004; Vann and Aggleton, 2004a), including learning the locations of specific objects (Vann and Aggleton, 2002; Parron and Save, 2004). Once again, animal studies have helped to investigate the role of the retrosplenial cortex in more detail by making it possible to compare sub-regions of the retrosplenial cortex. Clinical and neuroimaging studies have also emphasized the involvement of the retrosplenial cortex (area 29 and 30) in memory. First, Valenstein and colleagues (1987) argued that damage to the retrosplenial cortex was sufficient to cause anterograde amnesia. It is, however, worth noticing that the brain injury in their single case was probably not selective to the retrosplenial cortex and included as well as the splenium, the cingulum bundle and may have involved the fornix (Valenstein et al., 1987). Since then, the retrosplenial cortex has also been associated with a specific role in human navigation, such as topographical orientation (Maguire, 2001a; Epstein and Higgins, 2007; Iaria et al., 2007). In fact, Maguire (2001a) revealed the importance of the right retrosplenial cortex in navigation and orientation in human spatial tasks, while the retrosplenial cortex in the left hemisphere seems to be more involved, such as the left hippocampus, in episodic memory, specifically autobiographical event memory (Maguire, 2001b).

As mentioned earlier, the retrosplenial cortex is particularly sensitive to lesions of brain structures within the extended network. In order to get a better understanding of the retrosplenial cortex, I conducted a pilot experiment (not fully presented in this thesis) to study whether unilateral retrosplenial cortex lesions were enough to dysregulate its own activity (i.e. in the contralateral hemisphere). Animals were anaesthetised by intraperitoneal injection of sodium pentobarbital (60 mg/kg). Lesions were made unilaterally with radiofrequency, so comparisons of IEG activity (between subjects) were made between the non-lesioned hemisphere and separate surgical controls. Both groups (lesion and surgery control, n = 10) were trained in the identical standard working memory procedure in the radial-arm maze (Olton et al., 1978 and Chapter 4, experiments 3B, 4). Following the behavioural task, retrosplenial cortex activity was measured by immediate-early gene expression (c-*fos* and *zif*268).

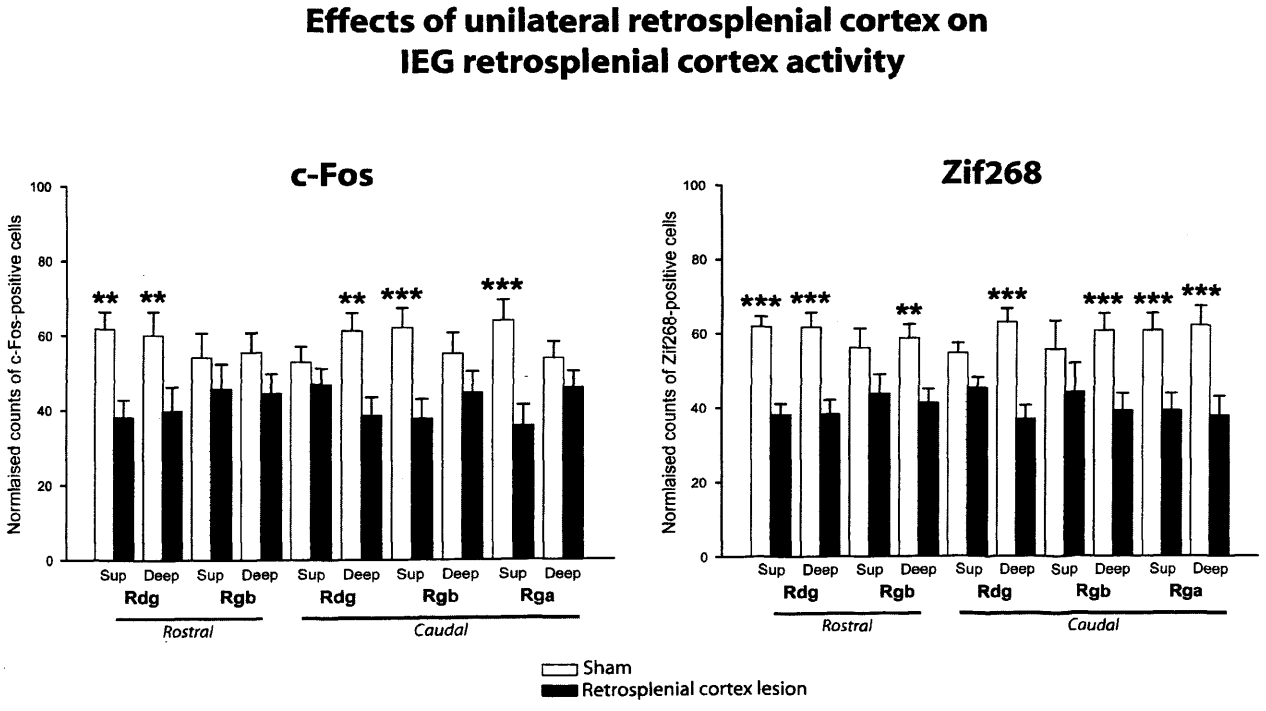

Figure 4. IEG activity in the retrosplenial cortex after unilateral retrosplenial cortex lesions. Normalised c-Fos counts (left) and Zif268 counts (right) in the retrosplenial cortex in the lesion group (black) and surgery control (white). All normalised percentages sum to 100. Errors bars refer to ± SEM of the

corresponding mean values. *** $p < 0.001$, ** $p < 0.01$. Abbreviations: Deep, deep layers; Rdg, retrosplenial dysgranular cortex; Rga, retrosplenial granular a cortex; Rgb, retrosplenial granular b cortex; Sup, superficial layers.

A decrease of IEG activity was found in the contralateral retrosplenial cortex after unilateral retrosplenial cortex lesions (Figure 4). These findings reveal that unilateral lesions of this specific brain region may partially disrupt its contralateral counterpart. Even though unilateral lesions in rats often appear to have only minimal effects on animal behaviour, our data suggest that unilateral lesions of the retrosplenial cortex might be unusually disruptive. The impact of such damage is likely to be most noticeable at the beginning of training.

Somatosensory demands

In behavioural experiments using immediate-early genes, the first step is to make sure that all animals of each group have matched the same sensory and motor demands during the behavioural task (Chapter 5, Shires and Aggleton, 2008); so differences in brain activity cannot be due to different experiences during the task. A way to get round this problem is to use unilateral lesions, as the comparison can then be made within animals. However this alternative was not possible in this pilot study as the aim was to assess the effects of retrosplenial cortex lesions on the activity of the contralateral retrosplenial cortex. So a surgical control group was needed.

The retrosplenial cortex hypoactivity found after unilateral retrosplenial cortex lesions was not as severe as the deficits obtained after hippocampal (Chapter 2) or mammillothalamic tract (Chapter 3) lesions, but was more similar to fornix lesions (Chapter 4). However, by analysing the control regions, I discovered some limitations with the findings. In particular there was a decrease of c-*fos* activity in two cortical areas (primary auditory and primary somatosensory cortices) that may reflect overall effects of the lesions throughout the brain or abnormal sensorimotor patterns following surgery.

Immediate-early gene experiments have to be carried out with great thought and with particular care given to control conditions.

Pairing of animals

Animals are also paired (in this pilot experiment, one unilateral retrosplenial cortex lesion animal, with one surgery control animal), so that during the immunohistochemistry procedures, the brain sections are processed together in the same pot. For the last immunohistochemistry step, positive cells are revealed by diaminobenzidine (DAB). The time and intensity of this procedure may vary between pots. For example, the reaction can be faster and stain darker the cells. By pairing the animals, variations between two immunohistochemistry reactions are minimised. Moreover, this pairing makes it possible to normalise the cell counting, and so reduce again variability between animals (see Chapters 2-5, Materials and Methods).

Histological control

When differences in IEG counts are found, another important control is to verify whether these changes are not due to alterations of the cytoarchitecture of the region of interest. Indeed, it is easy to imagine that cell loss in a brain area would lead to a lower count of IEG-positive cells. Indeed, a lesion of one specific region will deafferent another structure, which may be enough to induce shrinkage of the second brain area. For example, it has been shown that fornix damage isolates the mammillary bodies from their temporal lobe inputs, leading to mammillary body atrophy, (Loftus et al., 2000; Tsivilis et al., 2008), mostly due to the loss of neuropil (dendrites and axons). The aim of this histological control is to visualise and count the actual number of cells regardless of their activity. Two different cytoarchitectural markers have been used in this thesis: Nissl and NeuN (Chapter 2). One of the most traditionally used techniques is Nissl staining with cresyl violet, which stains endoplasmic reticulum. Since all cells contain endoplasmic reticulum, cresyl violet will stain both neurons and glial cells. The second marker is NeuN (Neuronal Nuclei); it

is a neuron-specific nuclear protein that can be visualised by immunohistochemistry, similar to c-Fos and Zif268. The counting procedure is also identical (e.g. software, microscope, number of slides) to the one used to count IEG-positive cells. However, this method is more expensive and takes longer to carry out compared to the Nissl-staining. In addition, it was shown, in Chapter 2, that similar results were found between the Nissl-stain and NeuN counts of cells.

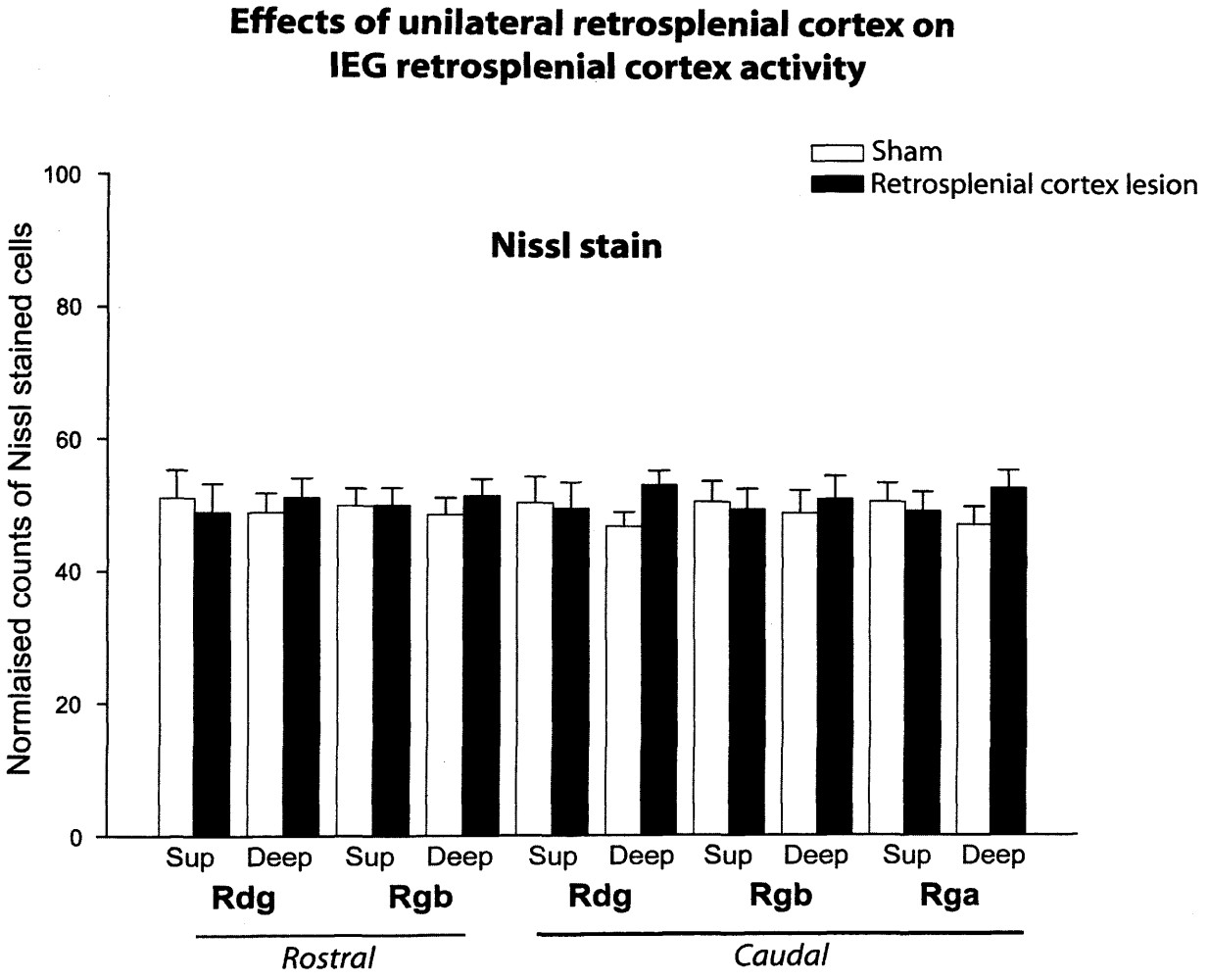

Figure 5. Normalised Nissl stained counts in the retrosplenial cortex in the lesion group (black) and surgery control (white) after unilateral retrosplenial cortex lesions. All normalised percentages sum to 100. Abbreviations: Deep, deep layers; Rdg, retrosplenial dysgranular cortex; Rga, retrosplenial granular a cortex; Rgb, retrosplenial granular b cortex; Sup, superficial layers.

In this pilot retrosplenial cortex lesion experiment, no significant changes in the number of Nissl-stained cells were found in the superficial and deep layers

of the three sub-regions (Rdg, Rgb, Rga) of the contralateral retrosplenial cortex after unilateral retrosplenial lesions (Figure 5), confirming that the lesions did not induce cell loss in the intact retrosplenial hemisphere. The counting method (number of photos, software, threshold) was also identical to the one used for IEG counts (see Chapter 2).

Cortical area controls

The final control is to verify that the IEG changes found (in this study a reduction of IEG-positive cells in the retrosplenial cortex following unilateral retrosplenial cortex lesion) are specific to the region of interest, and are not just a main effect throughout the brain. One approach is to measure the activity of brain areas that are linked to the region of interest. However, this may be misleading. For example, in a behavioural spatial task, linked regions may also be implicated in the same memory processes. A better control is to measure activity in cortical areas such as a sensorimotor area (e.g. primary auditory, visual, motor or somatosensory primary cortex), as any group differences might reflect abnormal sensorimotor patterns following surgery. However, the somatosensory demands of the behavioural task must be taken into account as the same time. Indeed, it would not be recommended to use the primary auditory area as a control comparison area in a task using different auditory stimuli. It would therefore be possible that activity changes occur in this area if auditory stimuli were not the same between groups. It is also the case that there are potential "back influences" upon sensory areas, e.g. the retrosplenial cortex in the rat projects to areas 17 and 18.

In our pilot study looking at the effect of unilateral retrosplenial cortex lesions on the activity of the retrosplenial cortex, although all the previous controls were used and validated, the latter (sensorimotor control area) highlighted some limitations of the conclusion of the study. As mentioned earlier, it was found that unilateral retrosplenial cortex lesions induce an overall decrease of the retrosplenial cortex activity in the non-lesioned hemisphere. In order to verify that this effect was not general to the whole brain, counts were made in

the primary auditory and primary somatosensory cortices. For this specific study, it was possible to measure two different controls with the control comparison areas. First, a within subject comparison was made of cortical areas between the lesion and non-lesion hemispheres. Second, a between subject comparison had to be made between the lesion group and the surgical control group. Indeed, a surgical control was necessary because the lesion group had only one retrosplenial cortex left, so the comparison of IEG counts in the retrosplenial cortex was made between the one retrosplenial cortex left in the lesion group and the retrosplenial cortex in the surgical control group. For both controls, a decrease of c-*fos* activity was found for both primary auditory and somatosensory cortices (Figure 6). These differences in IEG counts change the significance and the conclusions of the specificity of hypoactivity found in the retrosplenial cortex. These findings might reflect abnormal sensorimotor patterns following surgery. The anatomical connections of the retrosplenial cortex would lead one to expect changes in visual areas, but not in auditory cortex. As a consequence, the IEG findings of this pilot study are ambiguous and much more difficult to interpret.

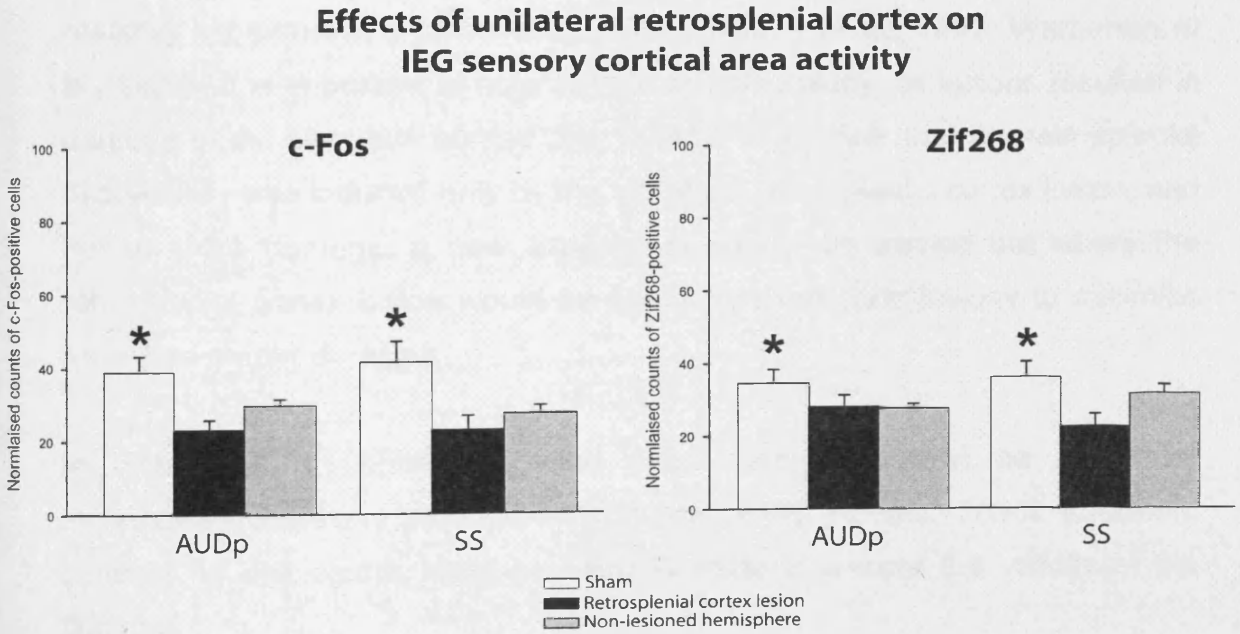

Figure 6. IEG activity after unilateral retrosplenial cortex lesions. Normalised c-Fos (left) and Zif268 (right) counts in sensory cortical areas in the lesion group (black), non-lesioned hemisphere (grey) and surgery control (white). All

normalised percentages sum to 100. Errors bars refer to ± SEM of the corresponding mean values. * $p < 0.05$. Abbreviations: AUDp, primary auditory cortex; SS, somatosensory cortex.

The first attempt (made by Dr. Guillaume L. Poirier) to make unilateral retrosplenial cortex lesions involved injection of neurotoxin (NMDA). However, this technique resulted in mild, but consistent damage in the retrosplenial cortex of the hemisphere opposite the lesion site. For this reason, in this study, the unilateral retrosplenial cortex lesions were made with radiofrequency. This lesion technique is non-specific in the sense that, contrary to excitotoxic lesions, it damages white matter in addition to tissue. For example, the radiofrequency lesion technique was used to damage fibre tracts, such as the mammillothalamic tract (Chapter 3) or the fornix (chapter 4). So one plausible explanation is that extra damage to fibres of passage (due to the radiofrequency technique) may have resulted in a more widespread hypoactivity throughout the brain. Indeed the rostral retrosplenial cortex is situated just above the cingulum bundle. The cingulum bundle carries projections from the anterior thalamic nuclei to temporal regions as well as to the cingulate cortices (Domesick, 1970; Aggleton et al., 1995). There is evidence that cingulum bundle damage is enough to produce spatial memory impairments (Neave et al., 1996; Neave et al., 1997; Warburton et al., 1998). It is important to note that, in the pilot study, all lesions resulted in damage in the cingulum bundle. So, in order to confirm that the retrosplenial hypoactivity was induced only by the unilateral retrosplenial cortex lesion, and not by extra damage, a new experiment should be carried out where the retrosplenial cortex lesion would be made by excitotoxic lesions to minimise any white matter damage.

In conclusion, in addition to the extra care that must be taken for immunohistochemistry procedures (Fritschy, 2008; Kovacs, 2008), additional controls for cell counts must be used in order to ensure the validity of the findings.

The use of IEG in behaviourally active animals

The immediate-early gene procedure has been increasingly used to study the effect of brain lesions upon activity of other brain areas (see Chapters 1-4). There is, however, another main advantage of this non-invasive technique. It is generally agreed now that immediate-early genes can be used as a marker of neural plasticity and learning (Nikolaev et al., 1991; Herdegen and Leah, 1998; Tischmeyer and Grimm, 1999; Kasahara et al., 2001; Fleischmann et al., 2003, but see Chapter 1). Therefore, it should be possible to highlight brain regions that are activated in different behavioural tasks (Wan et al., 1999; Vann et al., 2000c; Guzowski, 2002; He et al., 2002; Frankland et al., 2004; Poirier et al., 2008). So by using the IEG approach, it becomes possible to measure whether the region of interest is activated or involved in the behavioural task. Unlike fMRI, the measures of activity obtained by IEG technique are direct. Evidence for the integral role of IEGs in learning comes from antisense studies, where learning and memory can be disrupted by injection of IEG antisense (Grimm et al., 1997, but see Chapter 1; Guzowski, 2002; He et al., 2002; Seoane and Brown, 2007)

In conclusion, IEG expression imaging can lead to two different applications: (1) measuring brain region activity triggered by defined behavioural tasks; (2) measuring the effects of specific lesions upon other brain areas. However, these two applications can both help to get a better understanding of the role of a specific region. For example, behavioural studies using IEG expression show that the hippocampus subfields, the entorhinal cortex, the retrosplenial cortex, and the postrhinal cortex are activated by spatial tasks in the radial-arm maze (Vann et al., 2000c; Jenkins et al., 2003). These studies were followed by other studies coupling lesion and IEG technique. It was found that hippocampal lesions disturbed the activity of other brain regions such as the parahippocampal cortices, the retrosplenial cortex, and the anterior thalamic nuclei (Jenkins et al., 2006; Albasser et al., 2007). So the aim of combining the two approaches is to determine if the lesion/IEG findings highlight the same areas that are revealed in a normal brain IEG study

In Chapter 5, expression of the immediate-early gene c-*fos* was used to test for different patterns of temporal lobe interactions when rats explore either novel or familiar objects. Mapping visual recognition memory through IEG expression has in the past found a double dissociation between the perirhinal cortex (novel vs. familiar stimuli) and the hippocampus (novel vs. familiar spatial arrengement) using the paired-viewing procedure (Zhu et al., 1996; Wan et al., 1999). However, in this procedure, it was not possible to measure recognition memory behaviourally. That is why, a new paradigm suitable for behaviour and IEG expression analyses was designed (see Chapter 5). Our IEG findings confirmed that the discrimination of novel objects was accompanied by caudal perirhinal c-Fos increases and hippocampal subfield changes. In addition, structural equation modelling indicated the presence of pathways starting in the caudal perirhinal cortex that display a dynamic switch in their direction of effects from entorhinal cortex → dentate gyrus (perforant pathway) engagement with novel objects, compared with entorhinal cortex → CA1 field engagement (temporo-ammonic pathway) with familiar objects. This entorhinal switch not only substantiates the 'gatekeeper' hypothesis (Fernandez and Tendolkar, 2006), whereby, rhinal cortex moderates hippocampal processing but also indicates that the mechanism involves a change from temporo-ammonic (familiar) to perforant pathway (novel) influences.

As mentioned earlier, a new paradigm called the "bow-tie maze" was designed for the purpose of the experiment. The new task appears to have many advantages compared to previous tasks used in object recognition by combining positive aspects of the delayed non-matching to sample and the spontaneous exploration task. However, in order to validate this new one-session test for object recognition in rats, extra experiments were carried out (not presented in this thesis). Object recognition was assessed in animals with lesions of the perirhinal cortex, fornix and postcommissural fornix (Figure 7).

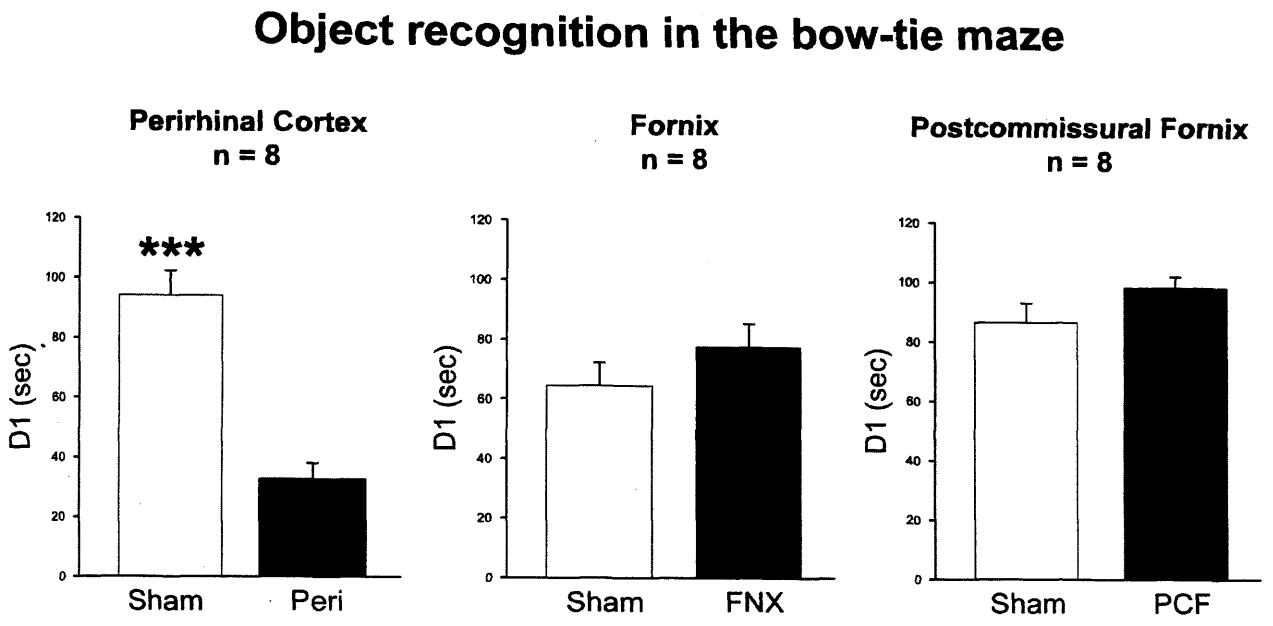

Figure 7. Exploration time as a measure of novelty discrimination by surgery controls (sham) in white and lesioned animals in black (left, perirhinal cortex; middle, fornix; right, postcommissural fornix). Mean D1 scores ($novel_{(sec)}$-$familiar_{(sec)}$) in seconds. Data are shown as mean ± SEM. *** $p < 0.001$.

All the control groups showed robust and reliable novelty discrimination, but only perirhinal cortex lesions impaired this task. Together with the results of the IEG experiment (Chapter 5), these results demonstrate the efficacy of this new behavioural task for assessing object recognition memory in rats and provide further evidence that the perirhinal cortex is required for recognition memory.

The particular importance of the caudal perirhinal cortex in object recognition?

In Chapter 5, special attention focused on the caudal part of the perirhinal cortex (Albasser et al., 2009). The perirhinal cortex (areas 35 and 36) is thought to be necessary for normal recognition memory. While the first evidence came from electrophysiological (Brown et al., 1987; Brown and

Aggleton, 2001) and lesion (Murray and Mishkin, 1986; Zola-Morgan et al., 1989; Meunier et al., 1993) studies with monkeys, subsequent studies of the rat have repeatedly shown that the perirhinal cortex appears to fulfil a very similar role (Mumby and Pinel, 1994; Zhu et al., 1996; Aggleton et al., 1997; Winters et al., 2004). Nevertheless, there is still a debate about different terminologies for the perirhinal cortex, allied to quite major differences in the placement of the perirhinal borders with its adjacent cortical regions. Burwell (2001) defines the perirhinal cortex as a longer region that can be subdivided in rostral (AP -2.80), mid (AP -3.80) and caudal (AP -4.80) perirhinal cortex AP relative to bregma, Paxinos and Watson, 1997); whereas Shi and Cassel consider only the caudal part as the perirhinal cortex proper (1999). Recent studies have highlighted different connection patterns for rostral, mid and caudal perirhinal cortex (Furtak et al., 2007; Van Strien et al., 2009).

A study by Albasser et al. (2009) examined two factors that might moderate the object-recognition deficit seen after perirhinal cortex damage. The first factor was whether the duration of active sampling and the length of the sample period alter discrimination performance in the spontaneous exploration task. Object recognition by normal rats was improved by extending the sample period time during which an object was first explored. Furthermore, there was a significant positive correlation between time spent in close exploration of the sample object and degree of successful novelty discrimination. In contrast, rats with perirhinal cortex lesions failed to benefit from increased close exploration and did not discriminate the novel object after the longest sample period. The second factor is more related to Chapter 5 and seeks to demonstrate whether varying the extent of the lesion has an effect on object discrimination performance. First, the extent of damage in different regions (perirhinal cortex, area Te2 and piriform/entorhinal cortices) was compared with the discrimination performance (Figure 8, left). Only perirhinal cortex damage correlated significantly with object recognition, with greater damage associated with poorer recognition. This correlation is consistent with that found in monkeys (Baxter and Murray, 2001). Our finding was then explored in more detail, and the extent of damage in the perirhinal cortex subdivisions was analysed (rostral, mid, caudal, but see Burwell, 2001;

Furtak et al., 2007). Interestingly, only the extent of damage in caudal perirhinal cortex significantly correlated with the discrimination performance (Figure 8, right).

So far, all previous perirhinal cortex studies have focused on the caudal part of the area (Mumby and Pinel, 1994; Zhu et al., 1996; Wan et al., 1999; Winters et al., 2004; Warburton et al., 2005; Griffiths et al., 2008), probably due to the debate over its border limitations (Shi and Cassell, 1999; Burwell, 2001). For the first time, direct comparisons were made in the same study between rostral, mid, and caudal perirhinal cortex damage, enabling us to highlight the importance of the caudal perirhinal. Consequently, these results complement those from the IEG study reported in Chapter 5.

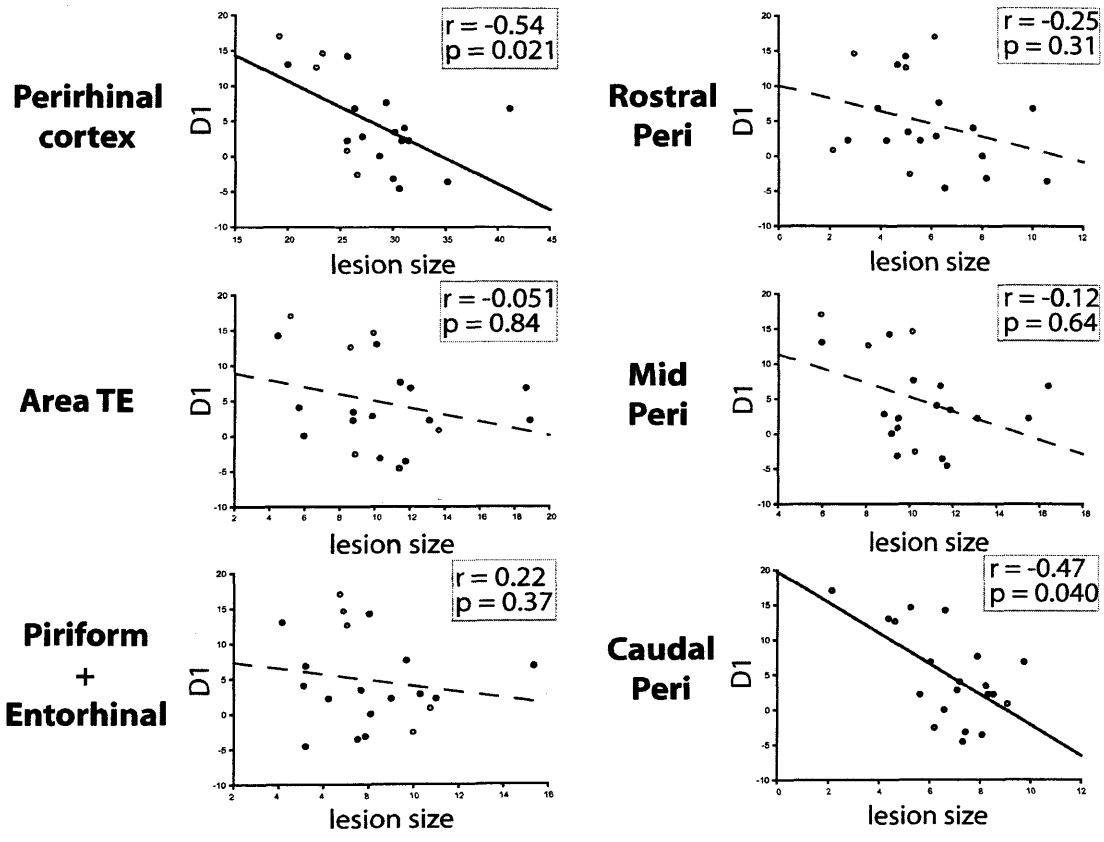

Figure 8. Pearson correlations between recognition performance (D1 scores) and extent of tissue loss in perirhinal cortex and in two adjacent cortical regions (left); and between D1 and the extent of tissue loss in the rostral, mid, and caudal perirhinal cortex (right). The partial regression results are given in the boxes (Albasser et al., 2009).

In Chapter 5, as mentioned earlier, expression of IEG was used to assess brain region activity induced by novelty/familiarity. Logically, following the findings of our previous study, activity was measured in the three sub-regions (rostral, mid, caudal) of the perirhinal cortex. Again, only the caudal perirhinal cortex showed a different pattern of activity with an increase of c-Fos counts induced by novelty. These two studies suggest a particular role of the caudal perirhinal cortex in object recognition. However, it cannot be fully concluded that only the caudal perirhinal cortex is involved in object recognition. Indeed, the three sub-regions within the perirhinal cortex are highly connected to each others (Furtak et al., 2007), so that their integrity may be of specific importance for recognition memory. A final experiment comparing rostral versus caudal perirhinal lesions would be needed to get a better understanding of the role of the different perirhinal cortex sub-regions.

One limitation of the use of IEG in this thesis is that I used only c-*fos* and *zif*268. Although they are the most widely studied IEGs, there exist many other IEGs: (1) other transcription factors like *jun*, *krox* 20 and (2) effectors, such as *arc*, *homer*. For example, Guzowski et al. (2001) compared three IEGs, *arc*, c-*fos*, *zif*268, after spatial learning in a water task. Overall it was found that the expression patterns for the three IEGs were quite similar, but that *arc* levels were most consistently correlated to behaviour.

The studies presented in my thesis all used immediate-early gene expression, as measured by c-*fos* or *zif*268, to extend our understanding of the neural processes of memory in rats. Throughout this thesis, the IEG methodology was used in combination with: (1) lesions to study the effects of distal damage on the extended hippocampal memory system (Chapters 2-4); (2) a new behavioural task, the bow-tie maze, to evaluate the activity of various brain areas occurring during object recognition (Chapter 5); and (3) structural equation modelling to reveal how brain structures within the same network interact together (Chapter 5). Consequently, this thesis reveals a number of ways in which immediate-early genes can provide a better understanding of memory networks.

From the three lesion/IEG studies presented in this thesis (Chapters 2-4), one specific brain region was highlighted. The retrosplenial cortex emerged as a unique node, in the network tested, as it was the region showing the most evident vulnerability to damage of several structures within the extended hippocampal memory system (see Table 1). As a result, the retrosplenial cortex showed a particular hypersensitivity to deafferentation from the medial diencephalon and the medial temporal lobe. The retrosplenial cortex, by its connections, may have a common role that helps to unify both the medial diencephalon and the medial temporal lobe. In conclusion, this thesis completes previous IEG studies by giving a better overall picture of the complexity of this extended hippocampal memory system. Damage to a region within this network markedly disrupts the extended hippocampal memory system, whether the damage is direct or indirect, e.g. hypoactivity in the retrosplenial cortex after hippocampal (direct) or mammillothalamic tract (indirect) lesions. My findings highlight four important structures within this network: the anterior thalamic nuclei, the mammillary bodies, the fornix and the hippocampus. Lesions of these four regions induce a widespread hypoactivity throughout the system. Even though they all decrease c-Fos levels in the retrosplenial cortex, their effects may vary in parahippocampal regions or in subicular cortex, e.g. only hippocampal lesions induce a reduction of c-*fos* activity in the perirhinal cortex (see Table 1 and Jenkins et al., 2006). Moreover, these lesions have different levels of effects upon other structures, e.g. retrosplenial activity is reduced by 15-20% after fornix lesions, but by 50% after hippocampal lesions. This difference may reflect the lack of fornix inputs to the retrosplenial cortex.

This thesis clearly gives further support for the notion of an extended hippocampal memory system, where damage to one of its structures may have radical effects on the rest of the system (Chapters 2-4). This notion of an interdependent system does not mean that the component structures all have the same functions (structural equation modelling, Chapter 5). This conclusion provides the next key challenge - to understand where and how these two putative models interact.

References

Abraham WC, Dragunow M, Tate WP (1991) The role of immediate early genes in the stabilization of long-term potentiation. Mol Neurobiol 5:297-314.

Abraham WC, Mason SE, Demmer J, Williams JM, Richardson CL, Tate WP, Lawlor PA, Dragunow M (1993) Correlations between immediate early gene induction and the persistence of long-term potentiation. Neuroscience 56:717-727.

Adelmann G, Deller T, Frotscher M (2004) Organizations of identified fiber tracts in the rat fimbria-fornix : an anterograde tracing and electron microscopic study. Anatomy and embriology 193: 481-493.

Aggleton JP (1985) One-trial object recognitions by rats. Q J Exp Psychol 37B:279-294.

Aggleton JP (2008) Understanding anterograde amnesia: disconnections and hidden lesions. Q J Exp Psychol (Colchester) 61:1441-1471.

Aggleton JP, Sahgal A (1993) The contribution of the anterior thalamic nuclei to anterograde amnesia. Neuropsychologia 31:1001-1019.

Aggleton JP, Saunders RC (1997) The relationships between temporal lobe and diencephalic structures implicated in anterograde amnesia. Memory 5:49-71.

Aggleton JP, Brown MW (1999) Episodic memory, amnesia, and the hippocampal-anterior thalamic axis. Behav Brain Sci 22:425-444; discussion 444-489.

Aggleton JP, Vann SD (2004) Testing the importance of the retrosplenial navigation system: lesion size but not strain matters: a reply to Harker and Whishaw. Neurosci Biobehav Rev 28:525-531.

Aggleton JP, Brown MW (2005) Contrasting hippocampal and perirhinal cortex function using immediate early gene imaging. Q J Exp Psychol B 58:218-233.

Aggleton JP, Brown MW (2006) Interleaving brain systems for episodic and recognition memory. Trends Cogn Sci 10:455-463.

Aggleton JP, Desimone R, Mishkin M (1986) The origin, course, and termination of the hippocampothalamic projections in the macaque. J Comp Neurol 243:409-421.

Aggleton JP, Neave N, Nagle S, Sahgal A (1995) A comparison of the effects of medial prefrontal, cingulate cortex, and cingulum bundle lesions on tests of spatial memory: evidence of a double dissociation between frontal and cingulum bundle contributions. J Neurosci 15:7270-7281.

Aggleton JP, Hunt PR, Nagle S, Neave N (1996) The effects of selective lesions within the anterior thalamic nuclei on spatial memory in the rat. Behav Brain Res 81:189-198.

Aggleton JP, Keen S, Warburton EC, Bussey TJ (1997) Extensive cytotoxic lesions involving both the rhinal cortices and area TE impair recognition but spare spatial alternation in the rat. Brain Res Bull 43:279-287.

Aggleton JP, Keith AB, Rawlins JN, Hunt PR, Sahgal A (1992) Removal of the hippocampus and transection of the fornix produce comparable deficits on delayed non-matching to position by rats. Behav Brain Res 52:61-71.

Aggleton JP, McMackin D, Carpenter K, Hornak J, Kapur N, Halpin S, Wiles CM, Kamel H, Brennan P, Carton S, Gaffan D (2000) Differential cognitive effects of colloid cysts in the third ventricle that spare or compromise the fornix. Brain 123 (Pt 4):800-815.

Albasser MM, Poirier GL, Warburton EC, Aggleton JP (2007) Hippocampal lesions halve immediate-early gene protein counts in retrosplenial cortex: distal dysfunctions in a spatial memory system. Eur J Neurosci 26:1254-1266.

Albasser MM, Davies M, Futter JE, Aggleton JP (2009) Magnitude of the object recognition deficit associated with perirhinal cortex damage in rats: Effects of varying the lesion extent and the duration of the sample period. Behav Neurosci 123:115-124.

Alexinsky T (2001) Differential effect of thalamic and cortical lesions on memory systems in the rat. Behav Brain Res 122:175-191.

Amaral DG, Cowan WM (1980) Subcortical afferents to the hippocampal formation in the monkey. J Comp Neurol 189:573-591.

Amaral DG, Witter MP (1995) The hippocampal formation. In: The Rat Nervous System, 2 Edition (Swanson LW, ed), pp 443-493. London: Academic Press.

Archer JS, Abbott DF, Waites AB, Jackson GD (2003) fMRI "deactivation" of the posterior cingulate during generalized spike and wave. Neuroimage 20:1915-1922.

Asahi T, Hirota K, Sasaki R, Mitsuaki Y, Roth SH (2006) Intravenous anesthetics are more effective than volatile anesthetics on inhibitory pathways in rat hippocampal CA1. Anesth Analg 102:772-778.

Asanuma M, Ogawa N (1994) Pitfalls in assessment of c-fos mRNA expression in the brain: effects of animal handling. Rev Neurosci 5:171-178.

Aupee AM, Desgranges B, Eustache F, Lalevee C, de la Sayette V, Viader F, Baron JC (2001) Voxel-based mapping of brain hypometabolism in permanent amnesia with PET. Neuroimage 13:1164-1173.

Bannerman DM, Yee BK, Good MA, Heupel MJ, Iversen SD, Rawlins JN (1999) Double dissociation of function within the hippocampus: a comparison of dorsal, ventral, and complete hippocampal cytotoxic lesions. Behav Neurosci 113:1170-1188.

Bannerman DM, Gilmour G, Norman G, Lemaire M, Iversen SD, Rawlins JN (2001) The time course of the hyperactivity that follows lesions or temporary inactivation of the fimbria-fornix. Behav Brain Res 120:1-11.

Bannerman DM, Deacon RM, Offen S, Friswell J, Grubb M, Rawlins JN (2002) Double dissociation of function within the hippocampus: spatial memory and hyponeophagia. Behav Neurosci 116:884-901.

Bannerman DM, Grubb M, Deacon RM, Yee BK, Feldon J, Rawlins JN (2003) Ventral hippocampal lesions affect anxiety but not spatial learning. Behav Brain Res 139:197-213.

Barbizet J (1963) Defect of memorizing of hippocampal-mammillary origin: a review. J Neurol Neurosurg Psychiatry 26:127-135.

Bast T (2007) Toward an integrative perspective on hippocampal function: from the rapid encoding of experience to adaptive behavior. Rev Neurosci 18:253-281.

Bast T, Wilson IA, Witter MP, Morris RG (2009) From rapid place learning to behavioral performance: a key role for the intermediate hippocampus. PLoS Biol 7:e1000089.

Baxter MG, Murray EA (2001) Opposite relationship of hippocampal and rhinal cortex damage to delayed nonmatching-to-sample deficits in monkeys. Hippocampus 11:61-71.

Baxter MG, Murphy KL, Crosby G, Culley DJ (2008) Different behavioral effects of neurotoxic dorsal hippocampal lesions placed under either isoflurane or propofol anesthesia. Hippocampus 18:245-250.

Bernabeu R, Thiriet N, Zwiller J, Di Scala G (2006) Lesion of the lateral entorhinal cortex amplifies odor-induced expression of c-fos, junB, and zif 268 mRNA in rat brain. Synapse 59:135-143.

Bisler S, Schleicher A, Gass P, Stehle JH, Zilles K, Staiger JF (2002) Expression of c-Fos, ICER, Krox-24 and JunB in the whisker-to-barrel pathway of rats: time course of induction upon whisker stimulation by tactile exploration of an enriched environment. J Chem Neuroanat 23:187-198.

Bliss TV, Lomo T (1973) Long-lasting potentiation of synaptic transmission in the dentate area of the anaesthetized rabbit following stimulation of the perforant path. J Physiol 232:331-356.

Bliss TV, Collingridge GL (1993) A synaptic model of memory: long-term potentiation in the hippocampus. Nature 361:31-39.

Braak H, Braak E (1991a) Alzheimer's disease affects limbic nuclei of the thalamus. Acta Neuropathol (Berl) 81:261-268.

Braak H, Braak E (1991b) Neuropathological stageing of Alzheimer-related changes. In: Acta Neuropathol (Berl), pp 239-259.

Brown MW, Aggleton JP (2001) Recognition memory: what are the roles of the perirhinal cortex and hippocampus? Nat Rev Neurosci 2:51-61.

Brown MW, Wilson FA, Riches IP (1987) Neuronal evidence that inferomedial temporal cortex is more important than hippocampus in certain processes underlying recognition memory. Brain Res 409:158-162.

Bullitt E (1990) Expression of c-fos-like protein as a marker for neuronal activity following noxious stimulation in the rat. J Comp Neurol 296:517-530.

Burwell RD (2001) Borders and cytoarchitecture of the perirhinal and postrhinal cortices in the rat. J Comp Neurol 437:17-41.

Byatt G, Dalrymple-Alford JC (1996) Both anteromedial and anteroventral thalamic lesions impair radial-maze learning in rats. Behav Neurosci 110:1335-1348.

Cahill L, McGaugh JL (1998) Mechanisms of emotional arousal and lasting declarative memory. Trends Neurosci 21:294-299.

Campeau S, Watson SJ (1997) Neuroendocrine and behavioral responses and brain pattern of c-fos induction associated with audiogenic stress. J Neuroendocrinol 9:577-588.

Carlesimo GA, Serra L, Fadda L, Cherubini A, Bozzali M, Caltagirone C (2007) Bilateral damage to the mammillo-thalamic tract impairs recollection but not familiarity in the recognition process: A single case investigation. Neuropsychologia.

Cassel JC, Cassel S, Galani R, Kelche C, Will B, Jarrard L (1998) Fimbria-fornix vs selective hippocampal lesions in rats: effects on locomotor activity and spatial learning and memory. Neurobiol Learn Mem 69:22-45.

Caulo M, Van Hecke J, Toma L, Ferretti A, Tartaro A, Colosimo C, Romani GL, Uncini A (2005) Functional MRI study of diencephalic amnesia in Wernicke-Korsakoff syndrome. Brain 128:1584-1594.

Charles DP, Gaffan D, Buckley MJ (2004) Impaired recency judgments and intact novelty judgments after fornix transection in monkeys. J Neurosci 24:2037-2044.

Chaudhuri A (1997) Neural activity mapping with inducible transcription factors. Neuroreport 8:iii-vii.

Clarke S, Assal G, Bogousslavsky J, Regli F, Townsend DW, Leenders KL, Blecic S (1994) Pure amnesia after unilateral left polar thalamic infarct: topographic and sequential neuropsychological and metabolic (PET) correlations. J Neurol Neurosurg Psychiatry 57:27-34.

Clayton DF (2000) The genomic action potential. Neurobiol Learn Mem 74:185-216.

Collingridge GL, Blake JF, Brown MW, Bashir ZI, Ryan E (1991) Involvement of excitatory amino acid receptors in long-term potentiation in the

Schaffer collateral-commissural pathway of rat hippocampal slices. Can J Physiol Pharmacol 69:1084-1090.

Cooper BG, Mizumori SJ (1999) Retrosplenial cortex inactivation selectively impairs navigation in darkness. Neuroreport 10:625-630.

Cooper BG, Manka TF, Mizumori SJ (2001) Finding your way in the dark: the retrosplenial cortex contributes to spatial memory and navigation without visual cues. Behav Neurosci 115:1012-1028.

Cotman CW, Monaghan DT, Ganong AH (1988) Excitatory amino acid neurotransmission: NMDA receptors and Hebb-type synaptic plasticity. Annu Rev Neurosci 11:61-80.

Coutureau E, Galani R, Gosselin O, Majchrzak M, Di Scala G (1999) Entorhinal but not hippocampal or subicular lesions disrupt latent inhibition in rats. Neurobiol Learn Mem 72:143-157.

Crosby C, Culley DJ, Baxter MG, Yukhananov R, Crosby G (2005) Spatial memory performance 2 weeks after general anesthesia in adult rats. Anesth Analg 101:1389-1392.

Cruce JA (1975) An autoradiographic study of the projections of the mammillothalamic tract in the rat. Brain Res 85:211-219.

Culley DJ, Baxter MG, Yukhananov R, Crosby G (2004a) Long-term impairment of acquisition of a spatial memory task following isoflurane-nitrous oxide anesthesia in rats. Anesthesiology 100:309-314.

Culley DJ, Baxter MG, Crosby CA, Yukhananov R, Crosby G (2004b) Impaired acquisition of spatial memory 2 weeks after isoflurane and isoflurane-nitrous oxide anesthesia in aged rats. Anesth Analg 99:1393-1397; table of contents.

Culley DJ, Yukhananov RY, Xie Z, Gali RR, Tanzi RE, Crosby G (2006) Altered hippocampal gene expression 2 days after general anesthesia in rats. Eur J Pharmacol 549:71-78.

Curran EJ, Akil H, Watson SJ (1996) Psychomotor stimulant- and opiate-induced c-fos mRNA expression patterns in the rat forebrain: comparisons between acute drug treatment and a drug challenge in sensitized animals. Neurochem Res 21:1425-1435.

D'Esposito M, Verfaellie M, Alexander MP, Katz DI (1995) Amnesia following traumatic bilateral fornix transection. Neurology 45:1546-1550.

Davis S, Bozon B, Laroche S (2003) How necessary is the activation of the immediate early gene zif268 in synaptic plasticity and learning? Behav Brain Res 142:17-30.

Delay J, Brion S (1969) Le Syndrome de Korsakoff. Paris: Mason.

Desgranges B, Baron JC, de la Sayette V, Petit-Taboue MC, Benali K, Landeau B, Lechevalier B, Eustache F (1998) The neural substrates of memory systems impairment in Alzheimer's disease. A PET study of resting brain glucose utilization. Brain 121 (Pt 4):611-631.

Dias N, Stein CA (2002) Antisense oligonucleotides: basic concepts and mechanisms. Mol Cancer Ther 1:347-355.

Dix SL, Aggleton JP (1999) Extending the spontaneous preference test of recognition: evidence of object-location and object-context recognition. Behav Brain Res 99:191-200.

Domesick VB (1970) The fasciculus cinguli in the rat. Brain Res 20:19-32.

Douglas RM, Dragunow M, Robertson HA (1988) High-frequency discharge of dentate granule cells, but not long-term potentiation, induces c-fos protein. Brain Res 464:259-262.

Dragunow M, Faull R (1989) The use of c-fos as a metabolic marker in neuronal pathway tracing. J Neurosci Methods 29:261-265.

Dragunow M, Peterson MR, Robertson HA (1987) Presence of c-fos-like immunoreactivity in the adult rat brain. Eur J Pharmacol 135:113-114.

Dragunow M, Abraham WC, Goulding M, Mason SE, Robertson HA, Faull RL (1989) Long-term potentiation and the induction of c-fos mRNA and proteins in the dentate gyrus of unanesthetized rats. Neurosci Lett 101:274-280.

Dragunow M, Goulding M, Faull RL, Ralph R, Mee E, Frith R (1990) Induction of c-fos mRNA and protein in neurons and glia after traumatic brain injury: pharmacological characterization. Exp Neurol 107:236-248.

Dudek SM, Bear MF (1992) Homosynaptic long-term depression in area CA1 of hippocampus and effects of N-methyl-D-aspartate receptor blockade. Proc Natl Acad Sci U S A 89:4363-4367.

Dusoir H, Kapur N, Byrnes DP, McKinstry S, Hoare RD (1990) The role of diencephalic pathology in human memory disorder. Evidence from a penetrating paranasal brain injury. Brain 113 (Pt 6):1695-1706.

Eichenbaum H, Stewart C, Morris RG (1990) Hippocampal representation in place learning. J Neurosci 10:3531-3542.

Eichenbaum H, Yonelinas AP, Ranganath C (2007) The medial temporal lobe and recognition memory. Annu Rev Neurosci 30:123-152.

Ennaceur A, Delacour J (1988) A new one-trial test for neurobiological studies of memory in rats. 1: Behavioral data. Behav Brain Res 31:47-59.

Epstein RA, Higgins JS (2007) Differential parahippocampal and retrosplenial involvement in three types of visual scene recognition. Cereb Cortex 17:1680-1693.

Fan X, Wang L, Thompson B (1997) The effects of Sample Size, Estimation Methods, and Model Specification on SEM Fit Indices. Paper presented at the annual meeting of American Educational Research Association. New York, NY.

Fazio F, Perani D, Gilardi MC, Colombo F, Cappa SF, Vallar G, Bettinardi V, Paulesu E, Alberoni M, Bressi S, et al. (1992) Metabolic impairment in human amnesia: a PET study of memory networks. J Cereb Blood Flow Metab 12:353-358.

Fernandez G, Tendolkar I (2006) The rhinal cortex: 'gatekeeper' of the declarative memory system. Trends Cogn Sci 10:358-362.

Fernandez G, Effern A, Grunwald T, Pezer N, Lehnertz K, Dumpelmann M, Van Roost D, Elger CE (1999) Real-time tracking of memory formation in the human rhinal cortex and hippocampus. Science 285:1582-1585.

Field TD, Rosenstock J, King EC, Greene E (1978) Behavioral role of the mammillary efferent system. Brain Res Bull 3:451-456.

Fleischmann A, Hvalby O, Jensen V, Strekalova T, Zacher C, Layer LE, Kvello A, Reschke M, Spanagel R, Sprengel R, Wagner EF, Gass P (2003) Impaired long-term memory and NR2A-type NMDA receptor-dependent synaptic plasticity in mice lacking c-Fos in the CNS. J Neurosci 23:9116-9122.

Fletcher PC, Frith CD, Grasby PM, Shallice T, Frackowiak RS, Dolan RJ (1995) Brain systems for encoding and retrieval of auditory-verbal memory. An in vivo study in humans. Brain 118 (Pt 2):401-416.

Fortin NJ, Wright SP, Eichenbaum H (2004) Recollection-like memory retrieval in rats is dependent on the hippocampus. Nature 431:188-191.

Frankland PW, Bontempi B, Talton LE, Kaczmarek L, Silva AJ (2004) The involvement of the anterior cingulate cortex in remote contextual fear memory. Science 304:881-883.

Fritschy JM (2008) Is my antibody-staining specific? How to deal with pitfalls of immunohistochemistry. Eur J Neurosci 28:2365-2370.

Furtak SC, Wei SM, Agster KL, Burwell RD (2007) Functional neuroanatomy of the parahippocampal region in the rat: the perirhinal and postrhinal cortices. Hippocampus 17:709-722.

Futterer CD, Maurer MH, Schmitt A, Feldmann RE, Jr., Kuschinsky W, Waschke KF (2004) Alterations in rat brain proteins after desflurane anesthesia. Anesthesiology 100:302-308.

Gabriel M, Lambert RW, Foster K, Orona E, Sparenborg S, Maiorca RR (1983) Anterior thalamic lesions and neuronal activity in the cingulate and retrosplenial cortices during discriminative avoidance behavior in rabbits. Behav Neurosci 97:675-696.

Gaffan D (1992) The role of the hippocampus-fornix-mammillary system in episodic memory. In: Neuropsychology of Memory, Second Edition (Squire LR, Butters N, eds), pp 336-346. New York: The Guildford Press.

Gaffan D (2001) What is a memory system? Horel's critique revisited. Behav Brain Res 127:5-11.

Gaffan D, Gaffan EA (1991) Amnesia in man following transection of the fornix. A review. Brain 114 (Pt 6):2611-2618.

Gaffan D, Hornak J (1997) Amnesia and neglect: beyond the Delay-Brion system and the Hebb synapse. Philos Trans R Soc Lond B Biol Sci 352:1481-1488.

Gaffan D, Parker A, Easton A (2001) Dense amnesia in the monkey after transection of fornix, amygdala and anterior temporal stem. Neuropsychologia 39:51-70.

Gage SL, Keim SR, Simon JR, Low WC (1994) Cholinergic innervation of the retrosplenial cortex via the fornix pathway as determined by high affinity choline uptake, choline acetyltransferase activity, and muscarinic receptor binding in the rat. Neurochem Res 19:1379-1386.

Gaiddon C, Loeffler JP, Larmet Y (1996) Brain-derived neurotrophic factor stimulates AP-1 and cyclic AMP-responsive element dependent transcriptional activity in central nervous system neurons. J Neurochem 66:2279-2286.

Galani R, Obis S, Coutureau E, Jarrard L, Cassel JC (2002) A comparison of the effects of fimbria-fornix, hippocampal, or entorhinal cortex lesions on spatial reference and working memory in rats: short versus long postsurgical recovery period. Neurobiol Learn Mem 77:1-16.

Garden DL, Massey PV, Caruana DA, Johnson B, Warburton EC, Aggleton JP, Bashir ZI (2009) Anterior thalamic lesions stop synaptic plasticity in retrosplenial cortex slices: expanding the pathology of diencephalic amnesia. Brain.

Ghosh A, Ginty DD, Bading H, Greenberg ME (1994) Calcium regulation of gene expression in neuronal cells. J Neurobiol 25:294-303.

Graff-Radford NR, Tranel D, Van Hoesen GW, Brandt JP (1990) Diencephalic amnesia. Brain 113 (Pt 1):1-25.

Griffiths S, Scott H, Glover C, Bienemann A, Ghorbel MT, Uney J, Brown MW, Warburton EC, Bashir ZI (2008) Expression of long-term depression underlies visual recognition memory. Neuron 58:186-194.

Grimm R, Schicknick H, Riede I, Gundelfinger ED, Herdegen T, Zuschratter W, Tischmeyer W (1997) Suppression of c-fos induction in rat brain impairs retention of a brightness discrimination reaction. Learn Mem 3:402-413.

Gudden H (1896) Klinische und anatomische Beitrage zur Kenntnis des multiplen Alkoholneuritis uber die Regerationsvorgange in peripheren Nervensystem. Archiv fur Psychiatrie und Nervenkrankheiten 28:643-741.

Guzowski JF (2002) Insights into immediate-early gene function in hippocampal memory consolidation using antisense oligonucleotide and fluorescent imaging approaches. Hippocampus 12:86-104.

Guzowski JF, Setlow B, Wagner EK, McGaugh JL (2001) Experience-dependent gene expression in the rat hippocampus after spatial learning: a comparison of the immediate-early genes Arc, c-fos, and zif268. J Neurosci 21:5089-5098.

Guzowski JF, Miyashita T, Chawla MK, Sanderson J, Maes LI, Houston FP, Lipa P, McNaughton BL, Worley PF, Barnes CA (2006) Recent behavioral history modifies coupling between cell activity and Arc gene transcription in hippocampal CA1 neurons. Proc Natl Acad Sci U S A 103:1077-1082.

Harada H, Kelly PJ, Cole DJ, Drummond JC, Patel PM (1999) Isoflurane reduces N-methyl-D-aspartate toxicity in vivo in the rat cerebral cortex. Anesth Analg 89:1442-1447.

Harding A, Halliday G, Caine D, Kril J (2000) Degeneration of anterior thalamic nuclei differentiates alcoholics with amnesia. Brain 123 (Pt 1):141-154.

Harker KT, Whishaw IQ (2002) Impaired spatial performance in rats with retrosplenial lesions: importance of the spatial problem and the rat strain in identifying lesion effects in a swimming pool. J Neurosci 22:1155-1164.

He J, Yamada K, Nabeshima T (2002) A role of Fos expression in the CA3 region of the hippocampus in spatial memory formation in rats. Neuropsychopharmacology 26:259-268.

Hemmings HC, Jr., Akabas MH, Goldstein PA, Trudell JR, Orser BA, Harrison NL (2005) Emerging molecular mechanisms of general anesthetic action. Trends Pharmacol Sci 26:503-510.

Henson RN, Rugg MD, Shallice T, Josephs O, Dolan RJ (1999) Recollection and familiarity in recognition memory: an event-related functional magnetic resonance imaging study. J Neurosci 19:3962-3972.

Herdegen T, Leah JD (1998) Inducible and constitutive transcription factors in the mammalian nervous system: control of gene expression by Jun, Fos and Krox, and CREB/ATF proteins. Brain Res Brain Res Rev 28:370-490.

Herdegen T, Kovary K, Buhl A, Bravo R, Zimmermann M, Gass P (1995) Basal expression of the inducible transcription factors c-Jun, JunB, JunD, c-Fos, FosB, and Krox-24 in the adult rat brain. J Comp Neurol 354:39-56.

Herrera DG, Robertson HA (1996) Activation of c-fos in the brain. Prog Neurobiol 50:83-107.

Hess US, Lynch G, Gall CM (1995a) Changes in c-fos mRNA expression in rat brain during odor discrimination learning: differential involvement of hippocampal subfields CA1 and CA3. J Neurosci 15:4786-4795.

Hess US, Lynch G, Gall CM (1995b) Regional patterns of c-fos mRNA expression in rat hippocampus following exploration of a novel environment versus performance of a well-learned discrimination. J Neurosci 15:7796-7809.

Hirao K, Ohnishi T, Matsuda H, Nemoto K, Hirata Y, Yamashita F, Asada T, Iwamoto T (2006) Functional interactions between entorhinal cortex and posterior cingulate cortex at the very early stage of Alzheimer's disease using brain perfusion single-photon emission computed tomography. Nucl Med Commun 27:151-156.

Hodges JR, Carpenter K (1991) Anterograde amnesia with fornix damage following removal of IIIrd ventricle colloid cyst. J Neurol Neurosurg Psychiatry 54:633-638.

Horel JA (1978) The neuroanatomy of amnesia. A critique of the hippocampal memory hypothesis. Brain 101:403-445.

Howell D (1987) Statitical Methods for Psychology. Belmont, California: Duxberry Press.

Howell DC (1982) Statistical Methods for Psychology. Belmont, California: Duxberry Press.

Howell DC (2002) In: Statistical methods for psychology Pacific Grove. CA: Duxbury.

Hu L, Bentler P (1998) Fit indices in covariance structure modeling: sensitivity to underparameterized model misspecification. Psychol Methods 3:424–453.

Hughes P, Dragunow M (1995) Induction of immediate-early genes and the control of neurotransmitter-regulated gene expression within the nervous system. Pharmacol Rev 47:133-178.

Hughes P, Lawlor P, Dragunow M (1992) Basal expression of Fos, Fos-related, Jun, and Krox 24 proteins in rat hippocampus. Brain Res Mol Brain Res 13:355-357.

Hughes PE, Alexi T, Walton M, Williams CE, Dragunow M, Clark RG, Gluckman PD (1999) Activity and injury-dependent expression of

inducible transcription factors, growth factors and apoptosis-related genes within the central nervous system. Prog Neurobiol 57:421-450.

Hunt SP, Pini A, Evan G (1987) Induction of c-fos-like protein in spinal cord neurons following sensory stimulation. Nature 328:632-634.

Iaria G, Chen JK, Guariglia C, Ptito A, Petrides M (2007) Retrosplenial and hippocampal brain regions in human navigation: complementary functional contributions to the formation and use of cognitive maps. Eur J Neurosci 25:890-899.

Insausti R, Herrero MT, Witter MP (1997) Entorhinal cortex of the rat: cytoarchitectonic subdivisions and the origin and distribution of cortical efferents. Hippocampus 7:146-183.

Jarrard LE (1989) On the use of ibotenic acid to lesion selectively different components of the hippocampal formation. J Neurosci Methods 29:251-259.

Jay TM, Glowinski J, Thierry AM (1989) Selectivity of the hippocampal projection to the prelimbic area of the prefrontal cortex in the rat. Brain Res 505:337-340.

Jeffery KJ, Abraham WC, Dragunow M, Mason SE (1990) Induction of Fos-like immunoreactivity and the maintenance of long-term potentiation in the dentate gyrus of unanesthetized rats. Brain Res Mol Brain Res 8:267-274.

Jenkins TA, Dias R, Amin E, Aggleton JP (2002a) Changes in Fos expression in the rat brain after unilateral lesions of the anterior thalamic nuclei. Eur J Neurosci 16:1425-1432.

Jenkins TA, Vann SD, Amin E, Aggleton JP (2004a) Anterior thalamic lesions stop immediate early gene activation in selective laminae of the retrosplenial cortex: evidence of covert pathology in rats? Eur J Neurosci 19:3291-3304.

Jenkins TA, Amin E, Brown MW, Aggleton JP (2006) Changes in immediate early gene expression in the rat brain after unilateral lesions of the hippocampus. Neuroscience 137:747-759.

Jenkins TA, Dias R, Amin E, Brown MW, Aggleton JP (2002b) Fos imaging reveals that lesions of the anterior thalamic nuclei produce widespread limbic hypoactivity in rats. J Neurosci 22:5230-5238.

Jenkins TA, Amin E, Harold GT, Pearce JM, Aggleton JP (2003) Distinct patterns of hippocampal formation activity associated with different spatial tasks: a Fos imaging study in rats. Exp Brain Res 151:514-523.

Jenkins TA, Amin E, Pearce JM, Brown MW, Aggleton JP (2004b) Novel spatial arrangements of familiar visual stimuli promote activity in the rat hippocampal formation but not the parahippocampal cortices: a c-fos expression study. Neuroscience 124:43-52.

Johnson T, Monk T, Rasmussen LS, Abildstrom H, Houx P, Korttila K, Kuipers HM, Hanning CD, Siersma VD, Kristensen D, Canet J, Ibanaz MT, Moller JT (2002) Postoperative cognitive dysfunction in middle-aged patients. Anesthesiology 96:1351-1357.

Jones MW, Errington ML, French PJ, Fine A, Bliss TV, Garel S, Charnay P, Bozon B, Laroche S, Davis S (2001) A requirement for the immediate early gene Zif268 in the expression of late LTP and long-term memories. Nat Neurosci 4:289-296.

Jongen-Relo AL, Feldon J (2002) Specific neuronal protein: a new tool for histological evaluation of excitotoxic lesions. Physiol Behav 76:449-456.

Joyce EM, Rio DE, Ruttimann UE, Rohrbaugh JW, Martin PR, Rawlings RR, Eckardt MJ (1994) Decreased cingulate and precuneate glucose utilization in alcoholic Korsakoff's syndrome. Psychiatry Res 54:225-239.

Jung MW, Wiener SI, McNaughton BL (1994) Comparison of spatial firing characteristics of units in dorsal and ventral hippocampus of the rat. J Neurosci 14:7347-7356.

Kapur N, Scholey K, Moore E, Barker S, Brice J, Mayes A, Fleming J (1994) The mammillary bodies revisited: their role in human memory functioning. In: Neuropsychological Explorations of Memory and Cognition: Essays in Honor of Nelson Butters (Cermak LS, ed), pp 159-190. New York: Plenum Press.

Kasahara J, Fukunaga K, Miyamoto E (2001) Activation of calcium/calmodulin-dependent protein kinase IV in long term potentiation in the rat hippocampal CA1 region. J Biol Chem 276:24044-24050.

Keene CS, Bucci DJ (2008a) Involvement of the retrosplenial cortex in processing multiple conditioned stimuli. Behav Neurosci 122:651-658.

Keene CS, Bucci DJ (2008b) Neurotoxic lesions of retrosplenial cortex disrupt signaled and unsignaled contextual fear conditioning. Behav Neurosci 122:1070-1077.

Kimpo RR, Doupe AJ (1997) FOS is induced by singing in distinct neuronal populations in a motor network. Neuron 18:315-325.

Kobayashi Y, Amaral DG (2003) Macaque monkey retrosplenial cortex: II. Cortical afferents. J Comp Neurol 466:48-79.

Kondo Y, Suzuki M, Mugikura S, Abe N, Takahashi S, Iijima T, Fujii T (2005) Changes in brain activation associated with use of a memory strategy: a functional MRI study. Neuroimage 24:1154-1163.

Korsakoff SS (1887) Disturbance of psychic function in alcoholic paralysis and its relation to the disturbance of the psychic sphere in multiple neuritis of non-alcoholic origin. Vestn Pshychiatrii 4, 2.

Kovacs KJ (1998) c-Fos as a transcription factor: a stressful (re)view from a functional map. Neurochem Int 33:287-297.

Kovacs KJ (2008) Measurement of immediate-early gene activation- c-fos and beyond. J Neuroendocrinol 20:665-672.

Kyd RJ, Pearce JM, Haselgrove M, Amin E, Aggleton JP (2008) The effects of hippocampal system lesions on a novel temporal discrimination task for rats. Behav Brain Res 187:159-171.

LaBar KS, Cabeza R (2006) Cognitive neuroscience of emotional memory. Nat Rev Neurosci 7:54-64.

Lanahan A, Worley P (1998) Immediate-early genes and synaptic function. Neurobiol Learn Mem 70:37-43.

Larsen M, Hegstad E, Berg-Johnsen J, Langmoen IA (1997) Isoflurane increases the uptake of glutamate in synaptosomes from rat cerebral cortex. Br J Anaesth 78:55-59.

Liang WS, Reiman EM, Valla J, Dunckley T, Beach TG, Grover A, Niedzielko TL, Schneider LE, Mastroeni D, Caselli R, Kukull W, Morris JC, Hulette CM, Schmechel D, Rogers J, Stephan DA (2008) Alzheimer's disease is associated with reduced expression of energy metabolism genes in posterior cingulate neurons. Proc Natl Acad Sci U S A 105:4441-4446.

Loftus M, Knight RT, Amaral DG (2000) An analysis of atrophy in the medial mammillary nucleus following hippocampal and fornix lesions in humans and nonhuman primates. Exp Neurol 163:180-190.

Lukoyanov NV, Lukoyanova EA, Andrade JP, Paula-Barbosa MM (2005) Impaired water maze navigation of Wistar rats with retrosplenial cortex lesions: effect of nonspatial pretraining. Behav Brain Res 158:175-182.

Mac Lean P (1949) Psychosomatic disease and the visceral brain; recent developments bearing on the Papez theory of emotion. Psychosom Med 11:338-353.

MacGibbon GA, Lawlor PA, Walton M, Sirimanne E, Faull RL, Synek B, Mee E, Connor B, Dragunow M (1997) Expression of Fos, Jun, and Krox family proteins in Alzheimer's disease. Exp Neurol 147:316-332.

Mackiewicz KL, Sarinopoulos I, Cleven KL, Nitschke JB (2006) The effect of anticipation and the specificity of sex differences for amygdala and hippocampus function in emotional memory. Proc Natl Acad Sci U S A 103:14200-14205.

Maguire EA (2001a) The retrosplenial contribution to human navigation: a review of lesion and neuroimaging findings. Scand J Psychol 42:225-238.

Maguire EA (2001b) Neuroimaging studies of autobiographical event memory. Philos Trans R Soc Lond B Biol Sci 356:1441-1451.

Mair WG, Warrington EK, Weiskrantz L (1979) Memory disorder in Korsakoff's psychosis: a neuropathological and neuropsychological investigation of two cases. Brain 102:749-783.

Malenka RC, Bear MF (2004) LTP and LTD: an embarrassment of riches. Neuron 44:5-21.

Manahan-Vaughan D, Kulla A, Frey JU (2000) Requirement of translation but not transcription for the maintenance of long-term depression in the CA1 region of freely moving rats. J Neurosci 20:8572-8576.

Markowska AL, Olton DS, Murray EA, Gaffan D (1989) A comparative analysis of the role of fornix and cingulate cortex in memory: rats. Exp Brain Res 74:187-201.

Martinez-Bisbal MC, Arana E, Marti-Bonmati L, Molla E, Celda B (2004) Cognitive impairment: classification by 1H magnetic resonance spectroscopy. Eur J Neurol 11:187-193.

McMackin D, Cockburn J, Anslow P, Gaffan D (1995) Correlation of fornix damage with memory impairment in six cases of colloid cyst removal. Acta Neurochir (Wien) 135:12-18.

Meguro K, Blaizot X, Kondoh Y, Le Mestric C, Baron JC, Chavoix C (1999) Neocortical and hippocampal glucose hypometabolism following neurotoxic lesions of the entorhinal and perirhinal cortices in the non-human primate as shown by PET. Implications for Alzheimer's disease. Brain 122:1519-1531.

Meunier M, Bachevalier J, Mishkin M, Murray EA (1993) Effects on visual recognition of combined and separate ablations of the entorhinal and perirhinal cortex in rhesus monkeys. J Neurosci 13:5418-5432.

Miao N, Frazer MJ, Lynch C, 3rd (1995) Volatile anesthetics depress Ca2+ transients and glutamate release in isolated cerebral synaptosomes. Anesthesiology 83:593-603.

Milbrandt J (1986) Nerve growth factor rapidly induces c-fos mRNA in PC12 rat pheochromocytoma cells. Proc Natl Acad Sci U S A 83:4789-4793.

Minoshima S, Giordani B, Berent S, Frey KA, Foster NL, Kuhl DE (1997) Metabolic reduction in the posterior cingulate cortex in very early Alzheimer's disease. Ann Neurol 42:85-94.

Mishkin M, Delacour J (1975) An analysis of short-term visual memory in the monkey. J Exp Psychol Anim Behav Process 1:326-334.

Mizumori SJ, Cooper BG, Leutgeb S, Pratt WE (2000) A neural systems analysis of adaptive navigation. Mol Neurobiol 21:57-82.

Moller JT, Cluitmans P, Rasmussen LS, Houx P, Rasmussen H, Canet J, Rabbitt P, Jolles J, Larsen K, Hanning CD, Langeron O, Johnson T, Lauven PM, Kristensen PA, Biedler A, van Beem H, Fraidakis O, Silverstein JH, Beneken JE, Gravenstein JS (1998) Long-term postoperative cognitive dysfunction in the elderly ISPOCD1 study. ISPOCD investigators. International Study of Post-Operative Cognitive Dysfunction. Lancet 351:857-861.

Morgan JI, Curran T (1986) Role of ion flux in the control of c-fos expression. Nature 322:552-555.

Morgan JI, Curran T (1991) Stimulus-Transcription Coupling in the Nervous System: Involvement of the Inducible Proto-Oncogenes fos and jun. Annual Review of Neuroscience 14:421-451.

Morgan JI, Cohen DR, Hempstead JL, Curran T (1987) Mapping patterns of c-fos expression in the central nervous system after seizure. Science 237:192-197.

Morris RG, Schenk F, Tweedie F, Jarrard LE (1990) Ibotenate Lesions of Hippocampus and/or Subiculum: Dissociating Components of Allocentric Spatial Learning. Eur J Neurosci 2:1016-1028.

Morrow BA, Elsworth JD, Inglis FM, Roth RH (1999) An antisense oligonucleotide reverses the footshock-induced expression of fos in the rat medial prefrontal cortex and the subsequent expression of conditioned fear-induced immobility. J Neurosci 19:5666-5673.

Moser E, Moser MB, Andersen P (1993) Spatial learning impairment parallels the magnitude of dorsal hippocampal lesions, but is hardly present following ventral lesions. J Neurosci 13:3916-3925.

Mufson EJ, Pandya DN (1984) Some observations on the course and composition of the cingulum bundle in the rhesus monkey. J Comp Neurol 225:31-43.

Mumby DG, Pinel JP (1994) Rhinal cortex lesions and object recognition in rats. Behav Neurosci 108:11-18.

Mumby DG, Pinel JPJ, Wood ER (1990) Nonreccuring-items delayed nonmatching-to-sample in rats: A new paradigm for testing nonspatial working memory. Psychobiology 18:321-326.

Mundy ME, Dwyer DM, Honey RC (2005) The role of the entorhinal cortex in perceptual learning. Acta Neurobiol Exp (Suppl) 65:69.

Murray EA, Mishkin M (1986) Visual recognition in monkeys following rhinal cortical ablations combined with either amygdalectomy or hippocampectomy. J Neurosci 6:1991-2003.

Neave N, Nagle S, Aggleton JP (1997) Evidence for the involvement of the mammillary bodies and cingulum bundle in allocentric spatial processing by rats. Eur J Neurosci 9:941-955.

Neave N, Nagle S, Sahgal A, Aggleton JP (1996) The effects of discrete cingulum bundle lesions in the rat on the acquisition and performance of two tests of spatial working memory. Behav Brain Res 80:75-85.

Nestor PJ, Fryer TD, Hodges JR (2006) Declarative memory impairments in Alzheimer's disease and semantic dementia. Neuroimage 30:1010-1020.

Nestor PJ, Fryer TD, Smielewski P, Hodges JR (2003a) Limbic hypometabolism in Alzheimer's disease and mild cognitive impairment. Ann Neurol 54:343-351.

Nestor PJ, Fryer TD, Ikeda M, Hodges JR (2003b) Retrosplenial cortex (BA 29/30) hypometabolism in mild cognitive impairment (prodromal Alzheimer's disease). Eur J Neurosci 18:2663-2667.

Nikolaev E, Werka T, Kaczmarek L (1992) C-fos protooncogene expression in rat brain after long-term training of two-way active avoidance reaction. Behav Brain Res 48:91-94.

Nikolaev E, Tischmeyer W, Krug M, Matthies H, Kaczmarek L (1991) c-fos protooncogene expression in rat hippocampus and entorhinal cortex following tetanic stimulation of the perforant path. Brain Res 560:346-349.

Novak CM, Smale L, Nunez AA (2000) Rhythms in Fos expression in brain areas related to the sleep-wake cycle in the diurnal Arvicanthis niloticus. Am J Physiol Regul Integr Comp Physiol 278:R1267-1274.

Olney JW, Sesma MA, Wozniak DF (1993) Glutamatergic, cholinergic, and GABAergic systems in posterior cingulate cortex: Interactions and possible mechanisms of limbic system disease. In Vogt B.A & Gabriel, M. (Eds). Neurobiology of Cingulate Cortex and Limbic Thalamus:Birkhäuser, Boston, pp. 558-580.

Olney JW, Wozniak DF, Farber NB (1998) Glumate receptor dysfunction and Alzheimer's disease. Restor Neurol Neurosci 13:75-83.

Olton DS, Walker JA, Gage FH (1978) Hippocampal connections and spatial discrimination. Brain Res 139:295-308.

Olton DS, Becker JT, Handelman GE (1979) Hippocampus, space, and memory. The Behavioral and Brain Sciences 2:313-365.

Olton DS, Walker JA, Wolf WA (1982) A disconnection analysis of hippocampal function. Brain Res 233:241-253.

Otani S, Marshall CJ, Tate WP, Goddard GV, Abraham WC (1989) Maintenance of long-term potentiation in rat dentate gyrus requires protein synthesis but not messenger RNA synthesis immediately post-tetanization. Neuroscience 28:519-526.

Paller KA (1997) Consolidating dispersed neocortical memories: the missing link in amnesia. Memory 5:73-88.

Papez JW (1937) A proposed mechanism of emotion. Arc Neurol Psychiatry 38:725-743.

Parkin AJ (1984) Amnesic syndrome: a lesion-specific disorder? Cortex 20:479-508.

Parkin AJ (1997) Memory and amnesia (2nd ed.). Oxford, UK: Blackwell.

Parron C, Save E (2004) Comparison of the effects of entorhinal and retrosplenial cortical lesions on habituation, reaction to spatial and non-spatial changes during object exploration in the rat. Neurobiol Learn Mem 82:1-11.

Paxinos G, Watson C (1997) *The Rat Brain in Stereotaxic Coordinates*. San Diego: Academic Press.

Paxinos G, Watson C (2005) The rat brain in stereotaxic coordinates, fifth edition. San Diego: Academic.

Pengas G, Hodges JR, Watson P, Nestor PJ (2008) Focal posterior cingulate atrophy in incipient Alzheimer's disease. Neurobiol Aging.

Poirier GL, Aggleton JP (2009) Post-surgical interval and lesion location within the limbic thalamus determine extent of retrosplenial cortex immediate-early gene hypoactivity. Neuroscience 160 (2): 452-469

Poirier GL, Amin E, Aggleton JP (2008) Qualitatively different hippocampal subfield engagement emerges with mastery of a spatial memory task by rats. J Neurosci 28:1034-1045.

Porte Y, Buhot MC, Mons NE (2008) Spatial memory in the Morris water maze and activation of cyclic AMP response element-binding (CREB) protein within the mouse hippocampus. Learn Mem 15:885-894.

Pothuizen HH, Aggleton JP, Vann SD (2008) Do rats with retrosplenial cortex lesions lack direction? Eur J Neurosci. 28(12): 2486-2498.

Pothuizen HH, Davies M, Albasser MM, Aggleton JP, Vann SD (2009) Granular and dysgranular retrosplenial cortices provide qualitatively different contributions to spatial working memory: evidence from immediate-early gene imaging in rats. Eur J Neurosci, *under review.*

Poucet B (1989) Object exploration, habituation, and response to a spatial change in rats following septal or medial frontal cortical damage. Behav Neurosci 103:1009-1016.

Preuss TM (1995) Do rats have prefrontal cortex? The Rose-Woolsey-Akert program reconsidered. J Cogn Neurosci 7:1-24.

Ratnakumari L, Hemmings HC, Jr. (1998) Inhibition of presynaptic sodium channels by halothane. Anesthesiology 88:1043-1054.

Reed LJ, Lasserson D, Marsden P, Stanhope N, Stevens T, Bello F, Kingsley D, Colchester A, Kopelman MD (2003) FDG-PET findings in the Wernicke-Korsakoff syndrome. Cortex 39:1027-1045.

Renou P, Ducreux D, Batouche F, Denier C (2008) Pure and acute Korsakoff syndrome due to a bilateral anterior fornix infarction: a diffusion tensor tractography study. Arch Neurol 65:1252-1253.

Sagar SM, Sharp FR, Curran T (1988) Expression of c-fos protein in brain: metabolic mapping at the cellular level. Science 240:1328-1331.

Sanderson DJ, Pearce JM, Kyd RJ, Aggleton JP (2006) The importance of the rat hippocampus for learning the structure of visual arrays. Eur J Neurosci 24:1781-1788.

Saunders RC, Aggleton JP (2007) Origin and topography of fibers contributing to the fornix in macaque monkeys. Hippocampus 17:396-411.

Scahill RI, Schott JM, Stevens JM, Rossor MN, Fox NC (2002) Mapping the evolution of regional atrophy in Alzheimer's disease: unbiased analysis of fluid-registered serial MRI. Proc Natl Acad Sci U S A 99:4703-4707.

Schlame M, Hemmings HC, Jr. (1995) Inhibition by volatile anesthetics of endogenous glutamate release from synaptosomes by a presynaptic mechanism. Anesthesiology 82:1406-1416.

Schmitt WB, Deacon RM, Seeburg PH, Rawlins JN, Bannerman DM (2003) A within-subjects, within-task demonstration of intact spatial reference memory and impaired spatial working memory in glutamate receptor-A-deficient mice. J Neurosci 23:3953-3959.

Schwartz WJ, Smith CB, Davidsen L, Savaki H, Sokoloff L, Mata M, Fink DJ, Gainer H (1979) Metabolic mapping of functional activity in the hypothalamo-neurohypophysial system of the rat. Science 205:723-725.

Scoville WB, Milner B (1957) Loss of recent memory after bilateral hippocampal lesions. J Neurol Neurosurg Psychiatry 20:11-21.

Seoane A, Brown MW (2007) Interfering with Fos expression impairs recognition memory in rats. British Neurosci Assocn Abstracts vol. 19:39.05.

Sharp FR, Sagar SM, Swanson RA (1993) Metabolic mapping with cellular resolution: c-fos vs. 2-deoxyglucose. Crit Rev Neurobiol 7:205-228.

Sheng M, Greenberg ME (1990) The regulation and function of c-fos and other immediate early genes in the nervous system. Neuron 4:477-485.

Shi CJ, Cassell MD (1999) Perirhinal cortex projections to the amygdaloid complex and hippocampal formation in the rat. J Comp Neurol 406:299-328.

Shibata H (1993) Direct projections from the anterior thalamic nuclei to the retrohippocampal region in the rat. J Comp Neurol 337:431-445.

Shibata H (1998) Organization of projections of rat retrosplenial cortex to the anterior thalamic nuclei. Eur J Neurosci 10:3210-3219.

Shibata H, Kondo S, Naito J (2004) Organization of retrosplenial cortical projections to the anterior cingulate, motor, and prefrontal cortices in the rat. Neurosci Res 49:1-11.

Shibata H, Honda Y, Sasaki H, Naito J (2009) Organization of intrinsic connections of the retrosplenial cortex in the rat. Anat Sci Int.

Shires KL, Aggleton JP (2008) Mapping immediate-early gene activity in the rat after place learning in a water-maze: the importance of matched control conditions. Eur J Neurosci 28:982-996.

Sokoloff L (1981) The deoxyglucose method for the measurement of local glucose utilization and the mapping of local functional activity in the central nervous system. Int Rev Neurobiol 22:287-333.

Sokoloff L, Reivich M, Kennedy C, Des Rosiers MH, Patlak CS, Pettigrew KD, Sakurada O, Shinohara M (1977) The [14C]deoxyglucose method for the measurement of local cerebral glucose utilization: theory,

procedure, and normal values in the conscious and anesthetized albino rat. J Neurochem 28:897-916.

Soonthon-Brant V, Patel PM, Drummond JC, Cole DJ, Kelly PJ, Watson M (1999) Fentanyl does not increase brain injury after focal cerebral ischemia in rats. Anesth Analg 88:49-55.

Spiers HJ, Maguire EA, Burgess N (2001) Hippocampal amnesia. Neurocase 7:357-382.

Squire LR, Zola-Morgan S (1991) The medial temporal lobe memory system. Science 253:1380-1386.

Squire LR, Wixted JT, Clark RE (2007) Recognition memory and the medial temporal lobe: a new perspective. Nat Rev Neurosci 8:872-883.

Sutherland RJ, Hoesing JM (1993) Posterior Cingulate Cortex and Spatial Memory: A microlimnology Analysis. In Vogt B.A & Gabriel, M. (Eds). Neurobiology of Cingulate Cortex and Limbic Thalamus:Birkhäuser, Boston, pp. 467-477.

Sutherland RJ, Whishaw IQ, Kolb B (1988) Contributions of cingulate cortex to two forms of spatial learning and memory. J Neurosci 8:1863-1872.

Swanson LW (1992) Brain maps: structure of the rat brain. Amsterdam: Elsevier.

Tabachnik BG, Fidell LS (1996) Using multivariate statistics, Ed 3. New York: HarperCollins.

Tischmeyer W, Grimm R (1999) Activation of immediate early genes and memory formation. Cellular and Molecular Life Sciences (CMLS) 55:564-574.

Tischmeyer W, Kaczmarek L, Strauss M, Jork R, Matthies H (1990) Accumulation of c-fos mRNA in rat hippocampus during acquisition of a brightness discrimination. Behav Neural Biol 54:165-171.

Todd MM, Weeks J (1996) Comparative effects of propofol, pentobarbital, and isoflurane on cerebral blood flow and blood volume. J Neurosurg Anesthesiol 8:296-303.

Tsivilis D, Vann SD, Denby C, Roberts N, Mayes AR, Montaldi D, Aggleton JP (2008) A disproportionate role for the fornix and mammillary bodies in recall versus recognition memory. Nat Neurosci 11:834-842.

Tulving E (1972) Episodic and semantic memory. In *Organization of Memory*, ed. E Tulving, W Donaldson, pp. 381-403. New York: Academic.

Tulving E, Markowitsch HJ (1997) Memory beyond the hippocampus. Curr Opin Neurobiol 7:209-216.

Tulving E, Markowitsch HJ, Kapur S, Habib R, Houle S (1994) Novelty encoding networks in the human brain: positron emission tomography data. Neuroreport 5:2525-2528.

Tung A, Herrera S, Fornal CA, Jacobs BL (2008) The effect of prolonged anesthesia with isoflurane, propofol, dexmedetomidine, or ketamine on neural cell proliferation in the adult rat. Anesth Analg 106:1772-1777.

Valenstein E, Bowers D, Verfaellie M, Heilman KM, Day A, Watson RT (1987) Retrosplenial amnesia. Brain 110 (Pt 6):1631-1646.

Van der Werf YD, Jolles J, Witter MP, Uylings HB (2003) Contributions of thalamic nuclei to declarative memory functioning. Cortex 39:1047-1062.

Van Elzakker M, Fevurly RD, Breindel T, Spencer RL (2008) Environmental novelty is associated with a selective increase in Fos expression in the output elements of the hippocampal formation and the perirhinal cortex. Learn Mem 15:899-908.

Van Groen T, Wyss JM (1990a) The postsubicular cortex in the rat: characterization of the fourth region of the subicular cortex and its connections. Brain Res 529:165-177.

Van Groen T, Wyss JM (1990b) Extrinsic projections from area CA1 of the rat hippocampus: olfactory, cortical, subcortical, and bilateral hippocampal formation projections. J Comp Neurol 302:515-528.

Van Groen T, Wyss JM (1990c) Connections of the retrosplenial granular a cortex in the rat. J Comp Neurol 300:593-606.

Van Groen T, Wyss JM (1992) Connections of the retrosplenial dysgranular cortex in the rat. J Comp Neurol 315:200-216.

Van Groen T, Wyss JM (2003) Connections of the retrosplenial granular b cortex in the rat. J Comp Neurol 463:249-263.

Van Groen T, Kadish I, Wyss JM (2004) Retrosplenial cortex lesions of area Rgb (but not of area Rga) impair spatial learning and memory in the rat. Behav Brain Res 154:483-491.

Van Groen TV, Vogt BA, Wyss JM (1993) Interconnections Between the Thalamus and Retrosplenial Cortex in the Rodent Brain. In Vogt B.A & Gabriel, M. (Eds). Neurobiology of Cingulate Cortex and Limbic Thalamus:Birkhäuser, Boston, pp. 123-150.

Van Strien NM, Cappaert NL, Witter MP (2009) The anatomy of memory: an interactive overview of the parahippocampal-hippocampal network. Nat Rev Neurosci 10:272-282.

Vann SD, Aggleton JP (2002) Extensive cytotoxic lesions of the rat retrosplenial cortex reveal consistent deficits on tasks that tax allocentric spatial memory. Behav Neurosci 116:85-94.

Vann SD, Aggleton JP (2003) Evidence of a spatial encoding deficit in rats with lesions of the mammillary bodies or mammillothalamic tract. J Neurosci 23:3506-3514.

Vann SD, Aggleton JP (2004a) Testing the importance of the retrosplenial guidance system: effects of different sized retrosplenial cortex lesions on heading direction and spatial working memory. Behav Brain Res 155:97-108.

Vann SD, Aggleton JP (2004b) The mammillary bodies: two memory systems in one? Nat Rev Neurosci 5:35-44.

Vann SD, Aggleton JP (2005) Selective dysgranular retrosplenial cortex lesions in rats disrupt allocentric performance of the radial-arm maze task. Behav Neurosci 119:1682-1686.

Vann SD, Albasser MM (2009) Hippocampal, retrosplenial, and prefrontal hypoactivity in a model of diencephalic amnesia: Evidence towards an interdependent subcortical-cortical memory network. Hippocampus. 19(11): 1090-1102.

Vann SD, Brown MW, Aggleton JP (2000a) Fos expression in the rostral thalamic nuclei and associated cortical regions in response to different spatial memory tests. Neuroscience 101:983-991.

Vann SD, Honey RC, Aggleton JP (2003a) Lesions of the mammillothalamic tract impair the acquisition of spatial but not nonspatial contextual conditional discriminations. Eur J Neurosci 18:2413-2416.

Vann SD, Saunders RC, Aggleton JP (2007) Distinct, parallel pathways link the medial mammillary bodies to the anterior thalamus in macaque monkeys. Eur J Neurosci 26:1575-1586.

Vann SD, Brown MW, Erichsen JT, Aggleton JP (2000b) Using Fos Imaging in the Rat to Reveal the Anatomical Extent of the Disruptive Effects of Fornix Lesions. J Neurosci 20:8144-8152.

Vann SD, Brown MW, Erichsen JT, Aggleton JP (2000c) Fos imaging reveals differential patterns of hippocampal and parahippocampal subfield activation in rats in response to different spatial memory tests. J Neurosci 20:2711-2718.

Vann SD, Kristina Wilton LA, Muir JL, Aggleton JP (2003b) Testing the importance of the caudal retrosplenial cortex for spatial memory in rats. Behav Brain Res 140:107-118.

Vann SD, Denby C, Love S, Montaldi D, Renowden S, Coakham HB (2008) Memory loss resulting from fornix and septal damage: impaired supra-span recall but preserved recognition over a 24-hour delay. Neuropsychology 22:658-668.

Vann SD, Tsivilis D, Denby CE, Quamme JR, Yonelinas AP, Aggleton JP, Montaldi D, Mayes AR (2009) Impaired recollection but spared familiarity in patients with extended hippocampal system damage revealed by 3 convergent methods. Proc Natl Acad Sci U S A 106:5442-5447.

Victor M (1987) The irrelevance of mammillary body lesions in the causation of the Korsakoff amnesic state. Int J Neurol 21-22:51-57.

Victor M, Adams RD, Collins GH (1971) The Wernicke-Korsakoff syndrome. A clinical and pathological study of 245 patients, 82 with post-mortem examinations. Contemp Neurol Ser 7:1-206.

Vogt BA (1993) Structural organization of cingulate cortex: Areas, neurons, and somatodendritic transmitter receptors. In: Neurobiology of Cingulate Cortex and Limbic Thalamus: A Comprehensive Handbook (VogtBAG, M., ed), pp 19-70. Boston: Birkhauser.

Vogt BA, Peters A (1981) Form and distribution of neurons in rat cingulate cortex: areas 32, 24, and 29. J Comp Neurol 195:603-625.

Von Cramon DY, Hebel N, Schuri U (1985) A contribution to the anatomical basis of thalamic amnesia. Brain 108 (Pt 4):993-1008.

Wakasugi M, Hirota K, Roth SH, Ito Y (1999) The effects of general anesthetics on excitatory and inhibitory synaptic transmission in area CA1 of the rat hippocampus in vitro. Anesth Analg 88:676-680.

Wan H, Aggleton JP, Brown MW (1999) Different contributions of the hippocampus and perirhinal cortex to recognition memory. J Neurosci 19:1142-1148.

Wan H, Warburton EC, Zhu XO, Koder TJ, Park Y, Aggleton JP, Cho K, Bashir ZI, Brown MW (2004) Benzodiazepine impairment of perirhinal cortical plasticity and recognition memory. Eur J Neurosci 20:2214-2224.

Wang J, Cottrell JE, Kass IS (2009) Effects of desflurane and propofol on electrophysiological parameters during and recovery after hypoxia in rat hippocampal slice CA1 pyramidal cells. Neuroscience.

Warburton EC, Aggleton JP (1999) Differential deficits in the Morris water maze following cytotoxic lesions of the anterior thalamus and fornix transection. Behav Brain Res 98:27-38.

Warburton EC, Aggleton JP, Muir JL (1998) Comparing the effects of selective cingulate cortex lesions and cingulum bundle lesions on water maze performance by rats. Eur J Neurosci 10:622-634.

Warburton EC, Baird AL, Morgan A, Muir JL, Aggleton JP (2000) Disconnecting hippocampal projections to the anterior thalamus produces deficits on tests of spatial memory in rats. Eur J Neurosci 12:1714-1726.

Warburton EC, Baird A, Morgan A, Muir JL, Aggleton JP (2001) The conjoint importance of the hippocampus and anterior thalamic nuclei for allocentric spatial learning: evidence from a disconnection study in the rat. J Neurosci 21:7323-7330.

Warburton EC, Koder T, Cho K, Massey PV, Duguid G, Barker GR, Aggleton JP, Bashir ZI, Brown MW (2003) Cholinergic neurotransmission is essential for perirhinal cortical plasticity and recognition memory. Neuron 38:987-996.

Warburton EC, Glover CP, Massey PV, Wan H, Johnson B, Bienemann A, Deuschle U, Kew JN, Aggleton JP, Bashir ZI, Uney J, Brown MW (2005) cAMP responsive element-binding protein phosphorylation is necessary for perirhinal long-term potentiation and recognition memory. J Neurosci 25:6296-6303.

Warrington EK, Weiskrantz L (1982) Amnesia: a disconnection syndrome? Neuropsychologia 20:233-248.

Whishaw IQ, Jarrard LE (1995) Similarities vs. differences in place learning and circadian activity in rats after fimbria-fornix section or ibotenate removal of hippocampal cells. Hippocampus 5:595-604.

Whishaw IQ, Maaswinkel H, Gonzalez CL, Kolb B (2001) Deficits in allothetic and idiothetic spatial behavior in rats with posterior cingulate cortex lesions. Behav Brain Res 118:67-76.

Winer MP (1971) Statistical principles in experimental design. New York: McGraw-Hill.

Winters BD, Forwood SE, Cowell RA, Saksida LM, Bussey TJ (2004) Double dissociation between the effects of peri-postrhinal cortex and hippocampal lesions on tests of object recognition and spatial memory: heterogeneity of function within the temporal lobe. J Neurosci 24:5901-5908.

Wirtshafter D (2005) Cholinergic involvement in the cortical and hippocampal Fos expression induced in the rat by placement in a novel environment. Brain Res 1051:57-65.

Witter MP, Groenewegen HJ, Lopes da Silva FH, Lohman AH (1989) Functional organization of the extrinsic and intrinsic circuitry of the parahippocampal region. Prog Neurobiol 33:161-253.

Witter MP, Wouterlood FG, Naber PA, Van Haeften T (2000) Anatomical organization of the parahippocampal-hippocampal network. Ann N Y Acad Sci 911:1-24.

Wyss JM, Van Groen T (1992) Connections between the retrosplenial cortex and the hippocampal formation in the rat: a review. Hippocampus 2:1-11.

Yang J, Zorumski CF (1991) Effects of isoflurane on N-methyl-D-aspartate gated ion channels in cultured rat hippocampal neurons. Ann N Y Acad Sci 625:287-289.

Yasuda Y, Watanabe T, Tanaka H, Tadashi I, Akiguchi I (1997) Amnesia following infarction in the right retrosplenial region. Clin Neurol Neurosurg 99:102-105.

Yoneoka Y, Takeda N, Inoue A, Ibuchi Y, Kumagai T, Sugai T, Takeda K, Ueda K (2004) Acute Korsakoff syndrome following mammillothalamic tract infarction. AJNR Am J Neuroradiol 25:964-968.

Zangenehpour S, Chaudhuri A (2002) Differential induction and decay curves of c-fos and zif268 revealed through dual activity maps. Brain Res Mol Brain Res 109:221-225.

Zhu XO, Brown MW, Aggleton JP (1995a) Neuronal signalling of information important to visual recognition memory in rat rhinal and neighbouring cortices. Eur J Neurosci 7:753-765.

Zhu XO, Brown MW, McCabe BJ, Aggleton JP (1995b) Effects of the novelty or familiarity of visual stimuli on the expression of the immediate early gene c-fos in rat brain. Neuroscience 69:821-829.

Zhu XO, McCabe BJ, Aggleton JP, Brown MW (1996) Mapping visual recognition memory through expression of the immediate early gene c-fos. Neuroreport 7:1871-1875.

Zhu XO, McCabe BJ, Aggleton JP, Brown MW (1997) Differential activation of the rat hippocampus and perirhinal cortex by novel visual stimuli and a novel environment. Neurosci Lett 229:141-143.

Zola-Morgan S, Squire LR, Amaral DG, Suzuki WA (1989) Lesions of perirhinal and parahippocampal cortex that spare the amygdala and hippocampal formation produce severe memory impairment. J Neurosci 9:4355-4370.

Zuschratter W, Gass P, Herdegen T, Scheich H (1995) Comparison of frequency-specific c-Fos expression and fluoro-2-deoxyglucose uptake in auditory cortex of gerbils (Meriones unguiculatus). Eur J Neurosci 7:1614-1626.